Hydrogeochemical conditions in the mine water of a flooding uranium mine – The Niederschlema/Alberoda deposit

Dissertation

for the attainment of the degree of

Doctor of Natural Sciences,

submitted by

Dipl.-Geol. Christian Wolkersdorfer

from Wendelstein, Middle Franconia, Germany

approved by the

Faculty of Mathematics and Natural Sciences

of the Clausthal University of Technology

Day of the oral examination:

6 November 1995

This thesis was published by
Institute for Geology and Palaeontology
of the Clausthal University of Technology.

English translation oft the
2. corrected edition, 2007

This text is the largely uncorrected DeepL translation of the original German text and reflects the knowledge of 1995

If in doubt, please refer to the German version.

My most current publications can be found at
www.wolkersdorfer.info/en/about-me/publikationen.html

Supervisor: **Univ.-Prof. G. Reik†, PhD**

Co-Supervisor: **Univ.-Prof. Dr. W. van Berk†**

Dedicated to all Wismut miners who gave their lives or health to provide the CPSU and SED dictatorships with the metal they used to threaten part of the world for half a lifetime.

“The only difference between a madman and me ist hat I am not mad”.

Salvador Felipe Jacinto Dalí y Domenech (1942)

Table of contents

1 Foreword

1.1 Introduction

With the completion of German unification, the Soviet-German Joint Stock Company (SDAG) Wismut became the property of the Federal Ministry of Economics. Until 1991, with few exceptions (KARLSCH 1993), it produced uranium exclusively for the Soviet Union (MAGER & VELS 1993). Thus the largest contaminated site in the new federal states was transferred to the responsibility of the Federal Republic of Germany at an estimated cost of 13 billion DM for remediation (FEDERAL MINISTER OF ECONOMICS 1993).

“Dealing with this legacy from 40 years of the GDR’s past is proving to be difficult and protracted,” says former Federal Environment Minister Dr. Klaus Töpfer (FEDERAL ENVIRONMENT MINISTRY 1994), “This is an elaborate large-scale project that is unprecedented on this scale in the world. For this reason, the highest demands are placed on all those involved. Contaminated site identification, remediation planning and conceptualisation must be carried out on a sound professional basis. The complete remediation of these mining sites will take years, if not decades”.

The aim of the present work, which is integrated into the remediation concept of Wismut GmbH, is to find a way to minimise the discharge of environmentally hazardous substances from the mine into the environment. To do this, the temporal and spatial changes in the concentrations of different water constituents in the seepage water and mine water of the former Niederschlema/Alberoda uranium mine must be clarified.

All results and process steps were obtained at the Institute of Geology and Palaeontology, Department of Engineering Geology, Clausthal University of Technology. They were discussed in the framework of the cooperation with the main department T1 of Wismut GmbH and verified at the local conditions of the Niederschlema/Alberoda mine (SDAG WISMUT & CLAUSTHAL UNIVERSITY OF TECHNOLOGY 1991).

The suggestion for the topic presented here came from Dr. Roland Hähne (former head of the Environmental Engineering Division) and Dipl.-Geol. Bernd Müller (former head of the group at the Office for the Environment/Chemnitz) in December 1990. At that time, SDAG Wismut was just leaving behind the period of strictest secrecy to become Wismut AG.

As a result of the political changes, the topics had to be adapted to the changed objectives and knowledge of SDAG Wismut, Wismut AG and Wismut GmbH, which led to unavoidable cutbacks in one or the other of the topics. In return, questions had to be added that had hardly been taken into account at the beginning of the work.

1.2 Acknowledgement

Work like this cannot be carried out without the help and support of a large number of people. This is especially true for the large number of measurements, water extractions and equipment installations at the Niederschlema/Alberoda mine.

I would therefore like to thank first and foremost my friend Günter Fröhlich and his colleague Gerd Lein from Sanierungsbetrieb Aue, who accompanied me on almost all my mining trips.

This would not have been possible without the cooperation of Dr. Jürgen Meyer and his superiors Dipl.-Chem. Jochen Schreyer, Dr. habil. R. Hähne (now HGC Chemnitz), Dr. M. Hagen and Prof. R. Gatzweiler from the main department T1 at Wismut GmbH in Chemnitz. They also ensured that the necessary contractual and legal basis for the cooperation was in place and that entry permits were obtained from the heads of the Aue remediation plant, Mr Christoph Rudolph and Mr Sigfried Geyer.

Special thanks go, of course, to my doctoral supervisor, Prof. Gerhard Reik, PhD, who made this work possible and was always available for discussions. I would like to thank Univ.-Prof. Wolfgang van Berk for kindly taking on the role of co-lecturer and for his expert support on chemical issues.

The biggest thanks, however, go to Ulrike. I owe my first contact with SDAG Wismut in December 1990 to her attentiveness during a customer meeting in Chemnitz.

Furthermore, I would like to thank the following individuals and institutions who have contributed to the success of my work to a greater or lesser extent:

Wismut GmbH, Dipl.-Ing. Udo Wirth zur Osten, Kathrin Huth, LUT Jena, Dr. K. Nindel, Dipl.-Geol. Jan Richter, Dipl.-Geol. Ulli Hiller, Kai Wagner, staff of Bayerische Vereinsbank Chemnitz, Dr. Thomas Rückwald, Dr. Kathrin Stein, Dr. Melanie Rieckhoff, Ms Hanna Brouwer, staff and colleagues of the Institute of Geology and Palaeontology, Dipl-.Geol. Helmut Fetzer, Library of the TU Clausthal, Klaus Schlüter, LogIn GmbH, Dr. Gerhard Lange, Dipl.-Geol. Wolfgang Büder, Siegfried Faßmann, Dipl.-Ing. Adam Jereczek, Dipl.-Chem. Volker Göbner, Familie Zier, Dipl.-Ing. geol. Irena Trebušak, Prof. Miran Veselič, Dason, Prof. Yuri Schukolyukov, Dr. Janine Teuppenhayn, Dipl.-Ing. oec. Ramona Olschewski, Georg Heindl, Herbert Zerbe (Institut Fresenius), Ponce Nguema.

Financial and non-material support was provided by the German Research Foundation Bonn (Re 920/1, 2), Wismut GmbH Chemnitz and the Hanns Seidel Foundation Munich.

2 Summary

For economic and environmental reasons, the former Niederschlema/Alberoda uranium mine near Aue in the Ore Mountains has been flooded since 1991. Wismut produced about 81,000 t of uranium there for the Soviet Union between 1945 and 1991.

The vein deposit, with pitchblende as the most important uranium ore, is located in contact and regionally metamorphically altered Ordovician to Devonian rocks in the contact area of the Auer Granite.

An open mine space with a volume of about 36 million m³, distributed over 50 main levels down to a depth of about 2000 metres, will be filled with water by the flooding, which is expected to last until the year 2000. Precipitation water penetrates the rock from the surface and enters the mine workings as seepage water via the mine workings. Permanent seepage inflows from fractures and faults are rare and almost non-existent below a certain level.

As the statistical and hydrogeochemical evaluations of analyses with up to 60 parameters each show, the waters in the mine can be assigned to three types: Seepage waters, intermediate waters and mine waters. All three types have substantially different chemical characteristics, with seepage water being the least mineralised and mine water the most. While seepage water and intermediate water show no statistically significant change in their physicochemical parameters during the study period from January 1991 to December 1994, the values of most physicochemical parameters of mine water increased more or less continuously until 1994. At the end of 1994, the increase in many parameters slowed down or came to a halt. This is either due to saturation of the water or a temporary equilibrium adjustment due to dissolution or precipitation of other phases.

To determine the hydrodynamic situation in the mine water, a tracer test and numerous depth-dependent temperature, electrical conductivity, pH and redox measurements were carried out. The tracer test with lycopod spores proved a complete mixing of the mine water in less than five weeks. The physicochemical measurements show a stratification of the water body with areas of varying thickness in which convection or diffusion predominate.

Comparisons of historical water analyses with those of today show that there are no substantial differences in the chemical properties of today's seepage water and the historical spring waters that flowed or flow into the Schlemabach and the Zwickauer Mulde.

In connection with the experience of mine flooding from the literature, it is evident that in Niederschlema/Alberoda the escape of water containing high levels of pollutants from the mine workings into the environment can be avoided. To this end, it is necessary to prevent vertical water pathways as far as possible by installing dam structures between levels that have yet to be determined. At open vertical connections that cannot be completely hermetised, seepage will overlay the mine water so that no contaminated mine water will enter the environment.

Résumé

Les hydrogéochimiques dans l'eau d'immersion d'une mine d'uranium – Le gisement de Niederschlema/Alberoda

Depuis 1991 l'ancienne mine d'uranium de Niederschlema/Alberoda près d'Aue dans le Erzgebirge (Monts Métallifères) inondée pour des raisons économiques et de protection de l'environnement. C'est ici qu'entre 1945 et 1991 la société Wismut produisait à peu près 81.000 tonnes d'uranium pour l'Union Soviétique.

Le gisement filonien avec pechblende comme le plus important minerai d'uranium se trouve dans la roche ordovicienne jusqu'à la roche dévonienne modifiée par métamorphose de contact et métamorphose régional dans l'auréole de contact du granit d'Aue. Jusqu'à l'an 2000 une mine au fond avec un volume d'environ 36 millions de m³, qui se répartit sur 50 étages principaux jusqu'à une profondeur d'environ 2000 mètres, sera rempli d'une immersion d'eau probablement jusqu'à l'an 2000. De la surface journalière des eaux de pluie pénètrent dans la montagne et atteignent comme eaux d'infiltration par la fracture dans toute la mine. Des afflux

d'eau d'infiltration durables provenant de fissurations ou de perturbations sont rares, pratiquement non existantes à partir d'un certain niveau.

Les eaux de mine peuvent être classifiées en trois types, comme le démontrent les évaluations statistiques et hydrogeochimiques des analyses avec jusqu'à 60 paramètres: eaux d'infiltration, eaux intermédiaires et eaux de mine. Ces trois types présentent de façon signifiante différentes caractéristiques chimiques, avec le moins de mineralisation des eaux d'infiltration pendant les eaux de mine sont plus fortement mineralisées. Les eaux d'infiltration et les eaux intermédiaires n'ont démontré du côté statistiques aucune modification signifiante de leurs paramètres physiquo-chimiques durant la période d'analyse entre janvier 1991 et décembre 1994, ce sont les taux de la plupart des paramètres physico-chimiques des eaux de mines qui ont plus ou moins augmenté jusqu'en 1994. En fin de 1994 l'augmentation de nombreux paramètres a ralenti ou s'est arrêtée. Cela est dû ou bien à une saturation des eaux ou bien à une réaction d'équilibre temporellement limitée.

Une analyse de Tracer et de nombreuses mesures de température de conductibilité, de facteur pH et de redox dépendant de la profondeur ont été réalisés pour déterminer la situation hydrodynamique dans les eaux de mine. L'analyse de Tracer avec des spores de lycopode (*Lycopodium clavatum*) a prouvé un mélange total des eaux de mines en moins de cinque semaines. Les mesures physico-chimiques démontrent une stratification du corps d'eau avec des sections de différentes importances, dans lesquelles existent convection et diffusion.

En comparant des analyses d'eau historiques avec celles d'aujourd'hui, on a pu constater qu'il n'existe pas de différences signifiantes entre les qualités des eaux d'infiltrations d'aujourd'hui et celles des eaux de sources historiques, qui s'écoulaient ou bien s'écoulent dans les ruisseaux de Schlemabach et de Zwickauer Mulde.

Compte tenu des expériences sur des immersions de mines décrites dans la bibliographie, l'exemple de Niederschlema/Alberoda nous démontre qu'il est possible d'éviter une sortie d'eau polluée de la mine dans l'environnement. Pour cela il est nécessaire d'éviter le plus possible l'écoulement vertical de l'eau en introduisant entre des étages encore à déterminer des constructions de barrages. Des eaux d'infiltrations vont être superposées aux eaux de mines aux liaisons verticales ouvertes qui ne peuvent être hermétiquement fermées de sorte que des eaux de mines contaminées n'atteindront pas l'environnement.

РЕЗЮМЕ

Кристиан Волъкерсдорфер: Гидрогеохимические соотношения в воде заводнений уранового рудника – Месторождение Нидершлемы/Алъбероды

С 1991 года бывший урановый рудник в Нидершлеме/Алъбероде под Ауе в Рудных горах по экономическим и экологическим причинам заводнетсяя. Там в период с 1945 по 1991 гг предпритиемя "Висмут" было произведено около 81,000 т урана для Советского Союза.

Жилъное месторождение с урановой смолкой из важнейшей урановой руды находится в горных породах силурийского-девонского периодов, преобразованных давлением, непогодой и вулканическими и располагающихся в области соприкосновения с ауеским гранитом.

Открытая подземная горная выработка объёмом приблизителъно в 36 миллионов м^3, разбитая на 50 главных подошв глубиной до приблизителъно 2000 м, заполнетсяя водой в резулътате заводнения, которое по всей видимости будет длитъся вплотъ до 2000 года. Воды, выпадающие в виде осадков, с земной поверхности проникают в породный массив и попадают в виде филътрационных вод через штолъни в сетъ подземных горных выработок шахты. Продолжителъные подтоки филътрационных вод из расселин и дислокаций редки и ниже определённого уровня уже практически не имеют места.

Как показывают резулътаты статистических и гидрогеохимических анализов с числом параметров в каждом отделъном случае до 60, воды в руднике можно классифицироватъ по 3 типам: филътрационные воды, промежуточные воды и шахтные воды. Эти 3 типа принципиалъно отличаются друг от друга по своим химическим характеристикам, причём фяилътрационна вода в наименъшей, а шяахтна вода в наиболъшей степени минерализированы. В то время как филътрационные и промежуточные воды в период исследований с нвар яя1991 по декабръ 1994 гг не показали статистически знаменателъных изменений их физико-химических параметров, значения для болъшинства физико-химических параметров шахтной воды до 1994 года в болъшей или менъшей степени последователъно росли. В конце 1994 года рост по многим параметрам призамедлился или полностъю приостановился. Это свзаноя либо с насыщением воды, либо с ограниченной во времени реакцией равновесия.

Для определения гидродинамической ситуации с шахтной водой были проведены трассовый опыт, а также многочисленные измерения температуры, проводимости, водородного показателя и окислителъно-восстановителъного потенциала, с учётом определённой глубины. Трассовый опыт с

порами плауна показал полное смешение шахтной воды за период менее чем в 5 неделъ. На основании физико-химических измерений было вывленоя наслоение водной среды с различными по мощности участками, в которых преобладают конвекция или диффузия.

Из сравнения анализов воды из истории с сегодншнимия становится сноя, что принципиалъных отличий в химических свойствах сегодншнихя филътрационных вод и родниковых вод из истории, тёкших или текущих в Шлемабах или Мулъде в Цвиккау, не существует.

На основании опыта по рудничным заводненимя из литературы вывлетсяяя, что выход воды с высоким содержанием вредных веществ из сети подземных горных выработок шахты в окружающую среду на месторождении Нидершлемы/Алъбереды предотвращаем. Для этого необходимо парализоватъ вертикалъные проходы для воды насколъко это возможно, поместив между пока ещё подлежащими определению подошвами перемычки. У открытых вертикалъных соединений, которые не могут быт полностъю герметизированы, слой филътрационных вод будет располагатъся над шахтной, так что загрзнёнаяя вода в окружающую среду уже не попадёт.

Povzetek

Hidrogeokemične razmere v vodi, ki zaliva uranov rudnik – ležišče Niederschlema/Alberoda

Nekdanji uranov rudnik Niederschlema/Alberoda, ki leži v bližini kraja Aue v nemškem Rudogorju (Erzgebirge) je iz gospodarskih in za okolje pomembnih razlogov že od leta 1991 v postopku zapiranja z zalivanjem. Tukaj je SDAG Wismut med leti 1945 in 1991 proizvedel okoli 81.000 t urana za Sovjetsko zvezo.

Čilno rudišče z uranovo smolo kot najpomembnejšim rudnim mineralom se nahaja v s kontaktno in regionalno metamorfozo spremenjenih ordovicijskih do devonijskih kamninah v kontaktnem območju granitove aureole.

Podzemni rudniški prostori z okoli 36 milionov m³ prostornine, ki se delijo na nekako 50 obzorij in segajo do globine približno 2.000 m, bodo predvidoma do leta 2000 z nenehnim zalivanjem zapolnjeni z vodo. Padavinska voda prodira z zemeljske površine v tla in teče kot pronicajoča voda v jamske prostore. Trajni dotoki pronicajoče vode iz razpok in prelomov so redki in pod nekim določenim nivojem se skoraj ne pojavljajo več.

Kot kažejo rezultati statističnih in hidrogeokemičnih analiz z občasno do 60 parametri, se rudniške vode ločijo v tri različne tipe: pronicajoče vode, vmesne vode in jamske vode. Vsi trije tipi kažejo precej različne kemične značilnosti, pri čemer je pronicajoča voda najmanj in jamska voda najmočneje mineralizirana. Medtem ko pronicajoče vode in vmesne vode v času trajanja preiskav od januarja 1991 do decembra 1994 niso pokazale statistično pomembnih sprememb fizikalnokemičnih parametrov, so vrednosti večine fizikalnokemičnih parametrov jamske vode bolj ali manj kontinuirano naraščale. Konec 1994 se je pri številnih parametrih to naraščanje upočasnilo ali ustavilo. Vzrok tega je v zasičenosti vode ali pa v časovno omejeni ravnovesni reakciji.

Za ugotavljanje hidrodinamičnih razmer v jamski vodi je bil izveden sledilni poizkus, kot tudi številne meritve z globino spreminjajočih se temperature, prevodnosti, pH in redoks potenciala. Sledilni poizkus z lisičjakovimi sporami je pokazal popolno mešanje jamske vode v manj kot petih tednih. Iz rezultatov fizikalnokemičnih meritev je mogoče ugotoviti meenakomerno slojevitost vodnega telesa. Prevladuje konvekcija ali difuzija.

Iz primerjave starejših analiz vode z današnjimi je razvidno, da ni kakšnih pomembnih razlik v kemični sestavi današnjih pronicajočih vod in vod nekdanjih izvirov, ki so se oz. se iztekajo v Schlemabach in v Zwickauer Mulde.

Primerjava z izkušnjami z zalivanjem jam opisanimi v literaturi kaže, da se je v primeru rudnika Niederschlema/Alberoda izlivu vode močno zasičene s škodljivimi snovmi v okolje mogoče izogniti. Pri tem je potrebno vertikalne vodne povezave kolikor je mogoče preprečiti tako se med obzorji, ki jih je potrebno še določiti, namestijo pregrade. Nad odprtimi vertikalnimi povezavami, ki jih ni mogoče popolnoma hermetično zapreti, bodo pronicajoče vode ostale nad jamsko vodo, tako da kontaminirana jamska voda ne bo prišla v okolje.

3 Problem

3.1 Inducement

On 2 July 1990, the flooding of the 10,179 m³ large –1800 level in the Niederschlema/Alberoda mine began by partially switching off the mine water pumps. It was not until 11 January 1991 that the controlled flooding process began with the flooding of level –1755 (G. FRÖHLICH, pers. comm.), the end of which will be reached in the year 2001/2 (FEDERAL MINISTER OF ECONOMICS 1995, WISMUT GmbH 1993a).

During and at the end of the flooding of a mine, the question arises as to the effects of the mine water on the hydrosphere in the immediate and wider surroundings of the mine. The problem here is that if the wrong procedure is followed during the closure of the mine, considerable amounts of environmentally hazardous substances can be released into the environment over decades or even centuries. Negative effects of mine water were already known in the 16th century, in AGRICOLA'S time (AGRICOLA 1994), and in more recent times various congresses and publications have dealt with environmental damage caused by mine water (GEOLOGICAL SURVEY OF SWEDEN, SWEDISH UNIVERSITY OF AGRICULTURAL SCIENCES 1991, UNIVERSITY OF MINING AND METALLURGY IN KRAKOW 1994, INTERNATIONAL MINE WATER ASSOCIATION 1991, INTERNATIONAL MINE WATER ASSOCIATION 1994, VESELIČ & TREBUŠAK in press, OFFICE OF WATER RESOURCES RESEARCH 1975). Acid mine waters are by far the most important compared to basic or neutral ones.

As early as 1989, the Aue mining operation had to clarify, under pressure from the Oberflussmeisterei (OFM) Chemnitz and the superordinate GDR Water Management Directorate Obere Elbe/Neisse, which pollutant discharges could be expected after the end of a controlled flooding of the Niederschlema/Alberoda mine (J. MEYER, pers. comm.). Above all, it was necessary to find out over what period of time which water constituents would escape and in what mass concentrations. To this end, SDAG Wismut carried out various laboratory tests on the solubility of uranium and arsenic in ore samples. They started in May 1989 and May 1990 (SDAG WISMUT 1991) and covered a period of one year and two years respectively (chapter 5.3).

FÖRSTER (1990) stated that "only few figures have been published on the mining of uranium in the Aue/Schlema, Ronneburg and Königstein mining areas". Although this is true only to a limited extent today, the need for research work "in the geochemical and biochemical fields to penetrate the reaction processes taking place in tailings piles and mine workings", which he pointed out at the time, has not changed (FÖRSTER 1990). Employees of the then Saxon Geological Survey (Dr. Andreas HARTSCH, pers. comm.) and various employees of SDAG Wismut also agreed that research on chemical and biochemical processes in the open and flooded mine workings was urgently needed.

3.2 Remediation concept of Wismut GmbH

The primary operational objective of Wismut GmbH is the rehabilitation of all areas and facilities that were used for the exploration, extraction and processing of uranium ore (RUNGE & BÖTTCHER 1994). To this end, the hazards emanating from the old sites must be eliminated or reduced to an acceptable level (WISMUT GmbH 1994a, GATZWEILER & MAGER 1993, MAGER & VELS 1993). In order to record the mining-related contaminated sites, Wismut drew up several remediation concepts (MAGER & VELS 1993) and a contaminated site register (KAUL 1991, RÖHNSCH & ETTENHUBER 1993), which is intended to serve the following purposes (BACHNER et al. 1993):

- Assessment of the overall situation
- Justification of the need for safeguarding and remediation measures
- Supporting the further economic development of the region through the containment of actually polluted areas and objects.

The result of the register of contaminated sites was the identification of well over 30 suspected sites that need to be investigated in more detail.

An essential component of remediation is environmental monitoring (GATZWEILER & MAGER 1993), which consists of static and dynamic monitoring. While static monitoring is used for long-term monitoring of the water, soil and air pathways independently of remediation, dynamic monitoring is used to control the remediation, recultivation and closure of mining facilities and mine dumps. The former includes, for example, hydrochemical environmental monitoring, seismic monitoring of flooding at the Niederschlema/Alberoda mine or radiometric inventory (KUYUMCU et al. 1994), the latter dust measurements or hydrochemical investigations of the flooding waters (WISMUT GmbH 1994a). In particular, the question of monitoring waters leaking from the mines can lead to difficulties, since there are still no legal regulations for waste water from uranium mines (GANS 1978) and the question arises as to how and whether the Radiation Protection Ordinance is to be applied. Chemotoxic elements on the one hand and elements of the uranium decay series (Tab.1) are discharged with the flooding water on the other hand. The former includes arsenic, for example, and the latter includes the extremely radiotoxic radium 226. For this reason, the discharges of uranium and radium at Wismut GmbH are recorded particularly precisely (Fig. 1) and compared with the approved annual discharges. In the following, following the terminology of Wismut GmbH, all waters that enter the Niederschlema/Alberoda mine workings or escape from there by means of technical aids (pumps) or by themselves, in a natural way (faults, water solution tunnels), are to be summarised under flooding water.

The results of the investigations suggest slightly higher average pollutant levels in the waters from the Niederschlema/Alberoda mine than in areas where no radioactive minerals occur. Accordingly, the overall goal of remediation, as formulated elsewhere by former employees of Wismut GmbH (KUYUMCU et al. 1994), can at most consist in restoring conditions that existed before uranium mining. Water treatmen beyond the geogenic background level is not economically justifiable.

The SI unit used since 1970 for the activity of a radioactive substance is the becquerel (Bq) named after the discoverer of radioactivity, Henri Becquerel. 1 Bq corresponds to one decay per second and replaces the old unit Ci (curie), which referred to the activity of one gram of radium and corresponded to $37 \cdot 10^9$ decays per second (BUTTERMANN 1987). Other units used in older literature for the activity of a litre of water were the Eman and the Mache unit (ME), between which the following relationship exists: 1 ME = 3.64 Eman = $3.64 \cdot 10^{-10}$ Ci L^{-1} = 13.468 Bq L^{-1} (GENSER 1932).

With regard to the annual discharges or the mass concentration of uranium, its chemotoxicity, rather than radiotoxicity, is to be regarded as the yardstick for possible limit values (GANS 1978).

Tab. 1: Longer-lived radionuclides of the uranium-radium decay series (from GANS 1978).

Nuclide	Half-life	Disintegration type
U 238	$4.51 \cdot 10^9$ a	α, γ, e^-
U 234	$2.47 \cdot 10^5$ a	α, γ
Th 234	24.1 d	β^-, γ, e^-
Th 230	8000 a	α, γ, e^-
Ra 226	1600 a	α, γ, e^-
Pb 210	22 a	β, γ, e^-
Bi 210	5.0 d	β^-
Po 210	138.4 d	α

In order to be able to achieve the rehabilitation goals mentioned at the beginning, the following tasks are to be fulfilled in the Aue rehabilitation enterprise (GATZWEILER & MAGER 1993):

- “Closure, disposal and custody of the pits in accordance with the regulations of the Mining Act and the radiation protection regulations, as well as the controlled flooding of the pits to the highest possible level. This is intended to restore the original hydrological conditions to a large extent.

- In several cases, it will be necessary to clean the escaping mine water in water treatment plants after the pits have been flooded, and landfill space will have to be made available for the solids produced in the process."

With an annual discharge of a hypothetical treatment plant of 6 … 7 · 10^6 m³ of water (WISMUT GmbH 1993a), about 6,000 … 20.000 t of solids, of which 5 … 23 t of uranium and 1 … 39 t of arsenic would have to be deposited (the calculation is based on the mean values and simple standard deviations of the mine water measured values from 1.1.1991 … 31.12.1994 from the Niederschlema/Alberoda mine in Table 28; numerical values rounded). Landfilling and handling such quantities of waste materials from a processing plant is not justifiable in the long term. Therefore, possibilities must be sought to dispense with a plant by means of controlled flooding or to shorten its period of use to an acceptable period (10 … 20 years).

All in all, it will take at least until 2003 before the contaminated sites of uranium mining in Saxony and Thuringia will be adequately cleaned up (GATZWEILER & MAGER 1993).

The results of the rehabilitation work up to the end of 1993 are summarised for the Schlema/Alberoda plant section in Table 2.

In a paper on "Flora and Vegetation in the Ronneburg Uranium Mining District", SÄNGER (1993) made the following demand for rehabilitation:

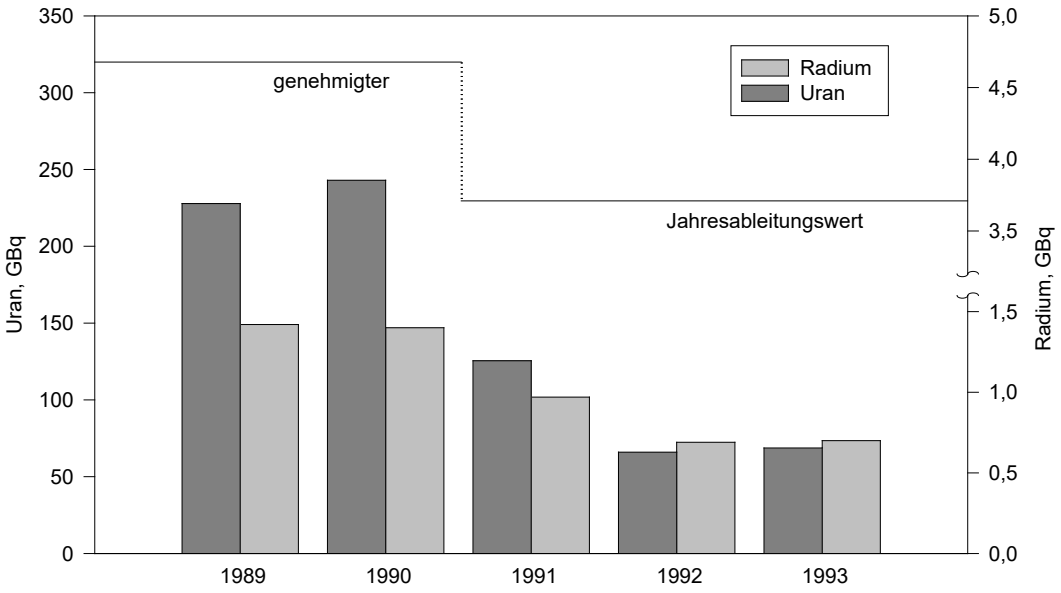

Fig. 1: Development of uranium and radium discharges of the Aue remediation plant, Schlema-Alberoda operation between 1989 and 1993. The authorised annual discharges for uranium are 320 GBq until 1990 and 230 GBq from 1991 onwards, for radium 4.7 GBq and 3.7 GBq annual discharges apply accordingly (WISMUT GmbH 1994a).

Tab. 2 Remediation work carried out at the Schlema/Alberoda site up to the end of 1993 (WISMUT GmbH 1994a).

Remediation work	Unit	Niederschlema/Alberoda
disposed mine workings	km	6.8
discarded workings	km	2
Dams	Piece	32
backfilled mines	m^3	1130
Stored shafts (number)	Piece	1
Stored shafts (scope)	m^3	10.932
Examination dies (number)	Piece	18
Examination dies (stored)	Piece	6
Investigative dies (custody started)	Piece	6
Examination dies (jacking)	m	350
Examination joints (reconstruction)	m	944
Investigative countersinks (Aufwältigung)	m	962
Examination sinks (backfilled)	m^3	9098
flooded mines	m^3	2,250,000

"The further remediation of tailings piles, tailings ponds and other contaminated sites should be carried out in compliance with the requirements of radiation protection in such a way that in the post-mining landscape it will be possible in future to ensure the protection of all natural developments and semi-cultural formations in open landscapes, because no conditions are to be conserved, but processes are to be enabled and their sequences guaranteed".

With regard to the tailings, whose hazardousness has repeatedly been falsely highlighted in the press (DOUGLAS & KLEINE-BROCKHOFF 1991, STAMM 1993), he concludes:

"The present results tend to indicate that the tailings of uranium ore mining seem to be less contaminated with heavy metals than previously assumed".

3.3 Water–rock–microorganism interactions

The development of the chemical composition of the seepage water (infiltration water) and the mine water is essentially influenced by the following criteria (partly according to VOIGT 1990):

- Size of the thermodynamic imbalance
- Geological and hydrogeological conditions
- time available
- Size of the active surfaces
- Amount of leachate
- physicochemical conditions
- Type of ore mining
- biological factors

KARRENBERG (1981) summarises the processes of water-mountain contact in the following way:

"The chemical composition of groundwater is largely determined by the rocks in which it resides or moves, primarily by dissolution of rock-forming minerals and selective precipitation of constituents in the cavities, with oxidation and reduction, sorption and ion exchange playing a significant role".

When investigating the hydrogeochemical conditions in the Niederschlema/Alberoda mine, the interactions between the inorganic and organic processes must also be taken into account. Unlike laboratory experiments with rocks from mine tailings, organic material is present in a mine (e.g. mine wood, faeces, paper), which bacteria and other lower organisms use together with oxygen to obtain nutrients. Since microbial activities have already been described from a wide variety of environments

(BAAS BECKING et al. 1960, NORDSTROM 1977), we will refrain from describing the processes in detail. An overview can be found in the chapter 4.9 chapter.

Only the consideration of all interlocking processes and factors affecting the flooding water of the Niederschlema/Alberoda mine creates the prerequisite for a prediction of the future mass concentration of various water constituents.

3.4 Model introduction and explanation of terms

In the chapter “Presentation of the model and explanation of terms” some of the more frequently used technical terms will be explained, as far as they are not explained in the relevant DIN standards (e.g. DIN 4049). Furthermore, a highly simplified model of the flooding process and the processes leading to the mobilisation of pollutants is to illustrate the complex interrelationships in the Niederschlema/Alberoda mine (Fig. 2).

This approach was chosen because the present work covers several subject areas with different technical terminology. These are essentially regional and historical geology, hydrogeology, hydrodynamics, engineering geology and mining. In addition, new terms are introduced or already known terms are redefined in the sense of the topic dealt with here.

Flooding of a mine is the gradual rise of water in the underground cavities (mine workings, mine buildings) after the water pumps in the mine have been switched off (mine drainage). In this process, the water rises in the more or less vertical (shafts), the horizontal (levels) and the mining-related (overhauls, excavations) mine workings. In the Niederschlema/Alberoda mine, the waters (infiltration waters, geological waters, meteoric waters) seep mainly through the loose rock cover and the weathering zone into the mine workings. There, they flow down the inverts, shafts and pipes of the mine drainage system to the rising water and raise the water level. Flooding is completed as soon as the water floods the deepest floor that is in contact with the surface (water solution gallery) or a water level is reached above which the water can be pumped to the surface.

All water that flows into, is in or emerges from the mine workings is referred to in this work as flood water.

The following model for the hydrodynamic behaviour of the flooding water in the mine workings is used as a basis: In the shafts, due to density differences (density flow, free convection), lighter water flows upwards until it meets a density limit (boundary layer) which it cannot overcome. Since the upwardly decreasing temperature at the concreted shaft walls presumably makes the most substantial contribution to density differences, the water cooled at the density boundary will sink after it cools in the centre of the shaft.

As soon as it has reached a certain temperature, thus density, again when it sinks in the shaft, the cycle begins anew (convection roller). Forced convection, which would be caused by actively introducing water, is not likely to drive large-scale convection. Likewise, laminar convection is unlikely, as the shaft internals and concrete roughness prevent it.

As soon as the water in two or more shafts is interconnected via one or more levels, open or closed convection circuits can be established in which the shaft acts as a thermosyphon. The consequence would be a complete mixing of the water within the interconnected pit areas.

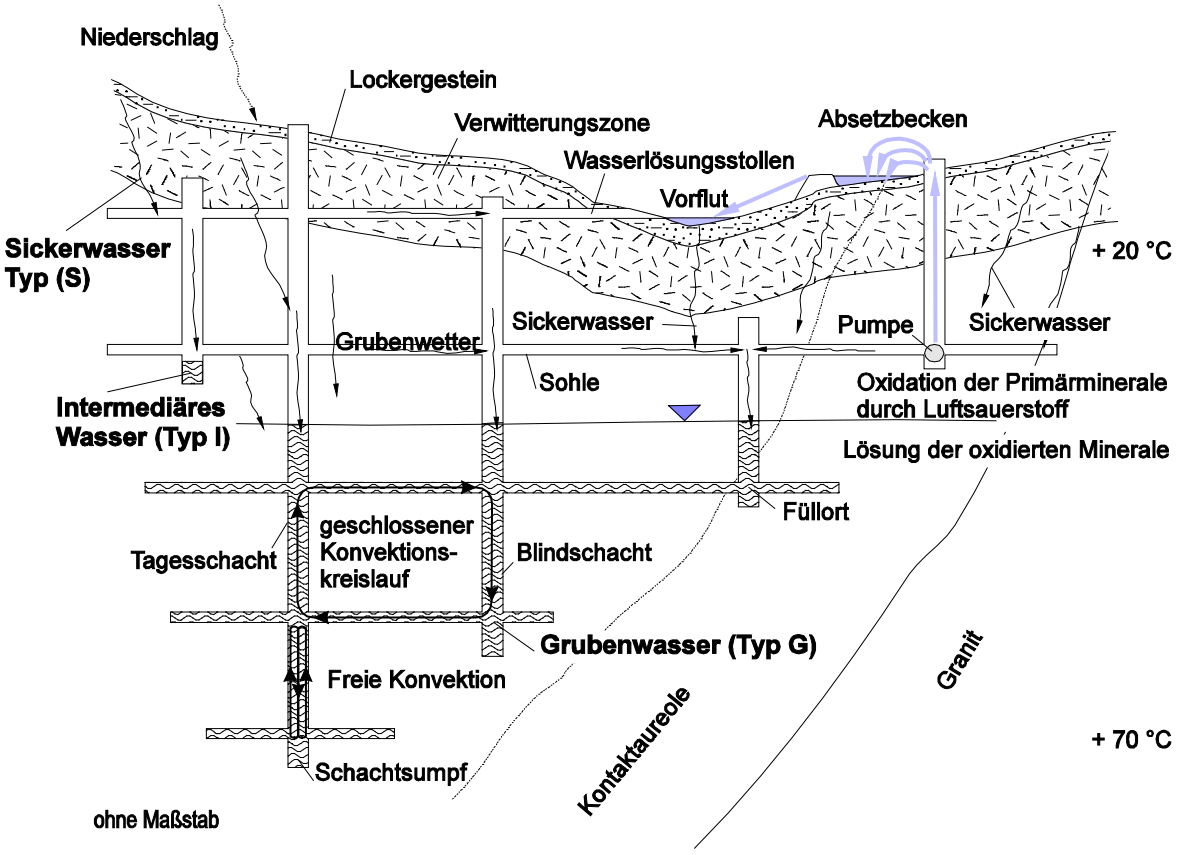

Fig. 2: Illustration of the principle processes during the flooding of the Niederschlema/Alberoda mine. Important terms are shown in the picture.

A thermosyphon is a fully or partially enclosed fluid circuit driven by temperature-induced density flow (GEBHART et al. 1988).

The terms seepage waters, intermediate waters and mine water are understood to mean flood waters that differ substantially in their chemical properties. A new term is introduced to distinguish between them, the deposit-specific boundary quotient. Each of the three chemically different water types can be spatially assigned to a mine area. Seepage waters are mostly waters that are above the flood water level. Intermediate waters are found in shafts or shaft sumps that are not in contact with the rising flood water. Finally, mine water is the water of the contiguous flood water body.

The mobilisation of substances is based on the following model: in the open mine workings, moist, oxygen-containing air (mine air) was able to weather the minerals on the exposed surfaces during the past maximum of 50 years. The amount of oxidised mineral phases increases depending on the amount of primary minerals and the age of the mine workings. The rising flood water dissolves the oxidised and non-oxidised solid phases, causing the mass concentrations in the flood water to increase. Since the amount of available substances depends on the contact time with the mine weathering and the degree of enrichment in the rock, the mass concentrations of dissolved species in the mine water will not remain constant during the flooding process.

The geochemical computer model WATEQ4F (version 2.0 of 30.10.91) with the standard data set was used to calculate the chemical-thermodynamic conditions in the floodwater. This thermodynamic data set provides a number of phases (range of a system with homogeneous chemical and physical properties) and reactions, with the help of which, among other things, the distribution of the chemical species (state form of a molecule or ion in a solution) can be calculated.

3.5 Objective and solution approach

The aim of this study is to find a way to minimise the discharge of pollutants from the mine workings into the environment after the end of flooding. For this purpose, it is necessary to clarify the following issues:

- Temporal change in the mass concentration of different water constituents in the seepage water and the mine water
- Buffer capacity of the mine water
- determinant responses
- maximum available cations/anions.

For this purpose, different data were used, which were obtained either within the framework of this work (TUC) or from Wismut GmbH (Wismut):

- Water analyses between January 1991 and December 1994 (Wismut, TUC)
- Tracer test with *Lycopodium clavatum* (TUC)
- Temperature measurements in several shafts (TUC, Wismut)
- Physicochemical measurement in several shafts (Wismut, TUC)
- Distribution of rocks in the mine field (TUC)
- regional CLARKE values for the deposit (Wismut).

The investigations are to provide Wismut GmbH and the responsible federal and state authorities with a working basis for the future hydrogeochemical development of the mine water. This will enable them to make decisions for medium- and long-term safeguards investments at the Niederschlema/Alberoda uranium mine.

The structure of this paper is as follows (chapter numbers in brackets):

As there are still few overall representations of the geological environment of the Niederschlema/Alberoda uranium mine, the work begins with a description of the geological conditions and the deposit itself (4). In order to understand how today's Wismut GmbH developed with its manifold problems, a historical outline is included (4.4). One focus is the description of the hydrogeological situation in the vicinity of the deposit before mining by SDAG Wismut (4.7). A summary of the microbial activities and weathering processes in a mine is intended to illustrate how the mobilisation of substances into the mine water takes place (4.8, 4.9).

This summary forms the transition to the chapter on the hydrogeochemistry of uranium, arsenic and radium as the most important pollutants in the Niederschlema/Alberoda mine (5). It is intended to allow a comparison between the situation in the Niederschlema/Alberoda region and other regions of the world, as well as to show the hydrogeochemical behaviour of these elements. The results of the column tests ("column test": test on the release of substances) will lead to the chapter on the empirical investigations and the actual situation in the mine (5.3).

The hydrogeochemical investigations are divided into two parts. In the evaluation part, the data material is essentially assessed mathematically and statistically (6.3). To forecast future pollutant development, the net neutralisation potential was determined (6.3.4.2). Then the hydrogeochemical milieu is characterised by chemical-thermodynamic equilibrium calculations in order to arrive at statements about the equilibrium-determining reactions (6.4).

In the chapter on the hydrodynamics investigations, the extensive physicochemical measurements are summarised (7). Together with these results and those of a literature research on mine flooding, a model of the hydrodynamic processes in the mine is developed (7.6).

Finally, the last chapter calculates the maximum pollutant loads that can be dissolved by hydrogeochemical processes and transported by hydrodynamic processes (8).

The work ends with considerations on the hydrogeochemical-hydrodynamic processes in the mine and the question of the necessity of a water treatment plant (9).

Fig. 3: Shaft 371 (“Hartenstein”) of the Niederschlema/Alberoda mine in the valley of the Zwickauer Mulde on 4 January 1991.

4 Niederschlema/Alberoda deposit

4.1 Introduction

Without knowledge of the geological relationships that lead to mineral formation in the rocks of an ore deposit or in an ore vein, it is not possible to interpret hydrogeochemical processes with sufficient accuracy. For this reason, the hydrogeochemical and hydrodynamic investigations of the flooding process begin with a summary of the surrounding geology of the Niederschlema/Alberoda mine.

A release of substances by the floodwater would not be possible to the extent described without weathering processes in the open mine workings. Since disulfide oxidation plays a key role in this release, it and the catalytically acting microbial processes are also presented in this chapter.

4.2 Geographical location

The main shaft of the Niederschlema/Alberoda mine, Shaft 371 (Fig. 3), is located in the Free State of Saxony, 28 km southwest of Chemnitz, between the Erzgebirge towns of Hartenstein and Aue at 365.2 mNN (Fig. 4, Fig. 10). In the north, the 22 km² measuring area of the Wismut Environmental Cadastre reaches close to Hartenstein, in the east to Lößnitz, in the southeast to Aue and in the southwest to Schneeberg. Within the area are Alberoda, Schlema and parts of Wildbad, Niederlößnitz, Aue and Schneeberg.

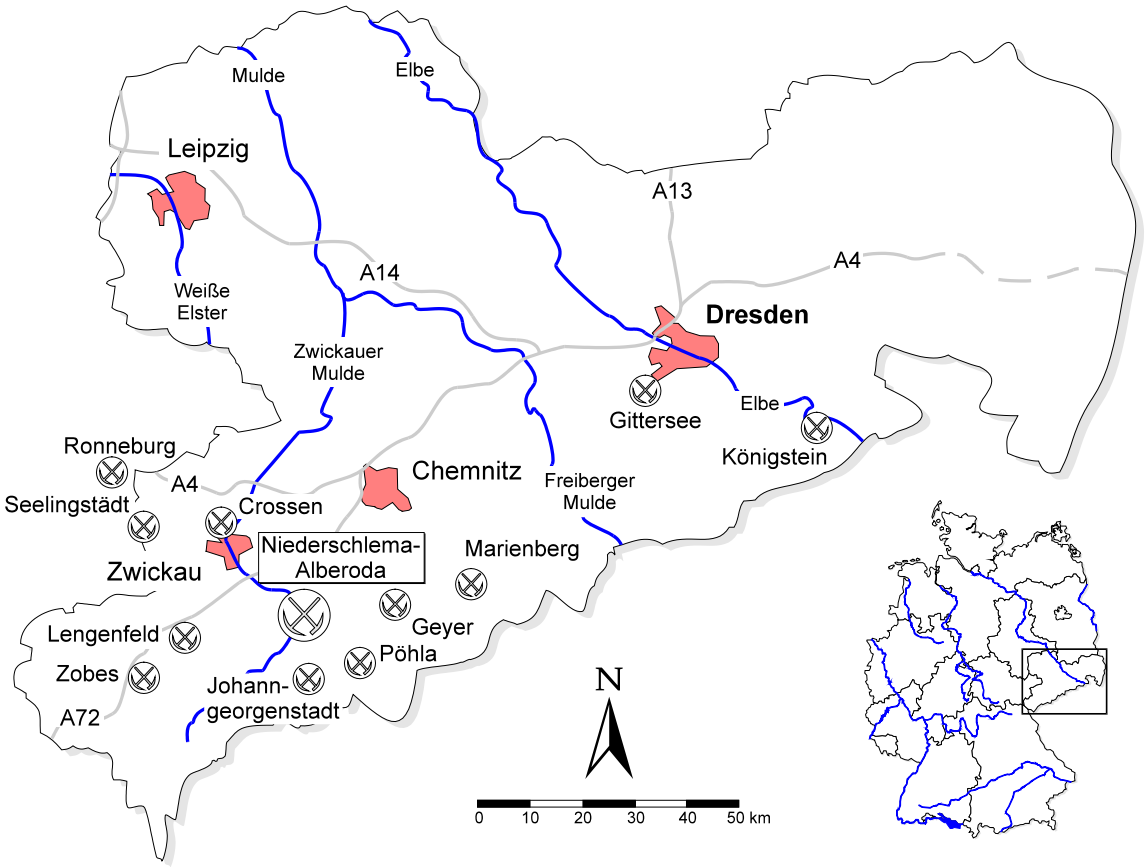

Fig. 4: General map of Saxony with the most important uranium ore deposits and the location of shaft 371 of the Niederschlema/Alberoda mine. In addition, the locations of the Seelingstädt and Crossen ore dressing plants and the open pit mine near Ronneburg.

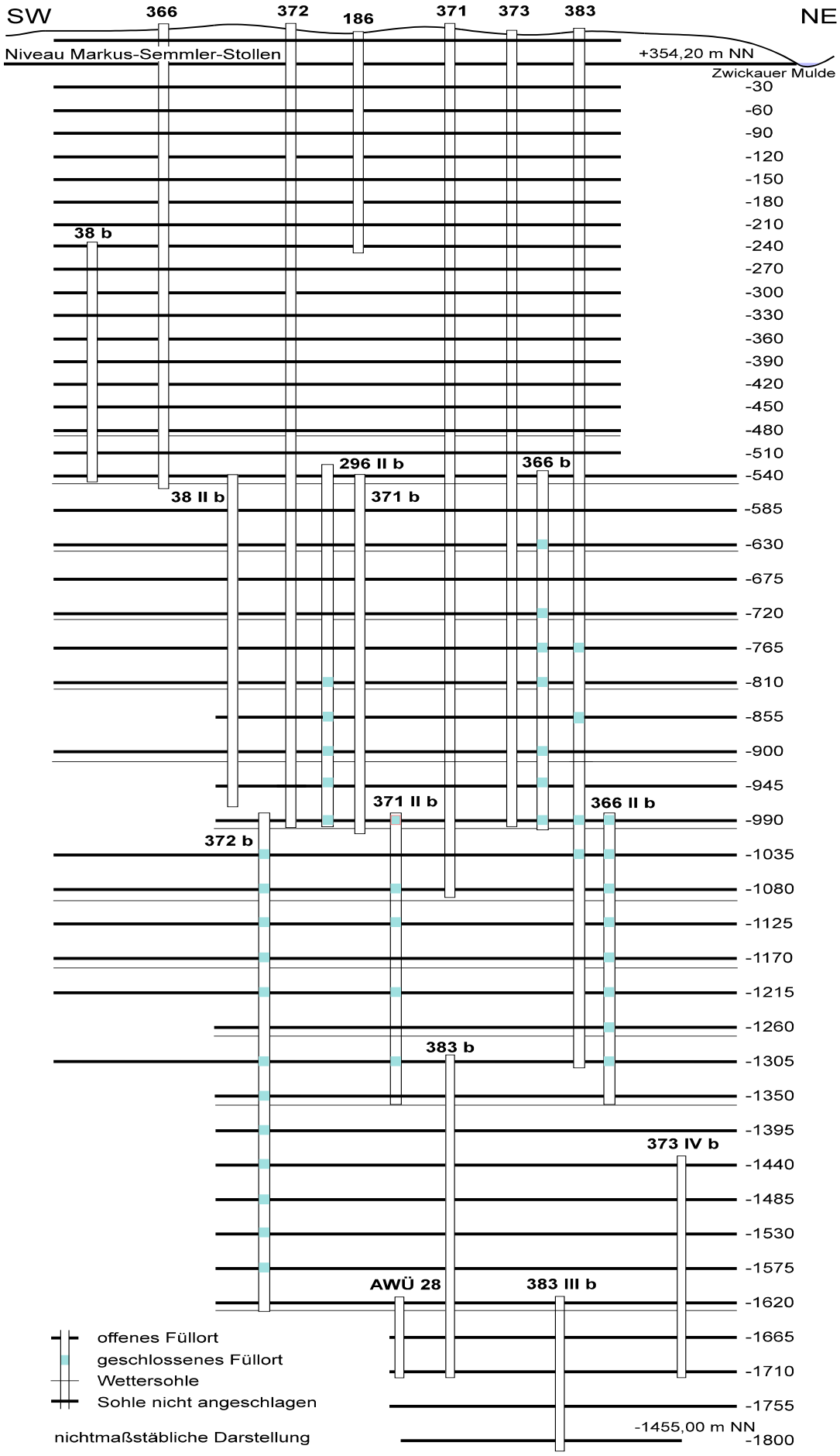

Fig. 5 Simplified and schematised view of the Niederschlema/Alberoda deposit with levels and the shafts mentioned in the text (compiled according to information provided by Wismut GmbH). The levels above the Markus-Semmler adit are only indicated.

The highest point, at 532.4 m a.s.l., is the 310 slag heap between Schneeberg and Wildbad, the lowest, at 312.4 m a.s.l., is the point where the Zwickauer Mulde leaves the measuring area in the north. The Zwickauer Mulde, which is fed by several small streams, flows from south to north (chapter 4.9) flow through the study area.

4.3 Mine building

During the active mining period, 50 main shafts were excavated in the Niederschlema/Alberoda deposit (object 9) and Oberschlema (object 2), whose names are derived from the average depth below the level of the Markus Semmler gallery, which was excavated in 1503. Inconsistent spelling e.g. in: SCHIFFNER 1908, SCHIFFNER & WEIDIG 1909, SCHIFFNER et al. 1911, WEIDIG 1912, GENSER 1932, GENSER 1933, WAGENBRETH 1990). Up to level -540, the average invert spacing was 30 m, below that, up to level –1800, construction was at 45 m intervals (Fig. 5). Additional ventilaton levels are or were located at levels –1626, –1356, –1266, –1176, –1086, -996, -906, -816 and -546. A further division of the mine workings subdivides them into six cascades, each bounded by two main winding levels (Tab. 6o).

The excavation was carried out by ridge jointing with backfilling (LANGE et al. 1991, BÜDER & SCHUPPAN 1992) by means of overcutting and ascending locations from the cross-cuts and field sections (Fig. 6), whereby a total of about 4150 km of roadways were excavated (BÜDER & SCHUPPAN 1992). There are different data on the floodable cavity, which vary between 35.6 and 49.4 million m³ (Tab. 3).

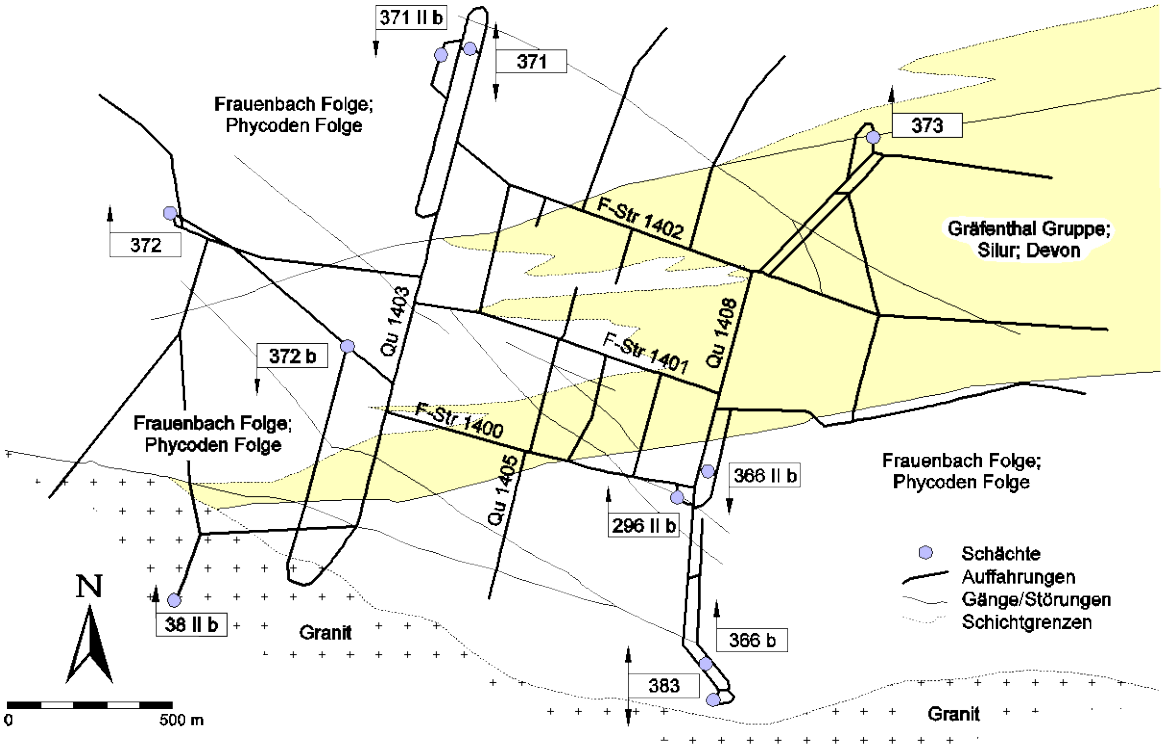

Fig. 6 Overview of level –990 of the Niederschlema/Alberoda- mine according to Wismut operating documents. As of 1 October 1986 with partial supplements until 1 May 1990. Tectonic elements modified according to BÜDER & SCHUPPAN 1992. Qu: crosscut, F-Str: field section.

Source	Cavities
J. MEYER (1994, pers. comm.)	35.6 m³
W. BÜDER (1992)	36.4 m³
Wismuth (ca. 1992, AP 2.1/B7)	49.4 m³
Wismut (ca. 1991, official document 4.0.28/254)	38.5 m³

Tab. 3: Open cavity of the Niederschlema/Alberoda and Oberschlema mines according to various sources between the –1800 level and the level of the Markus-Semmler adit.

The value from the service case 4.0.28/254 (Tab. 60) includes a volume of ≈ 9 … 10 million m³ of residual void space of the Oberschlema mine, which originates from data of the year 1983. Presumably, the difference to the 35.6 million m³ indicated can be explained by the fact that the residual cavity of Oberschlema was not determined more precisely until 1993/94. Accordingly, it amounts to about 6.6 million m³. The calculations in this paper are based on a volume of 36 million m³ of floodwater.

4.4 Historical development

4.4.1 From the Oak Forest to the Ore Mountains

When uranium ore mining near Aue and Pöhla ended in 1990, the fifth “Bergkgeschrey” in the Ore Mountains came to an end. This was preceded by mining periods in early history, the Middle Ages, the Renaissance and at the time of the Industrial Revolution (BEEGER et al. 1988).

Although there is no written or archaeological evidence for early historical mining (BÖTTCHER et al. 1991), recent geochemical investigations in the area of the Rote Weißeritz indicate mining around 1100 BC (!) (J. MATSCHULLAT, pers. comm.).

In 1168, silver was found for the first time near Christiansdorf and a little later today’s Freiberg was founded there. It was silver that gave the “Ferguna” or “Miriquidi", the oak or dark forest (BÖTTCHER et al. 1991), its wealth and eventually led to the name Erzgebirge. As the mines advanced to ever greater depths, technical problems arose which, in the 13th … 14th century, accompanied by wars, social unrest and a plague epidemic, finally led to the decline of medieval mining in the Ore Mountains.

As early as 1471, a new mining period began near Zwickau and Schneeberg when miners searching for ores stumbled upon rich silver deposits. Within a few decades, new mining towns sprang up and the invention of new mining techniques led to a previously unknown wealth. As the rich silver deposits of the oxidation and cementation zone diminished with increasing depth, a mining extinction began again in large parts of the Ore Mountains. The consequences of the 30 Years’ War and too little money for urgently needed hydraulic engineering also brought this period to an end. Only in the Schneeberg area did cobalt, nickel and bismuth ores ensure that mining did not come to a complete standstill.

With the founding of the Freiberg Mining Academy in 1765, a renewed upswing in mining in the Erzgebirge began. Mainly silver, cobalt, nickel, iron and bismuth were the target of the renewed activities. In addition, tungsten and uranium, discovered by KLAPPROTH IN 1789, were extracted during this period (KIRCHHEIMER 1978).

At the turn of the 19th to the 20th century, the reserves in the economically accessible depth range were exhausted, and the gradual closure of the Erzgebirge silver mines, which ended in 1913, began (BEEGER et al. 1988).

The last mining period of the Ore Mountains for the time being stems from the autarchy efforts of the Third Reich and the subsequent SED dictatorship. Between 1937 and 1990, lead, zinc, tin and uranium ores were mined in various places in the Ore Mountains, and the production quantities for all ores exceeded the sum of the previous mining periods. In the case of uranium ores, the Ore Mountains were even the third largest producer in the world (FEDERAL MINISTER OF ECONOMICS 1993).

4.4.2 From AG Wismut to Wismut GmbH

Even before Otto HAHN and Fritz STRASSMANN discovered nuclear fission in December 1938 (KIRCHHEIMER 1978), uranium ores were mined in the Ore Mountains for technical processes and paint production. The main place of discovery for uranium ores was St. Joachimsthal (Jáchimov) in Bohemia. Especially after P. CURIE, M. CURIE and G. BÉMONT found radium in 1898, there was increased uranium ore mining in the Ore Mountains (KIRCHHEIMER 1978). Compared to the quantities that could be sold after 1945 (about 100,000 t of metallic uranium), however, these were small at

about 1000 t (compiled according to KIRCHHEIMER 1978, BÖTTCHER et al. 1991 and SCHIFFNER 1908). In the autumn of 1945, Soviet geologists, supported by Professors Oscar OELSNER and Adolf WATZNAUER OF THE Freiberg Mining Academy (SCHÜTTMANN 1992), explored the potential of the uranium deposits at Sachsenerz-Bergwerks AG, and in the spring of 1946 AG Wismut was founded under the Red Army field number 27304 (BÖTTCHER et al. 1991, KARLSCH 1993). To what extent STALIN was informed about the uranium deposits of the Erzgebirge at Yalta in February 1945 must remain historical speculation for the time being (SCHÜTTMANN 1992, PAUL 1991). However, in view of the extensive literature on Erzgebirge uranium deposits published up to 1945 (KIRCHHEIMER 1978), this possibility should not be neglected. From the American side, the potential of existing uranium ore seems to have been estimated low, as PAUL (1991) tries to deduce. The assumption of KARLSCH (1993), according to which the Americans were "quite aware of the uranium deposits in Saxony and Thuringia", can be refuted by BAIN (1950), who wrote as late as 1950:

"The entire Erzgebirge region had about 1000 tons of recoverable U_3O_8 of industrial grade at the start of mining. Exploitation without regard to cost might raise the amount by 50 percent."

The region around Aue, Schlema, Schneeberg and Johanngeorgenstadt was fundamentally changed by SAG Wismut (Soviet Joint Stock Company Wismut), whose administration had been completely in Soviet hands since 30 May 1947 on the basis of Order 131 of the Soviet military administration (KARLSCH 1993). Shafts were built in the most diverse places, which explored the mountains in Aue and Schlema, initially from the level of the Markus Semmler adit, and from which pitchblende was extracted.

SAG Wismut, a state within a state, was transformed into SDAG Wismut (Soviet-German Joint Stock Company Wismut) on 1 January 1954 and, with a total capital of two billion marks, became the property of the GDR and the USSR in equal parts. There was still the obligation to sell the entire Yellow Cake (ammonium diuranate: $(NH_4)_2U_2O_7$) to the USSR. In addition to uranium mining in the Erzgebirge, mining operations near Dresden, Königstein in Saxon Switzerland and Ronneburg in Thuringia were added in the following years (Fig. 4). In addition, the uranium ore processing plant in Seelingstädt was built in 1960, where about 110 million tonnes of ore were processed until 1991 (WISMUT GMBH 1994b).

For SDAG Wismut's mining operations, the end began on 31 December 1989 (BÖTTCHER et al. 1991), which is reflected in the production figures of Yellow Cake (Fig. 7). In addition to the environmental damage caused by mining, the uneconomically high production costs were responsible for the mines' closure. Whereas in the 1960s they were still 100,-- GDR-mark/kg, they finally reached 350,-- GDR-mark/kg uranium ore (ANONYMOUS 1993).

As a result of German reunification on 3 October 1990, the GDR's shares became the property of the Federal Ministry of Economics. Between 3.10.1990 and 20.12.1991 SDAG Wismut called itself Wismut AG, without any legal basis. On 20 December 1991, SDAG Wismut became Wismut GmbH under the Wismut Act of 17 December 1991. This was preceded by negotiations with the USSR, which led to the signing of the German-Soviet intergovernmental agreement on 16 May 1991 regulating the takeover of the Soviet shares in Wismut by the Federal Republic. In this agreement, the USSR undertook to relinquish its shareholding and in return was released from the obligation to rehabilitate the company.

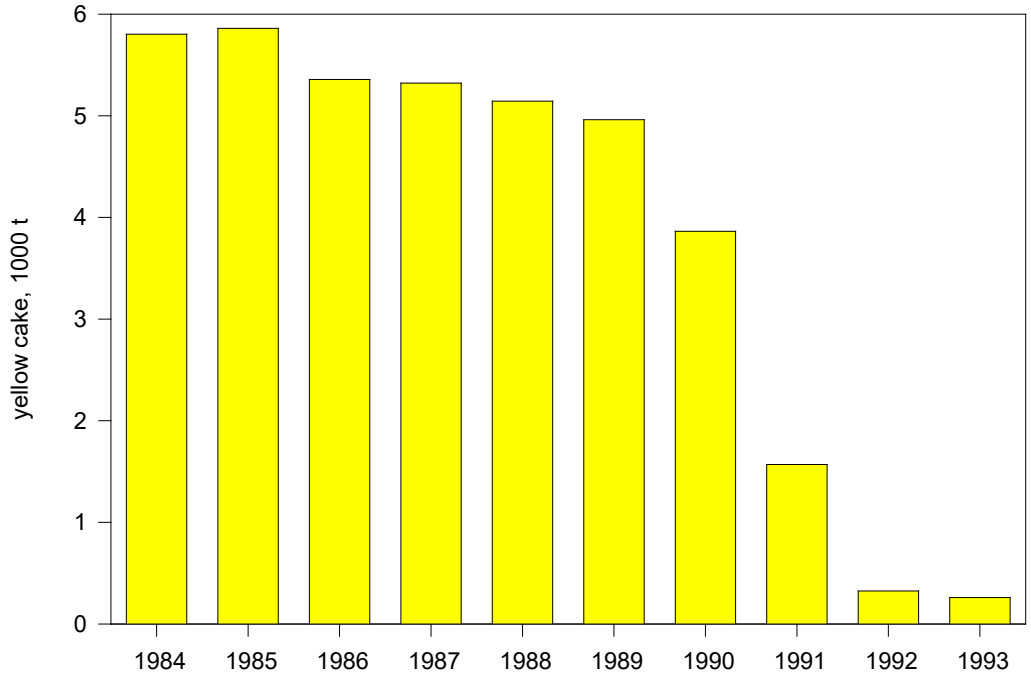

Fig. 7 Annual production of yellow cake by SDAG/GmbH Wismut between 1984 and 1993 (according to AMERICAN BUREAU OF METAL STATISTICS 1994, ANONYMOUS 1993, BARTHEL 1993).

The separation of the secondary operations (Wismut II) from the actual mining operations (Wismut I) represents a temporary conclusion in the development of Wismut. While the former have been operating under the name of DFA (Deutsche Fertigungs- und Anlagenbau GmbH) since 1 January 1992, the mining operations in Ronneburg, Königstein, Aue and Seelingstädt, which were renamed rehabilitation operations, retained the name Wismut GmbH (FEDERAL MINISTER OF ECONOMICS 1993). They have the task of decommissioning all Wismut operations in the long term, keeping them in safekeeping and rehabilitating contaminated sites (FRIEDRICH EBERT FOUNDATION 1992, FEDERAL MINISTER OF ECONOMICS 1992, RUNGE & BÖTTCHER 1994). On 1 January 1994, the Consulting Engineering division was spun off from the DFA and privatised under the name C&E (Consulting & Engineering) (Dr. RUNGE 1995, pers. comm.).

Part of the Aue remediation operation, which also includes the Pöhla-Tellerhäuser deposit, is the Niederschlema/Alberoda uranium deposit, 28 km southwest of Chemnitz'.

4.5 Geological conditions

4.5.1 Regional geological overview

4.5.1.1 Area delimitation

The Erzgebirge (Krušné hory), a pillar plateau in which the Niederschlema/Alberoda deposit is located, belongs to the Saxothuringian basement of the Bohemian Massif (DORN et al. 1992). Together with the Northeast Bavarian basement, the Saxon-Thuringian basement forms the Saxothuringian in the narrower sense. KOSSMAT (1927) defined the term more broadly and included in the Saxothuringian the entire area between the Moldanubian in the south and the Rhenoherzynian in the north. A simplified division divides the Saxothuringian into a synclinal and two anticlinal zones. The former is formed by the Thuringian Trough (Franconian Forest Palaeozoic), the latter includes the Central German Crystalline Threshold (e.g. Odenwald, Spessart) and the Fichtelgebirge-Erzgebirge Anticline.

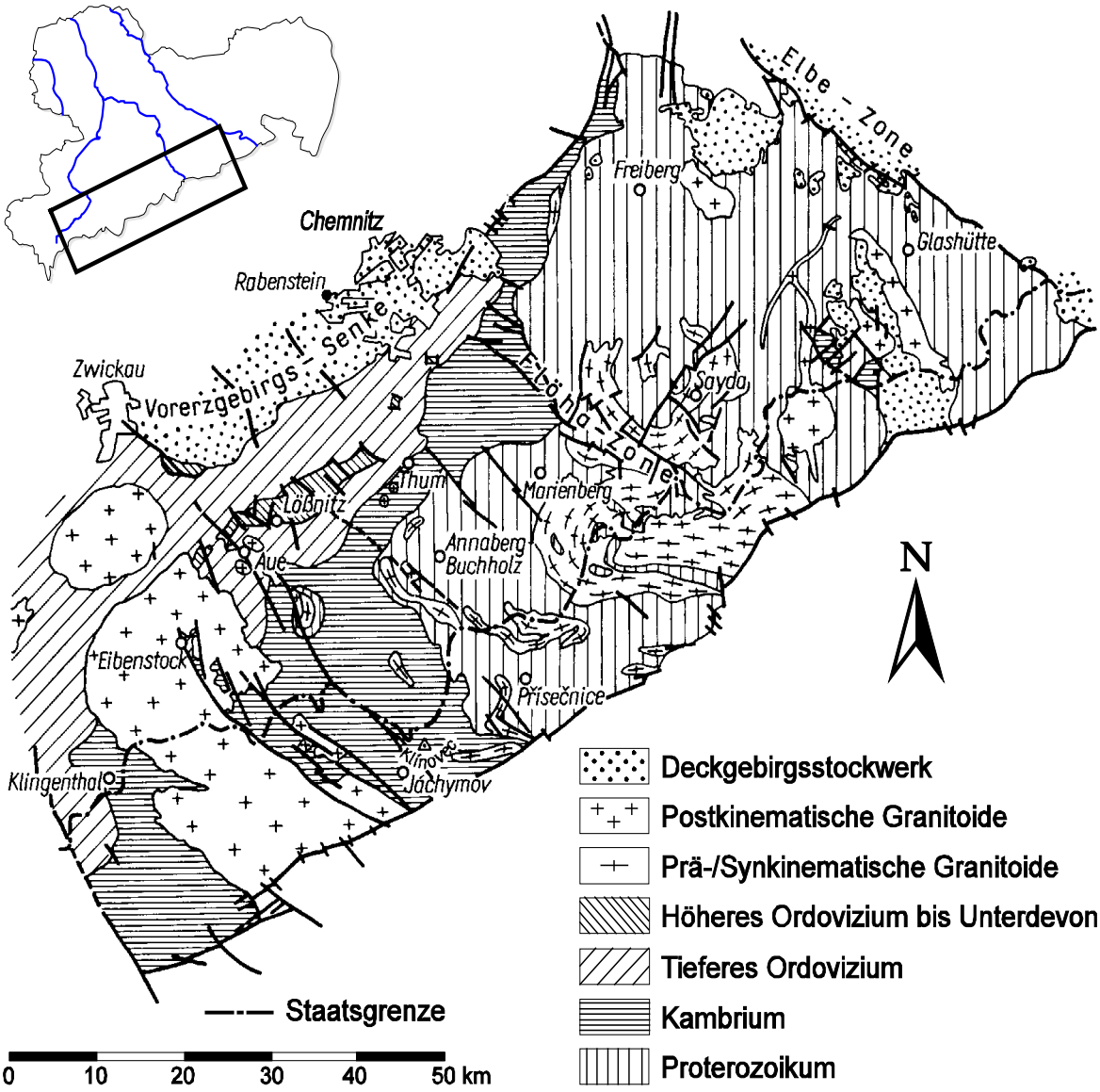

Fig. 8 Structural geological overview map of the Ore Mountains (partly modified from LORENZ & HOTH 1990).

To the northwest the Ore Mountains are bounded by the Variscan Molasse of the Erzgebirge Basin and to the northeast by the Central Saxon Fault (PIETZSCH 1951), which is followed by the western margin of the Elbe Valley Zone and the Saxon Cretaceous Depression (Fig. 8). South-east of the Erzgebirge, separated by the Erzgebirge fault, is the Bohemian Cretaceous Depression with the Tertiary Eger Graben and to the south-west, with a blurred transition, finally the Vogtland (DORN et al. 1992, PIETZSCH 1962). The highest elevations on Bohemian territory are the Keilberg (Klinovec) with 1244 mNN and on Saxonian territory the Fichtelberg with 1214 mNN (PIETZSCH 1962).

The mountains are part of the SW–NE trending Fichtelgebirgs-Erzgebirgs anticlinal zone. There, mesozonal ortho- and paragneisses strike out, interspersed with old and young Variscan granitoids.

A further subdivision is made into the morphologically less strongly divided Osterzgebirge and the more strongly divided Westerzgebirge (HENTSCHEL & SCHEFFLER 1991), the boundary of which is formed by the NNW–SSE running Flöhazone between Deutschneudorf and Flöha.

The lithostratigraphic processing of the Ore Mountains has not yet been completed in detail (LORENZ & HOTH 1990), and thus an overall representation of the processing area on a lithostratigraphic basis is not available. Also the “Grundriß der Geologie der Deutschen Demokratischen Republik” (ZENTRALES GEOLOGISCHES INSTITUT 1968) is based on the outdated lithological division of the Precambrian and Cambrian, therefore the “Grundriß” was only used where it could not be avoided. Nevertheless, in the following an attempt will be made to present the regional geological framework on

a lithostratigraphic basis. For the description of the lithological conditions for the time from the Precambrian to the Ordovician, the work of PIETZSCH (1962) is used, which is complemented by more recent individual presentations (LORENZ & HOTH 1990, LORENZ 1979, HOTH et al. 1979) and reviews (MRNA & SATTRAN 1980, ZENTRALINSTITUT FÜR PHYSIK DER ERDE 1989), among them from the Thuringian area (HOPPE & SEIDEL 1974), into the previously known and named groups and sequences (LORENZ & HOTH 1990).

4.5.1.2 Precambrian

The oldest rocks of the Ore Mountains are exposed in the Osterzgebirge. They are grouped together from the lying to the hanging to form the Osterzgebirgs Group, the Preßnitz Group and the Niederschlag Group (Tab. 4).

The Osterzgebirgs Group begins with biotite-orthoclase-plagioclase gneisses of the Freiberg sequence, followed by the gneisses, mica schists and quartzite of the Brand sequence and the gneisses of the Annaberg-Wegefarth sequence.

Pyrite-bearing metagreywackes, metaconglomerates and metabasites of the Reischdorf sequence as well as partly metavolcanic carbonate skarn horizons and muscovite gneisses of the Kupferberg sequence, both of which belong to the Preßnitz Group, are concordantly adjacent.

For the red gneisses (orthogneisses of granitic to granodioritic composition) in the rocks of the Preßnitz Group, a Prevariscan age is assumed. Presumably, the intrusions, whose main centres were the present-day gneisses of Sayda and Katharinenberg, began at the end of the Precambrian and extended into the Ordovician.

The Niederschlag Group consists largely of metamorphic siltstones and greywackes of the lying Schmiedeberg and hanging Kunnerstein sequence, which are classified in the Wendian (upper late Proterozoic) (HOHL 1985).

4.5.1.3 Cambrian

The Cambrian rocks exposed in the central and western Ore Mountains are divided into three groups: the Keilberg Group (± Lower Cambrian), Joachimsthal Group (± Middle Cambrian) and Thum Group (± Upper Cambrian). Characteristic rocks of the Keilberg Group, which in turn is subdivided into the Raschau-, Obermittweida and Fichtelberg sequences, are carbonate rocks. Included in these are locally varying proportions of quartz and garnet mica schists, which occur together with metagreywackes, metaconglomerates and metabasites. At the base of the Raschau sequence there is a transgression with a gap between the Kunnerstein and Raschau sequences which cannot be determined in detail (HOHL 1985). It possibly indicates a folding and uplift of the Precambrian rocks. The main component of the Fichtelberg sequence is a quartzitic rock sequence.

The Jáchymov Group is divided into the Grießbach and Breitenbrunn sequences. They are characterised by graphite-bearing mica schist horizons, metabasites and carbonate horizons, while quartzites and metagrawackes are clearly less prominent. In addition, branch mica gneisses with feldspar blasts are often intercalated in the aforementioned rocks.

The Thum Group, which is divided into the Herold and Halbmeiler sequences, has a similar rock content. However, it lacks the branch mica gneisses of the Joachimsthal Group. The almost complete absence of Cambrian rocks in the Eastern Erzgebirge is attributed to its threshold position during this time (DORN et al. 1992).

Tab. 4: Lithostratigraphic units of the Erzgebirge. c: Conglomerates, gf: graphite-bearing, gsf: Mica schist, k: Carbonates, mb: Metabasites, mc: metaconglomerates, mg: metagrauwackes, mugn: muscovite gneisses, ogn: orthogneisses, pgn: paragneisses, py: all pyrite-bearing, q: Quartzites (after LORENZ & HOTH 1990, ZENTRALINSTITUT FÜR PHYSIK DER ERDE 1989, LORENZ 1979, HOTH et al. 1979).

Formation	Gruppe	Folge	Gesteine	Mächtigkeit [m]
Ordovizium	Gräfenthal Gruppe	Lederschiefer Hauptquarzit Griffelschiefer	gsf, q	400
	Schwarzburg Gruppe	Phycoden Folge	gsf	300…400
		Frauenbach Folge	gsf, gf, q	300…800
±500 Ma	Thum Gruppe	Halbmeiler Folge	gsf, mb	<100…300
		Herold Folge	gf, gsf, q, mb	100…350
Kambrium	Joachimsthal Gruppe	Breitenbrunn Folge	gsf, q, mb	100…700
		Grießbach Folge	gsf, mugn, gf, ogn	600…1400
	Keilberg Gruppe	Fichtelberg Folge	gsf, q	0…600
		Obermittweida Folge	gsf, pgn, mb, c	150…750
		Raschau Folge	q, gsf, k	150…500
570±20 Ma	Niederschlag Gruppe	Kunnerstein Folge	pgn, mg, c	300…650
		Schmiedeberg Folge	pgn, mb, gsf	
	Preßnitz Gruppe	Kupferberg Folge	gsf, k, mb, ogn, mgn, pgn	300…1000
		Reischdorf Folge	pgn, q, mgn, mb, mc, py	700…1600
Präkambrium	Osterzgebirgs Gruppe	Annaberg-Wegefarth Folge	pgn, mg, mb, gf	800…1900
		Brand Folge	pgn, q, mugn, k, gf	200…600
		Freiberg Folge	pgn, mb, mugn, q	>2500?
1000±50 Ma				

4.5.1.4 Ordovician

At the time of the Ordovician, which begins without a stratigraphic gap to the Cambrian (PIETZSCH 1962), today's Ore Mountains come under the influence of the Thuringian facies (DORN et al. 1992, HOHL 1985). This consists mainly of clastic, terrestrial rocks that were deposited in a basin. Already at the beginning of the century the Ordovician rocks in the Vogtland could be stratigraphically divided (GRAUPNER 1928/29, JAEGER 1959, GAERTNER 1944). Although not all stratigraphic sequences of the Vogtland are present in the Erzgebirge (PIETZSCH 1962), the classification essentially also applies to the Ordovician rocks of the Erzgebirge (BRINKMANN & ZEIL 1986).

The Ordovician begins with the Schwarzburg Group, which consists of phyllites, quartzites and clay schists of the Frauenbach sequence and phyllites and quartzites of the Phycoden sequence. It ends on the slope with the lithostratigraphic strata Griffelschiefer, Hauptquarzit and Lederschiefer of the Gräfenthal Group, which consist of clay shales, quartzites, boulder clay shales and several iron ore horizons.

4.5.1.5 Silurian

In the Silurian, clayey-siliceous sequences were initially deposited, which towards the end (from about the Wenlockian onwards) changed into carbonate-rich sequences with diabases (HOHL 1985). Again, there is a great similarity between the Erzgebirge and the Vogtland conditions (DORN et al. 1992, PIETZSCH 1962). Compared to other European areas where a stratigraphic gap is present between Ordovician and Silurian (BRINKMANN & ZEIL 1986, HOHL 1985), the stratigraphic gaps found in the Vogtland and Erzgebirge can only be proven locally (PIETZSCH 1962). In general, continuous sedimentation from the Ordovician to the Devonian can be assumed for the Ore Mountains (BRINKMANN & ZEIL 1986).

The Silurian is divided into the Lower Graptolite Shales, the Ochre Limestone Group and the Upper Graptolite Shales which lead into the Devonian (PIETZSCH 1962, HOHL 1985). Some authors place the Upper Graptolite Shales completely in the Devonian (DORN et al. 1992, BRINKMANN & ZEIL 1986).

Main distribution area of the Silurian, Upper Ordovician and Devonian rocks is the Lößnitz-Zwönitzer Mulde, a strongly scaled synclinal structure (see chapter 4.5.2.2). There, alum shales, siliceous shales, clay shales and carbonates are found (DORN et al. 1992, PIETZSCH 1962), which were partly called "productive rocks" by Wismut together with the Devonian rocks, since a large part of the mineralisation occurs in them (SDAG WISMUT 1991, Tab. 13).

4.5.1.6 Devon

The Devonian begins concordantly to the Silurian with the Upper Graptolite Shales, whose sedimentation already began in the Upper Pridolian (BRINKMANN & ZEIL 1986, HOHL 1985).

This is followed by the Lower Devonian Tentaculite nodular limestone and the Tentaculite schists with the Nereïtes quartzite (named after Nereïtes, meandering grazing tracks of annelids or gastropods, KRUMBIEGEL & KRUMBIEGEL 1981), whose formation essentially corresponds to those of the Vogtland-Middle Saxon Synclinorium (DORN et al. 1992). On top of this, the Schwärzschiefer (HOHL 1985) OF THE Middle Devonian, resembling the Wissenbach shales of the Rhenoherzynikum, were deposited (PIETZSCH 1962).

In the Upper Devonian, diabase volcanism with shales and iron ores began (Planschwitz stage), the rocks of which are overlain by the cypridine shales and nodular limestones. The volcanism found in large parts of the Saxothuringian can be regarded as the initial volcanism of the Variscan orogeny (PIETZSCH 1962). Furthermore, the facies differentiation that had already begun in the Ordovician continued in the Upper Devonian (BRINKMANN & ZEIL 1986, PIETZSCH 1962), which led to the partial absence of Upper Devonian strata (PIETZSCH 1962). The beginning tectonic movements of the Variscan orogeny (Reussian phase and Breton phase) are also responsible for this absence (PIETZSCH 1962, BRINKMANN & ZEIL 1986).

4.5.1.7 Carbon

In the Lower Carboniferous, the main Variscan phase prevented sedimentation; in part, even existing sediments were eroded. Lower Carboniferous rocks are therefore only present in the Erzgebirge in the keratophyric tuffs near Lößnitz' (PIETZSCH 1962). In the closer vicinity, however, some Lower Carboniferous deposits are known between the northern edge of the Erzgebirge and the Granulitgebirge (strata of Borna-Hainichen, PIETZSCH 1962, HOHL 1985, BRINKMANN & ZEIL 1986), which can be regarded as molasse deposits (DORN et al. 1992).

During the main Variscan folding, acidic magmas rose, the mountain granites (OIC: Older Intrusive Complex) of the Viseum and Namurian (330 … 320 Ma). At the turn of the Westfalian/Stefanian (305 … 295 Ma), the Ore Mountain granites (YIC: Younger Intrusive Complex) intruded. Geochemical investigations in the Bohemian/Czech part of the Ore Mountains have shown that the Ore Mountain granites originate from the same source as the mountain granites (Fig. 9), in part even from the remelting of the mountain granites (STEMPROK 1992). At the same time, rhyolites (quartz porphyry), rhyodacites and granite porphyry were formed (DORN et al. 1992), for example at Schönfeld, Bärenfels, Bärenburg and Altenberg (PIETZSCH 1962). In the wake of the granite intrusions, the older part of the Erzgebirge ore deposits was formed (OELSNER 1958). However, a genetic relationship between the intrusions of the YIC and the uranium mineralisation cannot be deduced (SOKOLOVA & ACHEYEV 1972), as there are about 100 Ma between the age of the mineralisation (LEUTWEIN 1957) and the intrusion.

In contrast to the Osterzgebirge, where erosion has not yet exposed most granite deposits, the granites of the Westerzgebirge are exposed at the surface (DORN et al. 1992). Here as well as there, the deposits can be assigned to the older mountain granites or the younger Erzgebirge granites.

In the Western and Central Ore Mountains, the mountain granites include the porphyritic biotite-monzo granites of Karlsbad and Neudeck in Bohemia as well as Kirchberg, Bergen and Aue in Saxony. In the Eastern Ore Mountains, these include the granites of Tellnitz (Bohemia), Fleyh and Niederbobritzsch.

The Karlsbad Massif and the Eibenstock-Neudeck Massif also contain leucocrate tourmaline monzo granites and syeno granites of the younger Erzgebirge granites. These occur mainly in the granites of Ehrenfriedersdorf in the Middle Ore Mountains and Altenberg, Schellerhau, Zinnwald and Sadisdorf in the Eastern Ore Mountains (DORN et al. 1992, STEMPROK 1992). There, the associated tin-

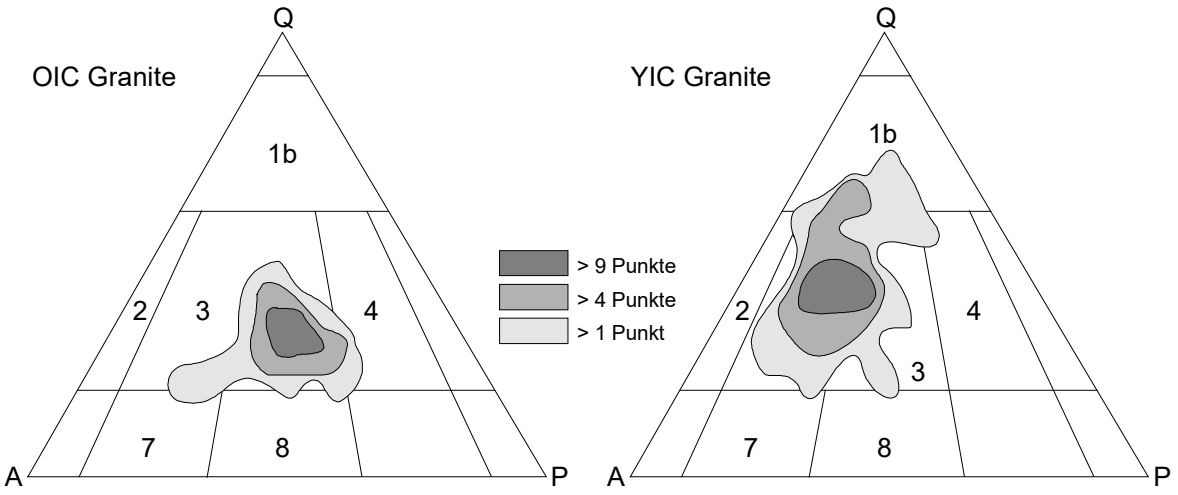

Fig. 9 Modal composition of the OIC granites (n = 33) and YIC granites (n = 87) in the STRECKEISEN diagram. OIC granites fall into the field of monzo granites, YIC granites lie at the boundary of monzo and syeno granites (after STEMPROK 1992). A: alkali feldspar, P: plagioclase, Q: quartz. 1 b: quartz-rich granitoids, 2: alkali feldspar granites, 3: syeno and monzo granites, 4: granodiorites, 7: quartz syenites, 8: quartz monzonites.

tungsten-molybdenum mineralisation had great economic importance (BAUMANN et al. 1979), which, however, dwindled with the political and economic turnaround in 1989/90.

In the vicinity of the granites, the series of the Erzgebirge and Vogtland, which are already present as regional metamorphic rocks, have been contact metamorphically altered and transformed into fruit schists, skarns, hornfels, carbonaceous schists and quartzites.

At the end of the Carboniferous, the Saxothuringian geosynclinal trough of the Variscan era was present as a new continental area. The Ore Mountains were continental and sediment deposition was concentrated in intermontane molasse basins. Erzgebirge (NE–SW) striking large saddles and large troughs with partly intense isoclinal folding and schistosity characterised the newly formed mountain range, which has since been predominantly an ablation area (PIETZSCH 1962).

4.5.1.8 Perm

At the turn of the Carboniferous and Permian periods, sedimentation of intramontane molasse sediments occurred, the remains of which are present today in the Altenberg quarry field and the Flöha transverse zone (DORN et al. 1992). In addition to conglomerates and sandstones, porphyry and coal seams were also found there (PIETZSCH 1962).

4.5.1.9 Jurassic, Chalk

During the Cenomanian and Turonian, marine and non-marine gravels and sands were deposited north and east of Freiberg, which are now diagenetically consolidated (PIETZSCH 1962, DORN et al. 1992). No further substantial sedimentation occurred during the younger Mesozoic (HENNINGSEN & KATZUNG 1992).

4.5.1.10 Tertiary

At the turn of the Oligocene/Miocene, clays, sands and gravels were formed. These sediments are remnants of fluviatile deposits of a northward draining river system of the Tertiary land surface, which were preserved, for example, under the protective basalt cover of the Pöhlberg near Annaberg-Buchholz. Other basalt deposits that formed in the wake of the basalt intrusions of the Duppau Mountains and Bohemian Uplands are found near Oberwiesenthal, near Scheibenberg, Seifen (Bohemia), Geiersberg or Wilisch (PIETZSCH 1962).

In the Lattorfian (Lower Oligocene) a depression begins in Bohemia, in which initially sands (e.g. Old Saddle Sandstone of the Old Saddle Formation between Karlovy Vary and Falkenau), later coals (Chattium: e.g. lignite basins of Saaz, Bilin and Falkenau in Bohemia) are deposited (DORN et al. 1992, PIETZSCH 1962).

The subsidence of the WSW–ENE striking Eger Graben is accompanied by the gradual tilting of the Erzgebirge, in the wake of which the Erzgebirgsabbruch was formed in the Burdigalian (PIETZSCH 1962). At this point, the southeastern floe sank by about 1000 m compared to the northwestern one (DORN et al. 1992). The uplift of the Erzgebirge caused a profound erosion of the high plateau of the Erzgebirge, with partial relief reversal (e.g. Pöhlberg near Annaberg-Buchholz), which is attributed to a previous, deep rock decomposition (PIETZSCH 1962).

4.5.1.11 Quaternary

The Ore Mountains were ice-free during the Quaternary, so that glacial sediments are missing. The ice had its southernmost limit in Saxony during the Mindel Glacial (Elster Glacial), when it penetrated approximately as far as the NE-SW trending line Reichenbach-Chemnitz-Nossen and the NW–SE trending line Nossen-Dresden-Bad Schandau.

One of the few known interglacial deposits dates from the Eemian interglacial and was exposed at the Klösterlein of Aue (“Interglacial of Aue”, PIETZSCH 1962). There BECK & WEBER (1897) described gravel, loam, clay and peat, in which various interglacial plants occurred, but which WOLF (1991)

places in the Brørup interstadial. Loess deposits on the northern edge of the Erzgebirge originate from the Würm glacial (Weichselian cold period).

However, mainly fluviatile sediments were deposited in the river valleys, which can be traced back to the weathering debris of the slopes and consist of loamy gravels, sands and slope debris.

As a consequence of the rising average annual temperatures, raised bogs formed on the clayey weathering layers of the granites and gneisses during the Holocene. Many of these are now destroyed by drainage (PIETZSCH 1962).

4.5.2 Local geological conditions

4.5.2.1 Introduction

Information about SDAG Wismut and areas where uranium ore mining was going on was subject to the strictest secrecy until the political changes in the GDR (SCHÜTTMANN 1992, KARLSCH 1993). This also applied to the geological conditions of the deposit and its surroundings, about which little published material was therefore available until 1989. Many publications contain only hidden references to uranium ore mining in the title (e.g. SHCHUROV & TIMOFEYEV 1966) and localities are often completely missing (e.g. YANISHEVSKY & KONSTANTINOV 1962, HARLASS & SCHÜTZEL 1965).

Regrettably, this secrecy has changed little to this day, a fact criticised in particular by Bundestag members Dr. Uwe JENS on 30 October 1991 and Dr. Klaus-Dieter FEIGE on 12 November 1992 in parliamentary speeches (JENS 1991, FEIGE 1992).

An indication of the strict secrecy to which Wismut was subject may be that in the work “Grundriß der Geologie der Deutschen Demokratischen Republik” (CENTRAL GEOLOGICAL INSTITUTE 1968) under the keyword uranium deposits there is only the following entry: “In Thuringia, uranium deposits are linked to the roughly equivalent clastic sediments in time (Zechstein 1, the author)”. Elsewhere, without an entry in the register, it says that “at greater distances from granite […] hydrothermal apomagmatic deposits [occur], especially lead-zinc-silver veins and uranium veins” (CENTRAL GEOLOGICAL INSTITUTE 1968, p. 255). In the comprehensive work “Geologie von Thüringen” (Geology of Thuringia) there are no references to uranium mining in the vicinity of Ronneburg (HOPPE & SEIDEL 1974).

The geologists of Wismut have left behind a comprehensive, geological work of cracks, which was not completely available for the present work for “reasons of secrecy”. Political and economic reasons only partially enabled the Soviet and German geologists to adapt their detailed mapping to the lithostratigraphic division of the Erzgebirge, which has been known at least since 1964 (LORENZ & HOTH 1990). In the older geological cross-sections of the deposit already published (BÖTTCHER et al. 1991, SCHRÖDER & LIPP 1990A, JANISCHEWSKIJ & KONSTANTINOW 1962, LANGE et al. 1991, BÜDER & SCHUPPAN 1992), the Wismut geologists therefore chose the same signatures for the phyllites of the Frauenbach sequence, for example, as for those of the Phycoden sequence.

In accordance with this fact, the description of the deposits in the present work is therefore mostly based on the lithological designations instead of the lithostratigraphical ones. It must be left to future researchers to process the extensive data on the geological conditions of the Niederschlema/Alberoda deposit in detail according to modern aspects.

4.5.2.2 Environmental geology

The Niederschlema/Alberoda vein deposit, “one of the largest vein deposits in the world” (BARTHEL 1993), is located in the Lößnitz-Zwönitzer-Zwischenmulde, an Erzgebirge (SW-NE) striking fold zone, northwest of the Erzgebirge Central Zone (BÜDER & SCHUPPAN 1992, DORN et al. 1992). There, rocks of the Halbmeiler sequence, the Frauenbach sequence, the Phycoden sequence and the Gräfenthal group of the Ordovician, Silurian and Devonian are exposed (Tab. 5), which were contact metamorphically altered in the area of the post-kinematic granites (DORN et al. 1992, BÜDER & SCHUPPAN 1992, LORENZ & HOTH 1990, LANGE et al. 1991).

The granites interconnected in the subsurface are the mountain granites of Aue, Kirchberg, Oberschlema, Auerhammer and Lauter and – at least in the vicinity of the deposit – the Ore Mountain granite of Eibenstock. Angles of 35 … 45° and northwesterly direction were determined for the dip of the granite surface in the deposit area (LANGE et al. 1991). In the wake of the granite intrusions, aplites and kersantites formed in the vicinity of the deposit, which are younger than the Erzgebirge granites and were formed in the Stefanian (older biotite kersantites) and in the Autunian (younger chlorite kersantites and aplites) (STEMPROK 1992, ZENTRALINSTITUT FÜR PHYSIK DER ERDE 1989). Their occurrence is linked to a tectonic zone of weakness that can be traced to Thuringia and Bohemia (Fig. 10, ZENTRALINSTITUT FÜR PHYSIK DER ERDE 1989), the Gera-Aue-Joachimsthal fault zone (in the Ronneburg area: Nejdeck-Crimmitschau fault; LANGE et al. 1991, BÜDER & SCHUPPAN 1992). The uranium deposits of Ronneburg/Thuringia (MEINEL 1993) and Joachimsthal/Bohemia are also located on this NW-SE striking fault. It continues in the form of the Finne fault through the entire Thuringian Basin to the Sondershausen area on the southern edge of the Harz Mountains (FRANZKE et al. 1992, DORN et al. 1992).

The typical rocks of the deposit are skarns, amphibolite schist, graphite schist, mica schist, metadiabase, kersantite, quartzite, pyroxene feldspar hornfels, limestones, granite, marble and fruit schist (JANISCHEWSKIJ & KONSTANTINOW 1962, SDAG WISMUT 1991, BÜDER & SCHUPPAN 1992). Their percentage distribution is shown in Fig. 11. Some main and trace elements of the most important lithological units can be taken from the table (Tab. 6). These results of ZETZSCHE (1994) ARE based exclusively on rocks from the Niederschlema/Alberoda deposit and are used in the calculations in chapter 8.3 used.

Interestingly, the regional CLARKE values of ZETZSCHE (1994) agree with those of PÄLCHEN et al. (1987) only in the main elements. In the minor elements there are in part substantial differences, which reach a power of ten, for example, in the Sr or Ba content of the phyllites.

The reasons for these differences cannot be definitively determined at this point, but the following causes are conceivable:

- Different area shares of the lithological units by the respective authors
- PÄLCHEN et al. (1987) did not include rocks of the northwestern Lößnitz-Zwönitzer syncline in their calculations
- systematic sampling error and too few analyses in PÄLCHEN et al. (1987)
- The composition of the rocks in the regional units under consideration is different.

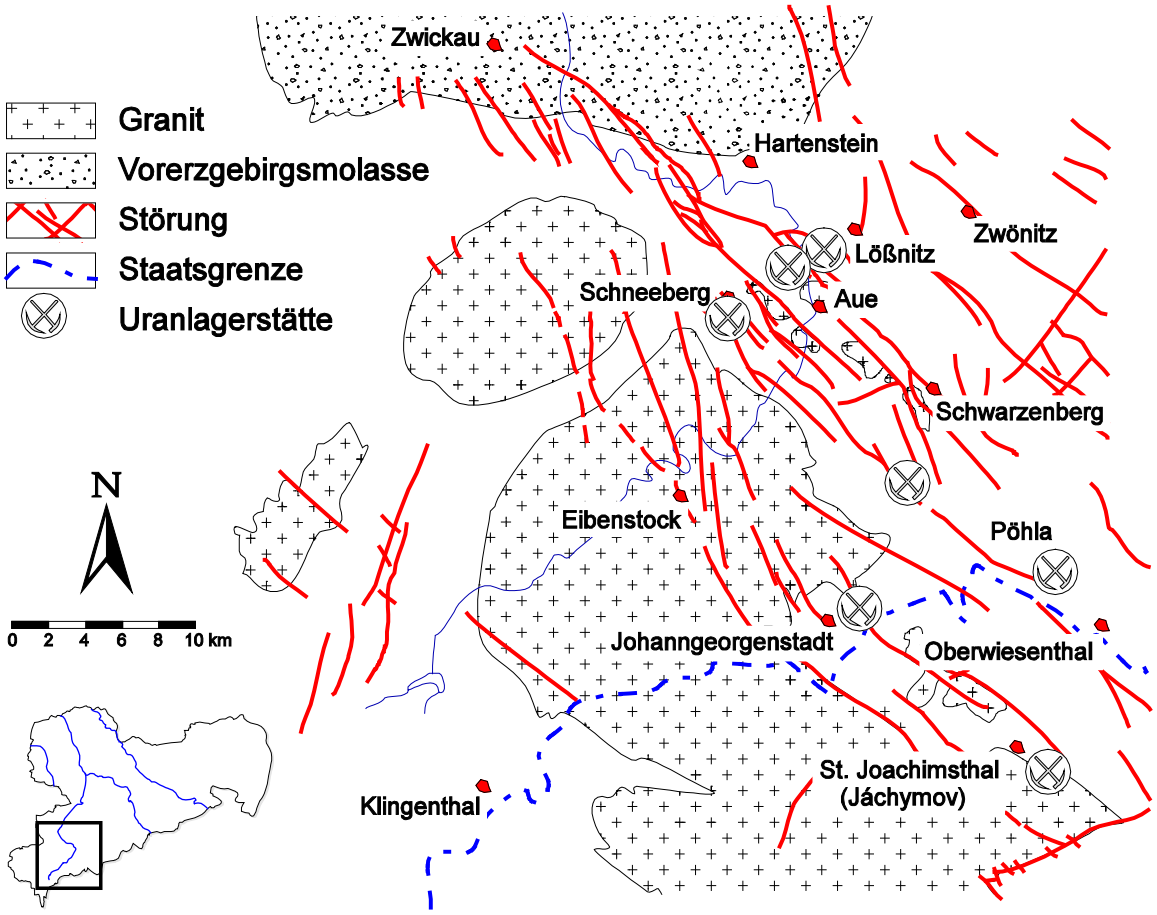

Fig. 10 Simplified tectonic overview map of the Gera-Aue-Joachimsthal fault zone between St. Joachimsthal and Zwickau as well as the Erzgebirge and mountain granites in its vicinity (modified after ZENTRALINSTITUT FÜR PHYSIK DER ERDE 1989, BÜDER & SCHUPPAN 1992).

Tab. 5 Lithostratigraphic profile for the deposits between Schlema and Alberoda (modified after ATSCHEJEW 1967 quoted after BÜDER & SCHUPPAN 1992).

Formation	Thickness	Rocks	Magmatite
Devon	max. 300 m	coarse-grained metadiabase	Granite
		fine-grained metadiabase	Aplite
		banded metadiabase	Biotite kersantite
		Limes	Chlorite kersantite
		Dark slates, fruit slates, mica rocks	
		Scarves (Skarnoids)	
Silurian	80 … 120 m	Alum slate	
		Alum and siliceous slate	
		carboniferous limestones	
		Carbon-bearing dark shales, fruit shales, mica rocks	
Ordovician Gräfenthal Group	150 … 120 m	Dark slates, fruit slates, mica rocks	
		Main quartzite	
		Dark calcareous slates	
Ordovician phycodes sequence	600 … 800 m	Light sericite-muscovite (biotite) schists, fruit schists, mica rocks	
		Quartzite slate	
		Scarves (Skarnoids)	
		fine-grained metadiabase	
		Gabbro-Diabase	

Tab. 6 Main and trace elements of the most important lithological units in the vicinity of the Niederschlema/Alberoda deposit (after ZETZSCHE 1994) as well as the acid production potential, neutralisation potential and net neutralisation potential of the respective rocks. Values marked with * according to WILDNER (1995, pers. comm.), from[+] the formulas 37 to 39. Major elements and pyrite in mass percent, minor elements in ppm, Ra in Bq g^{-1}, APP, NP and Net NP in g kg^{-1} $CaCO_3$. Cd (<1) and W (<10) each below detection limit. ud: homogeneous metadiabas (Upper Devonian), td: banded metadiabas (Upper Devonian), sk: hornfels (contact metamorphite), ks/l: alum and siliceous shales (Lower Graptolite shales, Silurian), ks/k: ochre limestone (Silurian), ds: dark phyllites (Gräfenthal Group), s: Light Phyllites (Phycode sequence), qs: Main Quartzite (Gräfenthal Group), G: Granite, Kb/Kh: Lamprophyre. APP: Acid production potential, NP: Neutralisation potential, Net NP: Net neutralisation potential.

Element	ud	td	sk	ks/l	ks/k	ds	s	qs	G	Kb/Kh
SiO_2	47,10	47,67	64,40	68,05	21,08	57,40	57,00	76,30	70,41	48,70
TiO_2	1,70	2,28	0,67	0,48	0,48	0,95	0,87	0,72	0,03	2,58
Al_2O_3	13,20	13,50	16,90	8,76	6,58	18,85	21,00	10,06	12,66	13,24
Fe_2O_3	3,40	3,25	0,90	1,60	2,45	1,70	1,75	4,98	0,03	2,68
FeO	10,90	8,10	4,60	4,00	3,06	6,45	5,05	4,36	5,30	7,18
MnO	0,18	0,16	0,09	0,08	0,36	0,08	0,11	0,10	0,16	0,21
MgO	5,30	4,30	1,70	1,68	5,70	2,94	2,11	1,30	0,64	4,14
CaO	8,40	11,75	0,59	1,64	28,88	0,95	0,51	0,56	1,28	5,84
NaO_2	3,20	2,25	0,96	0,60	0,30	2,00	1,20	1,94	3,53	3,89
K_2O	1,30	1,90	3,60	2,60	2,85	3,85	4,38	2,31	4,93	3,60
P_2O_5	<0,10	<0,14	10<0	0,60	0,20	.1<0.	1	0,10	0,13	0,73
S(ges)	0,21	0,39	<0.10<0	0,41	0,89	.1<0	.1		0,1* 0,2*	
$S\text{-}SO_4^{2-}$	<0,	10<0,	10<0,	10<0,	1<0,	1<0,	1<0,1			
H_2O	1,40	0,74	1,60	1,44	1,62	2,43	2,30	1,21	1,01	
GV	2,80	1,75	2,70	6,90	27,12	4,20	3,85			
F	0,08	0,11	0,10	0,20	0,12	0,10	0,1			
C(org.)	<0.10<0	0,13	.10<0	4,28	1,04	0,38	.1			
CO_2	0,18	0,34	0,30	0,18	25,25	0,51	0,45	0,38	.3*	6,43
Total	99,40	98,76	99,10	103,50		102,80	101,00	104,30	99,10	100,20
Pyrite	0,3*0	,7*		3*2*0,	3*0,	2*		0,2*0	,3*	
Ag<2<2	1	1	1	1	1	1	1	2		
As	46	23	26	74	44	26	21	22	4	60
B	15	18	14	20	15	12	10			
Ba 100	83	63	90	620	60	45				
Bi<1<1<1<1<1<1 9										
Co	40	51	20	17	17	23	16	7	6	60
Cu	52	48	24	61	61	15	18	15	1	38
Mo<4<4<4<4<4 10		10								
Ni	76	100	31	77	7	44	37	130	3,5	250
Pb	18	18	28	31	31	18	16	8	10	20
Ra<0	.05<0	.05	0,05	0,1	0,11	0,06	0,05		0,12	
Sb<0,		5<0,	5<0,	0,7	0,7	5<0,	5<0,5			
Se<0	.2<0	0,2	.2<0	2,1	2,1	.2<0.	2			
Sn<2<2<2<2<2<2		10,1								
Sr	125	115	33	120	120	42	36			
Th	2	6,1	12	6,8	6,8	15,5	15,5		17	
U<2	4	2,3	7	7	2	2,6		4		
V	89	120	42	165	165	53	27			
Zn	130	132	72	95	145	132	72	24	27	
APP-[+]	6	13	2	53	38	6	3	3	6	
NP-[+]	6	12	11	6	903	18	16	11	230	
Net NP[+]	0	-1	9	-47	865	12	13	-	8	224

JANISCHEWSKIJ & KONSTANTINOW (1962) were able to prove a clear relationship for the uranium mineralisation in the Erzgebirge between the uranium mineralisation and the lithological conditions on the one hand and the mineralisation and the fissure system on the other hand, which is discussed in more detail in the chapter 4.6 (the illustrations in this work leave no doubt that JANISCHEWSKIJ describes the Niederschlema/Alberoda deposit).

Apart from some gangue rocks and granites, all rocks are strongly isoclinally folded and tectonically interlayered. Fold axes and bedding planes strike ENE–WSW in the majority of the deposit area, in the southwestern part also N–S in isolated cases. The strata dip at 40 … 50° to the NW, accordingly the folds have a SE vergence (SCHRÖDER & LIPP 1990a, LANGE et al. 1991).

The controlling element for the deposit is the Gera-Aue-Joachimsthal fault zone. In its wake, NW–SE and NNE–SSW striking fault systems formed (ZENTRALINSTITUT FÜR PHYSIK DER ERDE 1989), to which the most important fault of the deposit also belongs: the *Roter Kamm* (red ridge). It separates the two granites of Oberschlema and Auerhammer (PIETZSCH 1962) from the rocks of the Halbmeiler, Frauenbach and Phycoden sequence and the Gräfenthal group, which adjoin to the northeast. In the Oberschlema granite area, the Roter Kamm was called the Gleesberg Wing, which are the only two historical vein names adopted by the Wismut miners (BÖTTCHER et al. 1991).

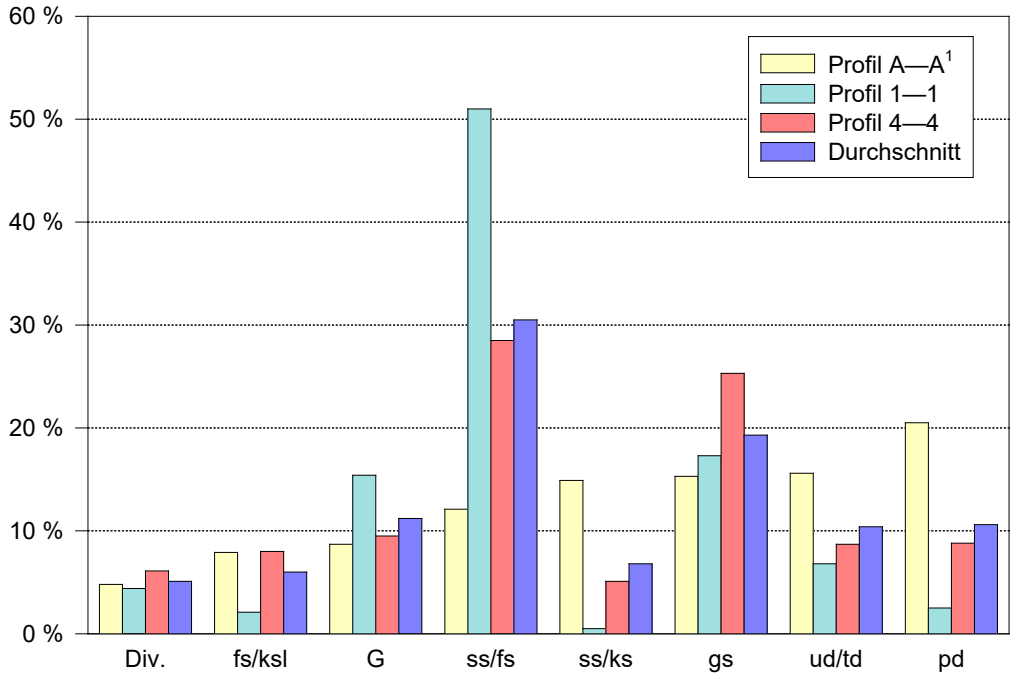

Fig. 11: Percentage distribution of rocks in the Niederschlema/Alberoda deposit based on geological maps and rock designations of Wismut GmbH. Div. (sk; A; Kb; Kh; qs; ks/l; ud): skarns, aplites, biotite kersantite, chlorite kersantite, quartzite schist, siliceous schist, fine-grained metadiabase; fs/ksl: fruit schist with siliceous schist layers; G: Granite; ss/fs: phyllite, light-coloured fruit schists; ss/ks: carbonaceous, dark phyllite; gs: light-coloured mica felses; ud/td: fine-grained and banded metadiabase; pd: coarse-grained metadiabase; Tab. 5. designations of the profiles correspond to the designation method of SDAG/GmbH Wismut, from which the deposit was usually represented in two longitudinal profiles (A-A¹, B-B¹) in SW–NE direction and eight transverse profiles (1-1 … 8-8) in NNW–SSE direction.

Tab. 7 Characterisation of the veins in the Schlema area (after BÜDER & SCHUPPAN 1992). Signatures indicate the intensity of uranium mineralisation. –: none, +: little, ++: much, +++: very much.

Direction of strike	Direction of incidence	Examples	Uranium ore
WSW–ENE	NNW	Union, Gera, Erna	++
WNW–ESE	±vertical	Bad Elster	+
NW–SE	S	Roter Kamm, Ruhmvoll, Schwerin, Beryll	+++
NE–SWN	W	Morgengänge in Oberschlema	–

The Roter Kamm also separates the historic silver ore deposit of Schneeberg-Neustädtel, whose deposits were exhausted in the 16th century (BÖTTCHER et al. 1991), and the uranium deposits of Niederschlema/Alberoda and Oberschlema. The fault zone, which is up to 10 metres thick, takes its name from iron and manganese oxides, which occur together with quartz, barite and fluorite of the eba formation (BAUMANN 1968) in the fault breccias and veins. The 5600 m long (SCHIFFNER et al. 1911) Roter Kamm dips at a jump height of 400 … 500 m (GENSER 1932) with 60 … 65° in northeast direction and strikes NW-SE. In the east, the deposit is also bounded by a fault zone, the NE-SW trending Affalter fault (SCHRÖDER & LIPP 1990a).

Historical maps of the area around Aue show ore veins which, in addition to the aforementioned directions, can also have a strike in ENE-WSW (“Geognostische Übersichtskarte des Erzdistricts von Schneeberg” in HAMANN & HAMANN 1990).

The ore mining in Niederschlema/Alberoda has opened up almost 200 veins of varying importance for uranium extraction (BÖTTCHER et al. 1991, BÜDER & SCHUPPAN 1992, JANISCHEWSKIJ & KONSTANTINOW 1962). Since not all of these veins strike above ground, further strike directions of the veins could only be determined by mining (Tab. 7). Not only the direction of strike, but also the intersection of the veins to form so-called ore nodes played a role in mining, which will be discussed in more detail in chapter 4.6.3 (JANISCHEWSKIJ & KONSTANTINOW 1962, BÜDER & SCHUPPAN 1992).

4.6 Properties of the deposit

4.6.1 Classifications

In the course of its history, 21 deposits were mined by Wismut in Saxony and Thuringia (Fig. 4), which can be assigned to five different deposit types (LANGE et al. 1991, FEDERAL MINISTER OF ECONOMICS 1993, MÜHLSTEDT 1992). Each of these deposits partly consists of further deposit parts (Tab. 8), the Ronneburg ore field, for example, consists of five mines.

Until the end of 1990, the GDR and the Federal Republic of Germany (220 kt of uranium metal) were among the three largest uranium producers in the world after the United States of America (334 kt of uranium metal) and Canada (240 kt of uranium metal) (FEDERAL MINISTER OF ECONOMICS 1993; FOR THE reasons for the contradiction with the data in the Tab. 8, see the legend there). However, this only takes into account the Saxon-Thuringian uranium ores that were mined after 1945. Between the first uranium mining in Saxony in 1825 (KIRCHHEIMER 1978) and 1945, a further 1000 t of uranium ore were mined (BAIN 1950).

DAHLKAMP (1993) places the uranium deposits of the Ore Mountains (“Schlema” in Tab. 8) in Type 3 (“Vein”) of his extensive classification (Tab. 9). He distinguishes a total of 15 types with 30 subtypes, of which type 3 is described as follows:

Tab. 8 Types of deposits and their mined ore reserves in Saxony and Thuringia (supplemented after MÜHLSTEDT 1992, FEDERAL MINISTER OF ECONOMICS 1993, BÖTTCHER et al. 1991). BÜDER & SCHUPPAN (1992) deviate from this and state 73 kt uranium for Niederschlema/Alberoda. It is possible that the data from BÜDER & SCHUPPAN (1992) REFER TO uranium metal, while the 248 kt in the table apply to yellow cake. BARTHEL (1993) assumes the cause of the differing mining figures to be different extraction and mining losses.

Wismuth type	Type DAHLKAMP	Characterisation	Deposits	UO_2 production
Ronneburg	16	Lenticular and stockwork deposits in Palaeozoic shales, limestones and diabases	Schmirchau, Reust, Paitzdorf, Beerwalde, Drosen, Dittrichshütte, Lichtenberg, Stolzenberg	111 kt
Schlema	3.1.2.2	hydrothermal vein deposits	Niederschlema/Alberoda	81 kt
			Tellerhäuser, Oberschlema, “Weißer Hirsch", Johangeorgenstadt, Antonsthal, Seiffenbach, Zobes, Bärenstein, Schneckenstein, Marienberg, Schneeberg, Pöhla, Geyer	21 kt
Königstein	4.1.1	Cretaceous sandstone deposits	Königstein, Pirna, Thürmsdorf, Rosenthal	19 kt
Culmitzsch	–	Seam-like deposits in calcareous-clayey sediments of the Zechstein	Culmitzsch, Sorge, Gauern	12 kt
Freital	14.1	uraniferous coal seams of the Rotliegendes	Heidenschanze, Bannewitz-Gittersee	4 kt
			Total	248 kt

Tab. 9 Classification of the Niederschlema/Alberoda deposit in the worldwide classification of uranium deposits according to DAHLKAMP (1993).

Type	Subtype	Class	Subclass	Designation	Characterisation	Example
3				Vein		
	3.1			Granite-related		
		3.1.2		Perigranitic		
			3.1.2.2	In metasediments, polymetallic	Ore Mountains	St. Joachimsthal, Karlsbad, Alberoda-Niederschlema, Pöhla-Tellerhäuser, Schneeberg, Johangeorgenstadt, Wittichen/ Black Forest

“Vein deposits consist of uranium mineralization in lenses or sheets or disseminations filling joints, fissures, breccias and stockworks in deformed and fractured rocks. Size and complexity of vein sets are variable. Distribution and intensity of mineralization are irregular. Principal uranium phases are pitchblende, uraninite, and coffinite. Gangue minerals are always present. Uranium may form monometallic mineralizations or polymetallic mineralizations. Associated metals include Co, Ni, Bi, Ag, Cu, Pb, Zn, Mo and/or Fe in the form of sulfides, arsenides or sulfarsenides. Wall rock alteration is commonly restricted to a narrow margin (<1 m)”.

Independently of the uranium deposit classification, there are further subdivisions in the Ore Mountains. VON CHARPENTIER (1778) and WERNER (1791) published the first systematic presentation of the mineral associations (“parageneses” after BREITHAUPT 1849) of the Ore Mountains (BAUMANN 1968). While WERNER had eleven “Gangerz formations” (quoted from BAUMANN 1968), today eight to ten mineral assemblages are distinguished on the basis of the mineralogical-paragenetic model (Tab. 10, BAUMANN 1968, Baumann 1992, Baumann 1994).

In addition, there are two further classifications in the Ore Mountains, which are based on the one hand on the morpho-structural position of the deposit and on the other hand on metallogenesis. The latter distinguishes thirteen different ore associations in the Ore Mountains (ZENTRALINSTITUT FÜR PHYSIK DER ERDE 1989), in which the Niederschlema/Alberoda deposit belongs to type X, "polymetallic association of the Younger Intrusive Complex (YIC), melanocrater type 1" (TISCHENDORF 1986).

No attempt will be made to adapt the paragenetic classification of Wismut according to BAUMANN (1967) to the metallogenetic one. Both have advantages, the latter above all that of establishing an age-related relationship between tectonic processes and the formation of deposits.

Since the paragenetic classification has already been used as a basis in other works on the uranium deposits of the Erzgebirge (HARLASS & SCHÜTZEL 1965, LEUTWEIN 1957, OELSNER 1951, JANISCHEWSKIJ & KONSTANTINOW 1962, SCHUPPAN et al. 1994), the same procedure will be followed here. Although BAUMANN has recently adapted his older classification to today's knowledge, the terms of his classification from 1967 (BAUMANN 1967) are used in this work, as the new terms have not yet become generally accepted.

Tab. 10 The ore formations of the Ore Mountains (BAUMANN 1968, ZENTRALINSTITUT FÜR PHYSIK DER ERDE 1989, HARLASS & SCHÜTZEL 1965, OELSNER 1958, BAUMANN 1992). For the problem of the eba formation see HARLASS & SCHÜTZEL (1965). In the sense of BAUMANN (1968, 1992) it is placed chronologically behind the uqk and eb Formation and is not to be regarded as the primary ore source in the sense of LEUTWEIN (1957). The grey shading of the bars indicates the relative abundance of the respective element. ags: silver sulfide, bafl: Baryte fluorite, BiCoNi: Bismuth cobalt nickel, BiCoNiAg: Bismuth cobalt nickel silver, dse: Dolomite-selenide, eb: Noble brown spar formation, eba: Iron baryte, fba: Fluorobaryte lead ore formation, flq: Fluorite-quartz, hmba: Hematite-baryte, kb: Gravelly-blende formation, kku: Comb quartz-calcite-uraninite, krsb: Carbonates-antimonides, krsf: Carbonates-sulfides, mgu: magnesium-carbonate-pechblende, polymetall.: polymetallic, qas: quartz-arsenides, qhm: quartz-hematite, qks/w: quartz-cassiterite/wolframite, qsf: Quartz-fluorite, rearrangement: rearrangements, uqk: uranium-quartz-calcite, W-Mo: tungsten-molybdenite. All designations are to be followed by the word "formation". As … Zn: Element symbols.

Formation	Gruppe	Folge	Gesteine	Mächtigkeit [m]
Ordovizium	Gräfenthal Gruppe	Lederschiefer Hauptquarzit Griffelschiefer	gsf, q	400
	Schwarzburg Gruppe	Phycoden Folge	gsf	300…400
		Frauenbach Folge	gsf, gf, q	300…800
±500 Ma	Thum Gruppe	Halbmeiler Folge	gsf, mb	<100…300
		Herold Folge	gf, gsf, q, mb	100…350
Kambrium	Joachimsthal Gruppe	Breitenbrunn Folge	gsf, q, mb	100…700
		Grießbach Folge	gsf, mugn, gf, ogn	600…1400
	Keilberg Gruppe	Fichtelberg Folge	gsf, q	0…600
		Obermittweida Folge	gsf, pgn, mb, c	150…750
		Raschau Folge	q, gsf, k	150…500
570±20 Ma	Niederschlag Gruppe	Kunnerstein Folge	pgn, mg, c	300…650
		Schmiedeberg Folge	pgn, mb, gsf	

4.6.2 Parageneses

4.6.2.1 Uranium

Apart from the Fe-Mn formation, which is present only marginally, at the “Roter Kamm” (BÜDER & SCHUPPAN 1992), all parageneses shown in Tab. 10 occur in the Niederschlema/Alberoda deposit (SDAG WISMUT 1991). Only the kku and mgu (in the Osterzgebirge: dse) formations were of economic importance for uranium production (SDAG WISMUT 1991, HARLASS & SCHÜTZEL 1965), for which formation ages of 280 … 220 Ma and 160 … 140 Ma, respectively, can be given in agreement on the basis of the determinations of LEUTWEIN (1957) and SHUKOLYUKOV et al. (1990, there uqk and eb formation). The average age of 50 pitchblende, mainly of the kku formation, in Niederschlema/Alberoda was determined to be 160 Ma by the Xe-Xe_{sn} method (SHUKOLYUKOV et al. 1994), with maxima at 153 Ma, 175 Ma, 197 Ma, 242 Ma and 270 Ma (BASAROWITSCH 1992, SHUKOLYUKOV et al. 1992).

According to LEUTWEIN (1957) (there eba Formation; he uses an older classification of the Erzgebirge formations, in which an eba Formation followed chronologically behind the kb Formation), only the kku and mgu Formation represent a uranium ore formation in the genetic sense, whereby, as HARLASS & SCHÜTZEL (1965) state, the kku Formation “would have to be regarded as the actual primary uranium formation in the narrowest sense”. According to the former, the uranium minerals in the younger formations are merely mobilisates from the kku and mgu formations.

During uranium mining, clear telescoping was often observed in the veins and fissures, and especially when approaching the Auer Granite, two to three formations occur in one vein (SDAG WISMUT 1991). The two main formations can be easily divided by their different carbonates. While calcite ($CaCO_3$) predominates in the kku formation, dolomite ($CaMg[CO_3]_2$) characterises the mgu formation.

The main uranium ore of the deposit, uraninite (pitchblende, UO_2), occurs in the veins of the kku formation as a kidney-shaped, X-ray crystalline mass (LEUTWEIN 1957, JANISCHEWSKIJ & KONSTANTINOW 1962), which indicates that it was precipitated as a gel at low temperatures (HARLASS & SCHÜTZEL 1965). THOMAS (1982, quoted from CENTRAL INSTITUTE OF EARTH PHYSICS 1989) determined homogenisation temperatures of 305 24± °C for the quartz of the kku (uqk) Formation from fluid inclusions, indicating catathermal formation. For the pitchblende itself, formation temperatures of 80 … 180 °C are given (HARLASS & SCHÜTZEL 1965), i.e. epithermal conditions. Coffinite ($U[SiO_4]$) was precipitated as another uranium mineral in the mgu formation. In the accessory rocks, the uranium content is relatively low and amounts to $2 \cdot 10^{-4}$ … $7 \cdot 10^{-4}$ mass percent (ZETZSCHE 1994, Tab. 6).

TISCHENDORF & UNGETHÜM (1968) made some investigations on the Eh-pH-ratios during the formation of these main uranium ore formations. From this it can be deduced that for the kku and mgu formations Eh values of –100 … –300 mV and pH values of 6 … 8 must have prevailed (Fig. 12).

Uraninite, which never occurs in nature in its ideal composition (DYBEK 1962), transforms during the weathering process into a mixture of the most diverse secondary minerals, which occur both in the mine workings and in the weathering zone of the deposit (Chapter 4.9). These include the less soluble uranyl silicates such as uranophane ($CaH_2[UO_2|SiO_4]_2 \cdot 5H_2O$) and the more soluble uranyl hydroxides called gummite (Tab. 11). This transformation (oxidation and hydration) product of uraninite is rubbery in character and consists essentially of minerals of the becquerelite-fourmarierite group (STRUNZ 1982). At the level of the Markus Semmler gallery, secondary minerals with which the water was in contact led to the high radioactivity of the radon waters of the former Oberschlema spa (Tab. 15, GENSER 1932), which was completely destroyed by the Wismut mining.

4.6.2.2 Arsenic

Arsenic occurs in the form of cobalt and nickel arsenides, more rarely as native arsenic, in the BiCoNi and ags formations. While the co-arsenides in the BiCoNi formation occur mainly together with native bismuth, the ni-arsenides can mostly be observed together with native silver (OELSNER 1958). The

most important arsenic mineral is löllingite ($FeAs_2$), but other arsenic compounds also occur (Tab. 12, OELSNER 1958, BAUMANN 1968, JANISCHEWSKIJ & KONSTANTINOW 1962).

According to Wismut's documents (SDAG WISMUT 1991), the proportion of arsenic compounds in the ore veins increased from the upper levels to the lower ones. Below level -990, 0.06 … 0.55 % arsenic by mass is given for the -ore and 0.07 % arsenic by mass for the waste rock, while the figure for waste rock is 0.002 … 0.007 % (Table 6).

Name	Formula	Described
Becquerelite	$6[UO_2(OH)_2]$-$Ca(OH_2)$-$4HO_2$	X
Billietit	$6[UO_2(OH)_2]$-$Ba(OH_2)$-$4HO_2$	
Clarkeit	$NaUO_{227}$	
Curit	$3PbO$-$8UO$-$4HO_{32}$	X
Fourmarierite	$8[UO_2(OH)_2]$-$2Pb(OH_2)$-$4HO_2$	X
Ianthinite	$[UO_2(OH)_2]$	
Masuyit	$[UO_2(OH)_2]$-HO_2	
Schoepit	$[UO_2(OH)_2]$-HO_2	
Uranosphaerite	$[UO_2(OH)_2$|BiOOH]	
Vandenbrandeit	$6[UO_2(OH)_2]$-$Cu(OH)_2$	
Vandendriesscheit	$8[UO_2(OH)_2]$-$Pb(OH_2)$-$4HO_2$	
Wölsendorfite	$6[UO_2(OH)_2]$-$3(Pb,Ca)O$	

Tab. 11: Compilation of the most important gummite-forming uranium minerals in which uranium is present in oxidation state VI (after DYBEK 1962 and STRUNZ 1982). The last column indicates whether the mineral has already been described for the Niederschlema/Alberoda deposit.

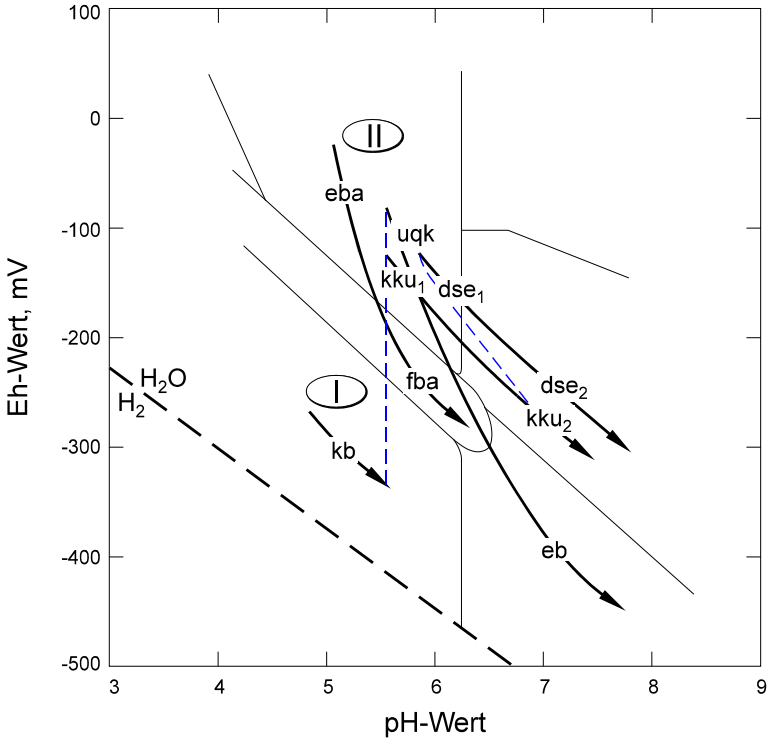

Fig. 12 Schematic representation of the Eh-pH ratios during the formation of the main ore formations (cycle I, II) for 100 °C, 203 kPa (modified after TISCHENDORF & UNGETHÜM 1968).

A special feature of the Niederschlema/Alberoda deposit is an unusually high As enrichment, which -was encountered between the levels -1305 and -1710 in the lying of a fault zone ("Union") ("ore node 191"). The grades there of 3.8 … 5.0 mass percent in the ore and 0.9 … 1.6 mass percent in the surrounding rock cannot be -regarded as representative for the entire area below level -1305.

The majority of all arsenic minerals in the BiCoNi Formation were first precipitated from the colloidal hydrothermal solution as a gel, which underwent collection crystallisation in a subsequent process. In the ags formation, since sufficient S^{2-} ions were available, sulfarsenides were formed from the molecular hydrothermal solution (HARLASS & SCHÜTZEL 1965).

4.6.2.3 Other element enrichments

In accordance with the character of a polymetallic deposit, further metal compounds occur in the vein mineralisations. These are, in order of atomic number, mainly manganese, iron, cobalt, nickel, copper, zinc, germanium, selenium, molybdenum, silver, indium, tin, antimony, thallium, lead and bismuth in varying concentrations (ZENTRALINSTITUT FÜR PHYSIK DER ERDE 1989). Average contents of some of these elements in the country rock are listed in the table (Tab. 6).

Tab. 61 gives an overview of which minerals have been described so far from Niederschlema/Alberoda. It has to be emphasised that in the kku-, mgu-, biconi- and ags-formation carbonates occur as gangue, whereby mainly calcite, dolomite and siderite are present. Pyrite and other sulfides occur in the Sn-W, mgu and biconi formations, but mostly in small amounts, which overall are probably lower than those in the rocks.

A special feature of the Erzgebirge is the selenium mineralisation of the mgu formation. Besides the insignificant precipitation of sulfides, such as galenite (PbS) and chalcopyrite ($CuFeS_2$), mainly selenides were formed, (e.g. clausthalite (PbSe)), which were occasionally extracted as ore (HARLASS & SCHÜTZEL 1965).

Tab. 12 Common (*italics*) and rare minerals from Niederschlema/Alberoda with arsenic as a formula component (after SCHRÖDER & LIPP 1990b and J. MEYER, pers. comm.).

Name	Formula	Name	Formula
Allemontite	Sb-As	Para-Rammelsbergite	$NiAs_2$
Annabergite	$Ni_3[As_2O_4]\cdot 8HO_2$	***Pharmacolite***	$CaH[AsO_4]\cdot 2H_2O$
Arsenic	As	Proustite	$AgAs_3S_3$
Arsenolamprit	*α*-As	***Rammelsbergite***	$NiAs_2$
Arsenolite	As_2O_3	Realgar	As_4S_4
Arsenopyrite	FeAsS	Rößlerit	$MgH[AsO_4]\cdot 7H_2O$
Atelestite	$Bi_2[O\|OH\|AsO_4$	***Safflorite***	$CoAs_2$
Auripigment	As_2S_3	Scorodite	$Fe^{3+}[AsO_4]\cdot 8H_2O$
Chloantite	$NiAs_3$	Skutterudit	$CoAs_3$
Cobaltin	CoAsS	***Symplesite***	$Fe_3^{2+}[AsO_{42}]\cdot 8H_2O$
Erythrin	$Co_3[As_2O_4]\cdot 8HO_2$	Tennantite	$Cu_3AsS_{3.25}$
Lautit	CuAsS	Uranospinite	$Ca[UO_2\|AsO_4]_2\cdot 10H_2O$
Löllingite	$FeAs_2$	***Weilit***	$CaH[AsO]_4$
Luzonite	Cu_3AsS_4	Xanthokon	Ag_3AsS_3
Maucherite	$Ni_{<3}As_2$	Zeunerit	$Cu[UO_2\|AsO_4]_2\cdot 10(16–10)H_2O$
Nickelin	NiAs		

4.6.3 Controlling factors of mineralisation

Within the Niederschlema/Alberoda mine, the occurrence of uranium mineralisation is linked to certain lithological and tectonic factors. One of the characteristics is that the mineralisation regularly declines when approaching the Auer granite (LANGE et al. 1991). Although there is a spatial relationship between the mineralisation and the granites of the Younger Intrusive Complex, a genetic relationship cannot be deduced (SOKOLOVA & ACHEYEV 1972), if only because of the different formation ages (SHUKOLYUKOV et al. 1990, LEUTWEIN 1957). The presentation of BÜDER & SCHUPPAN (1992), according to which the granite intrusion was followed by hydrothermal solutions, cannot be correct in its genetic-temporal sequence.

In principle, the rocks of the Niederschlema/Alberoda deposit are divided into productive and non-productive ones (JANISCHEWSKIJ & KONSTANTINOW 1962, SDAG WISMUT 1991, LANGE et al. 1991), whereby the productive rocks contained 95 % … 96 % of the uranium mineralisation (SOKOLOVA & ACHEYEV 1972, LANGE et al. 1991). During the transition from productive to unproductive rocks, it was often observed that the paragenesis of the veins changed. While in the former ore minerals and gangue minerals occur together, in the latter only 5 … 6 gangue minerals are present (JANISCHEWSKIJ

& KONSTANTINOW 1962). As various investigations show, ore enrichment was observed especially in the contact metamorphically altered rocks (JANISCHEWSKIJ & KONSTANTINOW 1962, SOKOLOVA & ACHEYEV 1972). The views on which rocks are to be described as productive differ between the individual authors, and are sometimes even contradictory (Tab. 13). From the table it can be deduced that the change in the chemical properties of the rock led to the precipitation of pitchblende from the hydrothermal colloid (Fig. 13). A dependence on the pyrite content of the rock was only observed by JANISCHEWSKIJ & KONSTANTINOW (1962).

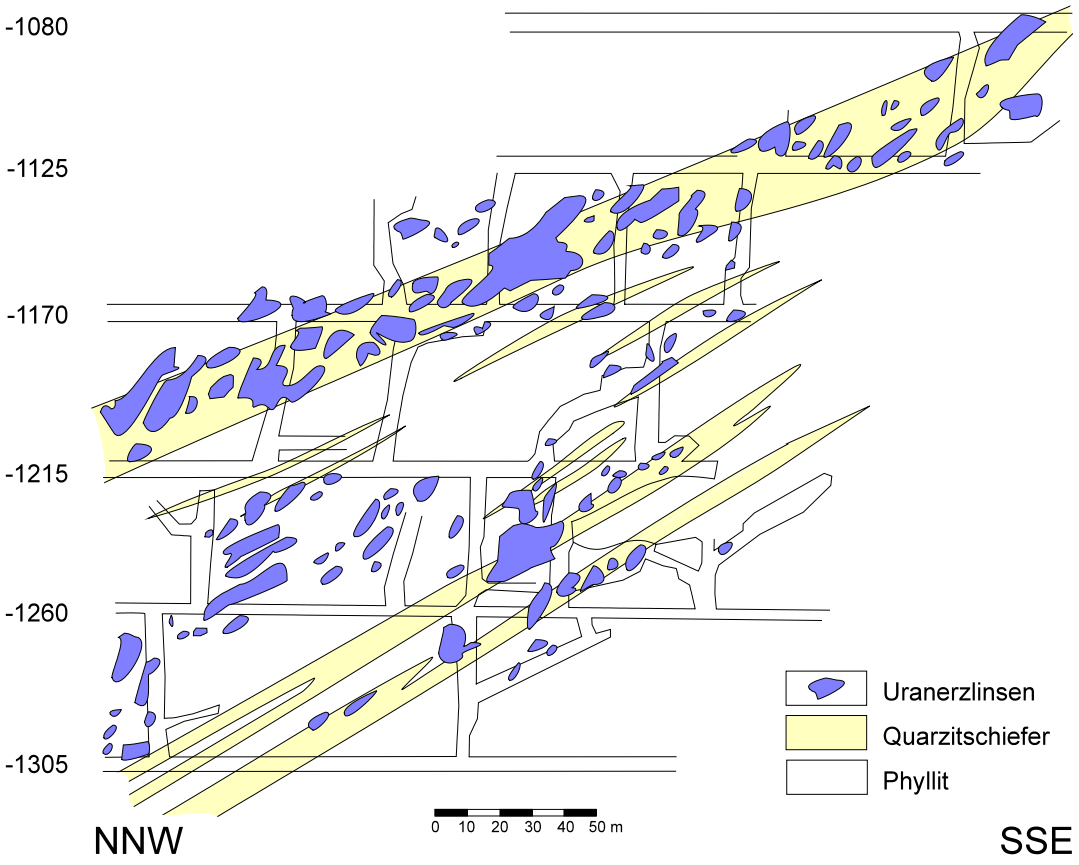

Fig. 13 Dependence of uranium mineralisation on lithology change. Shown is a outline of the “Beryll” vein at the level of levels –1080 to –1305 (modified after BÜDER & SCHUPPAN 1992).

Tab. 13 Productive rocks of the Niederschlema/Alberoda deposit according to various authors (SOKOLOVA & ACHEYEV 1972, SDAG WISMUT 1991, JANISCHEWSKIJ & KONSTANTINOW 1962, LANGE et al. 1991, SCHTSCHUROW & TIMOFEJEW 1966).

SOKOLOVA	Wismut	YANISHEVSKY	LONG	SHCHUROV
Basic and intermediate rocks	Amphibolite	Amphibolite slate (pyritised)	Amphybolite	Change of physico-chemical properties
Green albite-chlorite-limestone-silicate schists	Siliceous slate	Skarns (pyritised)	Lydite	Amphibolite
Albite-chlorite-limestone-silicate schist with carbonates, limestone, diabase and tuff	Alum slate	pyritised mica schists	Ribbon slate	Skarne
	carbon-bearing shales	Graphite slate (pyritised)	Carboniferous mica schists	
	Carbon-bearing phyllites			
	metamorphic diabase			

Besides lithological factors, tectonic factors are responsible for mineralisation. There is general agreement that apophyses and pinnae, if they are in contact with the main vein, are favourable for ore conduction (SHCHUROV & TIMOFEYEV 1966, YANISHEVSKY & KONSTANTINOV 1962). In addition, especially below the –990 level, intersections of dykes (“ore nodes”) have been shown to be ore enrichments (LANGE et al. 1991).

JANISCHEWSKIJ & KONSTANTINOW (1962) have compiled which vein types in the productive rocks are involved in ore conduction and in what proportion:

Apophyses	29 %
Aisle crosses	20 %
Gang aggradation	17 %
Diagonal trunks	16 %
multiple complicated veins	8 %
Flat incident faults	6 %
Simple veins	4 %

Particularly rich ore deposits are found where productive rocks and potentially ore-rich vein systems occur together (JANISCHEWSKIJ & KONSTANTINOW 1962). Unproductive rocks contain uranium mineralisation when certain tectonic structures are present.

4.7 Hydrological and hydrogeological conditions

4.7.1 Today’s situation

No recent publications are available on the hydrogeological conditions in the vicinity of the Niederschlema/Alberoda deposit. Therefore, for the description of the hydrogeological conditions, the project sketch prepared by Wismut for the prognosis of the flooding (SDAG WISMUT 1991) must be used for the most part.

In the metamorphic and plutonic rocks, fractures, faults, ore veins and fissures are the main potential movement paths for groundwater. During mining, water seepage occurred particularly frequently at intersections of ore veins and faults (SDAG WISMUT 1991). Even in marginal parts of the Bohemian Massif, a favourable water flow could generally be proven in the fault zones (KARRENBERG 1981).

Water moves subordinately in microcracks and in undisturbed rock, but its quantity is negligible because of the low permeability coefficients (Tab. 52) (KARRENBERG 1981), as performance quotients (yield) of wells in the Thuringian-Vogtland Slate Mountains show (Tab. 14). Only in the Silurian Ocherkalk are the performance quotients higher than those of the other rocks, presumably as a result of subrosion.

Tab. 14 Selected performance ratios (yields) of wells in pre- and early Palaeozoic rocks (after HECHT 1974).

Stratigraphic unit	Number of evaluations	minimal	maximum	Mean value
		Yield		
		L $s^{-1}m^{-1}$	L $s^{-1}m^{-1}$	L $s^{-1}m^{-1}$
Frauenbach layers	2	0.0008	0.013	0.007
Phycode layers	3	0.008	0.036	0.018
Main quartzite	4	0.005	0.167	0.092
Leather slate	5	0.008	0.052	0.021
Siliceous slate	10	0.007	0.661	0.274
Ochre lime	3	0.3	3.15	1.3
Diabase gemstone	14	0.002	2.62	0.25
Knotty limestone/knotty limestone slate	5	0	0.059	0.029

After drilling during mining, most fissure or crevice aquifers dry up after a short time (SDAG WISMUT 1991). This fact is in line with experiences from other crystalline regions in Europe, according to which the "crystalline shales are among the densest rocks" and shaly "rock areas […] are considered to be extremely poor in water" (KARRENBERG 1981).

Above the overlying rock, debris covers and soils are present which, compared to the unweathered rock, have substantially greater water pathways. The average thickness of the weathered zones and debris covers in the Eastern Erzgebirge is 0.4 … 1.2 m (SAKER & JORDAN 1977, SAKER & JORDAN 1979) and can even reach 2.0 m (THALHEIM & FIEDLER 1990a, THALHEIM & FIEDLER 1990b, ALTERMANN et al. 1988). Up to a depth of about 15 m, the bedrock is decomposed, with decomposition and k_f-values decreasing towards the bottom (SAKER & JORDAN 1977).

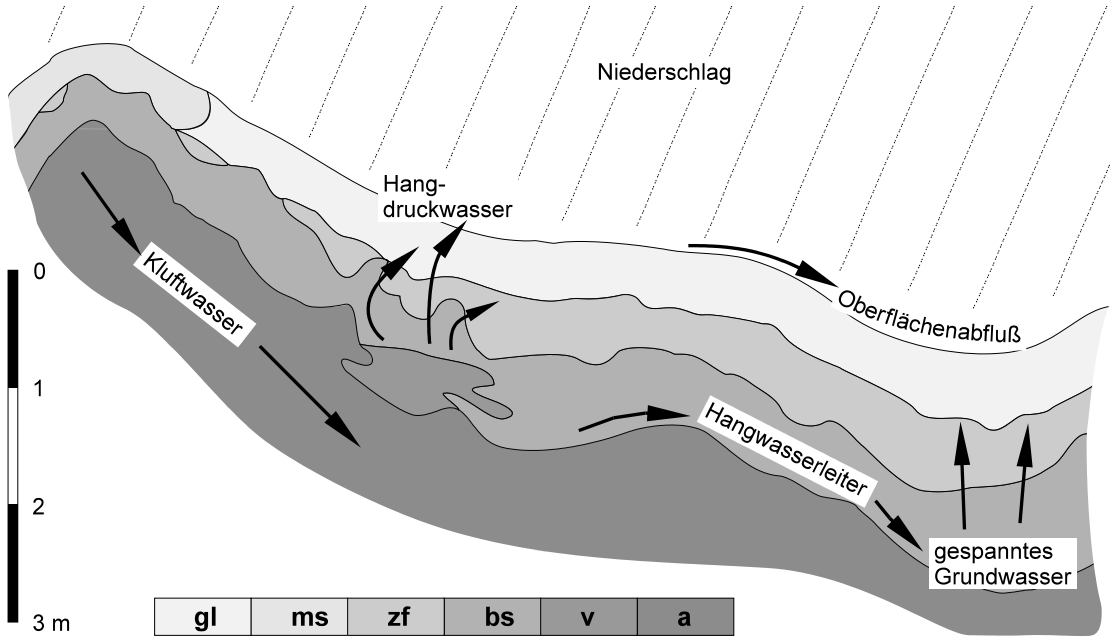

Fig. 14: Loose rock cover and waterway features in low mountain ranges using the example of the Harz Mountains (modified after ALTERMANN & WÜNSCHE 1991). As in the lower altitudes of the Erzgebirge (THALHEIM & FIEDLER 1990a, ALTERMANN et al. 1988), the upper cover is also missing in the Harz. gl: mountain loess, ms: middle debris, zf: intermediate flow soil, bs: base debris, v: older weathering residues, a: upstanding, loosened in the upper area.

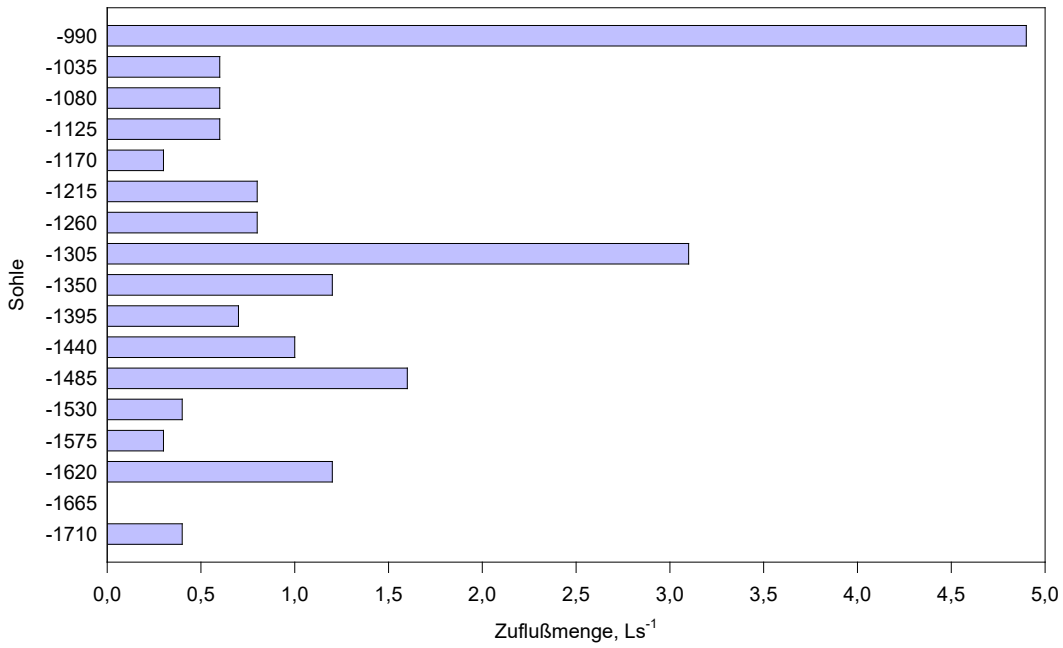

Fig. 15 Average inflow of water below and on level –990 in the years 1970 to 1982. Unit in L s^{-1} (modified after SDAG WISMUT 1991).

Investigations of weathering zones of gneisses in the Eastern Ore Mountains have yielded k_f-values between 10^{-6} and 10^{-4} m s^{-1} (SAKER & JORDAN 1977), which characterises the weathering zones as permeable according to DIN 18130. In the loess blankets of the Harz Mountains, the k_f-values range in the same range between 10^{-6} and 10^{-5} m s^{-1} (ALTERMANN & WÜNSCHE 1991).

In the course of mining, it was found that the weathering zone can reach 100 m deep and that groundwater movement in the weathered rock can be detected up to 240 m depth. Precipitation events influenced the water flow with a time delay up to 300 m depth (SDAG WISMUT 1991). In the Bohemian Massif, k_f-values of 10^{-7} … 10^{-6} m s^{-1} were determined for these depths (KARRENBERG 1981), in the Black Forest 10^{-8}… 10^{-9} m s^{-1} (STOBER 1995).

A simplified diagram of the structure of loose rock cover in the low mountain ranges, using the Harz mountains as an example, is shown in Fig. 14. The main water pathways are also recognisable there.

In the valley area of the Zwickauer Mulde, the main receiving water for the mining area, the sediments of gravels, sands and boulders are a maximum of 5 m thick. The river sediments in the tributaries are considerably less thick (SDAG WISMUT 1991). From south to north, the following watercourses flow into the Zwickauer Mulde in the area of the topographic map sheet Aue Nord (1407-12): Schwarzwasser, Lößnitzbach, Alberoder Bach, Schlemabach with Silberbach and Floßgraben, Wildbach, Bärengrundbach, Tieftalbach and Reitgrabenbach, the latter four being downstream of the Niederschlema/Alberoda mine.

The original hydrological conditions in the groundwater were permanently changed by mining. Above the Markus Semmler adit, the mountain range southwest of the Zwickauer Mulde was already extensively drained before Wismut mining began. From the tunnel mouth at 323.9 m a.s.l. on the Mulde to the north-east of Schlema railway station, the tunnel extends about 7 km in a south-westerly direction, beyond Schneeberg-Neustädtel. Its total length, including all side galleries, was 44 km (SCHIFFNER et al. 1911). To the north-east of the Zwickauer Mulde, the terrain was drained by the dewatering of shafts 371 and 208 to a maximum depth of 1800 metres, with about $7 \cdot 10^6$ m^3 of water being lifted annually (approx. 220 L s^{-1}).

By far the largest part of the inflowing waters are fissure and crevice waters above the –990 level. From there, about 90 % of the total inflowing water -flows or flowed into the mine (approx. 200 L s^{-1}). Only 10 % flowed into and below the –990 level (Fig. 15).

Most recently, about 6 … 7 · 10^6 m³ of water were lifted annually by Wismut; in addition, about 2 … 3 · 10^6 m³ of the water from the Markus Semmler adit could be discharged from shaft 15 II b into the Schlemabach. This results in an annual water volume of 8 … 10 · 10^6 m³. A comparison of these quantities with the quantities discharged from the Markus-Semmler adit before 1945 (5 … 9 · 10^6 m³ a^{-1}) makes it clear that the -seepage water flowing in between the Markus-Semmler adit and level –990 originates largely from the weathering zone above the Markus-Semmler adit level.

4.7.2 Historical situation of water chemistry

4.7.2.1 Before mining

Data on the hydrogeological situation before historical mining in the Ore Mountains are not available for understandable reasons. GERMANOV et al. (1958) investigated uranium mass concentrations of natural groundwaters in different regions of the former USSR. Some of their results can be transferred to the hydrogeological situation of the Ore Mountains before mining began.

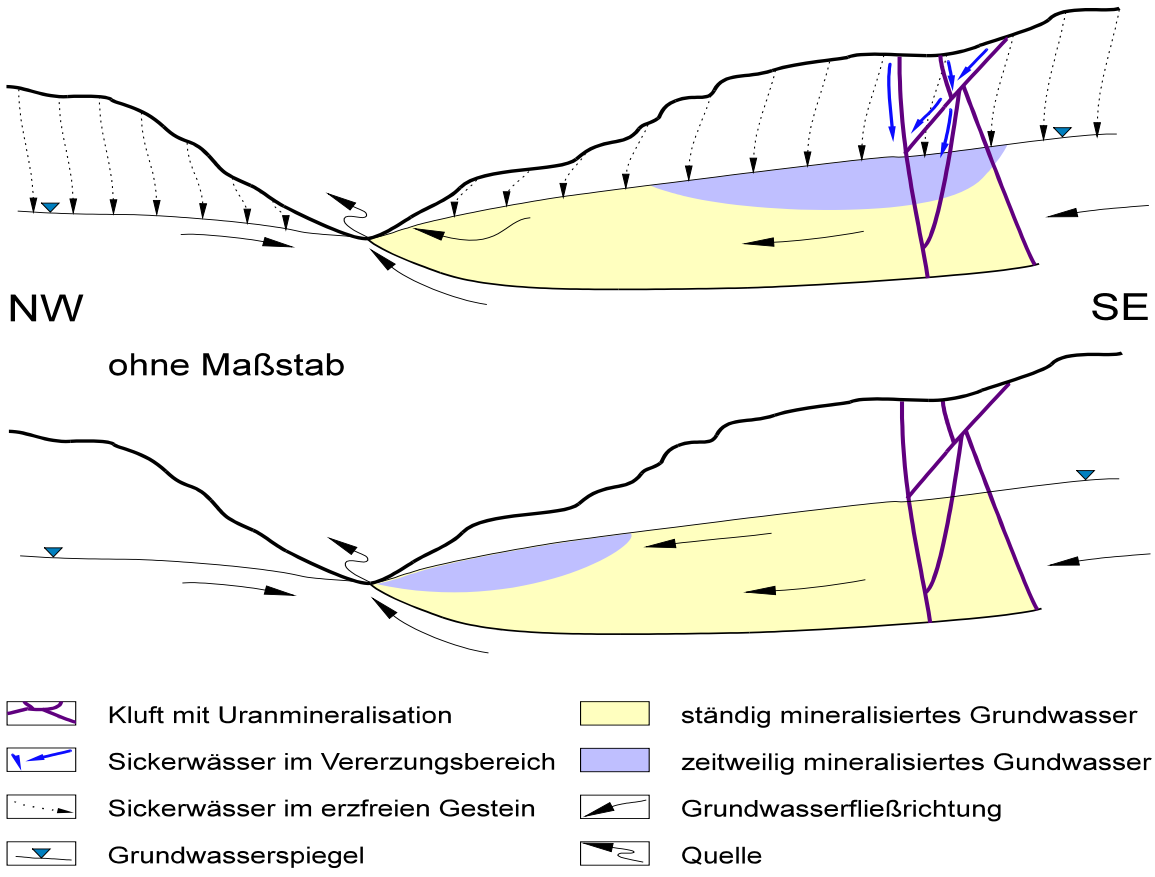

Fig. 16 Schematic sections of a uranium mineralisation in the Kendyktas Mountains, Tien Shan Mountains/Kyrgyzstan during (top) and after a precipitation event (bottom; modified after GERMANOV et al. 1958). During a precipitation event, water penetrates the mountains along the mineralised faults and increases the pollutant content in the groundwater discharge. After the end of the precipitation event, the pollutant front flows with the groundwater towards the source, where a temporally staggered increase of the outflowing water constituents occurs. “Temporarily mineralised groundwater” means that occasionally an above-average pollutant load is transported.

Tab. 15 Radioactivities of waters in the Markus-Semmler-Stollen, ordered by activity (SCHIFFNER & WEIDIG 1909, SCHIFFNER et al. 1911, GENSER 1932). Institut FRESENIUS (H. ZERBE, pers. comm.) determined 246,500 Bq L^{-1} in the Hindenburg Spring at the end of the 1930s.

Year of measure-ment	Measurement location	Radioactivity
		Bq L^{-1}
1932	Radium site, Hindenburg spring	181,818 (246,500)
1932	Radium site, Bismarck spring	40,404
1932	Frederick Wing	10,774
1932	Heinrich Wing, Borehole III	10,101
07.02.1911	Radium site, 25 m from Markus Semmler gallery	9,400 … 11,000
1932	Radium site, borehole I	8,350
19.10.1911	Radium site, 25 m from Markus Semmler gallery (*n* = 7)	7,886
19.09.1911	Radium site, Markus-Semmler adit inlet (*n* = 16)	5,375
23.11.1910	Radium site, 26.5 m from Markus Semmler gallery	4,539
1932	Radium site, radium die	4,444
1932	Radium site, borehole II	4,108
1932	Radium site, B-wing	4,040
1932	Heinrich Wing, Heinrich Swage	3,771
19.10.1911	Radium site, 34.5 m from Markus Semmler gallery (*n* = 5)	2,979
1932	Wolfgang Wing	1,886
1932	Gleesberg Wing	1,886
1932	Johannesflügel	1,347
23.03.1909	Maximilian Spat	1,048
07.01.1909	Eva Spat	640
1932	Young King David Wing	337
27.03.1909	Butcher morning walk	226
30.03.1909	Happiness Flats	218
30.03.1909	Transverse rock according to God's sending	191
30.03.1909	Türck flats	121
30.03.1909	unnamed spat on the cross with the lucky flat	110
27.03.1909	Gift of God Stollnort NW	86
30.03.1909	High spruce flats	55
26.03.1909	Priest spat	51
25.03.1909	Cross rock between New Year's Standing and Fresh Luck Morning Walk	31
05.01.1909	Sound of joy standing and hope of God flat	24
26.03.1909	Unnamed morning walk in the slope end of the Rappold Flachen	22
27.03.1909	Ascension wing	11

Tab. 16 Chemical analyses of some spring and well waters of the Schlema valley and Markus-Semmler-Stollen from 1909. Data in mg L^{-1} (SCHIFFNER et al. 1911). As far as possible, the measured values have been converted into quantities customary today. u.N.: below the detection limit or not detectable. Radium site (borehole) is identical with the Bismarck spring (Tab. 17).

Location	Ca	Mg	Fe/Al^{2+}	SO_4^{2-}	Cl	NO_3^-	H_2SiO_3
Weihnachtsfreuder Stollen	4,65	3,21	1,50	2,5	8,75	u.N.	13,6
Knietzschwasser	4,36	1,71	0,24	2,0	16,32	u.N.	6,2
Markus-Semmler-Stollen (Blaufarbenwerk)	6,48	2,00	0,32	12,2	8,06	8,86	12,7
Jung-König-Davider Flügel	7,13	4,59	0,63	11,9	9,02	8,88	8,1
Radiumort (mixed water)	13,62	6,79	5,93	26,8	12,71	u.N.	26,3
Radiumort (borehole)	14,77	7,03	1,05	28,2	15,55	u.N.	10,2

Due to the geological conditions of the Westerzgebirge, the Niederschlema/Alberoda deposit can be assigned to the oxidising type two according to GERMANOV et al. (1958). Its rock inventory is characterised by metamorphic rocks, intrusive and/or extrusive rocks. The pH values of the groundwaters in contact with the mineralisations generally range between 6.7 and 8.5, the Eh values between 0

and 525 mV, which corresponds to those of Niederschlema/Alberoda (Tab. 20). Under these oxidising conditions, microbially catalysed weathering reactions (chap. 4.9) lead to the transformation of poorly soluble, primary U(IV) phases into more easily soluble U(VI) phases. They dissolve in undersaturated seepage or groundwater and precipitate as secondary uranium phases when supersaturated. Depending on the groundwater level within the weathering zone of the rock, these secondary uranium minerals occur at depths of 100 … 200 metres. There, U(VI) phases can be dissolved again during precipitation periods and transported into the groundwater flow. At springs, the water then enters the surface part of the water cycle (Fig. 16).

GERMANOV et al. (1958) found the highest natural uranium mass concentrations in pH-neutral groundwaters in contact with pitchblende deposits. They ranged between 0.03 and 50 mg L^{-1} depending on the pH, with the higher values being characteristic of the infiltration zone of the mountains. At the springs, these values have already decreased to 0.001 … 0.03 mg L^{-1} U, provided there is a sufficiently long path between the ore veins and the spring (GERMANOV et al. 1958).

4.7.2.2 Beginning of mining until 1945

In Saxony, between 1908 and 1912, various researchers sought radioactive waters for healing purposes (SCHIFFNER 1908, SCHIFFNER & WEIDIG 1909, SCHIFFNER et al. 1911, WEIDIG 1912). Their main interest was less in hydrogeochemical analyses of the waters than in their radioactivities (Tab. 15).

According to GENSER (1932), no more highly active springs emerged above ground in 1932, since mining, especially the Markus-Semmler adit in its capacity as a water-solving adit, had caused a lowering of groundwater and a shift in the direction of groundwater flow. However, he suspects that highly active springs may well have been present before the Markus-Semmler adit was excavated. Activity measurements of more than 40 springs and wells in the Schlema valley from 1909 prove the relatively low activities of these waters, which at a mean discharge of 55 L s^{-1} (n = 42, s = 151 L s^{-1}, median: 25 L s^{-1}) had an activity of $\overline{x}$ = 165 Bq L^{-1} (n = 42, s = 159 Bq L^{-1}, median: 88 Bq L^{-1}). Chemical analyses were also carried out on some spring and well waters, which are incomplete from today's point of view, but should be cited here for reasons of comparison (Tab. 16, SCHIFFNER et al. 1911).

In the course of this prospecting for radioactive waters, R. FRIEDRICH (GENSER 1932, SCHIFFNER et al. 1911) discovered the Bismarck and Hindenburg springs of Bad Oberschlema, the latter of which, with 246,500 Bq L^{-1}, was considered the most radioactive healing spring in the world (Institut FRESENIUS, pers. comm. The data in CARLÉ 1975, p. 256 are not correct. There is both a calculation error and a transcription error).

The sites with radioactive waters were located within a section of only 500 m in various side galleries ("wings") of the Markus Semmler gallery, of which the 41 m long radium wing directly below the former bath provided the most highly active waters (GENSER 1932). Short transport routes of the water from the place of its enrichment with radon to the wells and springs are responsible for the high radioactivities (SCHIFFNER et al. 1911). It is possible that the wells were even sunk at the site of the enrichment, which is indicated by highly radioactive precipitates in a fissure in the radium wing (GENSER 1932). The first usable analyses of the water from the Bismarck and Hindenburg springs, excerpts of which are quoted in CARLÉ (1975), were carried out by the FRESENIUS Institute in 1933 (Tab. 17).

Further analytical values exist for the time before 1945 of cobalt and nickel, which amounted to 0.2 … 1 mg L^{-1} Co and 0.05 … 0.1 mg L^{-1} Ni in the flowing water of the Markus Semmler gallery. In stagnant waters of old mine workings, the values rose to 1 … 10 mg L^{-1} Co and 3 mg L^{-1} Ni as well as 0.05 mg L^{-1} Ag (LEUTWEIN & WEISE 1962).

In the years 1911 and 1962, 5 … 9 · 10^6 m^3 of water flowed out of the Markus-Semmler adit annually (SCHIFFNER et al. 1911, LEUTWEIN & WEISE 1962). This corresponds to the amount lifted by SDAG Wismut at the time of active mining in Niederschlema/Alberoda (Chapter 4.7.1).

Tab. 17 Chemical composition of the well water of the Bismarck Spring and the Hindenburg Spring. H_3PO_4, $HAsO_3$ and HBO_2 converted to PO_4^{3-}, As and B. $q^*_2 = -\log(n/n_{AsCa})$. Trace elements were determined by spectral analysis with the "Großer Quarzspektrographen für Chemiker von ZEISS". n.b.: not determined. Reproduction of the analysis with kind permission of the Institut Fresenius, Wiesbaden and the Kurgesellschaft Schlema mbH as successor of the radon bath Bad Oberschlema.

Parameter	Unit	Bismarckquelle	Hindenburgquelle
Date	–	February 1933	February 1933
Temperature	°C	9.5	9.2
electrical conductivity	mS cm^{-1}	0.133	0.137
pH value	–	6.6	6.6
Evaporation residue	mg kg^{-1}	190	180
Ca	mg kg^{-1}	18.42	17.38
Mg	mg kg^{-1}	11.49	11.95
Na	mg kg^{-1}	8.09	7.57
K	mg kg^{-1}	2.79	3.13
Fe	mg kg^{-1}	0.89	1.14
Mn	mg kg^{-1}	0.46	n.b.
Sr	mg kg^{-1}	0.42	n.b.
SO_4^{2-}	mg kg^{-1}	34.68	38.50
Cl	mg kg^{-1}	15.38	15.88
HCO_3^-	mg kg^{-1}	73.64	64.1
PO_4^{3-}	mg kg^{-1}	0.03	n.b.
As	mg kg^{-1}	0.01	n.b.
B	mg kg^{-1}	0.12	n.b.
$_2HSiO_3$	mg kg^{-1}	23.00	18.26
Li	mg kg^{-1}	0.13	n.b.
total CO_2	mg kg^{-1}	1.28	1.71
Trace elements	"smaller quantities"	Sr. Ba. Al. Mn. Fe. As. Si. B	
Trace elements	"Traces"	Be. Zn. Ni. Co. Cd. Wo. Mo. Sn. Cu. Pb. Ag	
Radioactivity	Bq L^{-1}	47,500	246,500
q^*_2	–	3.54	–

Tab. 18 Water analyses of the Zwickauer Mulde, the Schlema and the Silberbach from 1993 (WISMUT GmbH 1994a). before/after: before/after operational influence. FR: filter residue. $q_1^* = \log(n/n_{UAs})$, $q_2^* = -\log(n/n_{AsCa})$. The contamination with As is reflected in the smaller q_2 after the operational influence. m-xxx: name of monitoring location in the Wismut environmental register.

		Zwickau Mulde		Schlemabach		Silberbach	
		m-131	m-111	m-170	m-151	m-139	m-037
	Unit	before	after	before	after	before	after
pH	–	7.9	7.2	7.2	7.1	6.7	5.7
FR	mg L^{-1}	13	9	316	9	7	120
Ca	mg L^{-1}	19	25	24	37	14	37
Mg	mg L^{-1}	6	7	6	11	3	21
Fe	mg L^{-1}	0.23	0.51	1.63	0.33	0.12	7.40
SO_4^{2-}	mg L^{-1}	44	62	33	75	31	52
Cl	mg L^{-1}	15	18	125	41	81	19
HCO_3^-	mg L^{-1}	30	34	206	97	24	304
Hardness	°d	3.9	5.2	4.8	7.9	2.6	9.9
As	mg L^{-1}	0.011	0.023	0.054	0.13	0.0005	0.016
U	mg L^{-1}	0.005	0.020	0.019	0.012	0.001	0.005
Ra	mBq L^{-1}	15	15	<10	18	< 10	10
q_1^*	–	–0.84	–0.56	–0.96	–1.54	–0.20	–1.01
q_2^*	–	3.51	3.31	2.92	2.73	4.72	3.64

Tab. 19 Water analyses of mine water in the Markus-Semmler adit. The values represent mean values ($\bar{x}$) from four samples taken between April and June 1957. Standard deviation (s) and number of samples (n) are given in each case. In addition, q_2* = -log(n_{As}/n_{Ca}) and HCO_3^-* (from total hardness, Ca and Mg) were calculated. Units in mg L^{-1}, hardness in °d. pH and q_2 without unit. AR: Evaporation residue. RadAk: Radioactivity in Bq L^{-1}. Erika: Erika, am Querschlag 91; Bergkappe: Bergkappeschacht; Kreuz Anna: Kreuz Anna und Priesterschacht; Morgenstern: Morgenstern-Schimmelsberger Stollenflügel; Fleischer: Fleischer Morgengang-Schindlerschacht (after LEUTWEIN & WEISE 1962). In Table 1 of the original paper, some analytical values for Cu are obviously wrong (11.5 … 24 mg L^{-1}!). They were not taken into account here.

	Erika			Bergkappe			Kreuz Anna			Morgenstern			Fleischer			Mean values		
	$\bar{x}$	s	n	$\bar{x}$	s	n	$\bar{x}$	s	n	$\bar{x}$	s	n	$\bar{x}$	s	n	$\bar{x}$	s	n
pH	6.6	0.3	4	6.7	0.4	4	6.8	0.4	4	6.6	0.4	4	6.8	0.3	4	6.7	0.3	20
AR	569	124	4	220	28	4	206	6	4	332	13	4	181	45	4	302	157	20
RadAk	24.3	–	1	23.3	–	1	42.5	–	1	25.8	–	1	26.5	–	1	27.7	7.5	5
Ca	65.7	7.5	2	29.8	8.5	2	34.0	6.2	4	43.1	–	1	35.5	4.9	3	39.7	13.6	12
Mg	35.8	15.2	2	7.1	0.1	2	7.3	2.8	4	22.0	–	1	2.9	2.7	3	12.1	13.1	12
Na	7.9	6.2	4	4.9	1.4	4	4.9	1.5	4	7.0	2.2	4	4.1	1.6	4	5.8	3.2	20
K	2.8	0.3	4	2.4	0.4	4	2.1	0.1	4	2.4	0.6	4	2.2	0.7	4	2.4	0.5	20
Fe	1.11	1.16	4	0.37	0.10	4	0.17	0.19	4	0.32	0.15	4	0.38	0.22	4	0.47	0.59	20
Sr	0.15	–	1	0.11	–	1	0.06	–	1	0.06	0.07	2	0.07	–	1	0.08	0.05	6
SO_4^{2-}	318	18	4	81	43	4	59	25	4	167	60	4	59	26	4	137	107	20
Cl	17.6	0.5	4	16.0	4.8	4	11.7	1.2	4	14.4	0.6	4	8.6	0.8	4	13.7	3.8	20
$HCO^*_3^-$	35	1	2	68	31	2	46	21	4	–	–	–	35	27	3	45	23	11
Hardness	19.9	3.2	4	9.6	2.0	4	8.5	0.8	4	11.9	2.1	4	7.4	0.7	4	11.5	4.9	20
Al	0.31	–	1	0.02	0.01	2	0.03	0.03	3	0.03	0.02	4	0.02	0.03	4	0.05	0.08	14
As	0.36	0.08	2	0.04	0.02	3	0.29	0.32	3	0.17	0.19	4	0.42	0.25	4	0.25	0.23	16
Ba	0.03	–	1	0.13	–	1	0.05	0.02	2	0.06	0.01	3	0.04	0.03	3	0.06	0.03	10
Co	2.14	1.12	3	–	–	0	–	–	0	0.41	0.15	2	0.08	–	1	1.22	1.24	6
Cr	0.01	–	1	0.02	–	1	0.00	–	1	0.01	0.00	2	0.01	0.00	2	0.01	0.01	7
Cu	1.70	–	1	0.51	0.72	2	0.01	–	1	0.34	0.39	4	0.73	0.07	2	0.56	0.56	10
Ni	1.06	0.91	2	0.06	0.02	3	0.68	0.96	2	0.29	0.49	4	0.11	0.16	3	0.37	0.57	14
H_2SiO_3	18.6	3.1	4	19.9	3.5	4	27.9	2.5	4	16	1.9	4	25.6	2.7	4	21.6	5.2	20
Ti	0.06	–	1	0.01	0.00	2	0.17	0.27	3	0.05	0.04	3	0.04	0.04	2	0.08	0.14	11
Zn	0.68	0.25	2	0.04	–	1	–	–	0	0.19	0.12	4	–	–	0	0.31	0.29	7
q_2*	–	–	–	3.83	–	1	2.50	0.54	3	3.30	–	1	2.42	0.48	3	2.74	0.65	8

SCHIFFNER & WEIDIG (1909) preface their publication on radioactive waters of Saxony with a description of the mining conditions in the vicinity of the Markus-Semmler-Stollen. There they point out that water inflows into the pits occurred mainly where the contact between granite and metamorphic veins was formed. They write about the general water conditions:

“The ground waters have not increased towards the depths, because the water accesses consist mostly of open-cast waters, which decay into the depths and are therefore partly already discharged through stölln in the upper levels.”

4.7.2.3 After 1945

Unlike the surveys in Ronneburg and Königstein, there was no hydrogeochemical inventory in the Ore Mountains before mining began (J. MEYER, pers. comm.). Therefore, the information on the hydrogeochemistry of the waters in the study area is limited to the values tabulated by LEUTWEIN & WEISE (1962) (Tab. 19).

Information on the level-dependent substance content of the seepage water in the mine comes from SDAG Wismut (SDAG WISMUT 1991). These show that the mineralisation of the seepage water in the mine workings increases continuously from the top to the bottom at a roughly constant pH value (Fig. 17).

For comparison between today's flood waters and the unaffected situation before mining began, the mean values of water analyses from 1993 can be used, which were obtained by Wismut GmbH as part of environmental monitoring (Tab. 18). In terms of size, they correspond to the analyses of the Bismarck and Hindenburg springs.

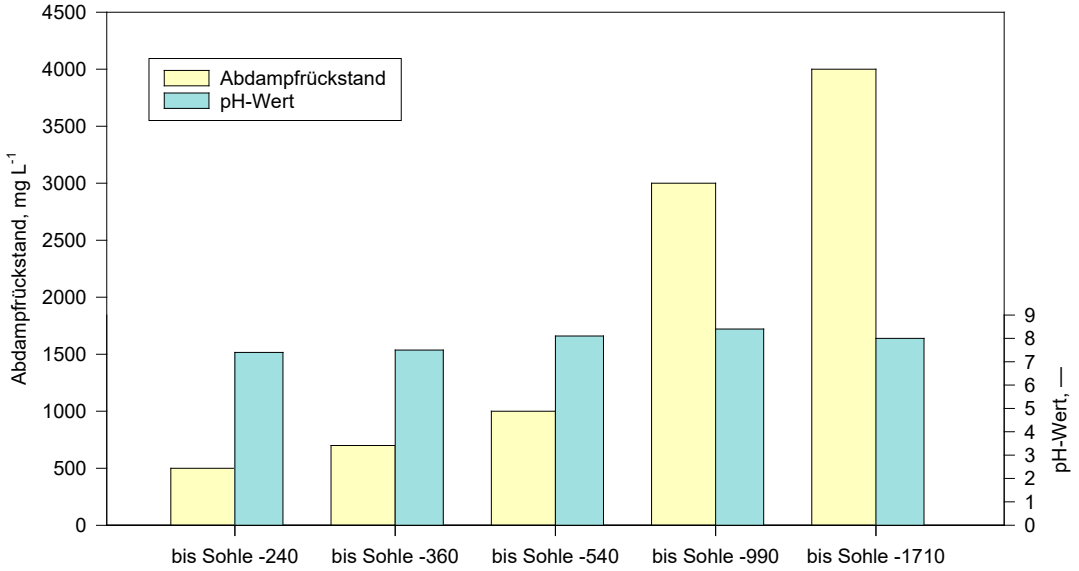

Fig. 17 Dependency of the evaporation residue and pH value on the level in the Niederschlema/Alberoda mine. With an almost constant pH value, the mass of the evaporation residue in the seepage water increases continuously from top to bottom (modified according to SDAG WISMUT 1991).

4.8 Microbial activities

Microorganisms play a role in a wide variety of processes in the natural and anthropogenic environment (BENEDIX et al. 1991). An essential aspect is the pH and Eh changes that their metabolism causes in water bodies and that can even lead to the formation of deposits. Furthermore, microorganisms make a decisive contribution to the composition of mineral parageneses by contributing to the formation of S^{2-}, SO_4^{2-}, CO_2, H_2S, HS^- and other ions and compounds (TISCHENDORF & UNGETHÜM 1965).

Eh-pH conditions of waters are important for the chemical reactions taking place and for the ions, complexes, phases or solubilities encountered. Therefore, the Eh and pH values naturally occurring in mine waters and seepage waters are important (Tab. 20). An example of the solubility of uranium as a function of CO_2 partial pressure and Eh value is shown in Fig. 18.

All bacteria catalytically involved in the leaching of metals and metaloids in the Niederschlema/Alberoda mine are chemoautotrophic (lithoautotrophic) organisms. So far, neutrophilic thiobacteria and *metallogenium* could be detected (Tab. 21), which belong to the GRAM-NEGATIVE eubacteria and, according to STRASBURGER et al. (1991), can be assigned to groups 8 and 10 of this class (evidence Dr. M. GRAFF, Institute for Microbiology at the Technical University of Braunschweig). Other disulfate-oxidising microorganisms are *Beggiatoa, Thiothrix*, *Sulfolobus, Thiobacillus acidophilus* or *Stibiobacter senarmontii* (LUNDGREN & SILVER 1980).

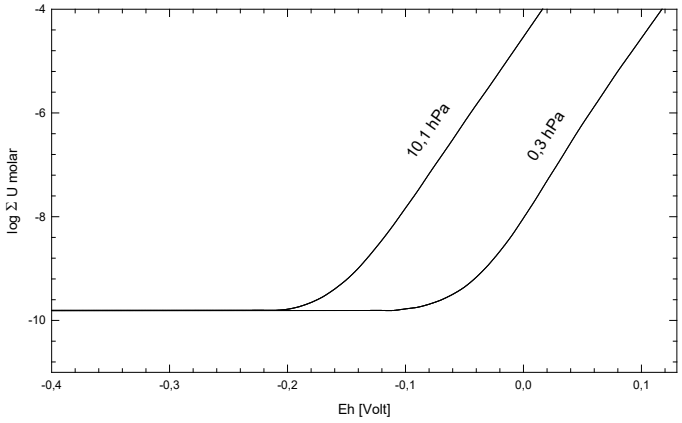

Fig. 18: Dependence of uraninite solubility on redox potential and CO_2 partial pressure, given as a function of log U molar (after LANGMUIR 1978). pH = 8, t = 25 °C.

Tab. 20 Eh and pH ranges of primary and oxidised mine waters and of ground waters (after BAAS BECKING et al. 1960, LISITSCHIN quoted from TISCHENDORF & UNGETHÜM 1965, Wismut measured data). *n*: Number of reported measured values.

n	Water	pH range	Eh range, mV
131	Mesozoic-Cenozoic sediments	6.1 … 8.3	-400 … +500
76	Groundwater	4.1 … 9.4	-90 … +600
23	Primary mine water	4.9 … 8.9	-110 … +200
33	Oxidised mine water	1.8 … 8.8	+120 … +830
44/59	Flood water Niederschlema/Alberoda (type S/type G)	6.4 … 8.8	+3 … +530

Tab. 21 Result of microbacterial tests for metals and metaloids leaching-relevant bacteria and physicochemical measurements on water samples from the Niederschlema/Alberoda mine. n.b.: not determined, n.n.: not detectable, *: measured value determined by Wismut GmbH.

	Shaft 366 b, level -540, (sample from -865 mNN)	Shaft 366 b, filling location invert -720	Crosscut 918, sole -540	Surge chamber, inlet, sole -540
Air temperature, °C	n.b.	13.6	22.8	16.0
Water temperature, °C	31.3*	13.0	24.4	17.5
pH	9.45*	8.10	7.33	7.73
Oxygen content, mg L^{-1}	2.5	10.0	7.2	9.5
Oxygen saturation, %	33	94	85	99
Redox potential Eh, mV	315*	345	335	365
neutral. thiobacilli (S^o-Ox.), L^{-1}	4.5 · 103	1.5 · 103	4.5 · 104	2.5 · 104
acid. Thiobacilli (S^o-Ox.), L^{-1}	n.n.	n.n.	n.n.	n.n.
acid. Iron oxidiser (Fe^{2+}-Ox.), L^{-1}	n.n.	0.4 · 103	n.n.	0.4 · 103

Chemoautotrophic organisms, in contrast to photoautotrophs, obtain their energy requirements from the oxidation of inorganic compounds. Here, the energy gain from the chemical reaction is used to phosphorylate ATP (adenosine triphosphate) from the reaction of ADP (adenosine diphosphate) with P^- (phosphate radical: PO_4^-) (reaction 1). ATP, in turn, is needed by organisms to enable movement processes, molecule and ion transport through the cell membrane and biosyntheses (VOGEL & ANGERMANN 1984). The chemical reactions take place inside the cell, which enables the uptake of the reactants into the cell interior. After the reaction, the cell excretes the products again, with the result that the pH and Eh values of the fluid change.

$$ADP + P^- \leftrightarrow ATP \qquad \Delta G^{\circ\prime} = +32\ kJ \quad (1)$$

There are two mechanisms of bacterial leaching of sulfides, direct and indirect (LUNDGREN & SILVER 1980, BOSECKER 1980). In the direct mechanism, there is cell contact between the sulfide and the bacterium, for example *Thiobacillus ferrooxidans*, and following the bacterially triggered reaction 5, iron(II) is oxidised to iron(III) (reaction 6). The indirect mechanism, on the other hand, takes place without cell contact and catalyses the oxidation of iron(II) to iron(III) in reaction 6.

The following reactions take place in *Thiobacillus thiooxidans, Beggiatoa* and *Thiothrix* within the cell:

$$2\ S^{2-} + 4\ H_3O^+ + O_2 \leftrightarrow 2\ S + 6\ H_2O \qquad (2)$$

$$2\ S + 6\ H_2O + 3\ O_2 \leftrightarrow 2\ SO_4^{2-} + 4\ H_3O^+ \qquad (3)$$

This releases $\Delta G^{\circ\prime} = -498$ kJ (reaction 3) of energy.

All the above-mentioned bacteria, apart from the strongly alkaline environment, are able to survive within wide pH and Eh ranges (Tab. 22) and in principle can be found in almost any mine water (BAAS BECKING et al. 1960). Other important parameters for optimal environmental conditions are: Temperature, O-content$_2$, CO-content$_2$, nutrient supply, grain size of the substrate and the concentration of metals and metaloids that may have a toxic effect on the organisms (LUNDGREN & SILVER 1980, BOSECKER 1980).

	pH range	Eh range, mV
Sulfate-reducing	4.2 … 9.9	–450 … + 115
Thiobacteria	1.0 … 9.2	–190 … + 855
Mine water	6.4 … 8.9	+ 3 … + 530

Tab. 22 Life ranges of bacteria in mine water (BAAS BECKING et al. 1960) and Eh-pH ranges of the mine water in the Niederschlema/Alberoda mine.

In addition, Thiobacillus species are used in technical processes involving the enrichment of metals from low-grade ores (NORDSTROM et al. 1989, NEAVILLE 1989). Microbially controlled leaching processes also run independently in the tailings of the Wismut mining (DAENEKE & BÜSSER 1991), the duration of which in Ronneburg can be up to 1000 years (HÄHNE 1992).

In the sixties EHRLICH (1963, 1964) proved by column experiments that microbial activities influence the release of elements from auripigment (As_2S_3), arsenopyrite (FeAsS) and enargite (Cu_3AsS_4) in an aqueous environment (pH 2 … 3.5). In the presence of *Ferrobacillus* or *Thiobacillus,* the mass concentration of Fe, As and Cu in the solution increased by up to six times after three weeks of experimentation compared to that without bacteria. The formation of HCl-soluble metal compounds insoluble in water was also increased. EHRLICH was able to prove that arsenites, arsenates and sulfate had formed in the bacterially treated columns after the end of the experiment, while only arsenites and sulfur ions were present in the untreated columns (EHRLICH 1963).

Uraninite is dissolved after reaction 16 dissolved, which indirectly accelerates *T. ferooxidans.* Reaction 4 on the other hand, proceeds by direct oxidation of the uranium(IV) by *T. ferrooxidans* acting as a catalyst (LUNDGREN & SILVER 1980):

$$2\ UO_2 + O_2 + 2\ H_2SO_4 \leftrightarrow 2\ U(VI)O_2SO_4 + 2\ H_2O \qquad (4)$$

NORDSTROM (1977) and BOSECKER (1980) have summarised which other sulfides *Thiobacillus ferrooxidans* oxidises and have been studied experimentally (Tab. 23). A description of the essential work on bacterial leaching of ores with the reaction mechanisms taking place is given by LUNDGREN & SILVER (1980) and BOSECKER (1980). Both works contain a detailed bibliography.

Tab. 23 Compilation of metal sulfides that occur in Niederschlema/Alberoda and can be oxidised by *T. ferrooxidans* or *T. thiooxidans* (NORDSTROM 1977, LUNDGREN & SILVER 1980, BOSECKER 1980). Greenokite has not yet been described from Niederschlema/Alberoda. However, it is always present as a secondary formation of sphalerite.

Mineral	Formula	Mineral	Formula
Antimonite	Sb_2S_3	Galenite	PbS
Arsenopyrite	FeAsS	Greenokit	CdS
Auripigment	As_2S_3	Markasite	FeS_2
Bismuthinite	Bi_2S_3	Millerite	β-NiS
Bornite	Cu_5FeS_4	Molybdenite	MoS_2
Chalcopyrite	$CuFeS_2$	Pentlandite	$(Ni,Fe)_9S_8$
Chalkosin	CuS_2	Pyrite	FeS_2
Cinnabarit	HgS	Pyrrhotine	FeS
Covellin	CuS	Sphalerite	α-ZnS
Enargit	Cu_3AsS_4	Tetrahedrite	$Cu_3SbS_{3.25}$

4.9 Weathering processes in a mine

Ore mining creates cavities in the rock, on the walls of which atmospheric oxygen and humidity cause the weathering of various minerals in the rock and the ore veins. Dissolution and redox processes lead to the formation of partly new compounds (FERNANDEZ-RUBIO et al. 1987). One of the most important of these processes in coal and metal mines is the oxidation of sulfides to sulfate, with pyrite oxidation being the most important. In addition, the dissolution of silicates or carbonates plays a role (Tab. 24).

Tab. 24 Selection of weathering processes that can take place in a mine (STUMM & MORGAN 1981, SIGG & STUMM 1994).

Type	Weathering reaction
Congruent solution	$SiO_2(s) + 2\ H_2O \leftrightarrow H_4SiO_4$
Incongruent solution	$3\ K[AlSi_3O_8](s) + 2\ H_2CO_3 + 12\ H_2O \leftrightarrow 2\ K^+ + 2\ HCO_3^- + 6\ H_4[SiO_4] + KAl_2[(OH)_2\|Al_3SiO_{10}](s)$
Redox reaction	$PbS(s) + 4\ Mn_3O_4(s) + 12\ H_2O \leftrightarrow Pb^{2+} + SO_4^{2-} + 12\ Mn^{2+} + 24\ OH^-$

The weathering process is generally not limited to the newly created surfaces of the drifts, shafts and workings, but extends far into the existing and newly created fissures and microfissures of the outcrop zones (Chapter 8.2). In principle, the processes correspond to those that take place in the weathering zone of ore deposits and lead to the formation of the oxidation and reduction zone of chemical weathering deposits. With the meteoric waters (seepage water) that enter the mine through the infiltration zone (seepage zone) and deep faults, the reaction products are transported into the mine water. In seepage-free areas, on the other hand, the rising floodwater releases the reaction products only after mine drainage has ceased.

Pyrite oxidation is the strongest acid formation process of all oxidation processes during weathering (STUMM & MORGAN 1981). Accordingly, the research work on it to date is extensive. As GOTTSCHALK & BUEHLER (1912) showed, the oxidation of pyrite or marcasite in aqueous solution is accompanied by the dissolution of other sulfides. In addition, the lowering of the pH value mobilises a large number of metals from the minerals, which only precipitate again during neutralisation.

In the absence of carbonates in a mine that could help neutralise the acidity produced, the mine or flood water becomes strongly acidic. pH values of mine waters of 3 and less are not uncommon in this oxidation process (STUMM & MORGAN 1981), and even pH values of 0.5 … 1.4 and –3.4 can occur (ALPERS & NORDSTROM 1990, NORDSTROM & ALPERS 1995).

The amount of water, contact time, the presence of buffers, the amount of available pyrite or marcasite and, to a decisive extent, its grain size are responsible for the pH value. The acid production increases with decreasing grain size (CARUCCIO et al. 1980), since a larger surface is available for the reaction.

The following reactions take place during the oxidation of pyrite and marcasite:

$$2\ FeS_2(s) + 7\ O_2 + 2\ H_2O \leftrightarrow 2\ Fe^{2+} + 4\ SO_4^{2-} + 4\ H^+ \quad (5)$$

In this reaction, the disulfide is oxidised to sulfate and four protons are released, which contribute to acidification. At the same time, iron(II) ions go into solution. As soon as pyrite or marcasite are used up, in a subsequent reaction step (reaction 6), iron(II) is oxidised to iron(III):

$$Fe^{2+} + O_2 + 4\ H^+ \rightarrow Fe^{3+} + 2\ H_2O \qquad \Delta G^{\circ\prime} = -67\ kJ \quad (6)$$

Iron(III) hydrolyses according to reaction 7 to iron(III) hydroxide:

$$Fe^{3+} + 3\ H_2O \leftrightarrow Fe(OH)_3(s) + 3\ H^+ \quad (7)$$

The protons released contribute to acid formation, while the iron hydroxide settles as a poorly soluble brown film on soles and butts or reacts with the sulfates to form jarosite ($KFe_3[(OH)_6|(SO_4)_2]$) and precipitates out of solution (LUNDGREN & SILVER 1980).

However, as long as pyrite is available for reaction, the iron(III) ion is reduced as follows:

$$FeS_2(s) + 14\ Fe^{3+} + 8\ H_2O \rightarrow 15\ Fe^{2+} + 2\ SO_4^{2-} + 16\ H^+ \quad (8)$$

acid and iron(II) ions are formed, which are fed into the cycle in reaction 6.

Microorganisms, for example *Thiobacillus ferrooxidans* or *Ferrobacillus ferrooxidans,* can catalyse reaction 6 and increase the reaction rate by a factor of 200 (RACKLEY 1976) to 10^6 (LUNDGREN & SILVER 1980) compared to that in the bacteria-free environment. Their presence neither leads to a shift in redox equilibria nor can they cause reactions that are excluded under given redox conditions (STUMM & MORGAN 1981, BARNES & CLARKE 1964, SIGG & STUMM 1994). From the reactions listed above it is clear that oxygen is necessary for pyrite oxidation (reaction 5). Reaction 8 on the other hand, takes place without oxygen, but the reaction rate is only sufficiently high at pH values below 3, since iron(III) hydroxide is formed preferentially above pH 3 (STUMM & MORGAN 1981). Corresponding to the pyrite oxidation, other sulfides go into solution, whereby the presence of pyrite accelerates the dissolution of these sulfides just as much (GOTTSCHALK & BUEHLER 1912, STUMM & MORGAN 1981) as the presence of microorganisms (NORDSTROM 1977, EHRLICH 1963).

Representative is the oxidation of sphalerite (-ZnS) and chalcopyrite ($CuFeS_2$) by iron(III) (NORDSTROM 1977):

$$ZnS(s) + 8\ Fe^{3+} + 4\ H_2O \leftrightarrow Zn^{2+} + 8\ Fe^{2+} + SO_4^{2-} + 8\ H^+ \quad (9)$$

$$CuFeS_2(s) + 16\ Fe^{3+} + 8\ H_2O \leftrightarrow Cu^{2+} + 17\ Fe^{2+} + 2\ SO_4^{2-} + 16\ H^+ \quad (10)$$

The proton release accelerates another process, namely the dissolution of carbonates, which leads to the buffering of the protons:

$$CaCO_3 + H^+ \leftrightarrow Ca^{2+} + HCO_3^- \quad (11)$$

$$CaMg[CO_3]_2 + 2\ H^+ \leftrightarrow Ca^{2+} + Mg^{2+} + 2\ HCO_3^- \quad (12)$$

Reaction 11 does not lead to reaction 5 or 8 proceed more slowly or not at all. Sulfate will therefore be formed in the same way in the presence of carbonates as without (TOLER 1982, BARNES & CLARKE 1964, STUMM & MORGAN 1981). However, due to the buffering of the protons, the solution of metals and metaloids according to equation 9 and 10 is reduced, since not enough Fe(III) is available from reaction 6.

Besides calcite and dolomite, other carbonates and hydroxides contribute to buffering, but partly only when calcite is no longer available and in other pH ranges (Tab. 25, BLOWES et al. 1994, JURJOVEC et al. 1995).

Mineral	Formula	pH buffer range
Calcite	$CaCO_3$	6.5 … 7.5
Dolomite	$CaMg[CO_3]_2$	6.5 … 7.5
Siderite	$FeCO_3$	4.8 … 6.3
Mixed carbonates	$(Ca, Mg, Fe, Mn)CO_3$	4.8 … 6.3
Gibbsite	$Al(OH)_3$	4.0 … 4.3
Ferrihydrite	$Fe(OH)_3$	< 3.5
Goethite	α-FeOOH	1.3 … 1.8
K-Jarosite	$KFe_3[(OH)_6](SO_4)_2]$	1 … 2 (laboratory experiment)
Aluminosilicates		1 … 2 (laboratory experiment)

Tab. 25 Mineral phases contributing to sequential pH buffering (BLOWES et al. 1994; goethite, K-jarosite and aluminosilicates added from JURJOVEC et al. 1995). The buffer ranges for K-jarosite and the aluminosilicates were determined in the column test.

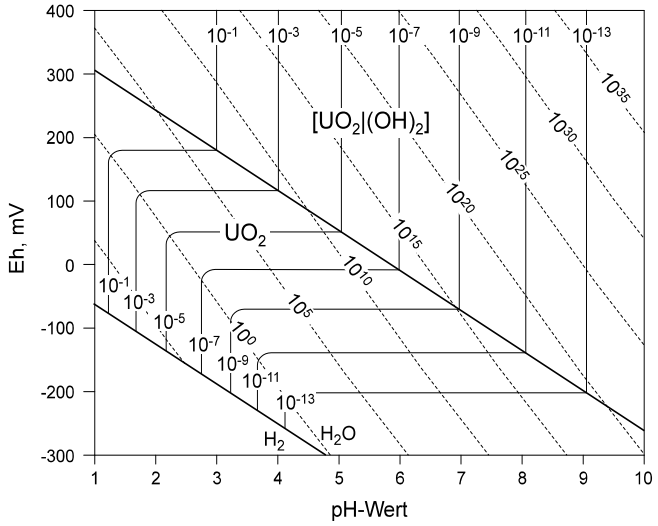

Fig. 19: Total activity (solid lines) and ratio (broken lines) of $(UO_2)^{2+}$ and U^{4+} in aqueous solution (modified after GARRELS 1955). There is an equilibrium with the solid phases UO_2 (uraninite) and $[UO_2|(OH)_2]$ (ianthinite).

The Ca^{2+} ion from equation 11 reacts together with Fe^{2+} and SO_4^{2-} from equation 5 and 8 to form gypsum and siderite (BLAIR et al. 1980):

$$Fe^{2+} + SO_4^{2-} + Ca^{2+} + CO_3^{2-} + 2\ H_2O \leftrightarrow FeCO_3(s) + CaSO_4 \cdot 2H_2O(s) \quad (13)$$

In the presence of ^{226}Ra from the uranium decay series, part of the calcium can be replaced (BLAIR et al. 1980) or, as described from the radon wing of the Markus-Semmler tunnel, precipitate directly as radium sulfate (GENSER 1932):

$$(^{226}Ra, Ca)^{2+} + SO_4^{2-} + 2\ H_2O \leftrightarrow (Ca^{226}, Ra)SO_4 \cdot 2H_2O\ (s) \quad (14)$$

Uraninite is only slightly soluble under normal conditions and has, depending on the temperature and the crystal structure, for reaction 15 has a solubility product of $10^{-60.6} \leq K_L \leq 10^{-52}$ (DYBEK 1962, LANGMUIR 1978):

$$UO_2 + 2\ H_2O \leftrightarrow U^{4+} + 4\ OH^- \quad (15)$$

In the acidic, oxidising environment, on the other hand, the solubility of uraninite increases substantially with the cooperation of bacteria (Fig. 19). Oxidation of the less soluble uranium(IV) phases to more soluble uranium(VI) phases occurs (reaction 16), whereby the $Fe_2(SO_4)_3$ originates from the pyrite oxidation (reaction 5) (LUNDGREN & SILVER 1980).

$$U(IV)O_2 + Fe_2(SO_4)_3 \leftrightarrow (VI)_2OSO_4 + 2\ FeSO_4 \quad (16)$$

5 Hydrogeochemistry of uranium, arsenic and radium

5.1 Introduction

In order to be able to classify the uranium, arsenic and radium concentrations in the waters of the Niederschlema/Alberoda mine in a worldwide comparison, the chapter “Hydrogeochemistry of uranium, arsenic and radium” compiles data on their concentrations. The comparability and reliability of the data were decisive factors in the selection.

Finally, the results of column tests on the mobilisability of arsenic and uranium are interpreted. They were conducted by SDAG Wismut and excerpts were made available for this work.

5.2 Empirical studies

5.2.1 Uranium

DYBEK (1962) and LANGMUIR (1978) cite various studies on the solubility of uranium in groundwater. The latter makes calculations in order to be able to indicate the uranium species present in each case as a function of the pH value. These confirm the chemical-thermodynamic equilibrium calculations of the programme code WATEQ4F (BALL & NORDSTROM 1991, BALL et al. 1981) and the statements on the complex formation of uranium made by them.

LOPATKINA (1964) and GERMANOV et al. (1958) obtained a linear relationship between total mineralisation and dissolved uranium in their solubility studies in a humid climate for flowing waters as a function of the metal mass concentrations of the rock through which the water flows. LANGMUIR (1978), on the other hand, limits the general validity of the LOPATKINA FORMULA, since it does not take sufficient account of the variability of the source rock, among other things. He therefore compiles a list of seven factors for the influences on uranium solubility in water:

- Uranium mass concentration of the source rock, sediments or soils and their dissolution possibility
- spatial distance of the water from the uranium-bearing rocks or minerals
- Degree of hydraulic separation of the water from fresh surface or ground waters.
- Climatic influences and their seasonal changes, especially the influence of evapotranspiration
- pH and Eh value of the water
- Concentration of compounds that can form uranium complexes or insoluble uranium compounds, such as carbonates, phosphates, vanadate, sulfate, fluoride, silicate, calcium or potassium.
- Presence of highly adsorptive materials such as organics, iron, manganese, titanium oxides/hydroxides and clays

Not every factor has an equal influence on the uranium mass concentration, rather they are spatially and temporally variable and can cancel each other out. Fig. 18 shows an example of the dependence of uraninite solubility on redox potential and CO_2 partial pressure. When the atmospheric CO_2 partial pressure (pCO_2 = 0.32 hPa) increases to that of an average groundwater (pCO_2 = 10.13 hPa), the uranium concentration increases 1000-fold under oxidising conditions. For the mine water of the Niederschlema-Alberoda mine, WATEQ4F calculates a CO_2 partial pressure of 30 hPa < pCO_2 < 100 hPa on the basis of the analyses, so that the solubility of uraninite in the mine water is even higher than under normal conditions. The reason for this is the formation of easily soluble uranyl-carbonate complexes.

FIX (1955) also lists a table with the minimum and maximum mass concentrations of the most frequently analysed parameters within the framework of 3500 surface and groundwater analyses (Tab. 26). Interestingly, according to FIX, the uranium mass concentration of mine waters varies in a wide interval. It is less important whether the mine produced uranium or not, but rather the pH value of the water. Thus, he was able to analyse mass concentrations of 0.005 to 0.535 mg L^{-1} uranium in uranium-producing mines, but the maximum mass concentration of 5.3 mg L^{-1} in a mine without uranium mineralisation (the pH value there was 2.5). CHERVET & COULOMB (1958) list uranium mass concentrations of up to 90 mg L^{-1} an for mine waters. Unfortunately, there is no information on the pH value prevailing there. FIX’s statement that no “extreme” uranium mass concentrations (several tens of

milligrams per litre) are to be expected at medium pH values (5.5 … 7.5) is of importance for the Aue remediation operation, as is the observation by MURAKAMI et al. (1958) that even at a relatively short distance from the deposit (700 m) the uranium mass concentrations of flowing waters have decreased to the background value as a result of dilution and adsorption to suspended particles.

Tab. 26 Minimum and maximum values of selected parameters of the 3500 waters examined by FIX (1955) in mg L^{-1}.

Parameter	Minimum	Maximum
U	< 0.00002	5.3
Fe (dead)	< 0.1	2310
Ca	0.6	1190
Mg	0.1	1520
Na	0.3	13400
K	0.1	1100
HCO_3^-	0	2630
SO_4^{2-}	0.7	8820
Cl	< 0.1	25000
AR	23	42200
pH	2.5	9.3

More precisely determined values are provided by PAČES (1969) for groundwater from the uranium mine of St. Joachimsthal in Bohemia. At pH values between 6.6 and 7.8 and Eh values of -89 … +57 mV, uranium mass concentrations of 0.017 … 9.000 mg L^{-1} (n = 4) could be measured.

Analyses of some “drip waters” were made by Wismut (SDAG WISMUT 1991) at the Niederschlema/Alberoda mine, where maximum uranium mass concentrations of 50 mg L^{-1} were measured; other seepage waters had predominantly mass concentrations of 0.001 … 0.01 mg L^{-1}.

In German ground and drinking waters < 0.03 … 3.62 µg L^{-1} (n = 107), in mineral waters < 0.03 … 11.58 µg L^{-1} (n = 22), in surface waters < 0.02 … 1.53 µg L^{-1} (n = 36) and in surface waters around uranium deposits (Black Forest, Fichtelgebirge) < 0.48 … 69.14 µg L^{-1} (n = 49) $_{238}U$ were determined (OBRIKAT & FUSBAN 1993).

A reference value for the global background level in surface and flowing waters is the average uranium mass concentration of 0.006 mg L^{-1} found by KOCZY et al. (1957), and 2.9 mg L^{-1} in the vicinity of uranium deposits of the pitchblende type (GERMANOV et al. 1958).

5.2.2 Arsenic

MOENKE (1956) determined arsenic contents of 0.02 … 0.35 mg L^{-1} at pH values between 2.1 and 6.0 in filtered discharge waters of the Feengrotten near Saalfeld, Saale. He showed that the mass concentration of arsenic depends on the pH value on the one hand and on the amount of filter residue on the other. Increasing suspended matter and pH values each reduce the arsenic mass concentration in the filtered water, whereby the suspended matter is attributed to iron hydroxides, among other things.

Arsenic mass concentrations of 0.1 … 2.23 mg L^{-1} (pH: 4.2 … 5.1) are reported from the Freiberg syncline, which are attributed to discharges of municipal wastewater, mine water and tailings leaching. The mine waters of the Davidschacht (kb formation, Rothschönberger Stollen) have an arsenic mass concentration of 1 mg L^{-1} at pH 4.2 (LEUTWEIN & WEISE 1962).

For the Schneeberg mining area (Weißer Hirsch, Siebenschlehn, Bergkappe, Adam Heber, Beustschacht) there is little meaningful material from the time before 1945: “Standing waters from old mine workings of arsenide parageneses contained considerable amounts of manganese, arsenic, cobalt and nickel” (source not given, quoted from LEUTWEIN & WEISE 1962).

Arsenic analyses by Wismut (SDAG WISMUT 1991) in “drip waters” of the Niederschlema/Alberoda mine show results of 0.01 … 0.1 mg L^{-1}; only at level -1305 did they reach a maximum value of 51.5 mg L^{-1} in 1969 in cross cut 1757. In the Markus-Semmler adit, water samples were taken at five

points in 1957 and analysed for some elements (Tab. 19). The arsenic mass concentrations ranged between 0.01 and 0.61 mg L^{-1}, at pH values of 6.1 … 7.2 (LEUTWEIN & WEISE 1962).

Results of the same order of magnitude exist for groundwaters from St. Joachimsthal, where arsenic mass concentrations of 0.05 … 0.28 mg L^{-1} were determined at pH values between 6.65 and 7.80 (n = 4, PAČES 1969).

5.2.3 Radium

Radium does not form its own minerals in nature, but is always associated with uranium minerals. It frequently occurs bound to uraninite, autunite, gummite, Ca-hydroxyapatite or coelestine, whereby the last two minerals are then called Ra-Ca-hydroxyapatite or Ra-coelestine (KUBACH & WEIGEL 1977). A comprehensive list of minerals containing radium was compiled by ERBACHER (1928).

In natural waters, radium occurs only in low mass concentrations (Tab. 27). It will normally not precipitate with its own radium phases, but always together with other compounds (KUBACH & WEIGEL 1977). In principle, it behaves like barium (WEIGEL 1977).

Together with calcium and iron, radium precipitates as a carbonate and with barium as a (Ba, Ra) sulfate, whereas a (Ca, Ra) sulfate is said to be thermodynamically unstable in the presence of barium (KUBACH & WEIGEL 1977). However, this is in contrast to GENSER (1932) and BLAIR et al. (1980), who both demonstrated a Ca-Ra sulfate. Another important factor for the precipitation of radium from aqueous solution, mainly in oxidising environments, is adsorption to Fe and Mn hydroxides, especially pyrolusite (-MnO_2).

In contrast to uranium, which mostly predominates in water as a uranyl ion, radium usually exists as a radium cation Ra^{2+} (STUMM & MORGAN 1981) about whose mobilisation there is still no sufficient understanding. Both an increase in temperature and in total mineralisation or sulfate content favour the leaching of radium from the corresponding mineral phases (KUBACH & WEIGEL 1977).

Only one radium analysis from the Hindenburg Spring could be found in the accessible literature. There, a Ra content of $5.8 \cdot 10^{-8}$ mg L^{-1} was determined in 1932 (GENSER 1932), which lies within the range given by GERMANOV et al. (1958). In carbonate rocks they determined radium mass concentrations of 10^{-9} … $2 \cdot 10^{-7}$ mg L^{-1}. From the uranium mine of Udaisagar, Rajasthan, India, a mass concentration of $1.5 \cdot 10^{-9}$ mg L^{-1} radium is reported. The radium mass concentrations of eastern Bavarian fluorspar mines are interesting. On contact with uraniferous fluorspar (CaF_2), the concentrations in the mine water reach $1.0 \cdot 10^{-9}$ … $1.0 \cdot 10^{-7}$ mg L^{-1} radium ($\bar{x} = 1.8 \cdot 10^{-8}$ mg L^{-1}, n = 31), for uranium-free fluorspar $4.0 \cdot 10^{-10}$ … $1.1 \cdot 10^{-8}$ mg L^{-1} ($\bar{x} = 2.4 \cdot 10^{-9}$ mg L^{-1}, n = 32; KUBACH & WEIGEL 1977). For the flowing waters around Aue, 3 … $4 \cdot 10^{-10}$ mg L^{-1} are determined in the inflow of the water discharges by Wismut GmbH (Tab. 27, FEDERAL MINISTER OF ECONOMICS 1992).

Tab. 27 Compilation of radium mass concentrations in waters of different origin, ordered by mass concentration. 1 Bq corresponds to a radium mass concentration of $2.703 \cdot 10^{-11}$ g.

Locality	Ra mass concentrations	Source
	mg L^{-1}	
Ore Mountains, Surface Waters	$3.2 \cdot 10^{-10}$ … $4.9 \cdot 10^{-10}$	Tab. 18
Eastern Bavaria, mine water fluorspar mine	$4 \cdot 10^{-10}$… $1.1 \cdot 10^{-8}$	KUBACH & WEIGEL 1977
Niederschlema/Alberoda, seepage water	$9.5 \cdot 10^{-10}$… $1.1 \cdot 10^{-8}$	Tab. 28, Mean value ± *s*
Eastern Bavaria, mine water fluorspar mine with uranium	$1 \cdot 10^{-9}$… $1 \cdot 10^{-7}$	KUBACH & WEIGEL 1977
Kendyktas Mountains, Kyrgyzstan, Groundwater	$1 \cdot 10^{-9}$ … $2 \cdot 10^{-7}$	GERMANOV et al. 1958
Udaisagar, India, mine water uranium mine	$1.5 \cdot 10^{-9}$	KUBACH & WEIGEL 1977
Niederschlema/Alberoda, mine water	$2.9 \cdot 10^{-8}$ … $8.4 \cdot 10^{-8}$	Tab. 28, Mean value ± *s*
Ore Mountains, Hindenburg Spring	$5.8 \cdot 10^{-8}$	GENSER 1932

5.3 Solution attempts

5.3.1 Description

In 1989 and 1990, SDAG Wismut carried out sixteen experiments to test the mobilisation of some elements in the ores of the Niederschlema/Alberoda deposit. The aim of these tests was to obtain reference values for a possible flooding of the mine.

Again for reasons of secrecy, the author only has excerpts from the test descriptions and the measured values (SDAG WISMUT 1991). Nevertheless, results were derived from the experiments that were included in the prognosis of the hydrogeochemical development of the floodwater.

Since the investigation of the rock material was to yield maximum values for the substance release, the rock samples were preferably taken from more mineralised areas. Precise information on the type of sampling and lithological conditions at the sampling point cannot be taken from the above-mentioned work. From the chemical analyses of CaO, MgO and Fe_2O_3, however, it can be assumed that the material is from the Phycoda sequence and the Lower Graptolite schists, mixed with ore.

Up to the time of sampling in 1987, the rock had been exposed to mine weathering for between 16 years and 1 year ($\bar{x}$ = 9 a, s = 4 a, n = 12) and was exposed to surface oxidation. It originates from the -540, -720, -765, -990, -1260, -1305, -1440, -1530 and -1620 levels and can therefore be assumed to be -representative of the mineralisation areas of the deposit, -at least in terms of vertical distribution. For the sampling in 1988, only depth data (-720, -1350, -1395, -1440, -1665) are available, but not the years of excavation.

The rock material was tested in three test series lasting 68 … 86 weeks (start: January 1989, May 1989 and May 1990) by column tests for the mobilisability of metals and metaloids, but especially uranium and arsenic. No information is available on the exact test conditions, only the type of dissolution test (“infiltrative”, “hydrostatic”) is given. One of the column tests was actively aerated, whereas the other fifteen columns were in contact with the atmosphere.

In the “infiltrative” test series, 0.5 … 1.5 L of tap water per day seeped through the columns. The water was always rich in oxygen and could oxidise the disulfide sulfur present. In contrast, 20 L of water were added once to the “hydrostatic” test series. There, the disulfide sulfur oxidation was able to successively consume the oxygen.

The quantities of water used are listed for 11 trials, the frequency of analysis or the quantities of water taken are missing. Water samples from two columns were analysed for their microbial activity. Microorganisms were not detectable in either column.

As, U, pH, Cu, Ni, Mo, Mn and Zn were determined in the columns, as well as O_2 and Ra in selected ones. Depending on the water temperature and the type of experiment, As values of 0.6 … 80 mg L^{-1} and U values of 0.5 … 180 mg L^{-1} (with the addition of H_2SO_4: 2000 … 5000 mg L^{-1}) were obtained,

whereby the pH value was almost constant at 7.2 … 8.4. When H_2SO_4 was added, the pH value decreased to 4 … 5, which indicates buffering by gibbsite or siderite. The oxygen content was determined to be 5 mg L^{-1} at 20 °C and 0 mg L^{-1} at 50 °C, and the radium activities were 10 … 17 Bq L^{-1} ($2.7 \cdot 10^{-7}$ … $4.6 \cdot 10^{-7}$ mg L^{-1}) after 10 months of experiment and 0.3 … 6 Bq L^{-1} ($8.1 \cdot 10^{-9}$ … $1.6 \cdot 10^{-7}$ mg L^{-1}) after 15 months of experiment. All mass concentrations of Cu, Ni, Mo, Mn and Zn ranged between 0.01 and 0.6 mg L^{-1}.

5.3.2 Results

Although no detailed chemical analyses are listed in the above-mentioned work (SDAG WISMUT 1991), some developments can be recognised at least in the dissolution behaviour of arsenic and uranium, some of which had already been described by DYBEK (1962) or LANGMUIR (1978).

Here, we will not deal with the sufficiently known influences of temperature, redox potential, pH value and interactions with other water constituents (DYBEK 1962), but rather with the substance mobilisation over a longer period of time. The uranium mass concentration adjusts differently depending on the water temperature. While water at 20 °C initially dissolves little uranium, and after 20 … 40 weeks an increase from 5 … 10 mg L^{-1} to an average of 100 mg L^{-1} can be observed, warm water (50 °C) initially has approx. 5 mg L^{-1} and after 8 … 10 weeks less than 1 mg L^{-1} dissolved uranium.

The reason for this does not seem to be the temperature itself, but the reducing conditions in the warm water, for which the O_2 content of 0 mg L^{-1} is a clue. Since part of the uranium in uraninite is always in the oxidised form (UO_2 … U_3O_8; DYBEK 1962), this U(VI) will go into solution during the first weeks. The oxygen of the freshly filled water is consumed by the oxidation of different sulfides, primarily pyrite and marcasite. After about four weeks, all the oxygen in the already oxygen-poor warm water seems to be used up, resulting in reducing conditions. The already dissolved U(VI) is replaced according to equation 17 the already dissolved U(VI) is reduced by Fe^{2+} from the pyrite oxidation to U(IV) and precipitates as UO_2. At the same time, the uranium mass concentration decreases to a constant 0.5 … 1 mg L^{-1}.

$$(UO^{+VI}_2)^{2+}(aq) + 2\ Fe^{2+} + 3\ H_2O\ UO\rightarrow^{+IV}_2(s) + Fe_2O_3(s) + 6\ H^+ \qquad (17)$$

In water at 20 °C, no reducing but oxidising conditions occur. The oxygen is available for pyrite oxidation, leads to the formation of $Fe(SO_4)_3$and enables the oxidation of U(IV) to U(VI) according to equation 16. Therefore, the uranium mass concentration increases up to 150 mg L^{-1}, a value that has not yet been described in the reviewed literature for occurrences in nature.

In the case of arsenic, the differences between 20 °C and 50 °C tap water are less marked. In both cases, the mass concentrations drop from an initial 5 … 11 mg L^{-1} to 0.5 … 2 mg L^{-1} after 42 weeks at the latest and remain constant until the end of the test series (Fig. 20).

What conclusions can be drawn from this for the chemical conditions in the floodwater?

Initially, the flooding water will dissolve the easily soluble uranium and arsenic phases until either a chemical equilibrium between the water and the phase is reached or the phase is completely dissolved. In the case of arsenic, higher mass concentrations will initially be present in the mine water, which will decrease after some time, presumably due to adsorption of the arsenic. In the case of uranium, either higher or lower mass concentrations occur in the mine water depending on the redox potential. Higher redox potentials, which are always present in the upper part of the water columns (chapter 7.4.3) lead to relatively higher, lower redox potentials to correspondingly lower mass concentrations.

As can be seen from the results of the column experiments, at first only those uranium phases seem to go into solution that already contain uranium in oxidation state VI due to weathering processes (Chapter 4.9). Only at a later stage can sufficient U(IV) be oxidised and contribute to higher mass concentrations through complexation.

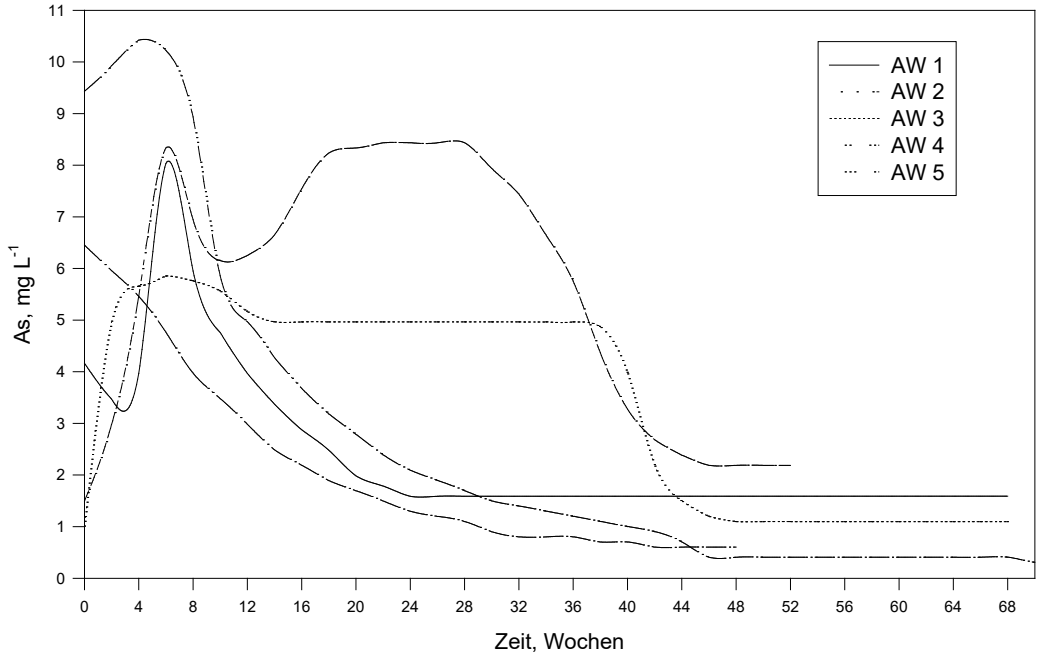

Fig. 20 Development of the arsenic mass concentration in the column tests AW1 … AW5 of SDAG Wismut (modified after SDAG WISMUT 1991).

6 Hydrogeochemical investigations

6.1 Introduction

The previous chapter described the geological processes that led to the genesis of the deposit and the accumulation of minerals in the rock and the veins. In addition, data on the hydrogeological conditions were collected in order to understand the relationship between water and rock.

The investigations on the hydrogeochemistry of the Niederschlema/Alberoda mine are now intended to describe the processes that lead to the release of substances from the minerals into the water. By means of chemical-thermodynamic equilibrium calculations, it will be investigated which phases are responsible for the control of the main constituents of the floodwater.

6.2 Material and methods

6.2.1 Sampling

Due to the restructuring within Wismut GmbH and the unresolved legal situation at the beginning of the period under review, it was not possible to optimally set up the underground sampling of the flooding water from the beginning. Rather, even without an existing monitoring programme, attempts were made to continuously monitor the flooding physicochemically. Most of the water sampling was carried out by employees of SDAG/GmbH Wismut, using different scoop vessels.

All samples were taken in the mine workings of the Niederschlema/Alberoda mine and filled into 1 … 5 L PVC sample bottles on site without prior filtering. While the sampling points on the non-flooded levels were directly accessible, the water samples from the flooded shafts could only be obtained with partly complex technical aids. For this purpose, the scoops were lowered either by means of electrically or manually operated steel winches 1 … 10 metres below the surface of the rising flood water and were retrieved after a short dwell time of 1 … 2 minutes. As far as the technical equipment allowed, temperature (WTW Oxi 96, measuring electrode EO 96), pH-value (Mauritius, pH ep2), oxygen content (WTW Oxi 96, measuring electrode EO 96) and electrical conductivity (WTW LF 90, measuring electrode KLE 1) were determined on site. The sample containers were usually taken to one of the laboratories on the same day without cooling and acidification and then kept there in the refrigerator until analysis.

The following major points of criticism of the sampling method, which could only be influenced to a limited extent by the author, should be emphasised, some of which only apply to the period from 1990 to the end of 1992:

- Initially unqualified sampling personnel
- wrong scoops
- Sampling partly at the water surface
- no sample filtering with 0.45 µm filter immediately after sampling
- no acidification with nitric acid immediately after sampling
- Partly missing temperature, pH, electrical conductivity and redox measurement on site
- No sufficient interlaboratory analyses in the laboratories
- irregular analysis of important chemical parameters
- no washing out of the sampling vessels with the respective sample.

Tab. 28: Mean values ($\bar{x}$), number of samples (n), standard deviations (s) and measurement units of the analysed and outlier-free parameters of Niederschlema/Alberoda separately for waters of types I, G, S. Standard deviations were given only for $n \geq 3$. For $n = 1$ the value in the column $\bar{x}$ corresponds to the measured value. COD: Chemical Oxygen Demand, TOC: Total Organic Carbon. The number of decimal places was chosen so that the smallest of the three values still has at least one valid place, but at least two places.

		Type S			Type I			Type G		
Parameter	Unit	n	$\bar{x}$	s	n	$\bar{x}$	s	n	$\bar{x}$	s
Temperature	°C	104	16.96	2.28	12	25.55	4.00	165	35.38	4.44
electrical conductivity	mS cm^{-1}	140	1.06	0.19	19	1.48	0.15	163	3.31	0.59
Eh value	mV	8	404.13	14.00	5	242.60	140.54	46	282.57	132.11
pH value	-	166	7.78	0.44	28	7.65	0.53	246	7.11	0.39
Filter residue	mg L^{-1}	98	21.23	31.08	13	29.95	39.70	130	61.09	85.76
Evaporation residue	mg L^{-1}	74	732.54	123.50	28	1101.57	431.37	199	2617.81	585.95
CSB	mg L^{-1}	-	-	-	-	-	-	66	70.92	10.90
TOC	mg L^{-1}	4	0.93	0.15	1	1.10	-	15	27.00	16.23
Ca^{2+}	mg L^{-1}	75	120.08	18.20	29	109.92	43.97	213	222.19	61.27
Mg^{2+}	mg L^{-1}	75	57.18	15.37	29	78.33	12.50	213	148.36	46.40
Na^{+}	mg L^{-1}	49	30.63	8.54	18	137.80	69.23	141	378.48	105.91
K^{+}	mg L^{-1}	36	4.36	1.07	18	9.73	7.11	119	37.14	4.85
Fe total	mg L^{-1}	53	0.10	0.13	9	0.33	0.37	98	2.66	2.31
Fe^{2+}	mg L^{-1}	5	0.02	0.01	10	0.11	0.07	51	2.46	2.18
Fe^{3+}	mg L^{-1}	4	0.04	0.02	8	0.59	0.87	34	1.60	1.95
Mn total	mg L^{-1}	13	0.26	0.82	5	0.51	1.01	158	2.80	1.21
NH_4^{+}	mg L^{-1}	2	0.07	-	2	0.25	-	58	0.68	0.76
Sr^{2+}	mg L^{-1}	8	0.99	0.39	-	-	-	17	2.64	0.48
SO_4^{2-}	mg L^{-1}	150	354.03	57.57	29	519.93	105.28	213	1138.36	263.68
Cl^{-}	mg L^{-1}	156	37.68	7.40	29	63.98	44.58	212	142.36	33.38
HCO_3^{-}	mg L^{-1}	74	187.65	37.47	28	270.53	82.30	209	889.52	264.71
NO_3^{-}	mg L^{-1}	143	9.18	1.90	25	2.88	1.07	146	2.17	1.54
NO_2^{-}	mg L^{-1}	-	-	-	4	0.03	0.02	36	0.06	0.12
CO_3^{2-}	mg L^{-1}	9	20.62	15.48	9	18.04	4.78	7	23.14	17.47
PO_4^{3-}	mg L^{-1}	14	0.14	0.10	13	0.29	0.10	72	4.42	2.07
F^{-}	mg L^{-1}	12	0.68	0.28	7	1.63	0.11	19	2.08	0.10
Total hardness	°d	154	30.24	3.86	29	33.28	7.50	213	65.21	15.86
Carbonate hardness	°d	41	8.53	1.44	16	12.04	0.90	106	42.09	8.41
Non-carbonate hardness	°d	36	19.54	2.98	12	19.33	2.39	83	28.02	6.30
O_2	mg L^{-1}	74	10.50	3.88	12	7.96	5.03	84	2.54	2.64
H_2S	mg L^{-1}	-	-	-	-	-	-	1	0.01	-
Ag	mg L^{-1}	-	-	-	-	-	-	1	0.08	-
Al	mg L^{-1}	21	0.21	0.02	11	0.26	0.25	62	0.37	0.22
As	mg L^{-1}	180	0.13	0.05	29	0.64	1.00	264	4.71	2.08
B	mg L^{-1}	4	0.04	0.03	1	0.06	-	4	0.20	0.12
Ba	mg L^{-1}	3	0.039	0.001	1	0.020	-	12	0.138	0.179
Be	mg L^{-1}	1	0.04	-	-	-	-	-	-	-
Bi	mg L^{-1}	2	0.07	-	-	-	-	8	0.07	0.03
Cd	mg L^{-1}	1	0.012	-	2	0.002	-	9	0.005	0.005
Co	mg L^{-1}	2	0.01	-	1	0.01	-	18	0.02	0.02
Cr	mg L^{-1}	1	0.003	-	1	0.015	-	28	0.005	0.006
Cs	mg L^{-1}	-	-	-	-	-	-	1	0.005	-
Cu	mg L^{-1}	11	0.02	0.03	6	0.03	0.03	38	0.03	0.03
H_2SiO_3	mg L^{-1}	16	15.89	1.23	16	15.48	2.26	75	32.49	7.06
Hg	mg L^{-1}	-	-	-	1	0.0001	-	2	0.0002	-
Li	mg L^{-1}	-	-	-	-	-	-	1	5.60	-
Mo	mg L^{-1}	2	0.027	-	3	0.031	0.002	10	0.199	0.179
Ni	mg L^{-1}	15	0.029	0.007	5	0.020	0.001	28	0.030	0.021
Pb	mg L^{-1}	9	0.005	0.003	11	0.008	0.007	39	0.011	0.008
Ra	mBq L^{-1}	86	218.03	183.06	25	565.32	286.89	141	2094.09	1013.33
Sb	mg L^{-1}	3	0.001	0.001	-	-	-	5	0.001	0.001
Se	mg L^{-1}	2	0.003	-	-	-	-	5	0.001	0.001
U	mg L^{-1}	176	0.78	0.30	28	2.07	0.50	260	2.82	0.90
V	mg L^{-1}	-	-	-	-	-	-	1	0.02	-
Zn	mg L^{-1}	25	0.03	0.03	14	0.12	0.18	66	0.11	0.14

Tab. 29 Analytical methods of the two laboratories in Aue and Chemnitz/Grüna. Br, Cs, $_2$HS, I, Rb, Si, SiO_2, and Th were analysed in external laboratories. Non-carbonate hardness calculated. Units in Tab. 28.

Parameter	Aue	Chemnitz/Grüna
Ag	Not analysed	DIN 38406-E22 (ICP-OES)
Al	Not analysed	DIN 38406-E9 (photometric) DIN 38406-E22 (ICP-OES)
Evaporation residue	DIN 38409-H1-1	DIN 38409-H1-1
As	photometric	DIN 38405-D18 (AAS hydride) DIN 38406-E22 (ICP-OES)
B	Not analysed	DIN 38406-E22 (ICP-OES)
Ba	Not analysed	DIN 38406-E22 (ICP-OES)
Be	Not analysed	DIN 38406-E22 (ICP-OES)
Bi	Not analysed	DIN 38406-E22 (ICP-OES)
Ca	DIN 38406-E32 -(titrimetric)	DIN 38406-E31 -(AAS flame) DIN 38406-E32 -(tirimetric)
Cd	Not analysed	DIN 38406-E191 DIN 38406-E192 DIN 38406-E22
Cl	DIN 38408-G4	DIN 38408-G4
Co	Not analysed	DIN 38406-E22 (ICP-OES)
CO_3^-	DEV D8	DEV D8
Cr	Not analysed	DIN 38406-E101 -(AAS flame) DIN 38406-E102 -(AAS furnace) DIN 38406-E22 (ICP-OES)
Chemical oxygen demand	Not analysed	DIN 38409-H41-1
Cu	Not analysed	DIN 38406-E71 -(AAS flame) DIN 38406-E72 -(AAS furnace) DIN 38406-E22 (ICP-OES)
Eh	DIN 38404-C6	DIN 38404-C6
F	Not analysed	DIN 38405-D41 -(ISE)
Fe	DIN 38406-E11 -(photometric)	DIN 38406-E22 (ICP-OES) DIN 38406-E11 -(photometric) DIN 38406-E191 -(AAS flame)
Filter residue	DIN 38409-H2-1	DIN 38409-H2-1
Total hardness	DIN 38409-H6	DIN 38409-H6, calculation
$_2HSiO_3$	Not analysed	Operating procedure (photometry)
HCO_3^-	DEV D8	DEV D8
Hg	Not analysed	DIN 38406-E124 -(AAS hydride)
K	Not analysed	DIN 38406-E13 (flame photometry)
Carbonate hardness	DIN 38409-H7	DIN 38409-H7
electrical conductivity	EN 26777:1993 (DIN 38404-C8)	EN 26777:1993 (DIN 38404-C8)
Mg	DIN 38506-E32/3 -(titrimetric)	DIN 38406-E31 -(AAS flame) DIN 38506-E32/3 -(titrimetric)
Mn	photometric	Flames AAS
Mo	Not analysed	DIN 38406-E22 (ICP-OES)
Na	Not analysed	DIN 38406-E14 (flame photometry)
NH_4^+	DIN 38406-E51 -(photometry)	DIN 38406-E51 -(photometry)
Ni	Not analysed	DIN 38406-E111 -(AAS flame) DIN 38406-E112 -(AAS furnace) DIN 38406-E22 (ICP-OES)
NO_2^-	Not analysed	DIN 38405-D10 (photometry)
NO_3^-	DIN 38405-D92 -(photometry)	DIN 38405-D92 -(photometry)
O_2	EN 25814:1992 (DIN 38408-G22)	EN 25814:1992 (DIN 38408-G22)
Pb	Not analysed	DIN 38406-E61 -(AAS flame) DIN 38406-E63 -(AAE furnace) DIN 38406-E22 (ICP-OES)
pH	DIN 38404-C5	DIN 38404-C5
PO_4^{3-}	photometric	DIN 38405-D11-4
Ra	emanometric	ULG 4/91 (emanometric)
Sb	Not analysed	DIN 38406-E22 (ICP-OES) DIN 38405-D18 (AAS hydride)
Se	Not analysed	DIN 38406-E22 (ICP-OES)
SO_4^{2-}	DIN 38405-D52 -(gravimetry)	DIN 38405-D52 -(gravimetry)
Sr	Not analysed	DIN 38406-E22 (ICP-OES)
Total Organic Carbon	Not analysed	DIN 38409-H3-1
U	ULG 2/91 (photometric)	ULG 2/91 (photometric) ULG 3/91 (fluorimetric); laser phosphorescence
V	Not analysed	DIN 38406-E22 (ICP-OES)
Zn	Not analysed	DIN 38406-E22 (ICP-OES) DIN 38406-E81 -(AAS flame)

The list shows that Wismut GmbH is not interested in the content of water-soluble substances, but in the total content including the colloidally bound ions. Until the end, no agreement could be reached between the author and Wismut GmbH on the question of whether the dissolved content or the total content should be determined in the water.

WENRICH-VERBEEK (1977) showed that filtration and acidification have a decisive influence on the uranium content of a water sample. In general, the uranium content is greater in the unfiltered samples than in the filtered ones, which is due to the adsorption of uranium compounds on suspended particles. Between sampling and analysis, this uranium goes into solution and therefore increases the uranium content in the water sample. Acidification of the unfiltered water would cause the uranium content in the analysis to be even higher than in the unfiltered sample.

MORIN (1990) demonstrated the difficulties that can arise in chemical analysis through ring analyses of waters from tailings piles of uranium mining. In particular, the experience of the laboratory, the chosen analytical method and the complex chemical matrix affect the results and determine their accuracy.

Since 1993, Wismut GmbH has been in the process of preparing and applying a quality management manual in accordance with ISO 9000, in which the quality and reliability of the measured values are specified (WISMUT GmbH 1994a). The question of the analysis of dissolved or total content of the water constituents to be analysed should definitely be included in this. In addition, the plausibility checks showed that Wismut GmbH passed on and still passes on analysis values that are not conclusive in themselves. In this study, these outliers are not included in the evaluation.

6.2.2 Analytical methods

Almost all water analyses were originally carried out by Wismut's own laboratories in Chemnitz/Grüna or in Aue. In the meantime, the former is an accredited laboratory that no longer belongs to Wismut GmbH. Depending on the laboratory, different procedures were used, which are listed in Tab. 28 are listed.

The results were also checked in other laboratories, including the LUT (Laboratory for Environmental Technology) in Jena and the Institute for Inorganic Chemistry at the Technical University of Clausthal. This showed that at least the order of magnitude of the measured parameters corresponded.

A detailed description of the analytical procedures will not be given here, since all analyses were carried out according to the standards that can be read in the German Standard Methods for Water Analysis (GESELLSCHAFT DEUTSCHER CHEMIKER 1982).

6.3 Evaluation

6.3.1 Graphical representation

For the statistical evaluation of the data from the 477 water analyses, it was necessary to classify them in order to be able to examine similar data collectives in each case. For this purpose, the data were entered into a PIPER and DUROV DIAGRAM (Fig. 22, Fig. 23). In addition, a log-As-Ca-U diagram was drawn up following WOLKERSDORFER (1994), which allows pit water and seepage water to be represented graphically (Fig. 24). The individual measuring points were given symbols according to their characteristics, which are identical for all figures (Tab. 30). The assignment was based on the clusters in the PIPER DIAGRAM and the position of the measuring points in the log-As-Ca-U diagram, whereby different measuring points in the same shaft were given the same type of symbol (e.g. m-363 and m-507).

Boxplots allow a clear visualisation of analytical values. These were created for 35 parameters of the water analyses of all measuring points, whereby the measuring points m-315, m-316, m-318, m-320, m-501, m-503, m-504, w-68 and w-92 were included in the measuring point SaSiWa (collective measuring point for seepage water). By means of boxplots different quantiles (10 %, 25 %, 50 %, 75 %

and 90 %), the mean value as well as values outside the 10 % and 90 % quantile can be displayed (Fig. 21). For normally distributed data, the mean and the median coincide. In contrast to the following statistical evaluation of the data, no elimination of outliers was carried out in order to record the complete range of the analysis values (Fig. 97 … Fig. 131).

In the PIPER DIAGRAM and type diagram according to FURTAK & LANGGUTH (from HÖLTING 1992), the water analyses of the Niederschlema/Alberoda mine can be divided into three types (Fig. 22). In the following, they are referred to as Type S (seepage waters), Type I (intermediate waters) and Type G (mine water) (Tab. 31).

Type S waters fall into field c of the type diagram, and are thus normally alkaline-earth, predominantly sulfatic waters. The waters of type I have a relatively slightly higher alkali content and are completely in field e, alkaline-earth waters with a higher alkali content, predominantly sulfatic. Type G water, which lies in the e and g fields of the type diagram, is characterised by further hydrogen carbonate and partial chloride uptake. It is thus an alkaline-earth, partly alkaline water with a higher alkali content, predominantly sulfatic.

Older water analyses from the Markus-Semmler-Stollen (number: 10, Tab. 19) and the Bismarck Spring (number: 1, Tab. 17) essentially coincide with type S, but have a slightly higher calcium content. In the type diagram they fall into fields c and b, which distinguishes them as normally alkaline-earth, hydrogencarbonate-sulfate to predominantly sulfate waters.

In order to keep the figure clear, the different water types were only graphically marked in the cation triangle of the PIPER DIAGRAM. The subdivision into three water types formed the basis for the following statistical evaluation.

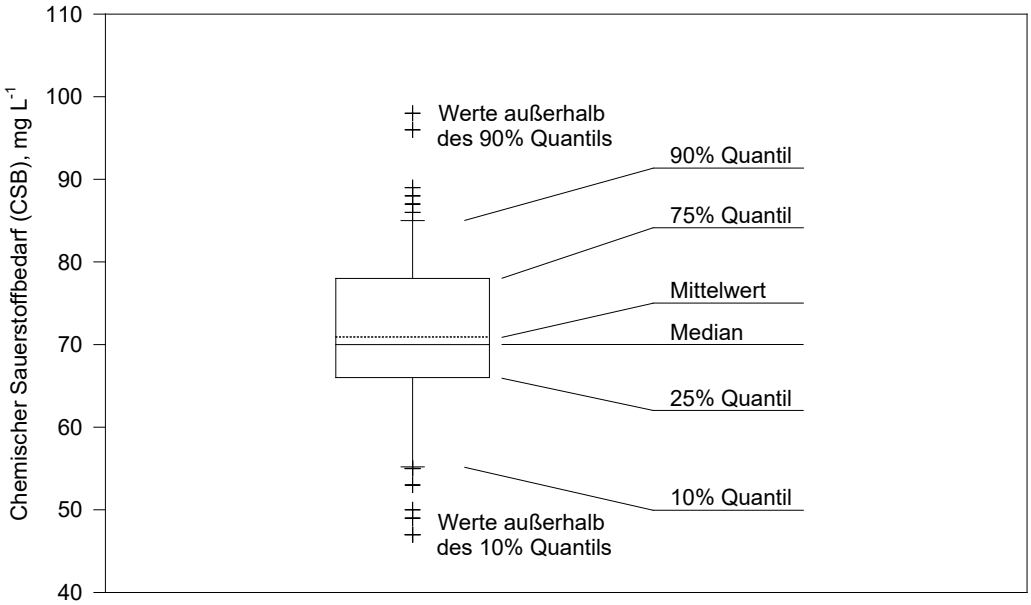

Fig. 21: Meaning of the lines of the boxplots using the example of all analytical values of the chemical oxygen demand (COD).

Tab. 30 Sampling points in the Niederschlema/Alberoda mine with the number of analyses and data points in the PIPER and DUROV DIAGRAMS. The allocation of the measuring points to the respective water type is based on the evaluation of the PIPER DIAGRAM. S: Seepage water, I: Intermediate water, G: Mine water. Shaft and roadway designations according to Wismut GmbH. FlWÜ: Escape route overburden, Ges.: Die, Q: Cross-cut, F-Str: Field section. The gridded symbols indicate measuring points with mine water character, squares and circles those with seepage character and diamonds those with intermediate character. In the case of changes in chemism in a shaft (e.g. 296 II b), the symbol first assigned was retained. To avoid an excessive number of symbols, measuring points with similar chemical characteristics were given the same symbol.

Measuring point	Designation	Symbol	Number	PIPER/DUROV	Type
m-107	Outflow of the Bohrbach dust basin, left side, pipe	○	169	41	S
m-308	Blind shaft 366 II b, to floor -990	△	115	48	G
m-315	Sole -540, F-str. 907 NW of Q 905	□	1	0	S
m-316	Sole -540, F-str. 906 NW of Q 903	□	1	0	S
m-318	Water lock 69, sole -540	□	1	1	S
m-320	Sole -540, Q 906a at F-str. 907	□	1	0	S
m-323	Blind shaft 371 II b, to floor -990	■	28	17	G
m-324	Blind shaft 372 b, to floor -990	▲	28	17	G
m-325	Blind shaft 296 II b, bottom -996, sump	◇	25	14	I
m-331	Blind shaft 366 II b, from bottom -990	●	44	14	G, 2 in I
m-332	Blind shaft 296 II b, from bottom -996	◇	3	1	G
m-362	Blind shaft 1 b	◆	10	9	G
m-363	Blind shaft 383 b	⬢	23	20	G, 3 in S
m-364	Blind shaft 383 III b	▽	4	3	G
m-365	FlWÜ2, soles -1665, -1710	▽	5	3	G
m-501	Blind shaft 186 b, bottom -540	□	2	1	S
m-503	Shaft 38, bottom -540	□	4	3	S
m-504	Blind shaft 38 II b, bottom -990	□	1	1	I
m-505	Shaft 383, bottom -1260	▽	1	1	G
m-506	Blind shaft 383 b, bottom -1485	▽	4	2	I, G
m-507	Blind shaft 383 III b, bottom -1665	▽	3	2	G
m-509	Sole -1485, Ges. 3	▽	1	1	G
m-510	Sole -1530, Q 2007	▽	1	1	G
w68	Sole -240, without place	□	1	0	S
w92	Sole -816, inlet	□	1	1	S

Tab. 31: Averaged percentage equivalent mass ratios of cations and anions of water types S, I and G in the PIPER and DUROV DIAGRAMS. Average mass contents in Tab. 28.

Water type	Designation	Ca	Mg	Na	HCO_3^-	SO_4^{2-}	Cl
Type S	Seepage water	50	38	12	25	67	8
Type I	Intermediate waters	30	40	30	30	62	8
Type G	Mine water	25	32	43	35	57	8

Another graphical representation possibility is the DUROV DIAGRAM presented in the former USSR by DUROV (quoted from CHILINGAR 1956). To enter the cations and anions in the diagram, they must be converted into their equivalent masses and their respective percentage share determined. In the quadrilateral diagram, the points are then obtained by horizontal or vertical projection of the points from the triangular diagrams. In total, five water classes numbered I to V can be distinguished in the DUROV DIAGRAM (CHILINGAR 1956).

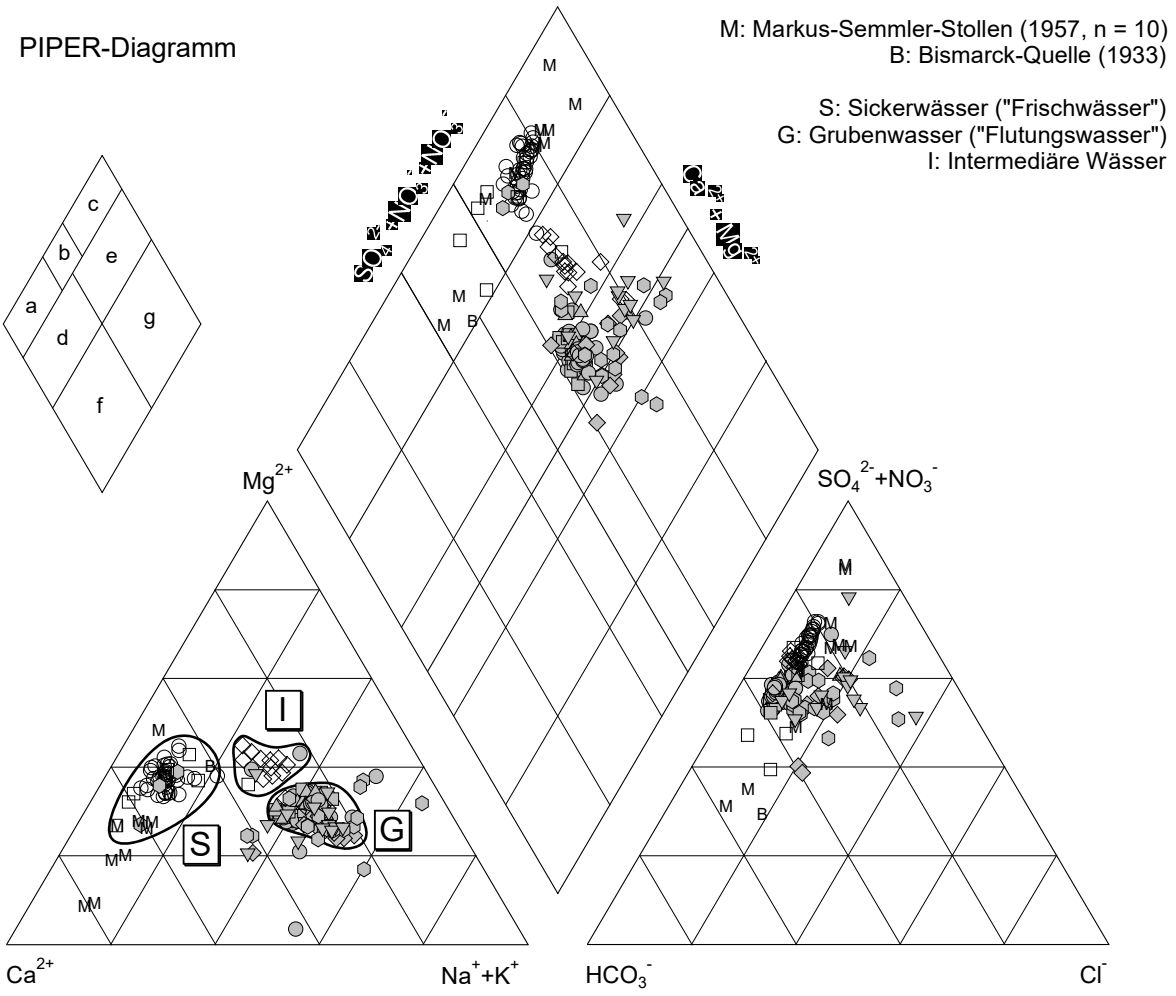

Fig. 22: PIPER DIAGRAM OF the water analyses of the Niederschlema/Alberoda mine. 212 value pairs, additionally 10 older analyses from the Markus-Semmler adit and one from the Bismarck spring. Legend s. Tab. 30. Small graph: Type diagram according to FURTAK & LANGGUTH (this from HÖLTING 1992).

Some of the water analyses from Niederschlema/Alberoda are secondary waters (Class II), but the majority are transitional waters between secondary and sulfatic waters (Class III). Primary (Class I), chloridic (Class IV) as well as alkali-bicarbonate waters (Class V) are completely missing.

Three analyses of the blind shaft 383 b (m-363) are in the range of type S waters. These are analyses 10, 25 and 26, which do not come from the flooding water, but from feed pipes into the blind shaft. The sampling location therefore differs from that of the 17 other samples from the blind shaft shown in the diagram. According to their character, they are clearly seepage water, which is also shown by the key figures q_1 and q_2.

At the beginning of the study period (1990 … 1991), the seepage water and the mine water hardly differed in their substance loads. Therefore, a possibility was sought to distinguish them from each other by means of ratios. q_1 and q_2 are the logarithms of two empirically determined quotients from the As, U and Ca substance quantities. By definition, the substance quantity n_x with the unit 1 mol is the quotient of the mass m and the molar mass M of the respective substance x:

$$n_x = \frac{m_x}{M_x} \qquad (18)$$

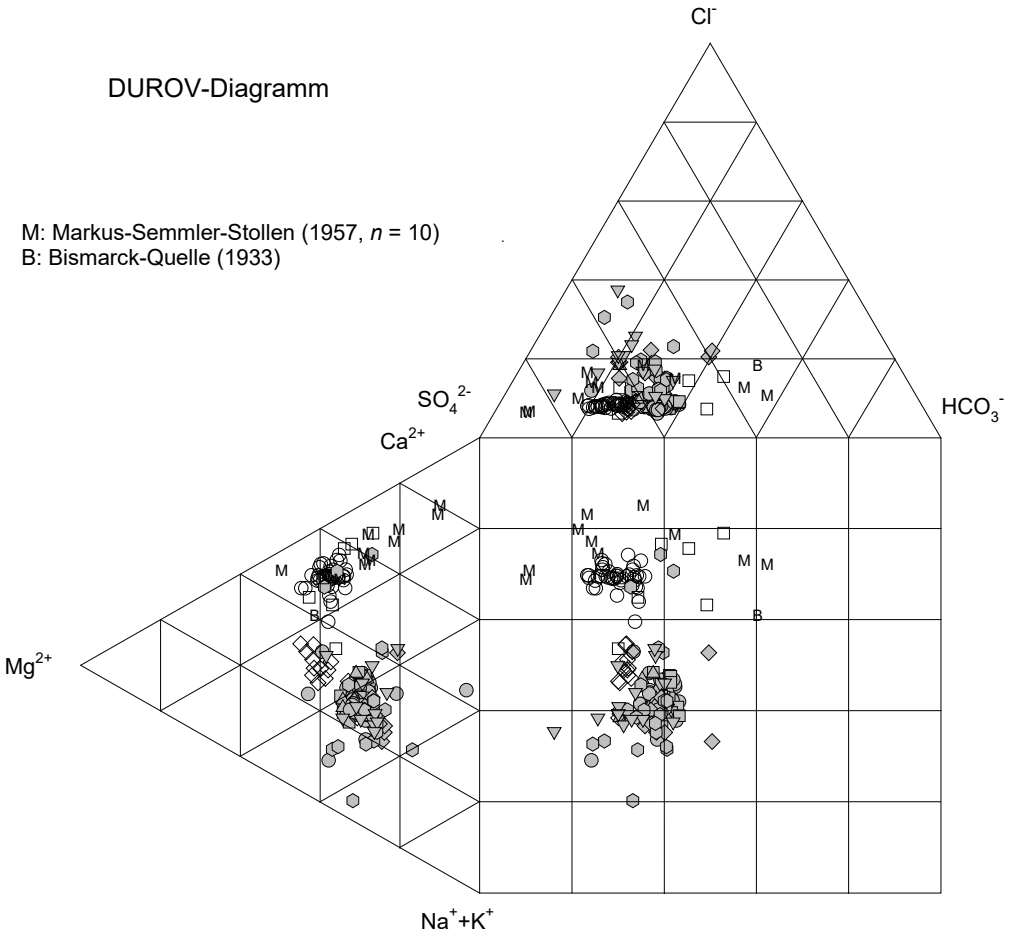

Fig. 23: DUROV DIAGRAM OF the water analyses of the Niederschlema/Alberoda mine. 212 value pairs, additionally 10 older analyses from the Markus-Semmler adit and one from the Bismarck spring. Legend see Tab. 30.

The following equations apply to the ratios q_1 and q_2:

$$q_1 = \log(\frac{n_U}{n_{As}}) \quad (19)$$

$$q_2 = -\log(\frac{n_{As}}{n_{Ca}}) \quad (20)$$

The log-As-Ca-U diagram shows that water of type G contains predominantly more uranium than arsenic. Type I and S waters, on the other hand, contain relatively more arsenic than uranium. Intermediate waters are characterised by lower n_{As}/n_{Ca} ratios than seepage waters. In most cases, the intermediate waters lie above the regression line of q_2 with respect to q_1 in the diagram, the seepage waters below.

It turned out that the histograms of q_1 and q_2 each have two maxima which can be assigned to a lognormal distribution. The smaller maxima in terms of value belongs to the measuring points of type G (m-308, m-323, m-324, m-331, m-332, m-362, m-363, m-364, m-365, m-505, m-507, m-509, m-510), the larger to those of type S or I (m-107, m-315, m-316, m-318, m-320, m-325, m-501, m-503, m-

504, m-506, w-68, w-92). Obviously, certain q_1 and q_2 exist that allow to distinguish waters of type G from those of types S and I. This q shall be referred to as the deposit-specific limiting index Q and, with a statistical certainty of, as $\alpha Q(\alpha)$. Depending on the approach, $Q(\alpha)$ is thus the index up to which $S = 1 - \alpha$ all q have the character of a mine water or that of a seepage water. In the log-As-Ca-U diagram (Fig. 24) only the upper boundary parameters $Q_1(\alpha)$ and $Q_2(\alpha)$ of the mine water are shown, since only the demarcation of mine water from the seepage water was of interest. As has been shown elsewhere (WOLKERSDORFER 1993), the boundary indices for two different deposits are not identical, so that the designation *deposit-specific* boundary indices seems justified.

The following null and counter hypotheses will therefore be tested to determine the upper boundary indices of the mine water and the lower ones of the seepage water:

H_0: $q_1(G)\ Q \leq_1 (G)$ H_1: $q_1(G) > Q_1(G)$ $\alpha = 0.05$ and 0.10

H_0: $q_2(G)\ Q \leq_2 (G)$ H_1: $q_2(G) > Q_2(G)$ $\alpha = 0.05$ and 0.10

H_0: $q_1(I,S)\ Q \geq_1 (I,S)$ H_1: $q_1(I,S) < Q_1(I,S)$ $\alpha = 0.05$ and 0.10

H_0: $q_2(I,S)\ Q \geq_2 (I,S)$ H_1: $q_2(I,S) < Q_2(I,S)$ $\alpha = 0.05$ and 0.10

To obtain the one-sided confidence intervals $\alpha = 0.05$ and $\alpha = 0.10$ of q_1 and q, all q_1 and q had to be transformed to obey approximately a normal distribution:

$$q_1' = \log(q_1 + 2.5) \quad (21)$$

$$q_2' = \log(q_2) \quad (22)$$

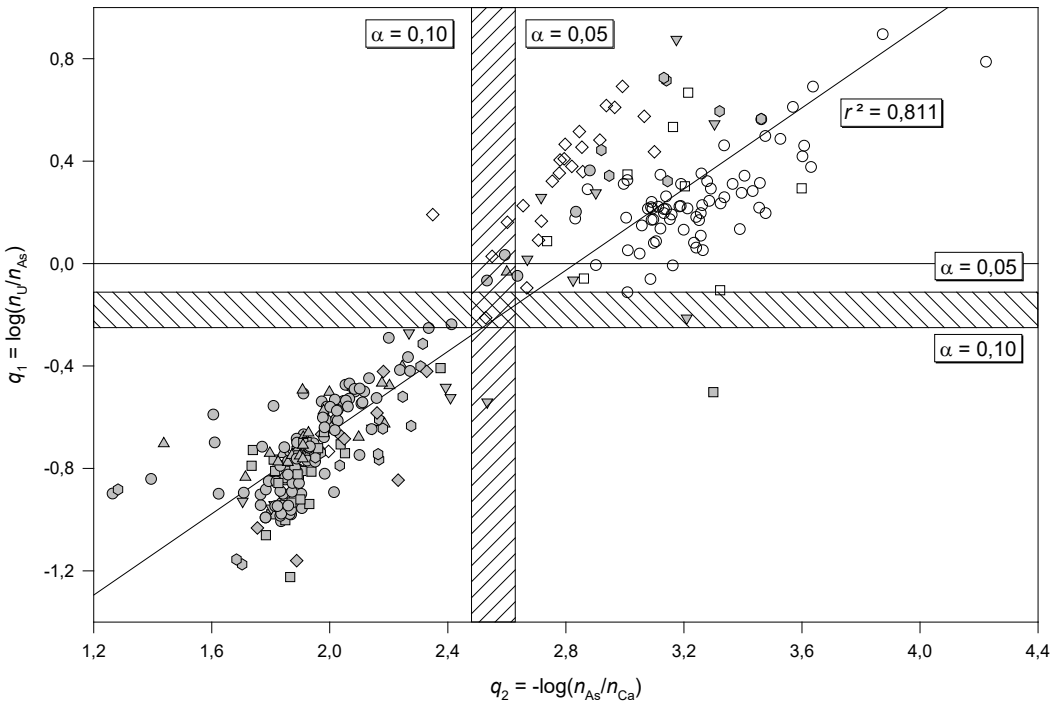

Fig. 24 log-As-Ca-U-diagram of the water analyses of Niederschlema/Alberoda between 12.4.1990 and 20.12.1994. 312 value pairs. $r^2 = 0.811$. Mine water (gridded symbols) is marked by its position below the hatched transition areas. Upper limits of mine water: $Q_2(0.10) = 2.48$, $Q_2(0.05) = 2.63$, $Q_1(0.10) = 0.-25$, $Q_1(0.05) = 0.-11$. Legend see Tab. 30. Further explanations in the text.

Of the four new quantities, the mean $\bar{x}$ and standard deviation s *were* calculated and the upper and lower limits of $Q_1(\alpha)$ and $Q_2(\alpha)$ were determined from these. The variable to be tested Z is:

$$Z = \frac{q' - \overline{x}}{s} \tag{23}$$

The results are summarised graphically in the log-As-Ca-U diagram (Fig. 24) and the table (Tab. 32). In the log-As-Ca-U diagram the area between $Q(0.10)$ and $Q(0.05)$ can be seen in the shaded area. It represents the transition area from seepage water to mine water.

Tab. 32 Calculation results of the deposit-specific boundary parameters $Q_1(\alpha)$ and $Q_2(\alpha)$ to distinguish between seepage water and mine water.

Value	Transformation	$\overline{x}$	s	n	Border	$Q(0.10)$	$Q(0.05)$
q_1(G)	$\log(q_1 + 2.5)$	0.2616	0.0714	261	upper	–0.25	–0.11
q_2(G)	$\log(q_2)$	0.3056	0.0696	214	upper	2.48	2.63
q_1(I,S)	$\log(q_1 + 2.5)$	0.4427	0.0395	203	lower	–0.03	–0.11
q_2(I,S)	$\log(q_2)$	0.4870	0.0549	102	lower	2.61	2.49

6.3.2 Statistical methods

6.3.2.1 Introduction

The analysis results were examined separately for seepage water (type S), mine water (type G) and intermediate water (type I) using statistical methods. The aim of the investigations is to describe the respective water types with statistical methods and to statistically substantiate their graphic allocation.

All statistical investigations were carried out on an 80486DX2 processor with the aid of the programme SigmaStat for Windows, the graphic representation with the graphic programme SigmaPlot for Windows (JANDEL SCIENTIFIC 1994b, 1994a). EXCEL for Windows and ACCESS for Windows (MICROSOFT CORPORATION 1993a, MICROSOFT CORPORATION 1994) were used as database programmes. The outlier test was carried out by a self-written macro in EXCEL.

6.3.2.2 Outliers and plausibility check

Some of the values from the water analyses of the Niederschlema/Alberoda mine deviate substantially from the mean value of the respective parameter. Therefore, statistical methods had to be used to prove whether they were outliers or whether they belonged to the population.

An “outlier” is a value in a sample that deviates substantially upwards or downwards from the other values. In order to identify whether the outlier belongs to the population or not, different statistical methods have been introduced into the literature, five of which are listed here as examples. The reason why possible outlier tests are presented in such detail is that there are always two questions to be answered when eliminating outliers: on the one hand, the “right” test method, and on the other hand, whether or not an outlier should be eliminated at all.

The significance of a statistical test tells us whether differences in the data sets are statistical or systematic. It is expressed by the probability with which the assumptions made in the test do not apply. A test result is usually significant if the probability of the assumption not being true is less than 0.01. Statistically significant test results therefore indicate a systematic relationship between two test variables.

If there is a normally distributed sample with n values, an outlier x_n can be recognised with the certainty $S = 1 - \alpha$ by the fact that it $_{(u);\,1-\alpha}$exceeds a threshold value x (STANGE 1970).

The threshold value is determined to:

$$x_{(u);\,1-\alpha} = + - \mu\sigma\, u_{(n);\,1-\alpha} \tag{24}$$

with

$$u_{(n);1-\alpha} = u_{\sqrt[n]{1-\alpha}} \tag{25}$$

where can be determined graphically $u_{\sqrt[n]{1-\alpha}}$, calculated or read from tables.

DOERFFEL (1965) presents a similar method according to GRAF, HENNING, GOTTSCHALK and DEHMEL (quoted from DOERFFEL 1965). In order to detect an outlier x_n, the mean value $\bar{x}$ and standard deviation s of the sample are determined without the value suspected of being an outlier. x_n can then be considered an outlier if applies:

$$x_n \; s </> \; \bar{x} \pm - g(1 - \alpha \; , \; n - 1) \tag{26}$$

$g(1 - \alpha \; , \; n - 1)$ is determined graphically as a function of the required statistical certainty and can be ≤applied for 4 $n \leq$ 1000.

The frequently used Nalimov test (KAISER & GOTTSCHALK 1976) or *r*-test (GOTTSCHALK & KAISER 1976) for outliers should no longer be used because it is statistically incorrect (KAISER & MÜHLBAUER 1983). This manifests itself in the formation of value collectives, with a scatter that does not correspond to the measurement method used.

KAISER & MÜHLBAUER (1983) present the SHAPIRO-WILKS TEST (W-test), in which a largest value x_n of the sample with standard deviation *s is* an outlier with certainty $S = 1 - \alpha$ if holds:

$$\frac{1}{(n-1)\cdot s^2}\left(\sum_{i=1}^{n/2} a_{n,n-i+1}\cdot\left(x_{n-i+1} - x_i\right)\right)^2 > w\left(1-\alpha\right) \tag{27}$$

The prerequisite for the application is a normal distribution of the sample with $n \geq 3$. This relatively complex test can be used especially for small samples, as it does not cause any distortion of the distribution. $w(1 - \alpha)$ can be taken from tables.

It is suggested by MEYER (1976) TO remove a value x_n from an $n \geq 10$ large sample if

$$x_n \pm \gtrless \bar{x} \; s - 4 \tag{28}$$

and $\bar{x}$ *s* are each to be calculated without the value x_n to be tested.

Due to the large amount of data, the test for the threshold value (STANGE 1970) could be used for the analyses of Niederschlema/Alberoda. It has the advantage that a test algorithm is easily programmable and the outlier-suspicious value does not have to be eliminated before the test. The statistical certainty was assumed to be $S = 0.99$.

The outliers were determined separately for the different measuring points and only addressed as such if it was not possible to clarify what caused the value to be too high or too low. Supplementary plausibility checks supported the decision-making process in all cases. A value that did not fit into the sample only by the outlier test, but seemed to be correct in the plausibility check, was not removed from the data set. Of the 8611 individual values, 0.6 % (52) had to be eliminated after the outlier test and plausibility check.

6.3.2.3 Mean value

For each water type, the mean values of the investigated parameters are calculated according to equation 29 (Tab. 28).

$$\bar{x} = \frac{1}{n}\sum_{i=1}^{n} x_i \tag{29}$$

Since the mean value is sensitive to outliers, the test was only carried out on outlier-free data material. Even a single analysis value that is too large or too small can simulate a result that does not

correspond to the real conditions. In the boxplots, on the other hand, the mean values of the entire data set of a parameter are shown for each measuring point.

6.3.2.4 Standard deviation

As with the mean value, the standard deviations (equation 30) was carried out on data sets free of outliers. The standard deviation shows how much the measured values scatter around the mean value (DAVIS 1986). Since the standard deviation for $n = 2$ corresponds to half the amount of the difference between the two measured values, the standard deviations in the table (Tab. 28) are only given if the number of measured values n is greater than 3. The relative standard deviations MSD (mean standard deviation) are not given, since they can easily be calculated from the mean value and the standard deviation s by division. $\overline{x}$ and the standard deviation s.

$$s = \sqrt{s^2} = \sqrt{\frac{1}{n}\sum_{i=1}^{n}(x_i - \overline{x})} \qquad (30)$$

The example of Ca shows that the values for seepage water are less scattered around the mean value than those for mine water.

6.3.2.5 No n-parametric analysis of variance (KRUSKAL-WALLIS test)

The aim is to test whether the water types S, I and G are significantly different from each other or whether type I possibly belongs to type S or G. The results are then used to determine whether the water types S, I and G are significantly different from each other. For this purpose, the analysis of variance or ANOVA (Analysis of Variance) is usually applied with the following null hypothesis (DAVIS 1986, JANDEL SCIENTIFIC 1994b):

H_0: = $\mu_1 = \mu_2 = \ldots = \mu_n$

As soon as at least one variance μ differs significantly from the others, the null hypothesis must be rejected.

For non-normally distributed samples, the ANOVA of the rank (KRUSKAL-WALLIS test) is used instead, whose test variable H *is* defined as follows (DAVIS 1986):

$$H = \frac{12}{N \cdot (N+1)} \sum_{j=1}^{k} \frac{\left(R_k - n_k \cdot (N+1)/2\right)^2}{n_k} \qquad (31)$$

with and $N = \sum_{j=1}^{k} n_k$ $R_k = \sum_{i=1}^{n_k} R(x_{ik})$, where $R(x_{ik})$ is the *i-th* rank of the *k-th* sampling.

H obeys approximately a χ^2-distribution for large amounts of data, so that the critical limits of H can be taken from the χ^2-distribution as a function of the degree of freedom $\nu = k - 1$ and the statistical certainty $S = 1 - \alpha$ tables.

For the most important parameters of the water analyses of Niederschlema/Alberoda all probabilities *P of* the null hypothesis are < 0.0001 (Tab. 33), so that it must be rejected. Consequently, types S, I and G are independent water types with significantly different chemistries.

Tab. 33 Result of the statistical evaluation of some main parameters with the KRUSKAL-WALLIS test (non-parametric analysis of variance of the rank). Critical values of the χ^2-distribution with the safeties α = 0.01, α = 0.05 and α = 0.10. Degree of freedom ν for all evaluations 2.

Parameter	*H*	*P* (α = 0.05)	Degrees of freedom	Critical value		
			ν	α = 0.01	α = 0.05	α = 0.10
As	333.4	< 0.0001	2	9.21	5.99	4.61
U	307.1	< 0.0001				
Ca	150.0	< 0.0001				
Mg	171.9	< 0.0001				
Na	127.9	< 0.0001				
SO_4^{2-}	281.4	< 0.0001				
Cl	277.3	< 0.0001				
HCO_3^-	193.2	< 0.0001				
PO_4^{3-}	52.1	< 0.0001				
Ra	173.5	< 0.0001				
pH	176.4	< 0.0001				

6.3.2.6 Multiple comparison (DUNN Test)

In order to statistically check the graphical allocation of the individual measuring points to the water types S, I and G, a multiple comparison can be applied, which compares several samples with each other individually. The DUNN test is applicable to all non-normally distributed samples with unequal variance (JANDEL SCIENTIFIC 1994b).

The differences from the mean values of the ranks, the distance of the differences *p,* the test variable *Q* and the probability *P are* calculated. *Q* is a measure of the difference between the samples, whereby it can be assumed that the difference between the samples is significant if *Q* is large. If *P is less than* 0.05, then the assumption of a significant difference between the two samples with less than 5% probability is false.

To verify the classification into three water types, the parameters As, U, Ca, Mg, Na, SO_4^{2-}, Cl and HCO_3^- were compared. At $Q > 10$ the difference between the measuring points is significant, i.e. they must not be combined in one water type, while at $Q < 1.0$ a similarity cannot be ruled out. The classification table (Tab. 57) shows that the classification based on graphical criteria (Tab. 30) can be considered statistically reliable.

6.3.2.7 Correlation (PEARSON Product Moment Correlation)

A measure of the linear dependence of two variables is the correlation coefficient r_P, which results from the parametric correlation (PEARSON Product Moment Correlation). For this purpose, the covariance COV_{jk} of the variables is formed and divided by the product of the standard deviations $s_j - s_k$ (YAMANE 1976):

$$r_{jk} = \frac{COV_{jk}}{s_j \cdot s_k} \quad (32)$$

whereby:

$$COV_{jk} = \frac{1}{n} \cdot \sum_{i=1}^{n} \left((x_{ij} - s_j) \cdot (x_{ik} - s_k) \right) \quad (33)$$

The values of r_P range from –1 to +1, with the sign indicating whether there is a negative or positive correlation (JANDEL SCIENTIFIC 1994b). A correlation coefficient of 0 indicates that there is no correlation between the two parameters. On the other hand, the greater the value of r_P, the greater the correlation between the two parameters, without this immediately resulting in a dependence of the two.

After each correlation, it is tested whether the correlation coefficient r_P *is* significantly different from 0. The associated two-sided null and counter hypothesis is (YAMANE 1976):

H_0: $r_{jk} = 0$

H_1: $r_{jk} \neq 0$

The probability of the *t*-statistic with degree of freedom $\nu = n - 2$,

$$t = \frac{r_{jk}}{\sqrt{\frac{1 - r_{jk}^{\ 2}}{\nu}}} \tag{34}$$

results from the two-sided density function of the *t*-distribution:

$$P(t \mid \nu) = 1 - F(t \mid \nu) \tag{35}$$

As soon as $P(t \mid \nu)$ is greater than 0.05, the null hypothesis must be rejected and the correlation coefficient r_P is not significant.

In the table of correlations (Tab. 58, Tab. 59) the probabilities *P are* tabulated in addition to the correlation coefficient r_P. No correlation coefficient can be calculated for parameter combinations that form fewer than 4 value pairs. These pairings are tabulated with ./.

To represent the large amount of data in the tables, the symbols tabulated below are used. Thus, all parameter combinations with the symbols ++< and --< show the highest correlation with the greatest significance. Not shown are parameters that do not show a significantly high correlation to other parameters. These include, for example, NH_4^+ or Cd.

Signa-ture	Regression coefficient (PEARSON correlation)	Test value *P*
++<	1,00 *r* o≥≥,6o	*P* < 0,1
- -<	-1,00 *r* ≤≤-0,6o	*P* < 0,1
+++	1,00 r o≥≥,8o	*P* o≥,1o
++	0,8o > *r* o≥,6o	*P* o≥,1o
+	0,6o > *r* +o≥,oo	Tab. 58
-	-0,6o < *r* ≤-0,oo	Tab. 58
- -	-0,8o < *r* ≤-0,6o	*P* o ≥,1o
- - -	-1,oo *r* ≤≤-0,8o	*P* o ≥,1o
<		*P* < 0,1o
>		*P* o ≥,1o
≪		*P* < 0.1o, *n* ≤ 8
./.	*n* < 3, correlation not possible	

6.3.3 Development over time

6.3.3.1 Introduction

Determined by the different nature of the water-mountain contact, the three water types show unequal temporal developments in the magnitudes of their constituents and physico-chemical properties over the four-year study period. The temporal variation is most pronounced for type G, while types S and I have almost constant properties. Type S seeps are in contact with the rock for between a few days and three months before they are either pumped to the surface from level -540 or flow further down into the mine workings. These are young meteoric waters in which the mass concentrations of the constituents are relatively low.

Type G mine water has been in the mine workings for more than four years in some cases and has been in contact with the rock or the surfaces in the mine workings from the time it entered the

underground part of the water cycle until today. Due to the long contact time, the water could partly be highly enriched with elements, whereby the mass concentration depends on the residence time on the one hand, and on the geochemical properties of the rock on the other hand.

Intermediate waters of type I are intermediate in character between those of types G and S. They are seepage waters that usually occur in a shaft in which – for whatever reason – no convection cell has yet built up (chapter 7.7).

All time courses have in common a decrease in the scatter in the individual values from about 1993 onwards. This indicates a more exact determination in the two laboratories, which leads to an increase in reproducibility. After a summary presentation of the respective water types in the chapters 6.3.3.2 … 6.3.3.4 is followed by a presentation of some essential water constituents and physical parameters in the chapters 6.3.3.5 … 6.3.3.16.

6.3.3.2 Type S

Overall, the physicochemical properties of the type S waters remained almost unchanged during the study period.

Only NO_3^- and O_2 as well as electrical conductivity and total iron mass concentration show a temporal dependence. All other parameters either have no temporal variation or only a variation that is not statistically significant.

The mass concentrations of NO_3^- and O_2 show an opposite course that varies with the season, with a maximum for NO_3^- in the first half of the year and for O_2 in the second half. Such a behaviour, however dependent on depth, can be observed during the stagnation period in lakes (STUMM & MORGAN 1981), where due to photosynthesis the oxygen concentration decreases with increasing nitrogen concentration. Therefore, it can be assumed that, in addition to substance inputs from agriculture, the seasonal change in substance turnover during photosynthesis plays a role in this seasonal course.

The slight decrease in electrical conductivity ($r^2 = 0.12$), which is accompanied by unrelevant decreases in potassium, chloride and phosphate mass concentrations, is probably due to the decrease in fertiliser use, which was associated with the decline of the LPGs (agricultural production cooperatives) after the collapse of the SED regime. Since some of the fertilisers contain iron, in the case of the Tangermünder Universaldünger (universal fertiliser) used in the GDR it is reportedly a trace element (VOIGT 1990), the decrease in iron mass concentration ($r^2 = 0.17$) can possibly also be explained by this.

Other parameters show a small, non-significant temporal dependence ($r^2 \leq 0.10$: As, U, pH, HCO_3^-, GH, Ra, Al, H_2SiO_3). This could be due to the increase in analytical reproducibility, which affects the numerical value of the regression coefficient.

6.3.3.3 Type I

A temporal change in the type I waters is only present for uranium and sodium. All other parameters seem to tend to decrease, but due to the small amount of data and a partly strong scattering, this is not numerically detectable.

It is not possible to determine with certainty to what the tendential increase in the uranium mass concentration and the decrease in the sodium mass concentration can be attributed. In both cases the regression coefficient r^2 is low (U: $r^2 = 0.11$, Na: $r^2 = 0.43$), but significant.

The explanation for this is the type of water inflow shown above (chapter 4.7). Easily soluble U(VI) compounds are dissolved by the infiltrating water, but since only little mineralised material flows around, the increase is relatively small. Conversely, the decrease in sodium mass concentration is due to a dilution effect caused by the inflow of infiltrating water.

6.3.3.4 Type G

Different temporal changes characterise water of type G, where about half of all parameters have a clear time dependence. This can be broken down as follows:

- continuous increase: SO_4^{2-}, Na, K, Ra, Leitf, Fe(II), NKH, Fe(III), Sr
- Increase to constant: Ca, Mg, AR, HCO_3^-, GH, temperature, KH, Al, $_2HSiO_3$
- Waste: pH, COD, Pb, Co, Mo, CO_3^{2-}, TOC
- Waste to Constance: Cl
- fluctuating: As, U, PO_4^{3-}
- insufficient values: OH^-, Hg, Ag, $_2HS$, Be, Li, Cs, U, Br, I, Rb, Th
- no dependence: $NO-_3$, Eh, Fe(ges), Cu, Cr, Cd, Se, Sb, F, B, Bi
- ± constant values: Mn, Zn, O_2, FR, NH_4^+, Ni, NO_2^-, Ba

Essentially, the strong increases in mass concentrations since the first quarter of 1994 have come to an end; in the case of arsenic and phosphate, a decrease in mass concentration is already evident. Uranium, on the other hand, is still increasing, because with the rise of mine water into higher, older mine workings, surfaces are available that have already been exposed to the oxidising conditions of the mine air for a long time. The dissolution behaviour of arsenic and uranium is almost consistent with the results of the column experiments described elsewhere (chapter 5.3). However, not only the geochemical behaviour of the two elements is responsible for this, but also a decrease in the arsenic content in the ore veins towards the upper levels (SDAG WISMUT 1991). Uranium is present in roughly constant quantities in the veins. Since the mass concentrations of Ca, Mg and hydrogen carbonate no longer increase, calcite and dolomite seem to be in solution equilibrium with the mine water.

6.3.3.5 pH value

During the study period, the pH of the floodwater was in the buffer range of the calcite and dolomite (Fig. 100). In the seepage water, the pH value is on average 7.8 and shows no significant temporal variation.

The same applies to the pH value of the mine water (Fig. 25), which, with an average of 7.1, is slightly below that of the seepage water and thus in the neutral range. A dependence on the measuring point cannot be determined.

A forecast of the future development of the pH value is given in chapter 6.3.4.2 a forecast is given.

6.3.3.6 Redox potential

As can be seen from chemical-thermodynamic equilibrium calculations (chapter 6.4), the redox potential is of great importance for the equilibrium setting of the phases of interest in the Niederschlema-Alberoda mine water. Nevertheless, only a few redox measurements from the seepage water and the mine water are available overall (Fig. 26, Fig. 99). Furthermore, the in-situ measurement results with a mobile multiparameter probe (LogIn GmbH, Gommern) partly deviate considerably from the potentials measured on site in the sampling container.

The few measurements in the seepage water (n = 8) are uniformly at 400 mV, whereas those of the mine water vary from 80 … 450 mV (n = 38; $\bar{x}$ = 280; s = 113, mean value only from the analyses that WATEQ4F used for calculation). With this relatively large range of measurement results, the question therefore arises as to which redox potentials are really present in the mine water.

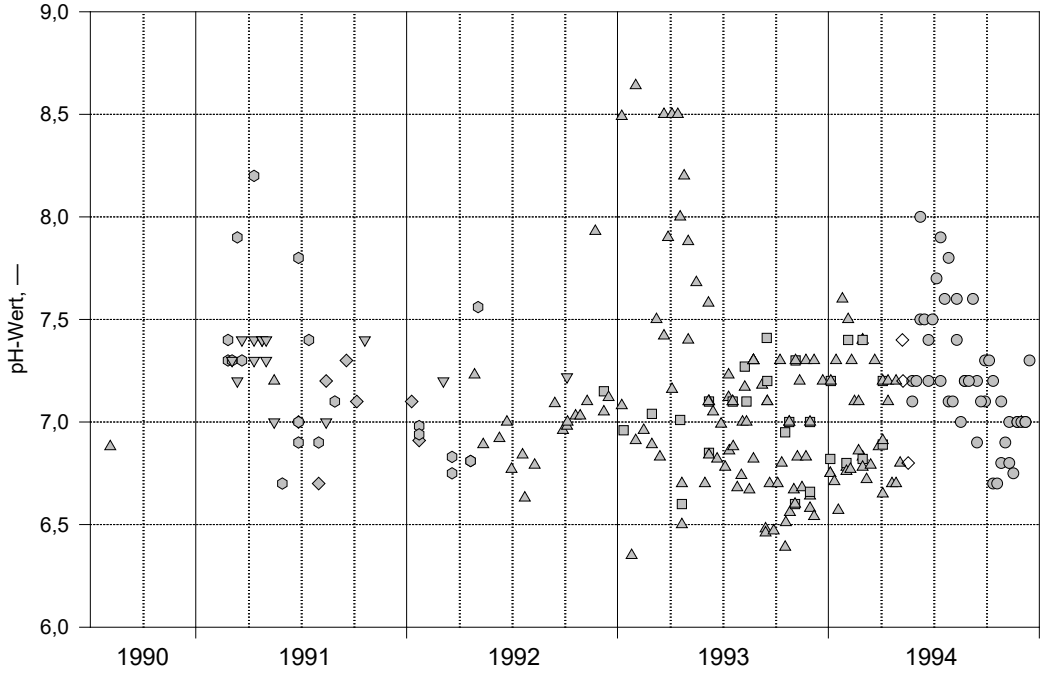

Fig. 25 Temporal development of the pH value for type G water between July 1990 and December 1994. 246 value pairs. Legend see Tab. 30.

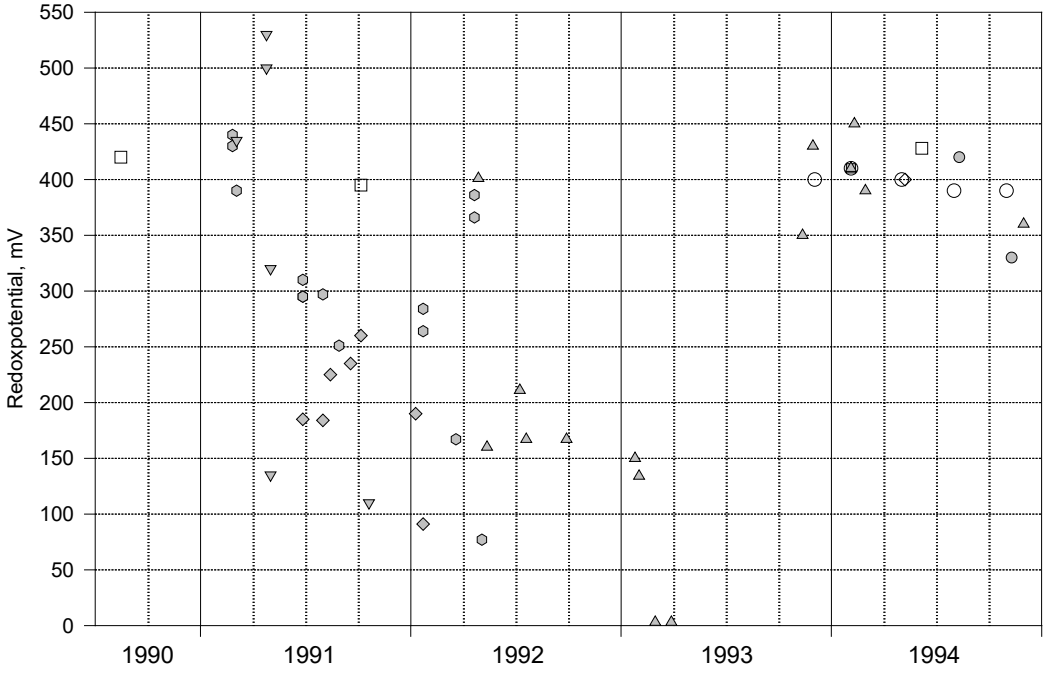

Fig. 26: Temporal development of the redox potential for water of type G (46 pairs of values) and type S (8 pairs of values; open circles and squares) between July 1990 and December 1994.

To determine this, the ratios of the mass concentrations of NO_3^-, NH_4^+, Fe^{3+} and Fe^{2+} in the mine water were compared with the Eh ranges in which these redox pairs react with each other in redox reactions. For both redox pairs, an Eh range of 200 … 400 mV results in terms of magnitude, as determined from the mean value of the redox potentials. This contrasts with the values of –50 … +50 mV and about 200 mV measured in situ -in the 296 II b shaft. In the -literature, –100 to +200 mV -are given for -primary mine waters -and +120 to +830 mV -for oxidised mine waters (BAAS BECKING et al. 1960). PAČES (1969) determined –89 … +57 mV in mine waters from Joachimsthal. -A rough calculation with the chemical-thermodynamic equilibrium program PHREEQE shows an equilibrium setting between water and the most important mineral phases at about +150 mV (VAN BERK 1995, pers. comm.). Based on the mean value and twice the standard deviation, there is therefore a range of interest of 50 … 500 mV.

Both types of measurements, the in situ and the on-site, are within the realm of possibility. A final decision on which redox potentials are “really” present in the mine water cannot be made at this point in time.

In the chemical-thermodynamic equilibrium calculation of the mine water analyses, the redox potential of the mine water was set at 300 mV based on the mean value of 280 mV.

6.3.3.7 Total hardness

The total hardness of the seepage water is 30 °d, which remained almost constant during the 4 years of the processing period. It is not possible to say which causes are responsible for the tendency to decrease from a little above 30 °d to a little below 30 °d.

From 1991 to the end of 1993, the total hardness of the mine water increased steadily. At the beginning of flooding it was 30 … 40 °d and reached about 80 °d in 1993, only to increase slightly from that time on (Fig. 27). Since calcite and dolomite are saturated or slightly supersaturated in the mine water (Tab. 37), the behaviour of the total hardness, which correlates well with Ca, Mg, HCO_3^{2-} and SO_4^{2-} (Tab. 58), is understandable.

6.3.3.8 Evaporation residue (“total mineralisation”)

In the leachates, the evaporation residue was about 800 mg L^{-1}, the numerical value of which decreased slightly at the end of 1994.

During the processing period, the evaporation residue in the mine water increased steadily (Fig. 28). Initially it was 1500 … 2000 mg L^{-1}, to reach about 3000 mg L^{-1} at the end of an almost linear increase until the end of 1993. In 1994, the evaporation residue remained at about 3000 mg L^{-1}, to rise again briefly to 3300 mg L^{-1} in the last quarter of 1994. Whether this was a sustained increase or only a short-term one cannot be read from the available data material.

The six water constituents Ca, Mg, Na, SO_4^{2-}, Cl^- and HCO_3^- almost all correlate well with the evaporation residue and contribute the main part to it. Since their mass concentrations did not increase substantially at the end of the processing period, a further increase of the exhaust steam residue as between 1991 and 1993 is not likely. Only when the pH range of the carbonate buffer is clearly undershot (approx. pH 5) will larger quantities of ions again go into solution.

In the leachates, the evaporation residue was about 800 mg L^{-1}, the numerical value of which decreased slightly at the end of 1994.

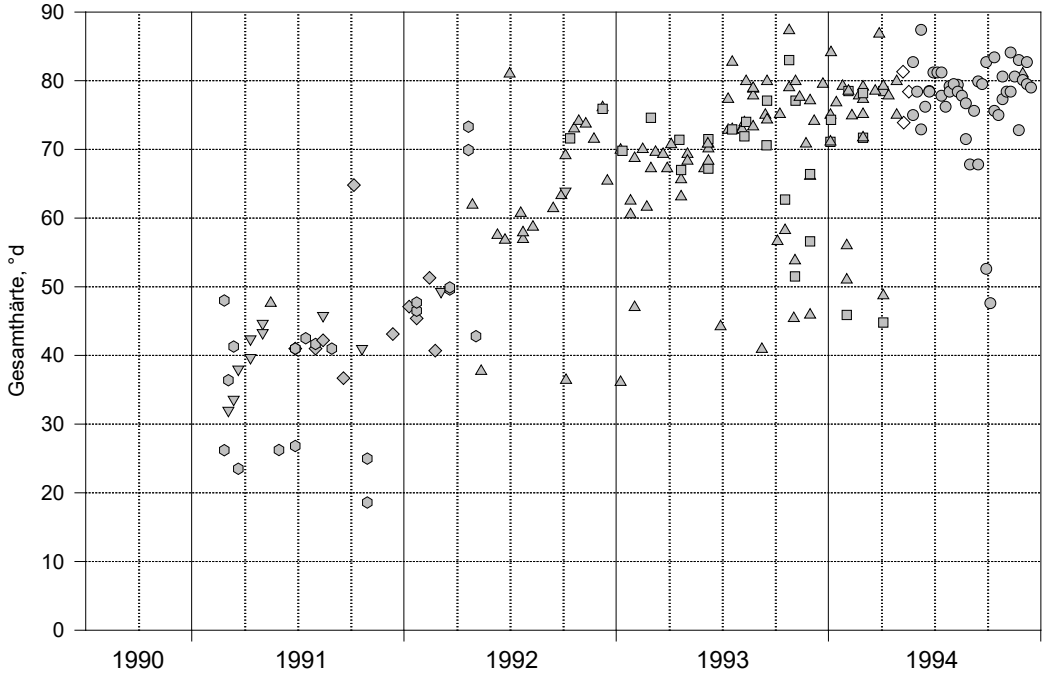

Fig. 27: Temporal development of the total hardness for type G water between January 1991 and December 1994. 213 value pairs. Legend see Tab. 30.

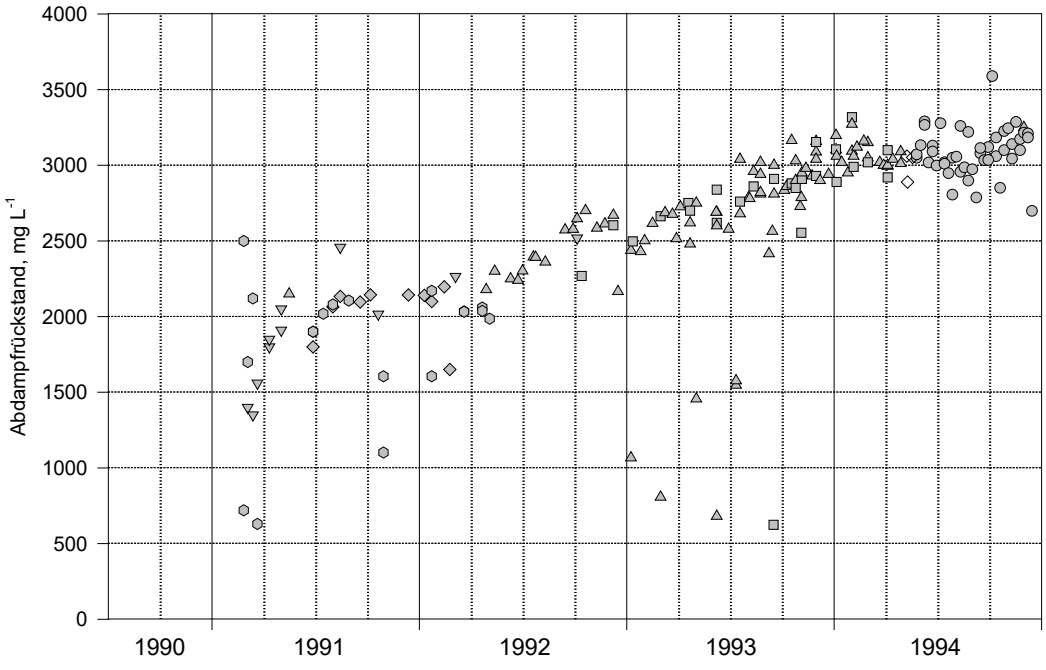

Fig. 28 Temporal development of the evaporation residue for type G water between January 1991 and December 1994. 199 value pairs. Legend see Tab. 30.

6.3.3.9 Uranium

In the seepage waters, the uranium mass concentration regularly ranged between 0.5 and 1 mg L^{-1} from 1990 to 1994 (Fig. 29). This is above the global background value (0.006 mg L^{-1}; KOCZY, TOMIC & HECHT 1957), but not above that with geogenically elevated uranium concentrations (2.9 mg L^{-1}; GERMANOV et al. 1958).

In the mine water, a drop in the uranium mass concentration is present in the first two quarters of 1993 (Fig. 30). In the calculations with WATEQ4F this decrease is recognisable in such a way that the saturation indices (chapter 6.4.3) of the least undersaturated uranium phases show a minimum (Schoepit, Rutherfordin, Ianthinit). Causes for this decrease could be dilution effects by seepage water, ascent of the mine water within an area with lower uranium contents of the rock, adsorption to clays or organic substances or a temporally interrupted mixing of the mine water. Interestingly, the decrease in uranium mass concentration coincides with the increase in mine water temperature, as observed in the 366 II b shaft, among others. Since uranium is less soluble with increasing temperature, a correlation is quite likely (LANGMUIR 1978). The positive correlation of uranium with temperature (Tab. 58) supports this assumption.

From the 3rd quarter of 1993, the uranium mass concentration begins to increase at a greater rate than before. At the end of 1994, mass concentrations of 4 … 5 mg L are $^{-1}$reached, which corresponds to an enrichment of 4 … 5 times compared to the leachates. Uranium correlates well with hydrogen carbonate (r_P = 0.63; $P \ll 0.01$) and total hardness (r_P = 0.72; $P \ll 0.01$), both of which appear to be heading towards a plateau. Therefore, a similar behaviour may occur for uranium, even if the regression (Chapter 6.3.4.5) suggests a further increase.

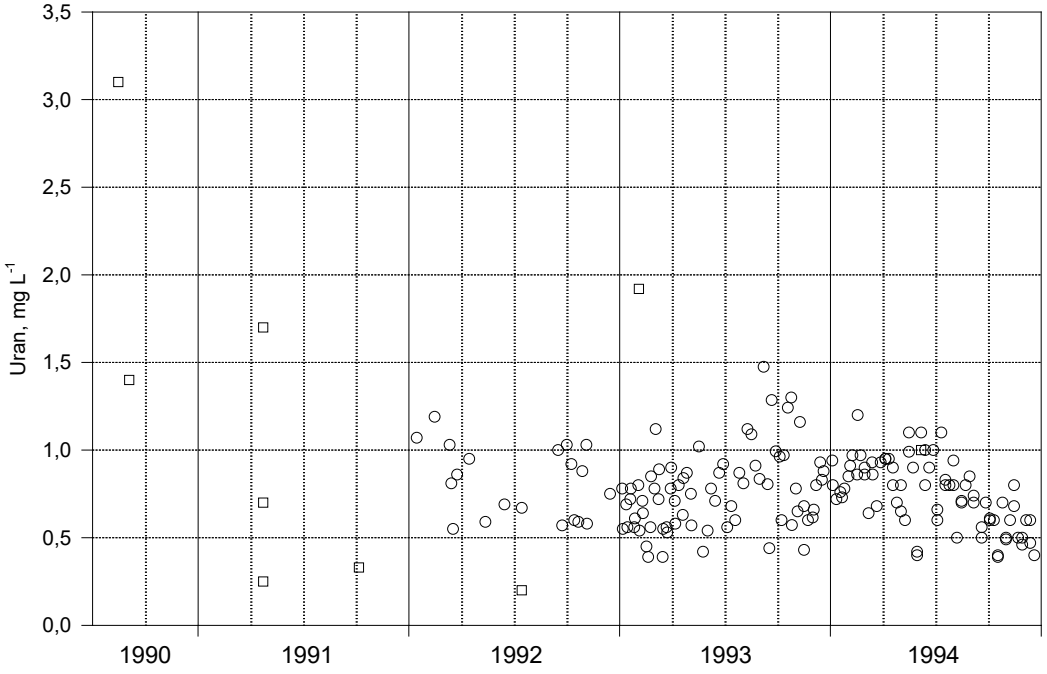

Fig. 29: Temporal development of the uranium mass concentration for type S water between July 1990 and December 1994. 176 value pairs. Legend see Tab. 30.

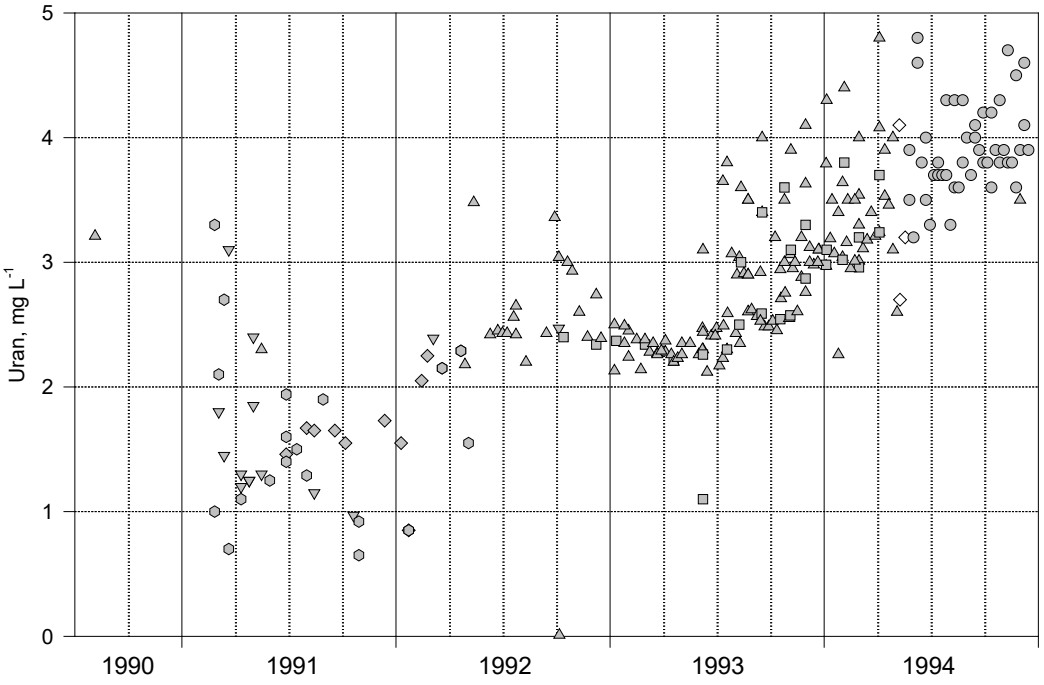

Fig. 30: Temporal development of the uranium mass concentration for type G water between July 1990 and December 1994. 260 value pairs. Legend see Tab. 30.

6.3.3.10 Arsenic

In the leachates, the arsenic mass concentration remained relatively constant between 0 and 0.2 mg L^{-1} (Fig. 31). Results of the same order of magnitude show groundwaters from the similar deposit of St. Joachimsthal, which have arsenic mass concentrations of 0.05 … 0.28 mg L^{-1} at comparable pH values (6.7 … 7.8) (n = 4, PAČES 1969).

From the beginning of 1991 to the end of 1992, however, the arsenic mass concentration in the mine water rose continuously from 0.1 mg L^{-1} to 7 mg L^{-1} (Fig. 32). From the beginning of 1993 it fell from this value to reach a value of 4 … 5 mg L^{-1} at the end of 1994. The good correlation of arsenic with hydrogen carbonate is due to the similar increase of both parameters until mid-1993. A year-by-year correlation shows the decline in the correlation of both parameters from 1993 onwards:

- 1991 r_P = 0.83 P < 0.01 n = 27
- 1991 … 1992 r_P = 0.90 P < 0.01 n = 60
- 1991 … 1993 r_P = 0.74 P < 0.01 n = 131
- 1991 … 1994 r_P = 0.62 P < 0.01 n = 208

Of the other parameters of the mine water, only phosphate shows a temporal behaviour similar to that of arsenic and is reflected in the good correlation of both parameters (r_P = 0.61, P < 0.01). Since in the scorodite ($FeAsO_4.2H_2O$), the least undersaturated arsenic phase, part of the arsenic is always replaced by phosphorus (VON PHILIPSBORN 1967), it is reasonable to assume that part of the phosphate in the mine water originates from the scorodite.

As the equilibrium calculations for the arsenic phases show, all primary arsenic minerals are clearly undersaturated in the mine water (-60 < SI < -8). Only a barium arsenate ($Ba_3(AsO_4)_2$), which does not occur in nature, is supersaturated in the mine water (SI ≈ +11) and will precipitate if it can form for kinetic reasons. Obviously, there is no correlation between the arsenic mass concentration and the

calculated chemical equilibrium settings. Therefore, other reasons must be responsible for controlling the arsenic mass concentration.

Arsenic is adsorptively bound to oxides and hydroxides by 22 … 55% in water (column As colloidal in Tab. 41). It is then no longer dissolved in water, but "adheres" to the surface of these solid phases. The strength of the bond between oxide or hydroxide and arsenic depends on the charge on the surface of the oxide or hydroxide. This in turn is influenced by the pH value. If the surface charge is positive, AsO_4^{3-} can bind to the oxides or hydroxides, whereas if the charge is negative, it is released into the mine water. The pH value at which the oxide or hydroxide surface is neutrally charged is called pH_{ZPO} (pH of zero point of charge). For FeOOH it is pH 7.8 and for ß-MnO_2 pH 7.2 (STUMM & MORGAN 1981).

Another cause for the decrease in the arsenic mass concentration in the mine water could be a dilution effect. From operational documents of SDAG Wismut (1991) it is known that the arsenic content in the rock increased with increasing depth. The rising mine water level therefore reaches areas with lower arsenic contents in the bedrock. Consequently, less arsenic is dissolved in the upper parts of the mine water body. A similar effect occurs when the supply of mobilisable arsenic is depleted.

6.3.3.11 Radium

The radium activity in the mine water increased continuously from the beginning of 1991 to the end of 1994 (Fig. 33). It was initially about 200 mBq L^{-1}, the value of the seepage water, and finally reached 3000 … 4000 mBq L^{-1}.

The way in which the radium activity is controlled or which mineral phase releases the radium could not be determined with certainty. Neither the correlation with other parameters nor the comparison of the radium activity with saturation indices of other solid phases yielded a solution to the problem (chapter 6.4.5).

BLAIR et al. (1980) show, using the example of groundwater in the downstream area of tailings piles in the Elliot Lake District/Ontario/Canada, that radium tends to increase with the sulfate mass concentration. This tendency is also present in the mine water of Niederschlema/Alberoda, but is not reflected in the correlation (Tab. 58) due to the strong scattering of the radium activities around the regression curve (r_P = 0.42).

6.3.3.12 Iron

In the case of iron, strongly fluctuating mass concentrations can be observed in the mine water between 1992 (there were no total iron determinations before March 1992) and the end of 1994 (Fig. 34). While the fluctuation range was initially between 0 and 3 mg L^{-1}, by the end of 1994 it had reached 0 … 8 mg L^{-1}. Overall, one could therefore speak of an increase in the iron mass concentration in the mine water. In the seepage water the iron content is 0 … 0.2 mg L^{-1}, i.e. a factor of 40 below that of the mine water. It is not clear what causes the strong fluctuation, but redox, adsorption and precipitation processes between sampling and the time of analysis seem most likely.

Most of the iron in the mine water comes from the oxidation of pyrite and marcasite, and partly from the dissolution of iron-containing compounds (e.g. siderite).

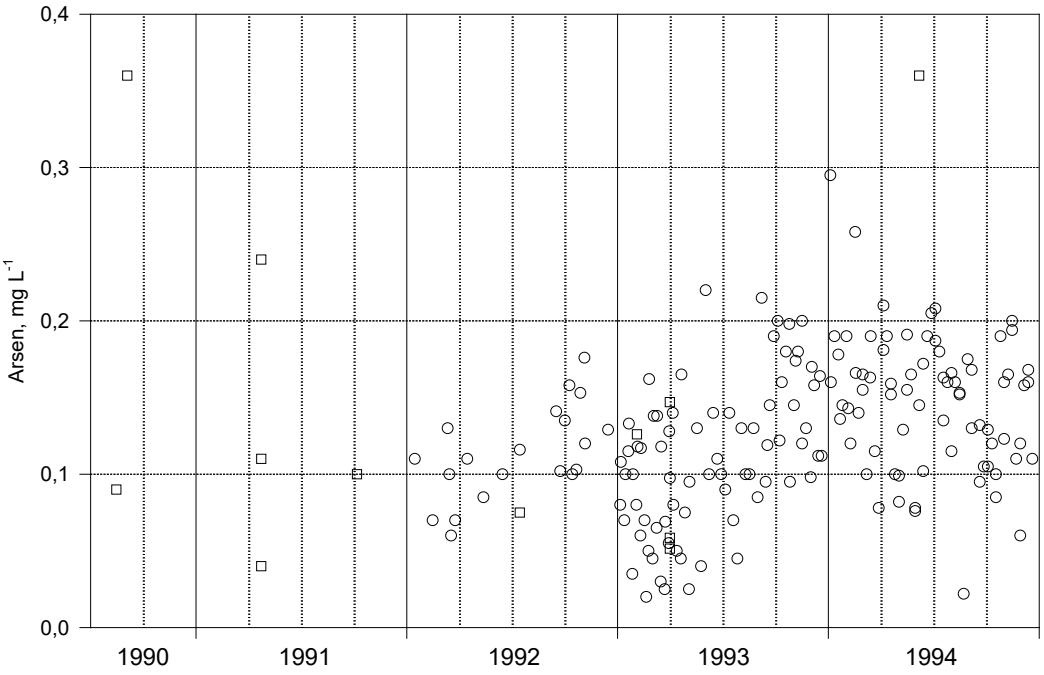

Fig. 31: Temporal development of the arsenic mass concentration for type S water between July 1990 and December 1994. 180 value pairs. Legend see Tab. 30.

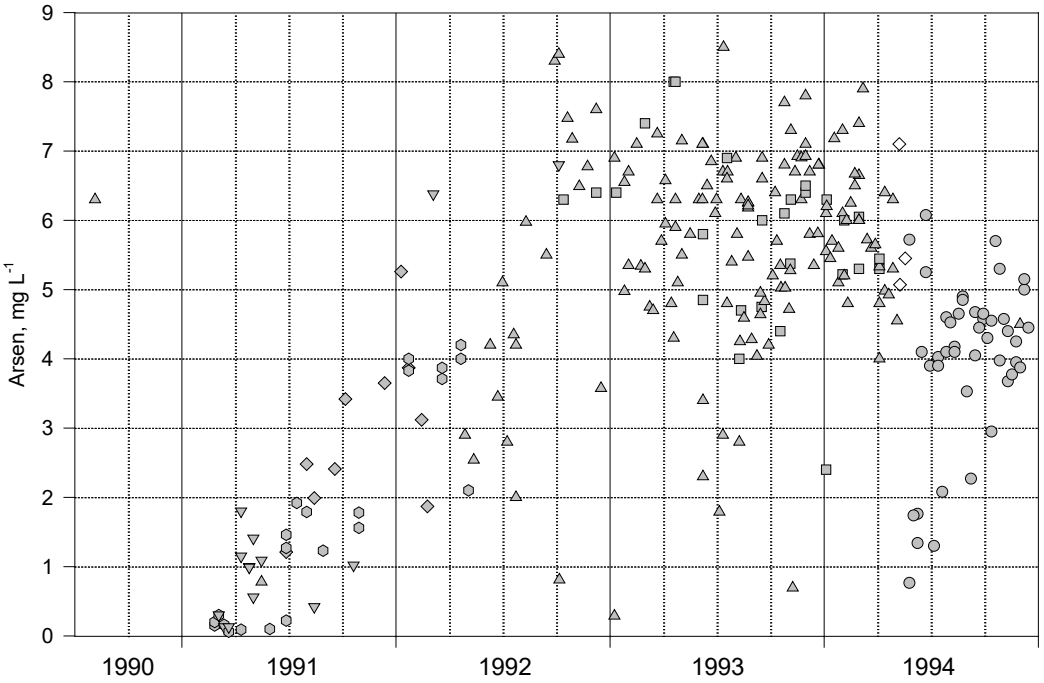

Fig. 32: Temporal development of the arsenic mass concentration for type G water between July 1990 and December 1994. 264 value pairs. Legend see Tab. 30.

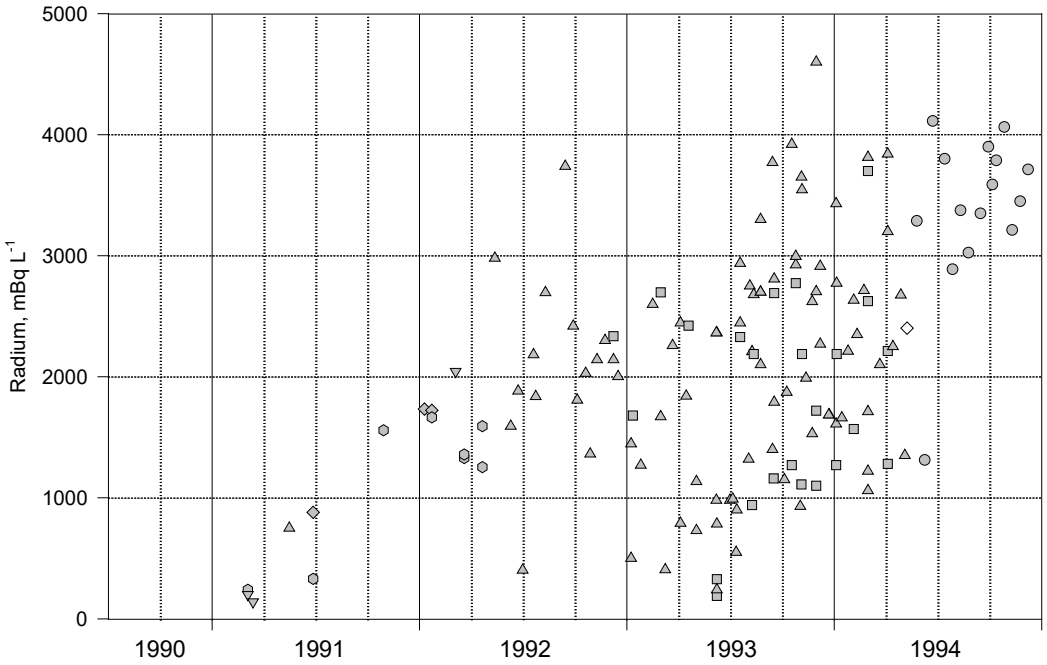

Fig. 33 Temporal development of the radium activity for type G water between January 1991 and December 1994. 141 value pairs. Legend see Tab. 30.

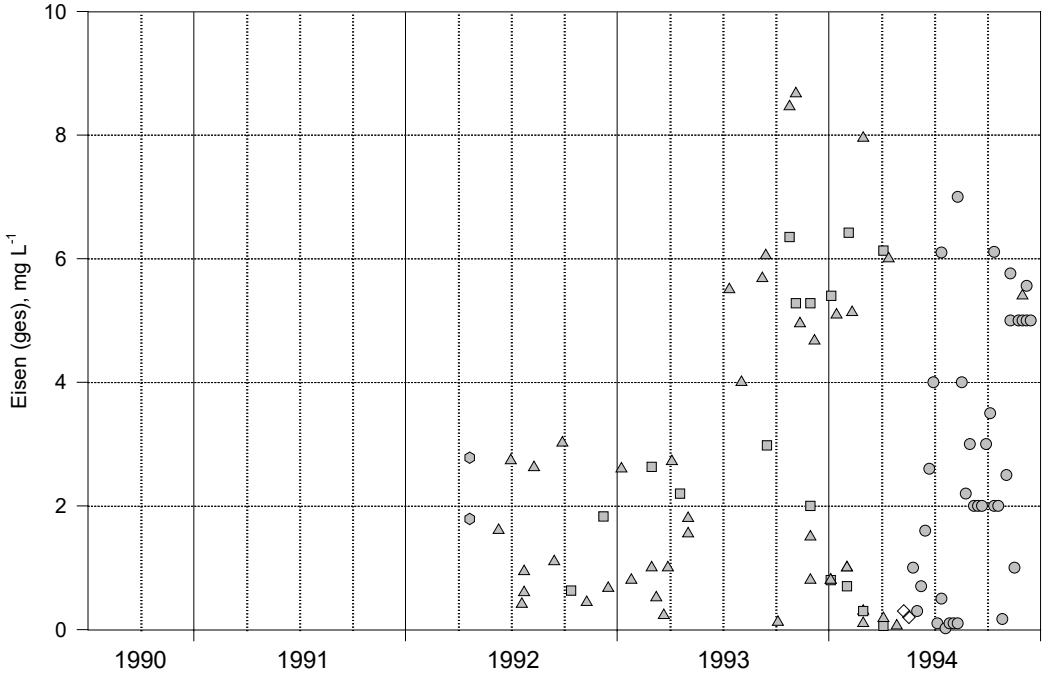

Fig. 34 Temporal development of the iron mass concentration for type G water between April 1992 and December 1994. 98 value pairs. Legend see Tab. 30.

6.3.3.13 Manganese

Like iron, manganese has a wide variation in its mass concentration, ranging from 0 … 2 mg L in $^{-1}$mid 1991 to 0 … 5 mg L^{-1} at the end of 1994 (Fig. 35). Again, it is not clear what causes this variation, but redox, adsorption and precipitation processes between sampling and time of analysis could also play a role. Compared to the leachates, the manganese mass concentration in the mine water is enriched by a factor of 100. As the equilibrium calculations show, there is an equilibrium between rhodochrosite and the mine water (Tab. 37). The manganese mass concentration is therefore controlled by this solid phase.

6.3.3.14 Sulfate

A continuous increase in sulfate content can be observed in the mine water, which levels off from the end of 1993 (Fig. 36). Initially, the mine water contained about 600 mg L^{-1} sulfate, rising to 1400 mg L^{-1} due to the oxidation of pyrite and marcasite and the microbial catalysis of these reactions.

6.3.3.15 Hydrogen carbonate

In the seepage waters, the hydrogen carbonate mass concentrations are about 150 … 250 mg L^{-1}. In contrast, an increase from these values to 1100 mg L^{-1} can be observed in the mine water. In 1993, mass concentrations of up to 1300 mg L^{-1} occasionally occurred (Fig. 37).

The mass concentration of hydrogen carbonate is mainly determined by the available amount of carbonates and carbon dioxide, i.e. the lime-carbonic acid equilibrium. In addition, HCO_3^- is formed from the dissociation of carbonic acid, which is formed by dissolving CO_2(g) in water. From the reactions 11 and 12 it can be seen that hydrogen carbonate is formed in the presence of calcite and carbon dioxide. For detailed descriptions of the complex reactions, their kinetics and equilibrium settings, please refer to the literature (e.g. STUMM & MORGAN 1981).

6.3.3.16 Chloride

Initially, the chloride mass concentrations of the mine water were 200 … 250 mg L^{-1} (Fig. 38), whereas the seepage water contained about 40 mg L^{-1} chloride. Until the end of 1991, the mass concentration in the mine water decreased steadily to remain constant at 140 mg L^{-1} until the end of 1994. Since the mobilisation of chlorides from the rock is unlikely to be of this magnitude and the supply of chlorides from the seepage waters is only small, the only possible source of the chloride is a substance that was used in mining. This is probably the dust binding agent magnesium chloride (G. Fröhlich, pers. comm.). After flooding of the last main level, it can be assumed that the chloride mass concentration in the mine water will decrease due to dilution. Between 1992 and 1994, dilution and dissolution balanced each other out. An estimate of the chloride mass concentration to be expected in the end is possible if the amount of magnesium chloride used is known.

6.3.3.17 Discussion and result

As can be seen from the time series of mass concentrations, the waters of type S and I have a constant chemical composition. In the case of water type G, on the other hand, the mass concentrations of many parameters rose continuously, to largely stagnate at a high level from the end of 1994. Care must therefore be taken not to allow this heavily contaminated water to enter the surface water cycle.

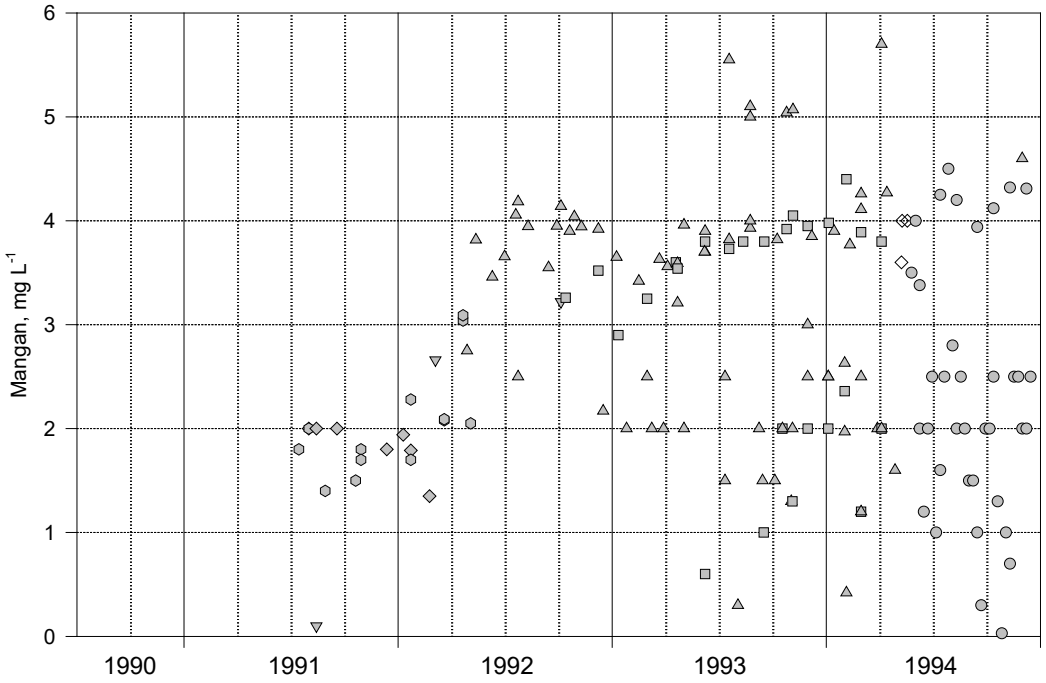

Fig. 35 Development of manganese mass concentration over time for type G water between July 1991 and December 1994. 158 value pairs. Legend see Tab. 30.

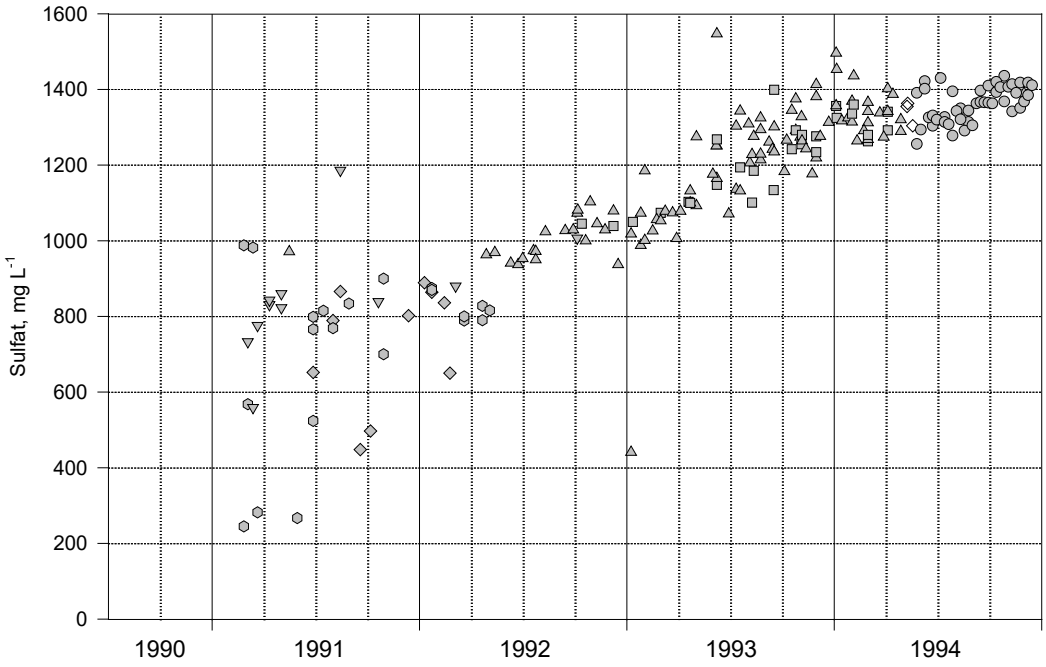

Fig. 36 Temporal development of the sulfate mass concentration for type G water between January 1991 and December 1994. 213 value pairs. Legend see Tab. 30.

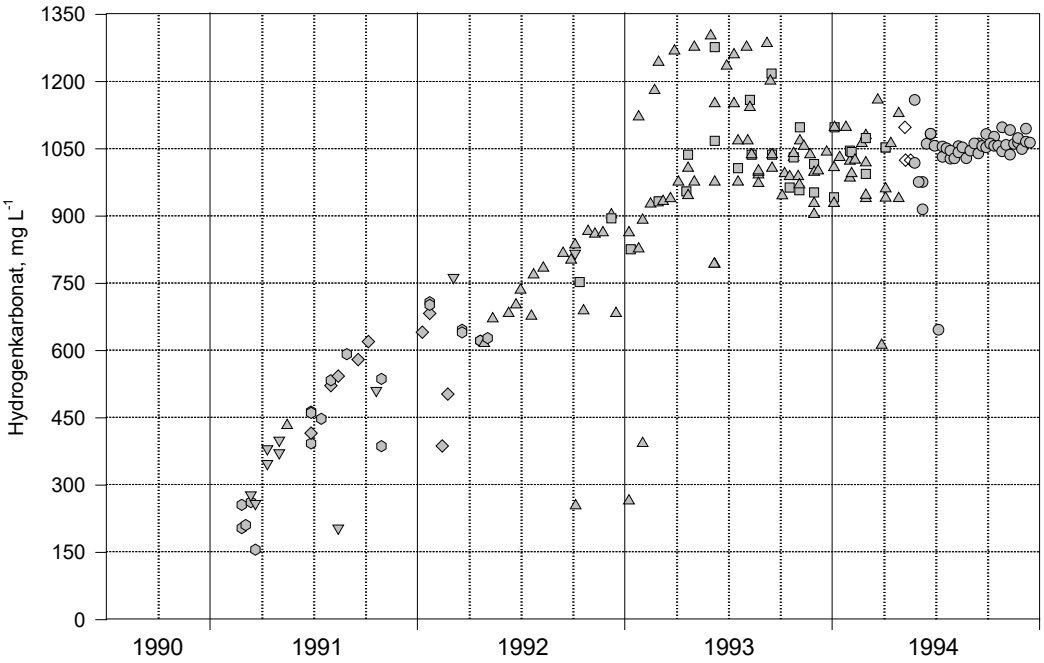

Fig. 37 Temporal development of the hydrogen carbonate mass concentration for type G water between January 1991 and December 1994. 209 value pairs. Legend see Tab. 30.

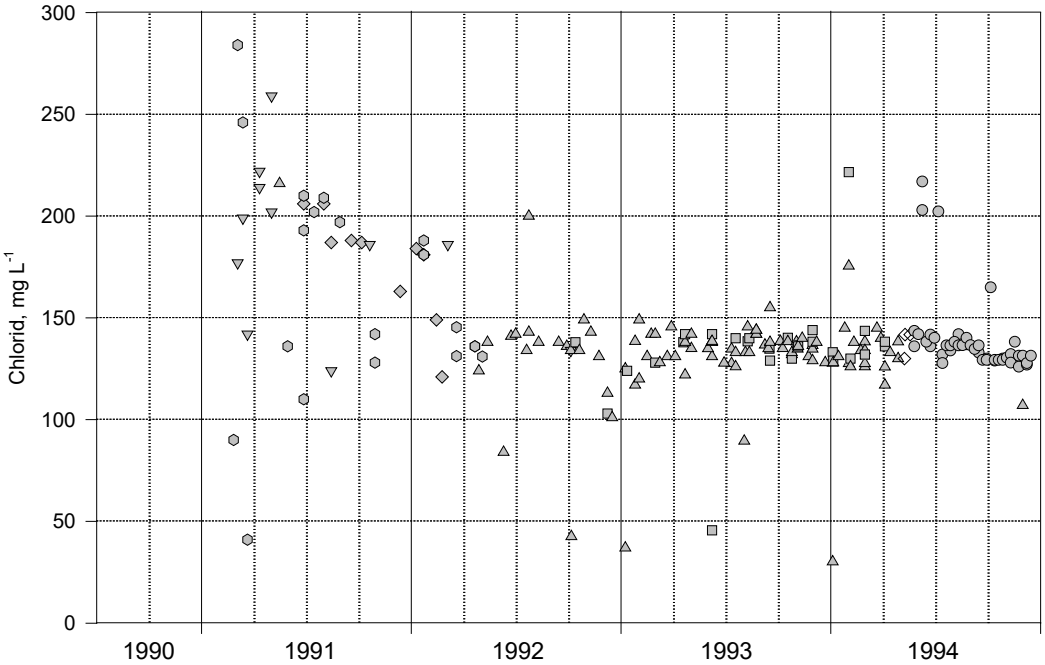

Fig. 38 Temporal development of the chloride mass concentration for type G water between January 1991 and December 1994. 212 value pairs. Legend see Tab. 30.

6.3.4 Forecast of future mass concentrations

6.3.4.1 Procedure and method of presentation

In order to be able to estimate the future development of the mass concentration, radium activities or values of some parameters of the type G water, mathematical-statistical regressions of time were carried out with respect to these values. Since the floodwater will have risen to the level of the Markus Semmler Dam in the year 2000 at the earliest, the graphs and predictions extend to the end of the year 2000. In order to be able to use the change in a parameter during the study period 1991 to 1994 as a basis for predicting its future change over time up to the year 2000, a number of assumptions were made:

- Substance mobilisation will remain in the same order of magnitude as before until the end of the forecast period (Sufficiently large substance reservoir)
- pH, Eh value and temperature will not change substantially
- Type and intensity of material transport in the mine workings remains about the same
- Direction of temporal change will remain the same
- no substances other than seepage are added to the mine water

The curve fitting programme TableCurve (JANDEL SCIENTIFIC 1992), with the help of which the fitting was carried out, provides linear and non-linear equations and determines, in addition to the equation parameters, the regression coefficient as well as three further key figures (regression coefficient corrected for degrees of freedom, standard deviation of the fit, *F-statistic*), with the help of which the optimal equation can be selected. In most cases it is not sufficient to use the equation with the highest regression coefficient or the highest *F-statistic to* predict future developments. Rather, knowledge about hydrogeochemical processes and the course of the prediction interval must also be used. Equations whose prediction interval opened up considerably after the end of 1994, so that theoretically any value was possible, were generally not taken into account. The same applies to equations with more than three parameters (except for the lognormal distribution for arsenic) or equations in which one parameter was very large (usually $>10^5$) or very small (usually $<10^{-5}$). Furthermore, it was assumed that parameters that are well correlated with each other will also be well correlated with each other in the future. For the forecast, their curves between 1995 and 2000 are therefore similar (e.g. SO_4^{2-} and exhaust residue).

In all graphs, the measuring points were assigned the symbols of the individual measuring points (Tab. 30). In addition, three different lines are shown: the curve fit (-- “Fit"), the 95 % confidence interval (- - “Confidence") and the 95 % prediction interval (- - “Predicted"). Within the 95 % prediction interval are 95 out of 100 values that would be determined by repeated measurements. The 95 % confidence interval, on the other hand, would contain 95 out of 100 curve fits of these 100 repeated measurements. All parameters of the correlation functions are given to a maximum of four valid digits, the correlation coefficients r^2 *to* three valid digits.

6.3.4.2 pH value

A tendency towards a decrease can be observed for the pH value (Fig. 39). However, the low regression coefficient of the linear regression of $r^2 = 0.02$ does not allow any statement as to whether this is a relevant decrease. The exponential function has the best regression coefficient ($r^2 = 0.035$), which nevertheless only indicates a trend. For the end of the year 2000, pH values of 6.4 … 7.7 can be expected within the 95 % prediction interval.

$$pH = a + b \cdot \exp^{\left(\frac{-t}{c}\right)}$$

a = 7.016; b = 1.785 · 10^{-1}; c = 6.220 · 10^{2}

At present, the pH value of the mine water is in the buffer range of the calcite and dolomite. Because of the importance of the pH value for the mobilisation of substances, special significance must be attached to its development (STUMM & MORGAN 1981). The question must therefore be clarified whether the protons released by disulfide sulfur oxidation can also be carbonately buffered in the future or whether acidification of the mine water can occur.

Two methods were chosen, which start from different approaches and can be transferred to the conditions in the Niederschlema/Alberoda mine.

Hardness-alkalinity relation

VOIGT (1990) presents a quotient of total hardness and alkalinity that was used by JACKS et al. (1984) and NORBERG (1985, quoted from VOIGT 1990) in Scandinavia (the quotient could not be found in JACKS et al. 1984!). Even slight increases in the quotient

$$R = \frac{2\left(\left[Ca^{2+}\right] + \left[Mg^{2+}\right]\right)}{\left(\left[HCO_3^{2-}\right] + 2\left[CO_3^{2-}\right]\right)} \tag{36}$$

can indicate long-term acidification in buffered media. This is caused by reactions that release protons and enhance weathering or exchange processes, which increase the total hardness in carbonate rocks. JACKS et al. (1984) demonstrated an increase in R long before the acidification of Scandinavian lakes.

As the graph (Fig. 40) shows, the hardness-alkalinity relation in the mine water remains constant. In the seepage water, on the other hand, the ratio increases substantially, which indicates a mobilisation of substances by acid rain.

Intermediate waters are again intermediate in their behaviour between seepage and mine water and show a slight increase.

LAPAKKO METHOD

Finally, a comparison of the acid production potential (APP) with the neutralisation potential (NP) was made according to the LAPAKKO METHOD (LAPAKKO 1990, LAPAKKO et al. 1995), which is used in the mining sector to answer the question of acidification of a system.

It calculates the acid production potential and the neutralisation potential with the unit g kg $^{-1}CaCO_3$ from the percentage content of disulfide sulfur, calcite and magnesite of a rock sample. A mine or tailings leachate will not acidify in contact with the rock if the net neutralisation potential (Net NP) is greater than zero. The calculation formulas are as follows:

$$APP = 31.25 - [S^{2-}],\ g\ kg^{-1}CaCO_3 \tag{37}$$

$$NP = 10 - [CaCO_3] + 11.9 - [MgCO_3],\ g\ kg^{-1}CaCO_3 \tag{38}$$

$$Net\ NP = NP - APP,\ g\ kg^{-1}CaCO_3 \tag{39}$$

As can be seen from the results (Tab. 34), the net neutralisation potentials of the rocks in the deposit area differ substantially from each other. Both the Lower Graptolite alum and siliceous shales (Net NP = -47) and the Upper Devonian banded metadiabase (Net NP = -1) have acidification potential, whereas the ochre limestone (Net NP = 856) and the lamprophyres (Net NP = 224) can buffer acidity. The weighted mean value of the net neutralisation potential from the percentage rock distribution is Net NP = 75 (APP = 8, NP = 83).

In summary, the three forecasts from regression, total hardness-alkalinity relation and net neutralisation potential show agreement that the mine water in Niederschlema/Alberoda will not acidify.

Tab. 34 Acid production potential (APP), neutralisation potential (NP) and net neutralisation potential (Net NP) of rocks of the Niederschlema/Alberoda deposit according to formulae 37 to 39. MgO, CaO, S-SO_4^{2-} and CO_2 from ZETZSCHE (1994). Values marked with * according to WILDNER (1995, pers. comm.). APP, NP and Net NP in g kg^{-1} $CaCO_3$. ud: homogeneous metadiabas (Upper Devonian), td: banded metadiabas (Upper Devonian), sk: hornfels (contact metamorphite), ks/l: alum and siliceous shales (Lower Graptolite shales, Silurian), ks/k: ochre limestone (Silurian), ds: dark phyllites (Gräfenthal Group), s: Light Phyllites (Phycode sequence), qs: Main Quartzite (Gräfenthal Group), G: Granite, Kb/Kh: Lamprophyre. MgO and CaO were converted into $MgCO_3$ and $CaCO_3$ according to their CO_2 ratio and the CO content.

	ud	td	sk	ks/l	ks/k	ds	s	qs	G	Kb/Kh
MgO, %	5,30	4,30	1,70	1,68	5,70	2,94	2,11	1,30	0,64	4,14
CaO, %	8,40	11,75	0,59	1,64	28,88	0,95	0,51	0,56	1,28	5,84
S(ges), %	0,2*	0,4*	0,05*	1,7*	1,2*	0,2*	0,1*	-	0,1*	0,2*
S-SO_4^{2-}, %	<0,10	<0,10	<0,10	<0,1	<0,1	<0,1	<0,1	-		
CO_2, %	0,18	0,34	0,30	0,18	25,25	0,51	0,45	0,38	0,3*	6,43
Pyrite, %	0,3*	0,7*	-	3*	2*	0,3*	0,2*	-	0,2*	0,3*
$MgCO_3$, %	0,3	0,4	0,7	0,3	16,4	1,3	1,2	-	0,4	9,6
$CaCO_3$, %	0,3	0,8	0,2	0,3	70,8	0,3	0,2	-	0,6	11,6
APP	6	13	2	53	38	6	3	-	3	6
NP	6	12	11	6	903	18	16	-	11	230
Net NP	0	-1	9	-47	865	12	13	-	8	224

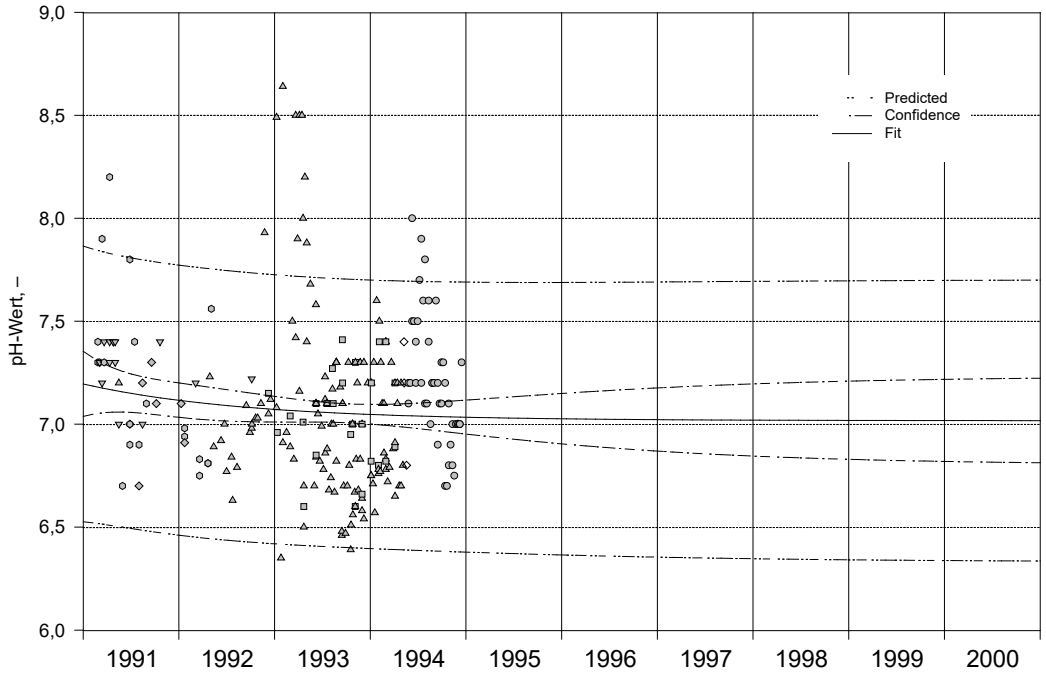

Fig. 39: Regression curve of time with respect to pH for type G water until the end of the year 2000. The assumptions of Chapter 6.3.4.1. 246 value pairs. Legend see Tab. 30.

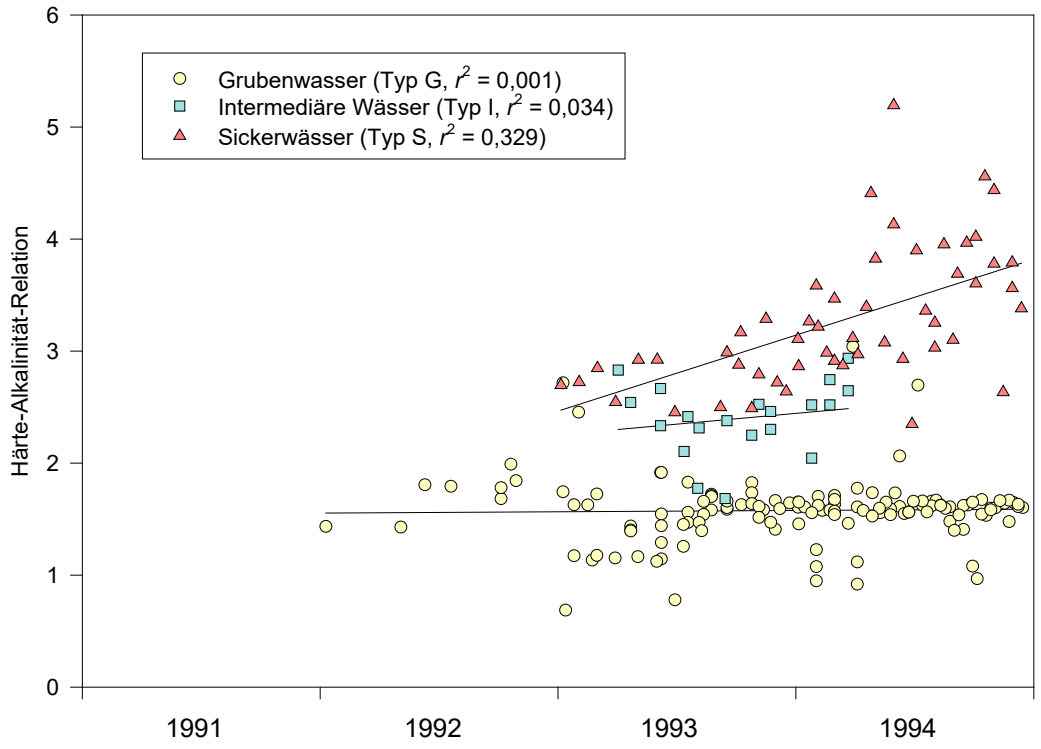

Fig. 40 Temporal development of the relationship between total hardness and alkalinity according to the formula of VOIGT (1990) between January 1992 and December 1994. 207 value pairs.

6.3.4.3 Total hardness

A continuous increase until the end of the forecast period is likely for total hardness (Fig. 41). With a regression coefficient of $r^2 = 0.651$ the equation found shows a good fit to the values from 1991 to 1994. The 95 % prediction interval is relatively narrow and suggests hardnesses of 90 … 140 °dH for the year 2000.

$$\text{Gesamthärte} = a + b \cdot t^c$$

$a = 1.784 \cdot 10^1$; $b = 2.281$; $c = 4.545 \cdot 10^{-1}$

6.3.4.4 Evaporation residue

Due to the good correlation of the Apdamp residue with the total hardness, a similar temporal development is present (Fig. 42). The regression coefficient is $r^2 = 0.819$; the equation describes the previous course satisfactorily accurately. With the assumptions made, mass concentrations of 3400 … 4200 mg L^{-1} can be expected within the 95 % prediction interval in the year 2000.

$$\text{Abdampfrückstand} = a + b \cdot \ln^2 t$$

$a = 5.837 \cdot 10^2$; $b = 4.770 \cdot 10^1$

6.3.4.5 Uranium

Due to the insufficiently explainable decline in the uranium mass concentration in the first half of 1993, the prognosis of the future development causes difficulties (Fig. 43). Therefore, a regression was first carried out for all values after mid 1993 and then for the entire measurement period. For the forecast for the year 2000, priority was given to the overall function that described both the overall

and the partial development after mid-1993 sufficiently well. Until 2000, uranium mass concentrations of 5 … 7 mg L^{-1} are to be expected within the 95 % prediction interval (rounded to 1 mg L^{-1}).

$$\text{Uran} = a + b \cdot \sqrt{t}$$

$a = 1.378 \cdot 10^{-1}$; $b = 9.315 \cdot 10^{-2}$

Since the uranium solubility depends on the pH-value and the predictability of the pH-value by means of the regression (s. chapter 6.3.4.2) has only a low degree of certainty, the interval is only valid for the case of an approximately constant pH value. Taking into account empirical results (chap. 5.1), the falling trend of the pH value and the constant saturation index of the least undersaturated uranium phases (Fig. 51), an interval of 3 … 6 mg L^{-1} is more likely to be assumed.

6.3.4.6 Arsenic

Compared to all other parameters, the arsenic mass concentration shows a peculiar course (Fig. 44), the regression of which was only possible in connection with the interpretation of the column experiments on uranium and arsenic solubility (Fig. 20, SDAG WISMUT 1991). Within the 95 % prediction interval and the assumptions listed above, arsenic mass concentrations of 0 … 4 mg L^{-1} may be expected in the year 2000 (rounded to 1 mg L^{-1}).

$$\text{Arsen} = a + b^{-\left[\frac{\ln(t \cdot c^{-1})}{2 \cdot d}\right]^2}$$

$a = 7.364 \cdot 10^{-1}$; $b = 5.326$; $c = 8.117 \cdot 10^{2}$; $d = 6.144 \cdot 10^{-1}$

From the relatively large regression coefficient of $r^2 = 0.630$, it cannot be concluded that the arsenic mass concentration will actually conform to the lognormal distribution in the future. Because of the sorption of arsenate on oxide and hydroxyl surfaces, a slight change in pH of only 0.2 units can exceed or fall below the pH_{PZC} (zero point of charge) and lead to a renewed increase or decrease in the mass concentration.

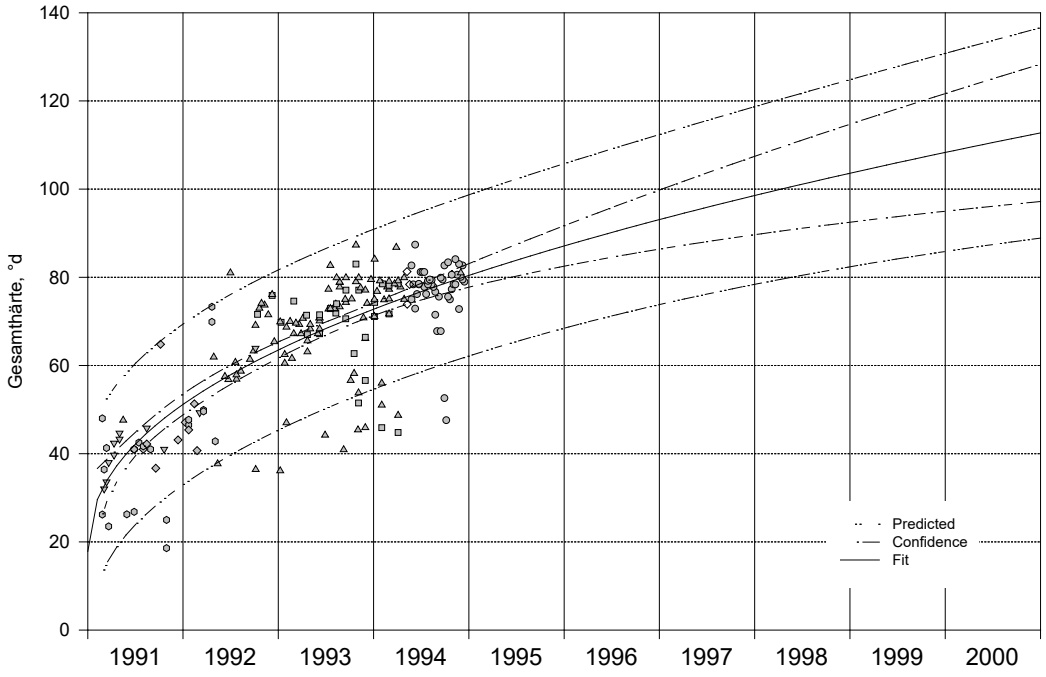

Fig. 41: Regression curve of time with respect to total hardness for type G water until the end of the year 2000. The assumptions of Chapter 6.3.4.1. 213 value pairs. Legend see Tab. 30.

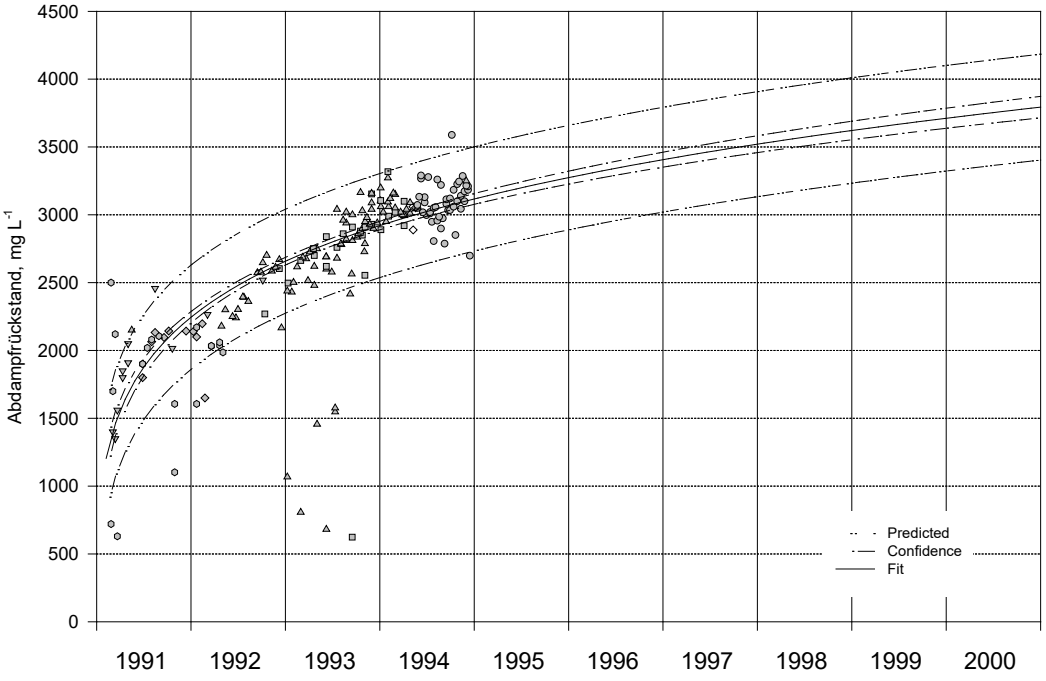

Fig. 42: Regression curve of time with respect to the evaporation residue for type G water until the end of the year 2000. The assumptions of Chapter 6.3.4.1. 199 pairs of values. Legend see Tab. 30.

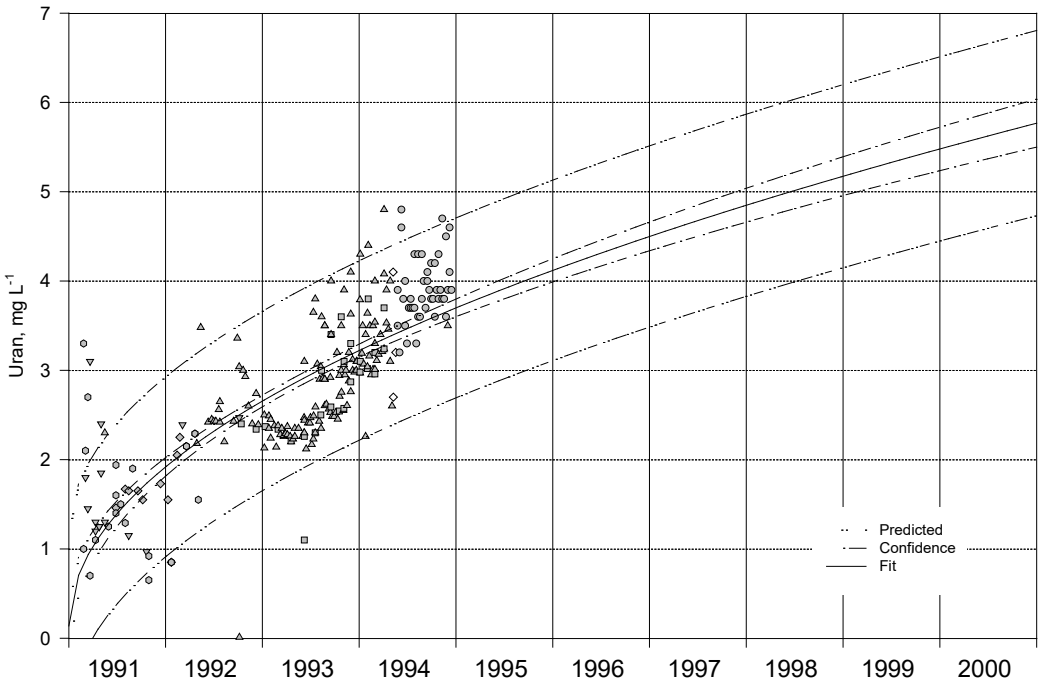

Fig. 43: Regression curve of time with respect to the uranium mass concentration for type G water until the end of the year 2000. The assumptions of chapter 6.3.4.1. 260 value pairs. Legend see Tab. 30.

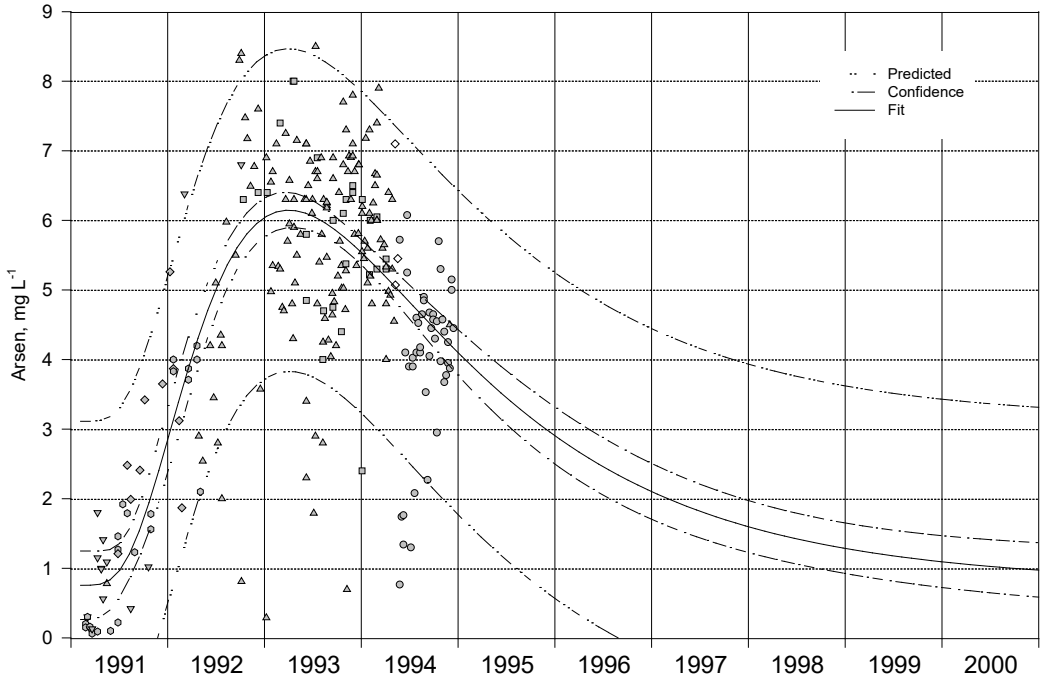

Fig. 44: Regression curve of time with respect to arsenic mass concentration for type G water until the end of the year 2000. The assumptions of chapter 6.3.4.1. 264 pairs of values. Legend see Tab. 30.

6.3.4.7 Radium

It was already shown at an earlier time that radium activity is highly scattered (WOLKERSDORFER 1993). From the wide 95 % prediction interval and the low regression coefficient of $r^2 = 0.256$ it can be seen that a prediction of radium activity remains in the realm of speculation (Fig. 45). However, the increasing trend evident in 1993 has not ended and will probably continue into the year 2000. This is confirmed by the good correlation with the evaporation residue, whose prognosis also points to an increase (Tab. 58).

$$\text{Radium} = a + b \cdot \sqrt{t}$$

$a = -4.680 \cdot 10^2$; $b = 8.627 \cdot 10^1$

6.3.4.8 Sulfate

For the sulfate mass concentration, similar to the regression of the uranium, two adjustment steps were carried out to account for the deviating development from 1993. In addition, the measured values from 1991 and 1992 were weighted only half as much as those from 1993 and 1994 in the overall regression (Fig. 46).

The results of the regression with $r^2 = 0.826$ suggest sulfate mass concentrations of 1500 … 1900 mg L^{-1} for the year 2000 within the 95 % prediction interval (rounded to 100 mg L^{-1}).

$$\text{Sulfat} = a + b \cdot \ln^2 t$$

$a = 5.491 \cdot 10^1$; $b = 2.480 \cdot 10^1$

6.3.4.9 Hydrogen carbonate

Depending on whether greater weight is attached to the overall development or the partial development from mid-1992 onwards, either higher or lower future hydrogen carbonate mass concentrations result. Therefore, two different equations with approximately the same regression coefficient for the mass concentration can be found. The limit of the 95 % prediction interval of the two equations below (Fig. 47) was determined by setting either the maximum value of the upper interval limit or the minimum value of the lower interval limit as the new interval limit. A plot of the prediction interval was omitted to keep the graph clearer. Furthermore, the values up to mid 1992 received only one tenth of the weighting of the remaining values.

The hydrogen carbonate mass concentration will thus, based on the assumptions in the chapter 6.3.4.1 will be 1000 … 1500 mg L^{-1} at the end of the year 2000.

$$\text{Hydrogenkarbonat} = a + b \cdot \exp^{\left(\frac{-t}{c}\right)}$$

a = 1.146 · 10^3; b = -1.108 · 10^3; c = 4.996 · 10^2

r^2 = 0.760 (equation 1)

$$\text{Hydrogenkarbonat} = \exp^{\left(a + \frac{b}{\sqrt{t}}\right)}$$

a = 7.505; b = -1.897 · 10^1

r^2 = 0.771 (equation 2)

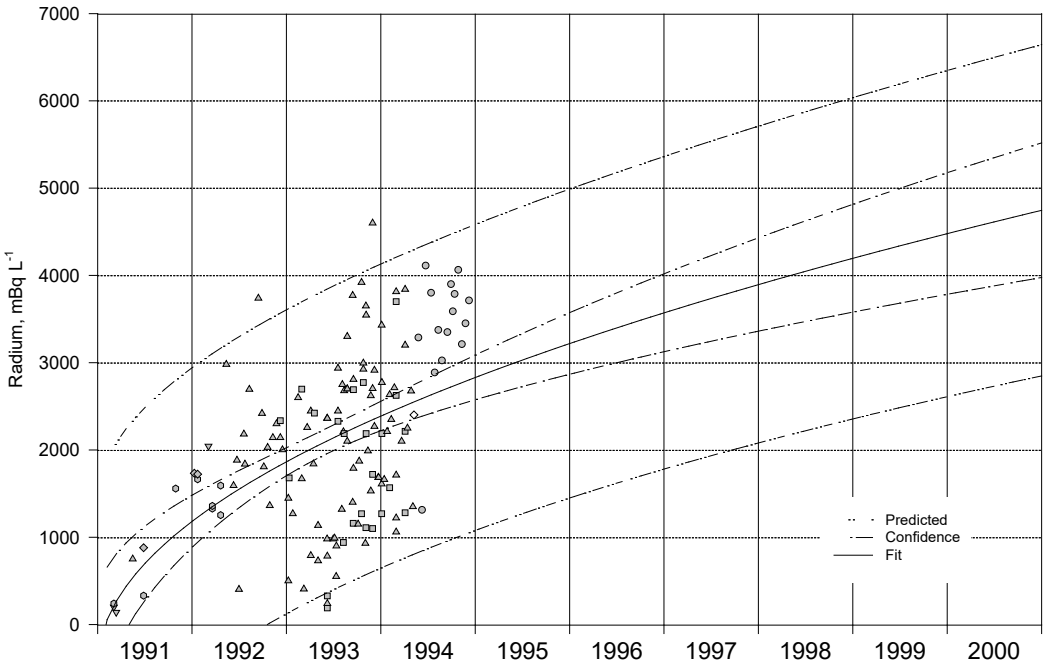

Fig. 45: Regression curve of time with respect to radium activity for type G water until the end of the year 2000. The assumptions of Chapter 6.3.4.1. 141 pairs of values. Legend see Tab. 30.

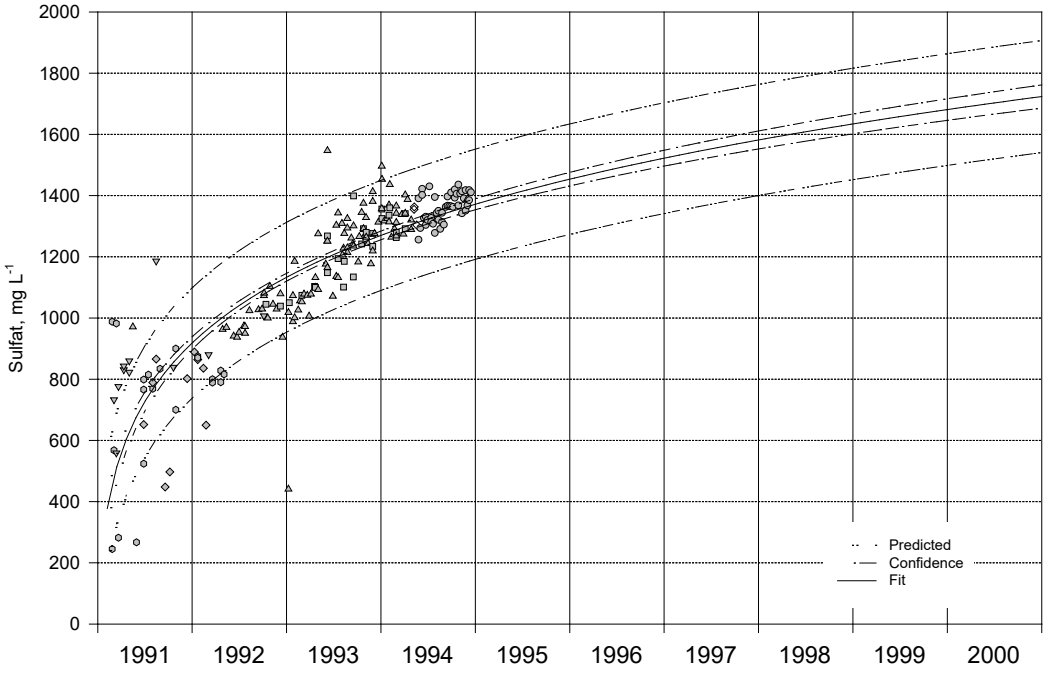

Fig. 46: Regression curve of time with respect to sulfate mass concentration for type G water until the end of the year 2000. The assumptions of the chapter apply. 6.3.4.1. 213 pairs of values. Legend see Tab. 30.

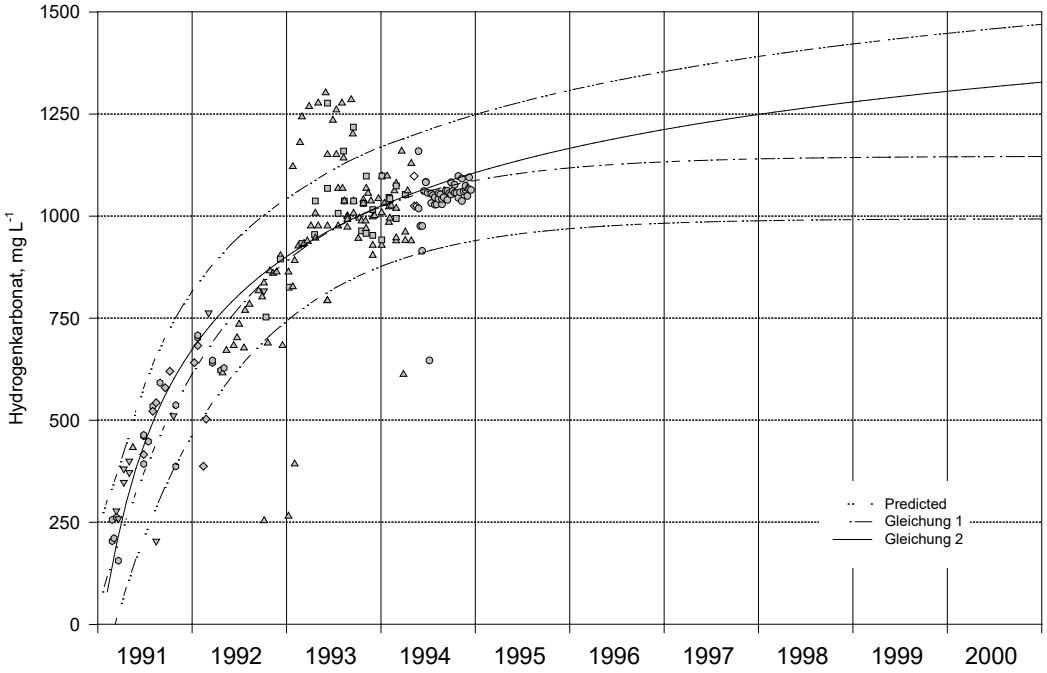

Fig. 47: Regression curve of time with respect to hydrogen carbonate mass concentration for type G water until the end of the year 2000. The assumptions of the chapter apply. 6.3.4.1. 209 pairs of values. Legend see Tab. 30.

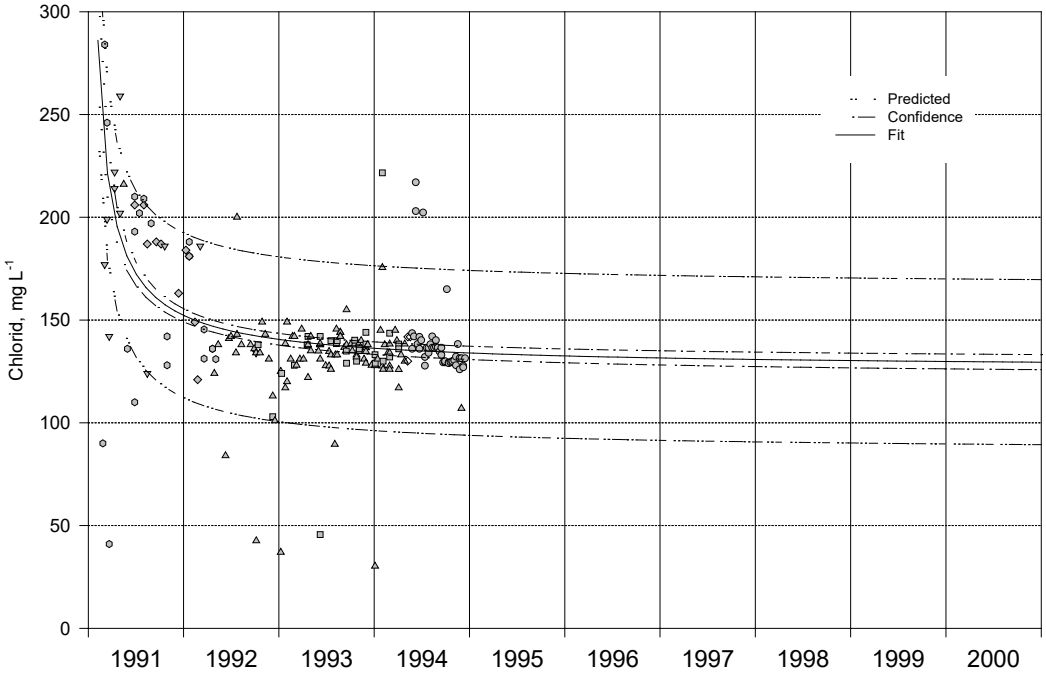

Fig. 48: Regression curve of time with respect to the chloride mass concentration for type G water until the end of the year 2000. The assumptions of Chapter 6.3.4.1. 212 pairs of values. Legend see Tab. 30.

6.3.4.10 Chloride

As the regression of the chloride mass concentration shows, no major change in the chloride mass concentration is to be expected (Fig. 48).

With a regression coefficient of $r^2 = 0.637$ and within the 95 % prediction interval, 90 … 170 mg L^{-1} are to be expected (rounded to 10 mg L^{-1}).

$$\text{Chlorid} = a + \frac{b}{t}$$

$a = 1.261 \cdot 10^2$; $b = 9.021 \cdot 10^3$

6.4 Chemical-thermodynamic equilibrium calculations

6.4.1 Basics

The aim of the chemical equilibrium investigations is to gain information about the saturation state of various solid phases and the distribution of uranium and arsenic species in the flood waters. From this, together with the investigations on the mass concentrations, conclusions are to be drawn for the future hydrogeochemical development of the waters in the Niederschlema/Alberoda mine. The following questions regarding the chemical equilibria are to be answered:

- did the equilibria of the leachates change between 1991 and 1994?
- will the equilibria of the mine water change after 1994?

In order to investigate chemical equilibria in complex aqueous solutions, computer-aided geochemical models based on thermodynamic data of important equilibrium reactions are used. The prerequisites for this are the following assumptions (SCHULZ & KÖLLING 1992, NORDSTROM et al. 1990):

- chemical equilibrium between the species involved and the water,
- Mass constancy of the ions involved,
- the constants of the reactions involved are known with sufficient precision,
- all essential reactions are taken into account by the programme.

The performance of the available computer programs varies and depends both on the thermodynamic data set used ($\Delta G°$ or K_L) and on the programme-specific iteration procedures. We will not go into this in detail here, but refer to the literature (NORDSTROM et al. 1979, DEUTSCHER VERBAND FÜR WASSERWIRTSCHAFT UND KULTURBAU 1992, WOLERY 1992, DAVELER & WOLERY 1992, KÖLLING 1988). An essential element of any chemical equilibrium model is "thermodynamic consistency" (NORDSTROM et al. 1990), which is achieved by optimally matching the individual thermodynamic constants of the reactions within their accuracies. For this reason, it is only possible to a limited extent to transfer the thermodynamic constants of one data set to another. Furthermore, not every reaction taking place in the natural system can be taken into account – if only because of the lack of thermodynamic data – since these reactions are often not sufficiently known (WOLERY et al. 1990). However, computer models can be used to estimate equilibrium states, as shown by the remarks of NORDSTROM et al. (1979).

When examining the computer programs for a modelling of the equilibrium states in the waters of the Niederschlema/Alberoda mine, the choice fell on the program code WATEQ4F with its standard data set in version 2.0 of 30.10.91 (BALL & NORDSTROM 1991, BALL et al. 1981). In particular, the large number of uranium species incorporated and the successful application of WATEQ in uranium prospecting (RUNNELLS & LINDBERG 1981) justified this choice. A description of the functioning and structural design of WATEQ4F is given by BALL & NORDSTROM (1991) and DEUTSCHER VERBAND FÜR WASSERWIRTSCHAFT UND KULTURBAU (1992). In addition to the parameters analysed in each case, WATEQ4F requires the pH value, the redox potential and the water temperature for calculation.

Tab. 35 List of the output calculation results of the chemical-thermodynamic computer model WATEQ4F.

Dissolved ions

- Analysed mass concentration, ppm
- Calculated mass concentration, ppm
- Analysed molality, mol dm^{-3}
- Calculated molality, mol dm^{-3}
- Proportion of the compounds of the corresponding ion, %.
- Activity, 1
- Activity coefficient, 1
- Negative decadic logarithm of the activity coefficient, 1

Ratios

- Weight ratio from the analysed mass concentration
- Molar ratio from the analysed molality

Fixed phases

- Saturation index: $\log(IAP/K_{L,T})$
- Ion activity product: log(IAP)
- Standard deviation of the ion activity product
- Solubility constant: $\log(K_{L,T})$
- Standard deviation of the solubility constant

Tab. 36 Complete list of possible input values for the chemical-thermodynamic computer model WATEQ4F.

Cations

Ca^{2+}, Fe_{ges}, Fe^{3+}, K^+, Mg^{2+}, Mn^{2+}, Na^+, U_{ges}, $U^{4+/6+}$, Ag^+, Al^{2+}, Ba^{2+}, Cd^{2+}, Co, Cr, Cu^+, Mo, Ni, Pb, Se, Sr, V, Zn, B, Br, Cs, Li, Rb, As

Anions

Cl^-, F^-, I^-, HCO_3^-, NO_3^-, PO_4^{3-}, SO_4^{2-}, CO_3^{2-}, NO_2^-

Other

Evaporation residue, Eh value, electrical conductivity, pH value, temperature, SiO_2, H_2S, NH_4^+, O_2

After reading the input file generated by the self-made VISUAL BASIC program (MICROSOFT CORPORATION 1993b) WIN_WQ4F from an MS Access data set (MICROSOFT CORPORATION 1994), WATEQ4F checks the input for the percentage difference of the cation-anion balance (equation 40)

$$\Delta\text{Ionen} = \frac{(\Sigma\text{Kationen} - \Sigma\text{Anionen}) \cdot 100}{(\Sigma\text{Kationen} + \Sigma\text{Anionen}) \cdot 0{,}5} \ [\%] \qquad (40)$$

and performs the iterative calculation if its amount is less than 30 %. WATEQ4F then calculates various parameters (Tab. 35) for a maximum of 648 solid phases and 366 dissolved ions (species), the amount of which can be 4 … 12 closely printed DIN A4 pages, depending on the number of analysis values entered (Tab. 36).

In order to be able to process this amount of data, WIN_WQ4F extracts the parameters of the fixed phases (Tab. 35) from the output file of WATEQ4F, which are then displayed graphically with MS EXCEL (MICROSOFT CORPORATION 1993a) and SigmaPlot (JANDEL SCIENTIFIC 1994a).

Not all of Wismut GmbH's water analyses contain the parameters temperature, pH value and redox potential that are necessary for the calculations of WATEQ4F. Other parameters important for the calculation are also sometimes missing. Therefore, only those analyses were used where at least Ca, Mg, Na, SO_4^{2-}, HCO_3^-, Cl, As and U were given. The missing temperatures, pH values and redox potentials were determined as follows, based on the results of Tab. 28, taking into account Tab. 20 and the redox reactions occurring in natural waters (STUMM & MORGAN 1981):

	Redox potential	Temperature	pH value
Water type S	400 mV	17.0 °C	7.0
Water type I	370 mV	25.6 °C	7.0
Water type G	300 mV	35.4 °C	7.0

6.4.2 Calculations

Based on the thermodynamic data set, WATEQ4F calculated the chemical equilibria of a total of 291 phases with which the floodwater can react. From these, in turn, all phases that appear to be relevant for the mineralisation of the mine water were selected by comparing the saturation indices. Radium phases or species are not included in the WATEQ4F data set. Therefore, statements on the chemical-thermodynamic equilibrium setting of the water with radium phases or on the distribution of radium species are not possible.

6.4.3 Saturation indices

The mass concentrations of the constituents in the mine water are caused by geochemical reactions of the solid phases. Water that is out of equilibrium will, in the course of time, move towards a state of equilibrium. For this purpose, solid phases that are undersaturated with respect to the water – as far as they are available – go into solution, while supersaturated phases precipitate.

The quotient SI (saturation index) of the ion activity product (IAP) and the temperature-dependent solubility product ($K_{L,T}$) of the solid phase of interest is used as a measure of supersaturation or undersaturation, whereby unwieldy numerical values are avoided by logarithmisation. Supersaturation is then expressed by a positive SI, undersaturation by negative SI (BALL & NORDSTROM 1991), while in the saturated state SI = 0. The definition of the saturation index is as follows:

$$\text{SI} = \log\left(\frac{\text{IAP}}{K_{L,T}}\right) \qquad (41)$$

Tab. 37 Minerals and phases which, due to their saturation indices, are decisive for the chemical composition of the mine water. SI: Saturation index. X: Mineral has already been described for the Niederschlema/Alberoda deposit. $Mn_3(AsO_4)_2.8HO_2$ does not occur as a mineral, manganese hornesite is $(Mn, Mg)_3(AsO_4)_2.8HO_2$ (STRUNZ 1982). -1: Phase does not occur as a mineral. Calculations of the saturation indices with WATEQ4F and its standard data set.

Mineral	Formula	Described	SI
Calcite	$CaCO_3$	X	+0.5 … +1
Dolomite	$CaMg(CO_3)_2$	X	0 … +2
Magnesite	$MgCO_3$		0 … +0.5
Siderite	$FeCO_3$	X	± 0
Strontianite	$SrCO_3$		-1.4 … -0.4
Rhodochrosite	$MnCO_3$	X	± 0
Huntite	$CaMg_3(CO_3)_4$		± 0
Plaster	$CaSO_4$	X	-1 … -0.5
Baryte	$BaSO_4$	X	+0.4
Coelestine	$SrSO_4$		-1 … -0.6
Jarosite	$KFe_3[(OH)_6\|(SO_4)_2]$		-2 … +2
Alunite	$KAl_3[(OH)_6\|(SO_4)_2]$		0 … +2
Fluorite	CaF_2	X	-0.5
Goethite	FeOOH	X	+8
Gibbsite	$Al(OH)_3$		+2
-1	Cu_2FeO_4		+16
-1	$Fe_3(OH)_8$		0 … +4
Quartz	SiO_2	X	+0.4 … +0.6
Greenalit	$Fe_2[(OH)\|Si_4O_{10}]$		± 0
Hydroxyapatite	$Ca_5[OH\|(PO_4)_3]$	X	-1 … +5
Mansfieldite	$AlAsO_4.2\ H_2O$		-5
Scorodite	$FeAsO_4.2\ H_2O$	X	-4 … -3
Manganese-Hörnesite	$Mn_3(AsO_4)_2.8\ H_2O$		-4
Ianthinite	β-$[UO\|_2(OH)_2]$		-4
Schoepit	$[UO\|_2(OH)_2].H_2O$		-4
Rutherfordin	$[UO\|CO_2]_3$		-5 … -3
Na-Autunuit	$Na_2[UO\|PO_{24}]_2$	X	-4

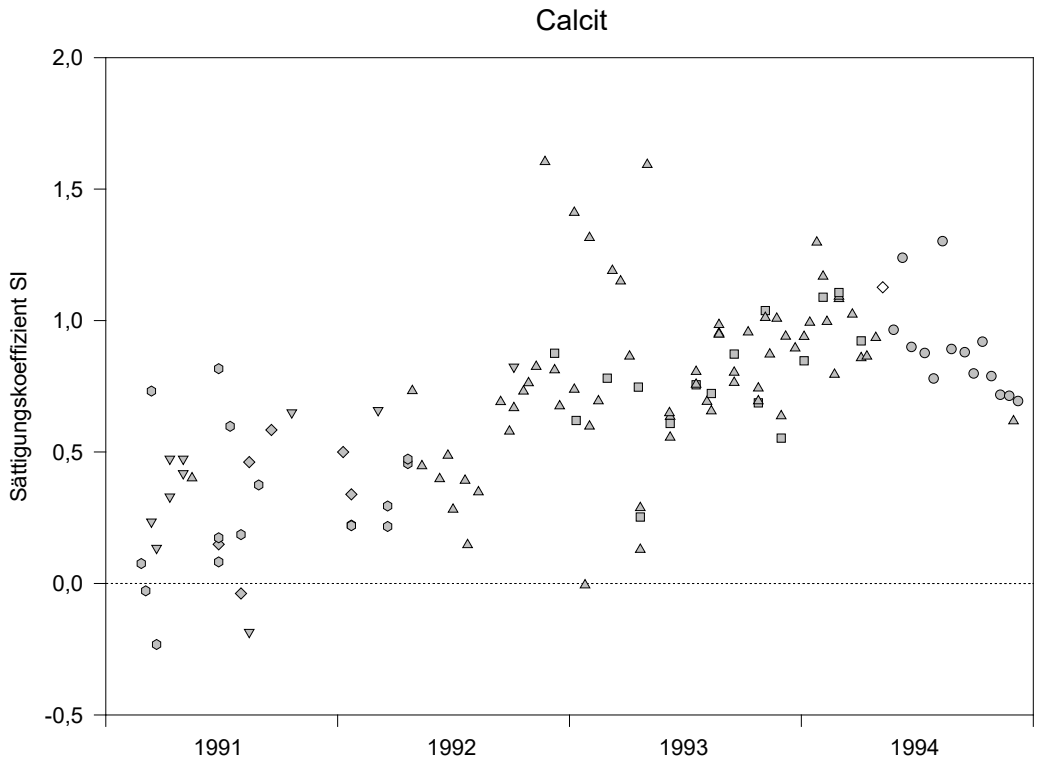

Fig. 49: Saturation index of calcite in mine water between 1991 and 1994. The saturation index increased steadily from 0 to about +1 from 1991 to the beginning of 1994. The mine water is now slightly supersaturated with calcite. Symbols according to Tab. 30.

For example, the saturation index for siderite in equilibrium with aqueous solution (log $K_{25\,°C}$, from NORDSTROM et al. 1990) is calculated as follows

$$FeCO_3 \leftrightarrow Fe^{2+} + CO_3^{2-} \qquad \log K_{25\,°C} = -10.45 \quad (42)$$

to

$$SI = \log\left(\frac{\{Fe^{2+}\} \cdot \{CO_3^{2-}\}}{10^{-10,45}}\right) \quad (43)$$

In Anglo-Saxon literature SI is called “saturation index” (e.g. BALL & NORDSTROM 1991, BALL et al. 1981, WOLERY 1992) and is consistently translated as „Sättigungsindex“ by German-speaking authors. This may be a linguistically correct translation, but it is mathematically incorrect, as the above quotient is not an index, but a coefficient. In German language, therefore, the term „Sättigungskoeffizient“ should be used instead.

The time it takes for a solid phase to reach saturation depends on various factors such as pH value, redox potential, temperature and the presence of other species and solids. The reaction kinetics are of essential importance. A phase that is strongly supersaturated in water (in mine water, for example, almost all phyllosilicates) but cannot form for kinetic reasons will not precipitate (SCHULZ & KÖLLING 1992).

As the chemical-thermodynamic equilibrium calculations show, only a few mineral phases play a role in the composition of the mine water. Among the phases that are decisive for the limitation of molecules and ions in the water (limiting phases), carbonates, sulfates, oxides and oxyhydrates contribute to the equilibrium setting. Interestingly, these minerals, listed in Table 37, coincide for the most part with those that NORDSTROM et al. (1990) consider essential for the water-mountain reactions. The

mineral phases in the table can be considered saturated when -1 < SI < +1. To illustrate the carbonate saturation, the saturation indices of calcite are shown as representative of these minerals (Fig. 49). Due to the large kinetics of its solution reaction, it has a limiting effect on the calcium mass concentration (SCHULZ & KÖLLING 1992).

Since the saturation indices of the three and four least undersaturated arsenic and uranium phases, respectively, are quite low, these minerals contribute to the arsenic and uranium mass concentration only via dissolution (Tab. 37). A controlling phase for the arsenic and uranium in the flood waters is not present. Because of the importance of the arsenic and uranium phases for the later discharge of the mine water into the Zwickauer Mulde, the following descriptions will essentially be limited to these phases. The other uranium and arsenic phases (uranium: a total of 30, arsenic: a total of 14) are not considered, as their saturation indices indicate that they are insignificant for the mine water chemistry. To prove this, the uranium and arsenic mass contents of water analysis 502 (-m331, 10 November 1994) were varied until WATEQ4F calculated a saturation of the respective mineral in the water (Tab. 38). As can be seen from the table, the saturation concentrations of all uranium and arsenic phases are far from the mass concentrations present in the mine water (Fig. 30, Fig. 32). Together with their clear undersaturation, this is an indication that the uranium and arsenic mass concentrations at the pH-Eh ratios of the mine water are not controlled by chemical-thermodynamic equilibrium reactions, but by other processes, such as solution or sorption.

The saturation indices of the three least undersaturated arsenic phases (Fig. 50, Tab. 39) were examined to see whether they correlate with the pH value, the arsenic mass concentration, the evaporation residue or the CO_2 partial pressure calculated by WATEQ4F. A correlation with the redox potential was not possible due to an insufficient number of measured values. In addition, the three minerals were correlated with the aluminium, manganese and total iron mass concentration (formula components), whereby it turned out that the saturation indexe of scorodite and manganese hörnesite increases with increasing iron and manganese mass concentration, respectively, as expected. A relationship between the saturation and the aluminium mass concentration does not exist.

Tab. 38 Selected uranium and arsenic minerals with theoretical uranium and arsenic mass concentrations that would be necessary in the mine water to achieve saturation with the corresponding mineral. None of the figures represent real expected mass concentrations, rather they are calculated mass concentrations to illustrate the degree of undersaturation.

Uranium mineral	Equilibrium concentration
Na-autunite	400 mg L^{-1}
Schoepit	670 mg L^{-1}
Ianthinite	700 mg L^{-1}
Rutherfordin	780 mg L^{-1}
K-Autunit	1050 mg L^{-1}
Autunit	1100 mg L^{-1}
Saleeit	1200 mg L^{-1}
Sr-Autunit	1800 mg L^{-1}
Bassetit	2200 mg L^{-1}
Gummit	2500 mg L^{-1}
Uranocircite	2500 mg L^{-1}
Przhevalskit	2600 mg L^{-1}
Uraninite	2800 mg L^{-1}
H-Autunit	4200 mg L^{-1}

Arsenic mineral	Equilibrium concentration
Manganese-Hörnesite	450 mg L^{-1}
Scorodite	2900 mg L^{-1}
Mansfieldite	$\gg$ 10,000 mg L^{-1}
Köttingit	$\gg$ 10,000 mg L^{-1}
Annabergite	$\gg$ 10,000 mg L^{-1}
Claudedite	$\gg$ 10,000 mg L^{-1}
Arsenolite	$\gg$ 10,000 mg L^{-1}

The procedure for the uranium minerals was similar to that for the arsenic minerals. There was hardly any correlation between the four minerals and the CO_2 partial pressure, the evaporation residue, the

pH value and the uranium mass concentration (Tab. 40). The same can be observed for the sulfate and phosphate mass concentration. The correlation with other physicochemical parameters of the mine water did not yield relevant results for schoepite, rutherfordine and ianthinite either. Only Na-autunite is significantly positively correlated with Sr (r_P = 0.795), SO_4^{2-} (r_P = 0.686), U (r_P = 0.656), Mn (r_P = 0.640) and Fe_{ges} (r_P = 0.559).

From the time course (Fig. 51) and the pH-Eh dependence of the saturation indices of Na-autunite, schoepite, rutherfordine and ianthinite, the undersaturation of these secondary uranium minerals compared to the mine water can be clearly seen (Fig. 55, Fig. 56).

Tab. 39 Qualitative correlation between selected arsenic phases and CO partial pressure$_2$ (pCO_2), evaporation residue (AR), pH and arsenic mass concentration. -[1]: no correlation available.

Phase	pCO_2	AR	pH value	As mass concentration
Mansfieldite	positively correlated	Negatively correlated	Negatively correlated	-[1]
Scorodite	positively correlated	positively correlated	Negatively correlated	-[1]
Manganese-Hörnesite	Negatively correlated	positively correlated	clearly positively correlated	positively correlated

Tab. 40 Qualitative correlation between selected uranium phases and CO partial pressure$_2$ (pCO_2), evaporation residue (AR), pH and uranium mass concentration. -[1]: no correlation available.

Phase	pCO_2	AR	pH value	U mass concentration
Na-autunite	-[1]	positively correlated	-[1]	-[1]
Schoepit	Negatively correlated	-[1]	-[1]	-[1]
Ianthinite	Negatively correlated	-[1]	-[1]	-[1]
Rutherfordin	-[1]	-[1]	-[1]	-[1]

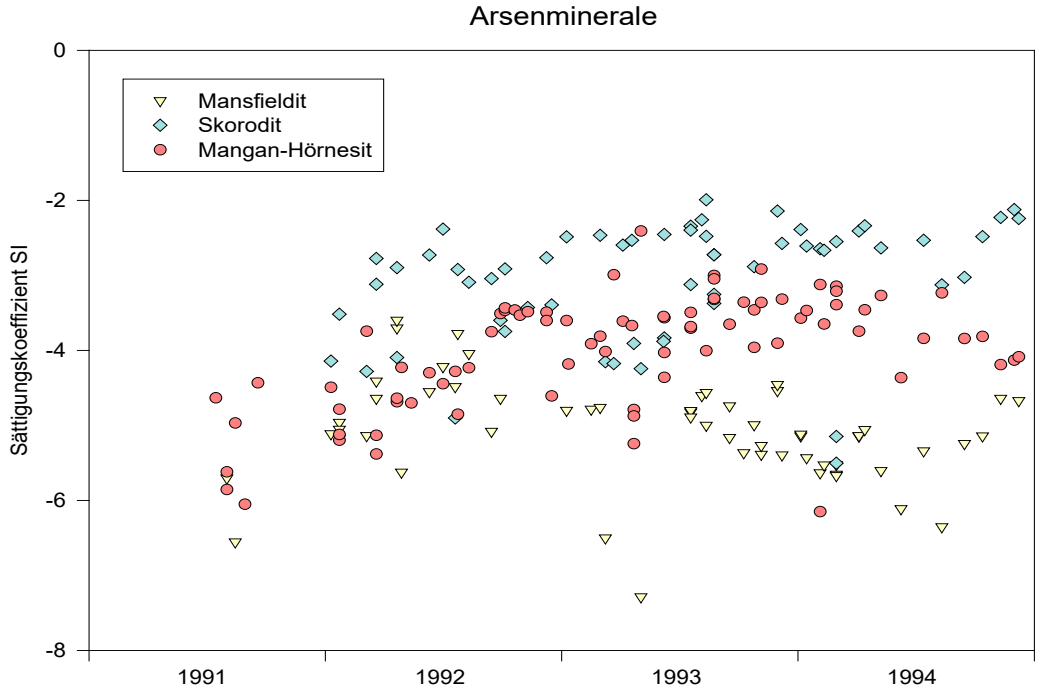

Fig. 50: Saturation indices of selected arsenic minerals in the mine water of the Niederschlema/Alberoda mine between 1991 and 1994.

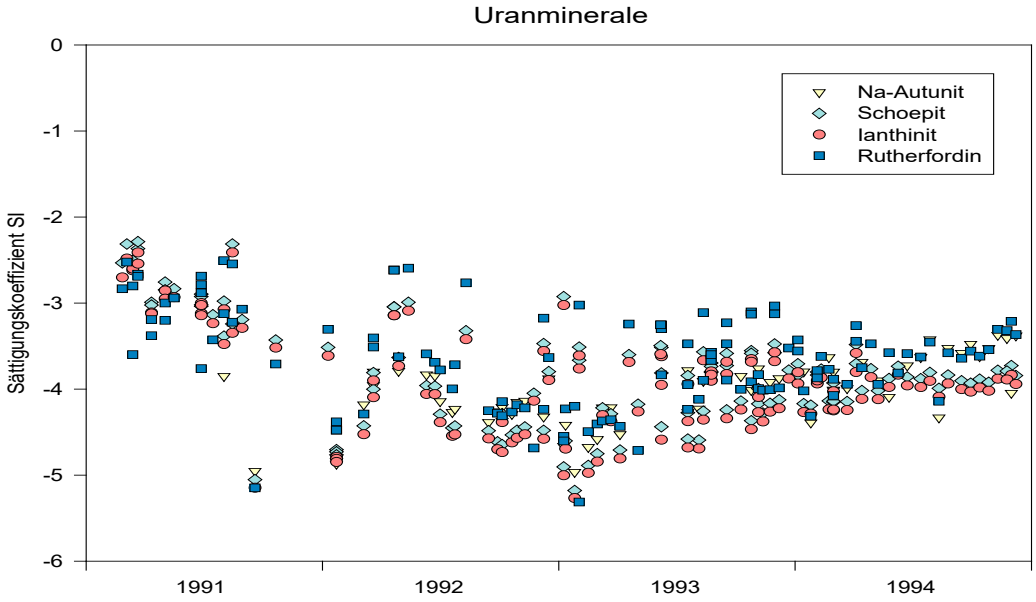

Fig. 51 Saturation indices of selected uranium minerals in the mine water of the Niederschlema/Alberoda mine between 1991 and 1994. The saturation index of the primary mineral uraninite ranges between -10 and -8.

6.4.4 Development of uranium and arsenic species

Both uranium and arsenic are present in different species in the mine water of the Niederschlema/Alberoda mine. Uranium(VI) is complexed to more than 98 % as a uranyl ion (Fig. 52), and arsenic is bound to more than 99 % in the first and second dissociation stage of arsenic acid (Fig. 53). From the chemical analyses of the species distribution of arsenic, a similar distribution is evident (Tab. 41, Fig. 54).

Since a large part of the uranium in the mine water is in the form of the uranyl phosphate complex ($UO_2(HPO_4)_2^{2-}$), only the calculations of WATEQ4F were used to investigate the uranium species distribution, where PO_4^{3-} was indicated in the analysis. In future, an analysis of the PO content$_4^{3-}$ in the mine water may no longer be dispensed with.

Up to pH 7.3, the uranium species are dominated by the uranyl phosphate complex $UO_2(HPO_4)_2^{2-}$, at higher pH values by the carbonate complex with $UO_2(CO_3)_3^{4-}$. Between pH 7 and 8, up to 20 % of the uranium exists bound as the carbonate complex $UO_2(CO_3)_2^{2-}$. In the Eh range of interest of about 50 to 500 mV, there is no dependence of the type of uranyl complex on the Eh value, since the oxidation number of the uranium does not change (SCHADE 1982). Only at redox potentials below 50 mV was there an increase in the saturation index of uraninite (Fig. 55). This result agrees with the theoretical calculations carried out by LANGMUIR (1978) on the uranium species distribution.

The predominance limit between $HAsO_4^{2-}$ and $H_2AsO_4^-$ is pH 6.5 in the mine water of the Niederschlema/Alberoda mine. Since only a few waters in the mine have a pH value below this limit, the arsenic is thus mostly present in the second dissociation stage of arsenic acid. Within the most frequently measured pH values, this is 70 … 90 % of all arsenic. Arsenic shows no significant dependence of the species on the Eh value between 50 mV and 500 mV Eh value, as corresponds to the predominance diagram calculated by SPERLING & MERKEL (1992).

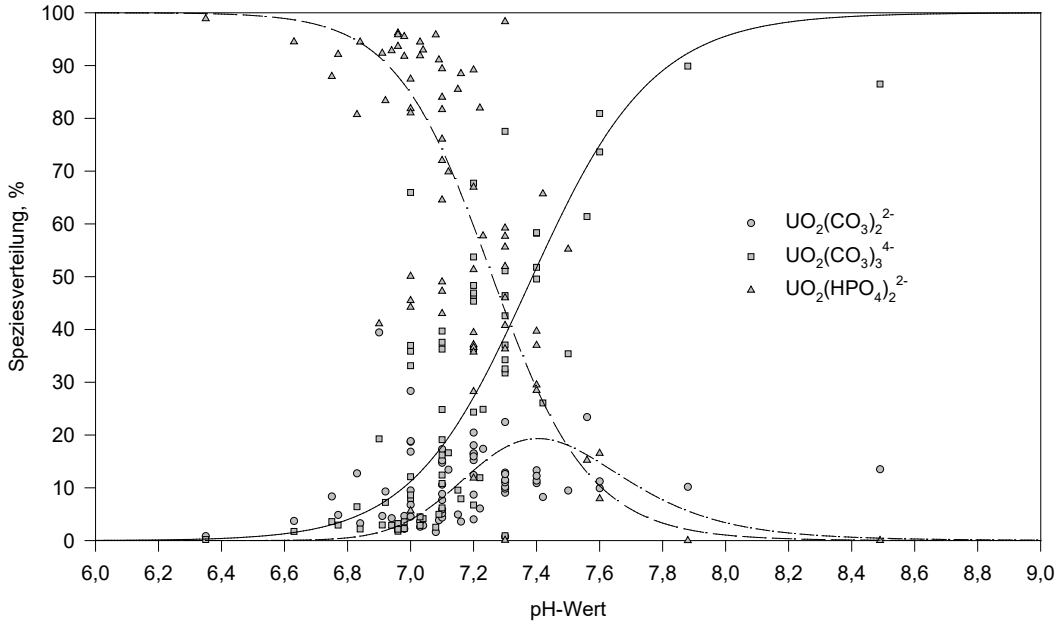

Fig. 52: Distribution of uranium species in the mine water of the Niederschlema/Alberoda mine as a function of the measured pH values. Eh value about 300 mV, 70 data pairs.

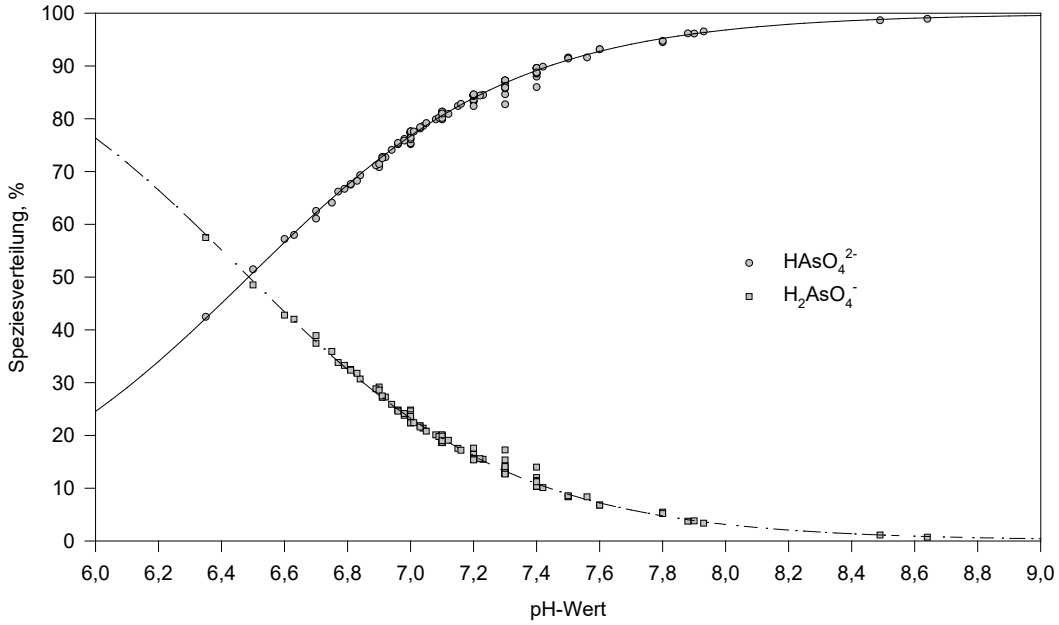

Fig. 53: Distribution of arsenic species in the mine water of the Niederschlema/Alberoda mine as a function of the measured pH values. Eh value about 300 mV, 131 data pairs.

Tab. 41 Ratio of arsenic(III) to arsenic(V) and of colloidally as well as cationically and anionically bound arsenic species in the mine water of the Niederschlema/Alberoda mine. The deviation of the 1st analysis compared to the following ones is due to influences by matrix effects, which were only controlled by the Institute of Inorganic and Analytical Chemistry of the TU Clausthal in the following analysis 2. Arsenic with Perklin Elmer Hybrid AAS, uranium with Dr. Lange photometer CADAS 50, colloids with ultrafilter Amicon 500 D, cation/anion exchanger Dowex III/IV.

No	Date	Shaft	As ges	As^{3+}	As^{5+}	Arsenic	Arsenic	Arsenic	pH	Eh
			mg L^{-1}			colloidal	anionic	cationic		mV
1	07.12.92	366 II b	1,204	50,2 %	49,8 %	available	> cationic	< anionic	7,1	n.b.
2	25.01.93	366 II b	11,95	4,2 %	95,8 %	21,8 %	92,2 %	7,8 %	6,4	150
3	26.10.93	372 b	8,41	12,0 %	88,0 %	55,2 %	85,9 %	14,1 %	7,0	n.b.
4	26.10.93	371 II b	7,96	6,0 %	94,0 %	42,5 %	81,5 %	18,5 %	7,0	n.b.
5	26.10.93	366 II b	8,28	9,4 %	90,6 %	39,7 %	82,8 %	17,2 %	7,0	n.b.
6	15.03.94	366 II b	11,75	1,8 %	98,2 %	29,1 %	68,5 %	31,5 %	6,8	n.b.
7	15.03.94	372 b	11,08	1,8 %	98,2 %	23,9 %	68,3 %	31,7 %	n.b.	n.b.
8	01.12.94	366 II b	2,861	5,9 %	94,1 %	24,9 %	67,7 %	32,3 %	7,0	360

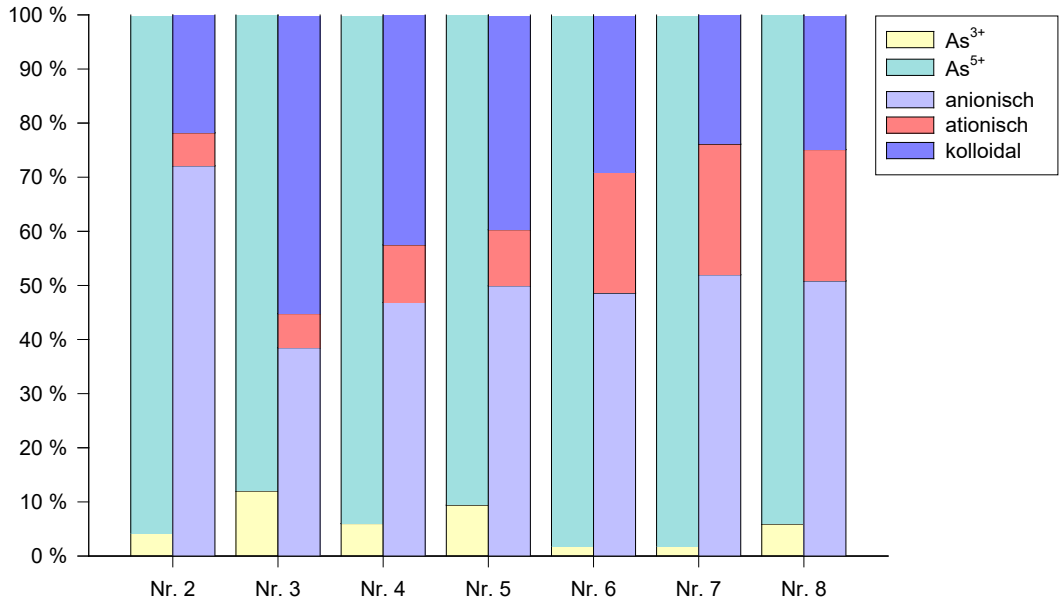

Fig. 54 Graphical representation of the ratio of arsenic(III) to arsenic(V) (right column) and of colloidal as well as cationically and anionically bound arsenic species (left column) in the mine water of the Niederschlema/Alberoda mine. No. 2: 25.01.93, 366 II b; No. 3: 26.10.93, 372 b; No. 4: 26.10.93, 371 II b; No. 5: 26.10.93, 366 II b; No. 6: 15.03.94, 366 II b; No. 7: 15.03.94, 372 b; No. 8: 01.12.94, 366 II b. Tab. 41.

6.4.5 pH-Eh dependencies of the saturation indices of selected minerals

In a further step, by varying the pH and Eh values in the representative analysis 502, it should be shown at which pH-Eh conditions a uranium or arsenic phase would be saturated relative to the mine water. In a natural system, a change in pH or Eh alone will never occur without a simultaneous change in other parameters. Therefore, especially in the case of uraninite, it cannot be assumed that, for example, with a pH of 7.0 and a redox potential of 0 mV, the equilibrium concentration of uranium corresponds to that from analysis 502.

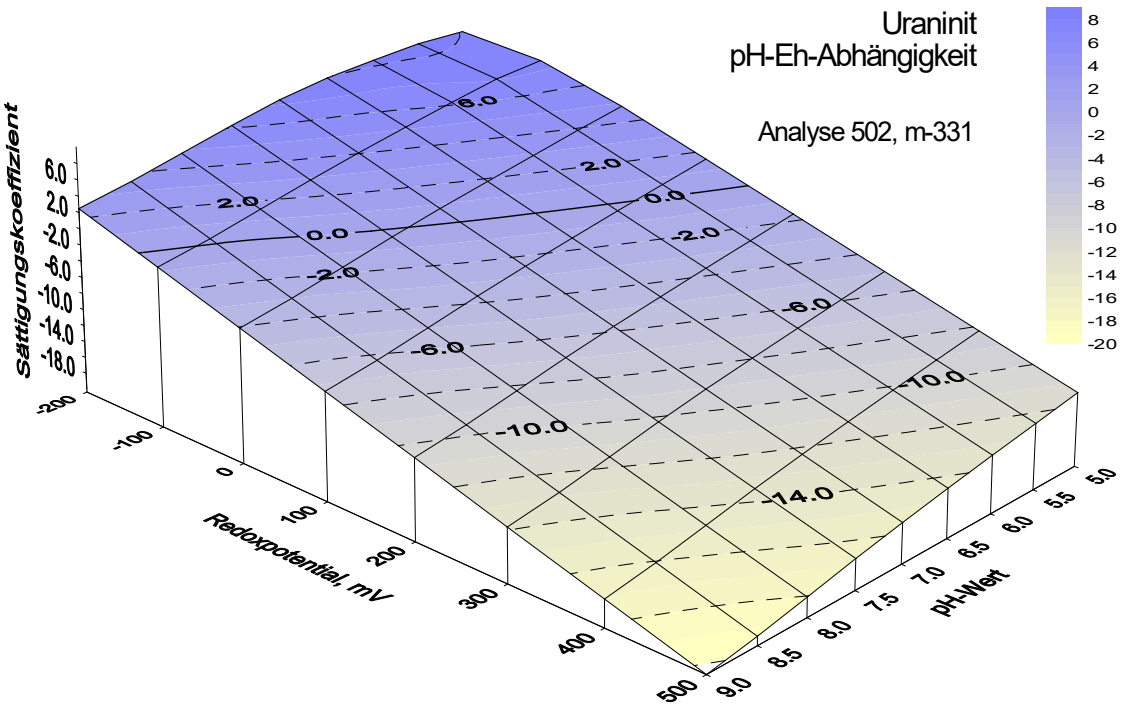

Fig. 55: Dependence of uraninite saturation at Eh values of -200 … 500 mV and pH values of 5.0 … 9.0. Calculation basis is water analysis 502 of 10 November 1994 (shaft 366 b, -m331).

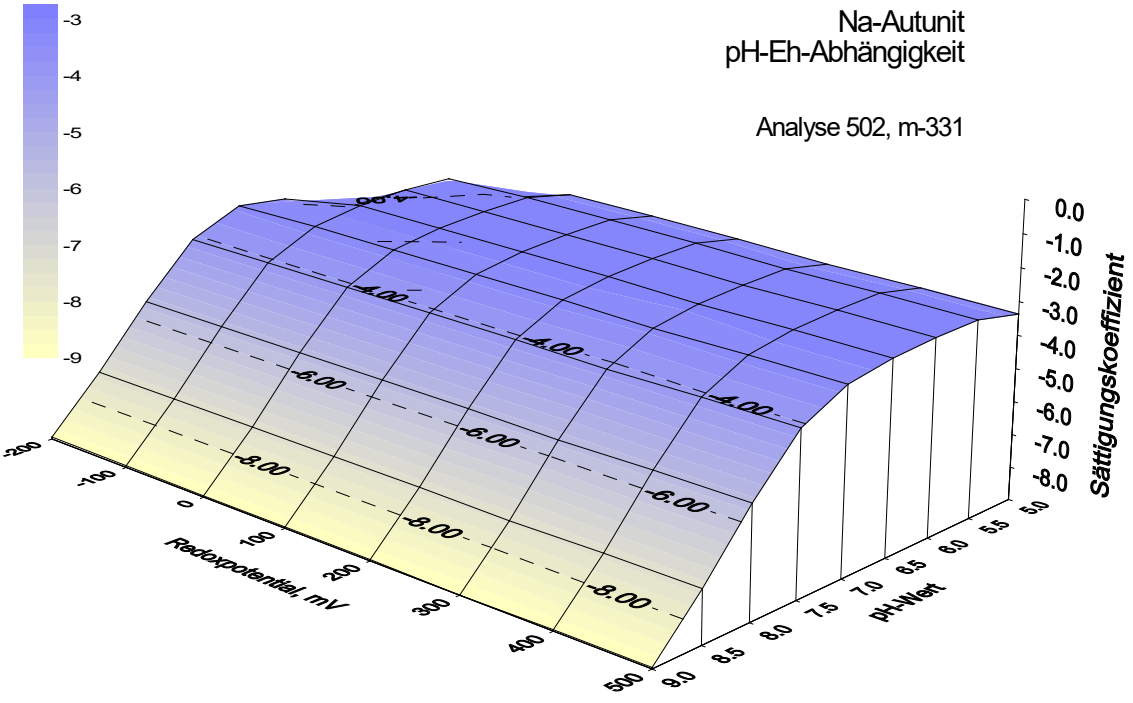

Fig. 56 Dependency of Na-autunite saturation at Eh-values of -200 … 500 mV and pH-values of 5.0 … 9.0. Calculation basis is water analysis 502 of 10 November 1994 (shaft 366 b, -m331).

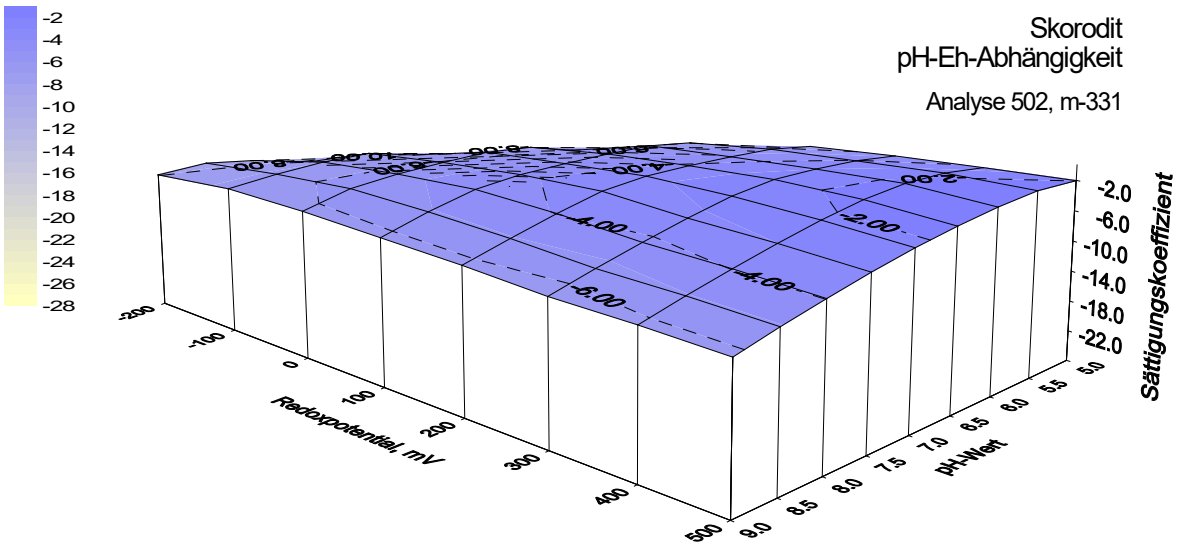

Fig. 57 Dependence of scorodite saturation at Eh values of -200 … 500 mV and pH values of 5.0 … 9.0. Calculation basis is water analysis 502 of 10 November 1994 (shaft 366 b, -m331).

To calculate the pH-Eh dependencies of the saturation indices of analysis 502, the pH value was increased from 3.0 to 11.0 in steps of 0.5, the redox potential from -200 mV to 500 mV in steps of 100 mV (the analytical value of 330 mV was also added). The 144 hypothetical water analyses were then calculated with WATEQ4F and subsequently evaluated as described above. To show the dependence of the saturation index on the two physicochemical parameters, a three-dimensional plot was made for pH values between 5.0 and 9.0 and Eh values from -200 to 500 mV. The pH value was scaled from the acidic to the basic environment so that the pH dependence of the uraninite saturation can be seen better, which increases strongly in the acidic, reducing environment. A graphical evaluation was only done for uraninite, Na-autunite and scorodite (Fig. 55, Fig. 56, Fig. 57).

As can be seen from the figures, only uraninite reaches hypothetical saturation in the area of interest. The other two minerals are always undersaturated.

6.4.6 Correlation with radium

As indicated in the chapter 5.2.3 the radium in natural systems rarely forms its own radium phases, but is mostly bound to another solid phase. It would then be expected that the radium activity in the mine water correlates with the saturation of this phase, since with increasing saturation of this phase compared to the mine water, more radium is released into the water. Conversely, when saturation equilibrium is reached, radium is diadochously bound in these phases and is no longer available to the solution equilibrium.

The PEARSON correlation coefficient was used to test the extent to which a relationship exists between the radium activity and the saturation of individual phases. A significant positive correlation was found with gypsum ($Ca[SO_4]$-$2H_2O$), jarosite ($KFe_3[(OH)_6|(SO_4)_2]$), Na-autunite ($Na_2[UO|PO_{242}]$-10-12 H_2O) and K-autunite ($K_2[UO|PO_{242}]$-10-12_2 HO).

The radium activity is probably controlled by one or more of these radium-containing phases. Which one it is cannot be said without in-depth investigations because of the strong variability of the radium activity. On the basis of the compilation by KUBACH & WEIGEL (1977), it can be assumed that radium is released into the flooding water via the solution of the autunite. The results of BLAIR et al. (1980) suggest that gypsum has a decisive role in setting or even limiting radium activity (chapter 5.2.3).

6.5 Results

The most important individual results of the statistical investigations are those of the KRUSKAL-WALLIS (Tab. 33) and the DUNN test (Tab. 57), as they provide statistical evidence for the distinction of three types of water. Mine waters, intermediate waters and seepage waters, whose classification was originally based on the PIPER and DUROV DIAGRAMS, are significantly different from each other and can be discussed separately, as is done here.

As the chemical-thermodynamic equilibrium calculations with WATEQ4F show, the carbonates, gypsum and some other mineral phases in the mine water are saturated. Oxides and hydroxides are supersaturated and will precipitate out of the mine water. Uranium and arsenic minerals are consistently undersaturated compared to the mine water.

The saturation indices of many phases asymptotically approached a certain value between 1991 and 1994, which they had almost reached towards the end of the processing period. Most curves tend to run in the direction of an equilibrium setting (SI 0), so that the saturation indices of these phases will approach 0 in the future.

All important cations (Ca, Mg, Mn, Sr, Ba) in the mine water are controlled by carbonates or sulfates. The carbonate solution causes the observed increase in hydrogen carbonate mass concentration in the mine water. The controlling solid phase to adjust the silicate mass concentration is quartz, for phosphate it is apatite and sulfate is controlled by gypsum. The WATEQ4F calculations also show that CO_2 is outgassed from the mine water and can reach several percent by volume above the water surface.

Since the saturation index of the uranium and arsenic minerals is clearly in the negative range, the arsenic and uranium mass concentrations are not controlled by the equilibrium setting between the minerals and the water. For both arsenic and uranium, the mass concentration at which saturation towards a mineral would occur is far from the measured mass concentrations. Two conclusions can be drawn from this. On the one hand, the poorly soluble, primary uranium and arsenic minerals (pitchblende, löllingite) only slowly release their metal contents into the mine water under the current – and also expected future – pH-Eh conditions. On the other hand, there are not enough easily soluble secondary uranium minerals to cause saturation of the mine water with the respective metal. In the case of arsenic, control of mass concentration is by adsorption to oxides and oxihydrates. At least some differentiated arsenic analyses show up to 55 % colloidally bound arsenic. Uranium is probably also partially bound to oxides and oxyhydrates, and its adsorption to organic components is equally probable.

The uranium and arsenic species of the mine water vary significantly with the pH value. While more than 98 % of uranium(VI) occurs in the uranyl ion ($UO^{+VI}{}_2{}^{2+}$), arsenic(V) is present in the arsenate ($AsO^{+V}{}_4{}^{3-}$). A dependence of the oxidation number on the Eh value could not be observed between 50 and 500 mV.

No equilibria were calculated with radium. Nevertheless, the correlation of radium activity with the saturation indices of other mineral phases shows that radium is released by the solution of autunite and possibly controlled by gypsum precipitation.

7 Hydrodynamic Investigations

7.1 Introduction

The previous chapter described the processes that lead to the release and control of substances. Here follows a description of the processes that cause the transport of the released substances within the flooded water body.

For flow modelling, and to be able to estimate the large-scale movement of mine water in the Niederschlema-Alberoda mine, data are needed. This includes, for example, the flow velocity, flow direction or temperature of the water. The modelling itself is not part of this work, but will be produced by orders from Wismut GmbH as part of project studies.

The diagram (Fig. 58) shows which hydrodynamic and hydrogeochemical data are necessary, among other things, to create a CFD model (computer-aided fluid dynamics) of the mine. In the present work, first results of the hydrodynamic investigations are used to gain information about the mixing of the mine water in the mine workings. Before that, an optimal tracer and a feeding probe and sampling method had to be developed that could be used under the special conditions in the Niederschlema/Alberoda mine.

7.2 Tracer test

7.2.1 Choice of tracer

There are four tracer methods for investigating flow conditions in water (HÖLTING 1992):

- Radioactive isotopes
- Dyes
- Salts
- Drift materials

In principle, the four methods must meet the following requirements, although not every method has all of them (KÄSS 1991):

- No natural occurrence of the tracer
- good analytical detectability (even in large dilutions)
- Water-soluble or dispersible
- resistant
- No interaction between tracer and medium
- economic
- Physiologically harmless

In order to clarify the flow situation in the Niederschlema/Alberoda mine, each method was checked to see whether it could be used in the floodwater. Apart from the drift method, the respective reasons for not using it (Tab. 42) lie in the physicochemical properties of the flood water. Therefore, in cooperation with Wismut GmbH, the choice fell on a drift test, in which several feed points and one or two extraction points were planned.

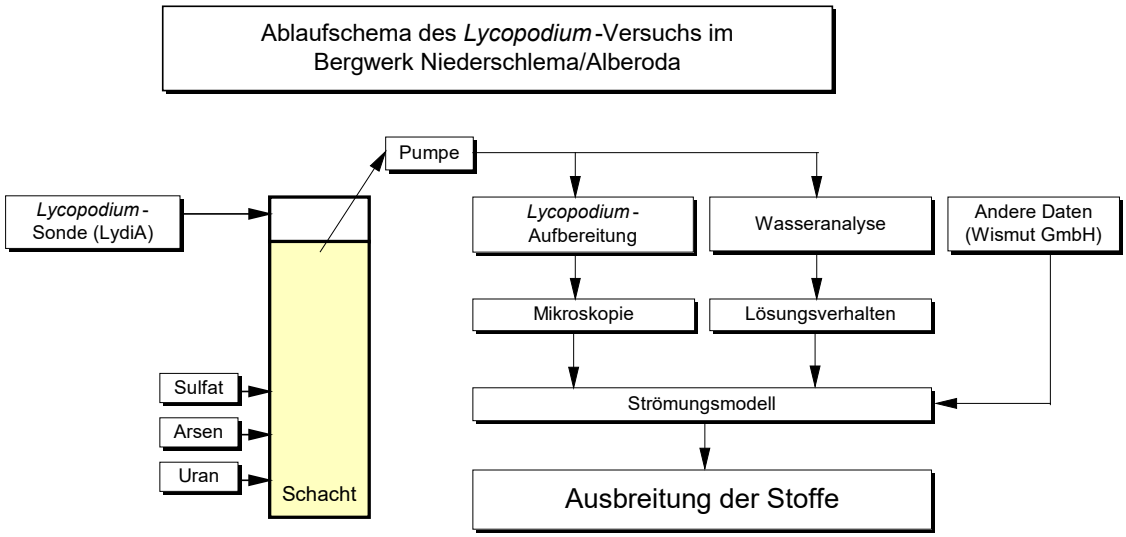

Fig. 58 Schematic representation of the *Lycopodium experiment* and related topics for data acquisition for flow modelling.

Tab. 42 Tracer methods with their disadvantages in the Niederschlema/Alberoda uranium mine.

Method	Disadvantage
Radioactive isotopes	Isotopes present in the flood water can interfere with the determination, when using tritium (^{3}H), age determination of the water is no longer possible, granting of approval questionable
Dyes	Interaction dye–flooding water
Salts	Flood water is heavily loaded with elements in question; large quantities of salt would be necessary
Drift materials	special pumps and filters necessary

From the theoretically possible drift experiments, the spore drift experiment with *Lycopodium clavatum* (club moss) first used by MAYR (1953) was selected (*"Lycopodium experiment"*). On the one hand, the spores are resistant to external environmental influences, on the other hand, they can be coloured with dyes (MAURIN & ZÖTL 1960) and added to the flooding water at various points.

7.2.2 Experimentation

Between January and May 1992, staining experiments were carried out on *Lycopodium clavatum* spores *with* six dyes (safranin, fuchsin, bismarck brown, crystal violet, Nile blue, malachite green) to determine which of them is stable in water. Although the dye-spore combinations showed no changes in the laboratory experiment, unknown processes caused discolouration in the in situ experiment (see below). All spores were stained according to a procedure modified by the author following the procedure in MAURIN & ZÖTL (1960) as follows:

Dissolve 20 g tetra-sodium diphosphate in 2300 mL distilled water and heat to boiling over a medium flame for about 10 minutes with stirring. Then 1000 g *Lycopodium clavatum* spores *are* weighed out in a pot and mixed with the heated water. To obtain a stirrable spore slurry, additional distilled water without tetra-sodium diphosphate must occasionally be added to the spore-water mixture. The spore slurry is then boiled for 10 minutes at a maximum of 90 °C so that all spores are evenly wetted. The azo dye is then added, which is prepared from 10 g of the solid dye and 125 mL of ethyl alcohol. In order to obtain an even colouring of all spores, the spore slurry with the dye must be boiled for one to two hours at a maximum of 90 °C. The spore slurry is then added to the dye. At the end, 10 mL of formaldehyde is added to the slurry while stirring to prevent moulding of the spores. The pot is left to cool for one to two days with the lid closed. The spores are then washed by filtering them using a

vacuum pump and sufficient quantities of distilled water. The washed spores are placed in the drying oven at a maximum of 70 °C for about 3 days and are then sieved to separate impurities (beetles and plant components) from the spores (0.125 mm sieve according to DIN 4188). Usually, about 90 % of the original amount of spores remain after sieving, the rest are impurities and stuck-together spores.

On 11 May 1992, 904 g of bismarck brown spores (49.5 %, $n = 2.61 \cdot 10^{11}$) were added to the floodwater via the pipe system, and on 12 May 1992 another 924 g of fuchsine spores (50.5 %, $n = 2.67 \cdot 10^{11}$) were added at pump station 296 II of level -996. At this time, the floodwater was at the level of intermediate level -1312 (water level: -967.6 mNN, volume: approx. $3.3 \cdot 10^6$ m³). While the bismarck brown spores were fed in at level -1620 near the SKW station (screw cold water station) at shaft 383 b, the fuchsine ones entered the flooding water via level –1395 at die III (Fig. 59). To avoid mutual contamination, the pipeline system was flushed with 100 m³ of water per hour for 19 hours between the two feeds. Assuming that the spores are statistically distributed in the mine water body, one litre of flooding water should contain about 80 spores of each colour. For the detection of spores in the pumped water, this theoretical number had to be sufficient to be able to detect a total of at least one spore per colour and litre of water (MAURIN & ZÖTL 1960 give a failure rate of 99 %).

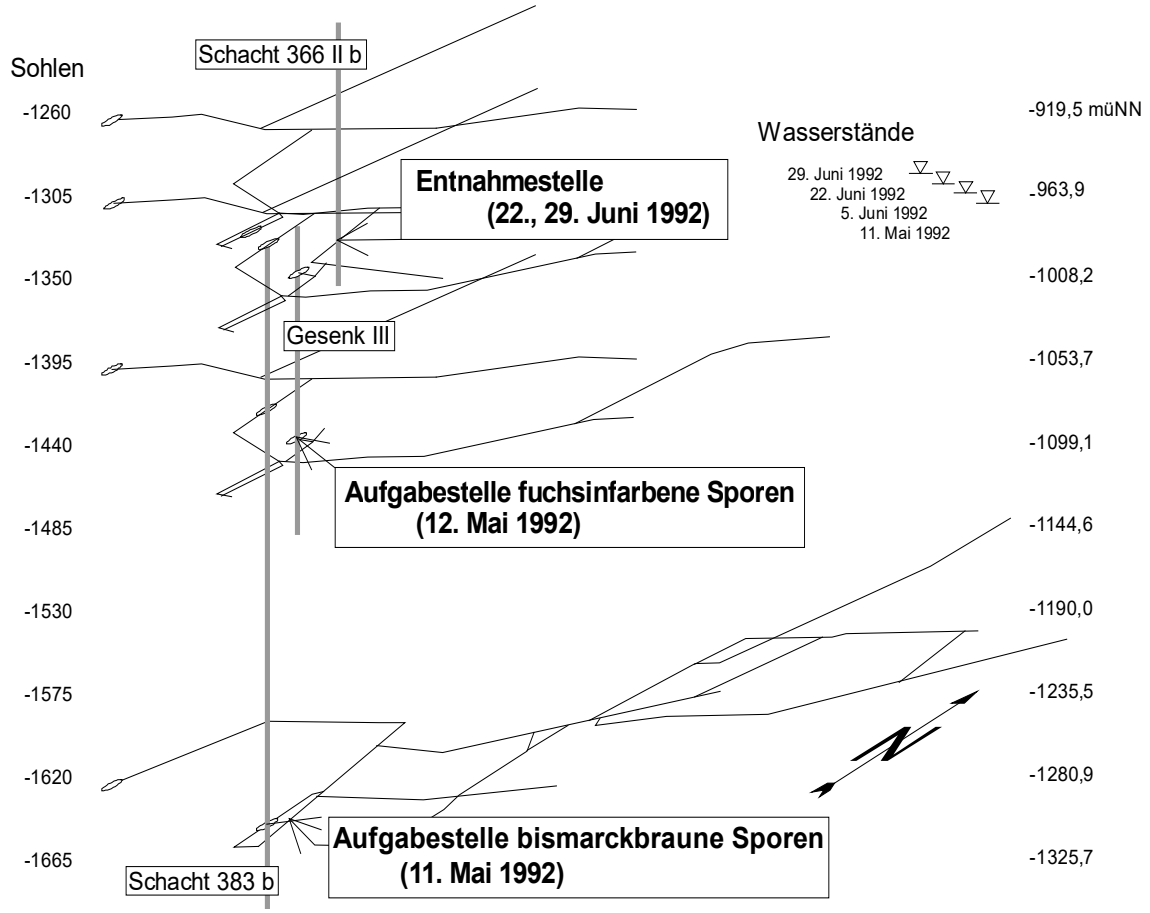

Fig. 59 Geometric conditions in the *Lycopodium* trial. Only the most important shafts (383 b, Gesenk III, 366 II b) and floor cracks (-1260, -1305, -1395, -1620) are shown in simplified form. For classification in the entire mine workings, compare Fig. 5.

Due to operational reasons (too high radon content and too low oxygen content in the mine air of the -1260 level), it was only possible to start installing a *Lycopodium* net (NY 41 HC, Hydro-Bios/Kiel) and a submersible pump (PLEUGER mini-submersible pump) with a capacity of 167.6 mL min^{-1} on the –1260 level at shaft 366 II b on 5 June 1992 at 12:40 p.m. (water level: -960.9 mNN). On two days, 22 June (water level: -956.1 mNN) and 29 June 1992 (water level: -950.6 mNN), the net was cleaned and the residues were filled into glass bottles. Due to heavy algal, bacterial and mould infestation on

the net and wooden frame (Fig. 60), the experiment had to be stopped prematurely at about 09:30 o'clock on 29 June 1992 after sampling.

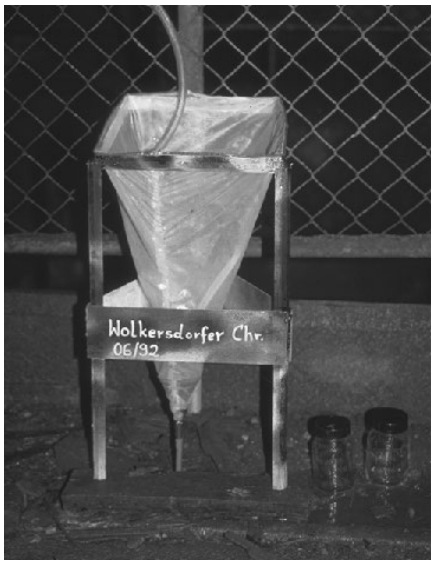

Fig. 60 Installed *Lycopodium* net at shaft 366 II b on level –1260. Hight of the wooden frame about 50 cm.

During the 24 days of the sampling period, the controlling miners emptied the *Lycopodium* net several times. They feared that the net would be irretrievably destroyed by the slimy masses (probably *Beggiatoa*). Therefore, the spores in the samples of 22 and 29 June 1992 represent only a small percentage of the spores actually pumped out. Furthermore, the miners used the PLEUGER PUMP TO fill several 100 litres of water into canisters that were sent for chemical analysis. Based on the pumping times given above, this amounts to about 333 hours of pumping time with a pumped water volume of 3300 L and about $2.64 \cdot 10^5$ spores per colour.

Despite the sources of error, the spore counts of the two dried net residues have been determined. During the count, greenish-yellow spores were found in addition to fuchsia and bismarck brown ones.

The sum of bismarck brown and greenish yellow spores almost corresponds to the number of fuchsine spores (Fig. 61). Presumably, chemical processes cause a discolouration of the bismarck brown. At which structural site of the azo dye the change occurs or which causes are responsible for it is not known. A series of experiments with several dye-water combinations also failed to clarify the matter.

Notwithstanding this, it can be deduced from the *Lycopodium* experiment that on 29 June 1992, i.e. after 49 days, the flooding water in the study area is completely mixed, since the numerical ratio of recovered spores of each colour corresponds to that of the spore quantities added.

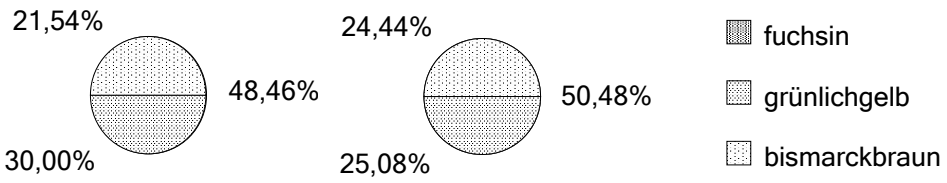

Date	fuchsin	Greenishyellow	Bismarckbrown	Sum
22.06.1992	63	39	28	130
29.06.1992	159	79	77	315
Total	222	118	105	445
Loss				99,8 %

Fig. 61: Results of the spore count from the samples of 22nd (left) and 29th June 1992 (right).

7.2.3 Description of the *Lycopodium* probe (LydiA)

A disadvantage of the May 1992 tests was that it was not possible to feed the spores into the mine water at an exact point in time, but only indirectly via the pipeline system. For the injection of the spores in a mine with its special conditions, the following requirements should be fulfilled:

- Time of release determinable (at least 60 minutes after positioning of the probe)
- Locally accurate feed, even in lower areas
- No mixing of different colours when feeding in
- Reliable opening mechanism of the feed probes
- No contamination of the water body passed through by means of uncontrollably released spores.

In principle, there are three possibilities of a probe closure:

- mechanical-electronic
- explosive electronic
- chemical.

During the preliminary considerations it became apparent that a chemical seal would work most reliably under the physicochemical conditions and the high pressures to be expected in the Niederschlema/Alberoda mine. At the same time, the requirement had to be met that neither the chemical seal nor the spores should be damaged or fall out during the loading of the probe.

The substance for the chemical seal must meet the following requirements:

- easy solubility
- Stability against external pressure
- Protection of the spores during the draining and dissolving phase

Based on this catalogue of requirements, a total of four spore probes (LydiA: *Lycopodium Injection Probe*, ***Lycopodium* Apparatus**) with different pressure equalisation and closure mechanisms were designed and tested in the course of this work. LydiA1 to LydiA3 are based on a spring-piston mechanism that moves freely in an aluminium piston as soon as the probe closure opens. Rubber seals on the lid and cap ensure that water only passes through the chemical seal to the spores. LydiA4, on the other hand, consists of specially designed parts bonded together by polyvinyl alcohol (PVA).

From 2 April 1992 to 16 June 1992, experiments were carried out with various PVAs to determine their solubility in water (Tab. 43). The PVA granulate was dissolved according to the leaflet no. 2160.890 “Polyviol” of Wacker-Chemie GmbH or the brochure “Moviol Polyvinylalkohol” of Hoechst AG. Based on the tests, MOVIOL 4-88 and Polyviol g 04/140 turned out to be the most suitable for chemical sealing.

In eight individual experiments between 8 November 1994 and 22 June 1995, each with 8.5 g PVA dissolved in 20 … 40 mL water, LydiA4 was sealed using 2 to 4 PVA layers. It could be shown that optimal bonding occurs with 8.5 g PVA with 20 mL water and three layers, whereby the time to break apart is 6 … 10 hours and the duration of complete spore emergence is again about 5 … 8 hours (Tab. 44).

In summary, LydiA4 is suitable to be used in the mine in accordance with the requirements of chapter 7.2.3 in the mine. An in-situ test can only take place again when the water level in the Niederschlema-Alberoda mine is high enough to be able to extract water with the PLEUGER MINI PUMPS.

Tab. 43 Solubility behaviour of 1 … 2 mm thick PVA films in 1000 mL cold distilled water. The sample quantity for film production was chosen in such a way that the PVA grains were just soluble in 20 mL distilled H_2O under heating. The amount of dispersion LL 869 was chosen so that a film of approx. 2 mm thickness was formed after drying.

Name	Manufacturer	Solubility behaviour	Quantity g
Moviol 4-88	Hoechst	very good	3.1
Moviol 4-98	Hoechst	bad	2.0
Moviol 40-88	Hoechst	moderate	3.6
Polyviol g 04/140	Wacker	good	3.8
Polyviol g 28/10	Wacker	bad	1.7
Dispersion LL 869	Wacker	bad	13.0

Tab. 44 Results from the eight trials with LydiA4 between 8 November 1994 and 22 June 1995 [2]: not carried out, [1]: complete exit was not awaited.

PVA weights	H_2O allowance	Layers	Probe breakage	Spore weighing	Exit time
g	mL		h:min	g	h
8,5	40	2	-[1]	-[1]	-[1]
8,5	20	2	-[1]	-[1]	-[1]
8,5	20	4	7:08	-[1]	-[1]
8,5	20	3	Aborted after 9 hours		
8,5	20	3	5:50	-[1]	-[1]
8,5	20	3	10:15	718	-[2]
8,5	20	3	10:07	803	8
8,5	20	3	8:09	772	5

7.2.4 Experiments with azo dyes

In two series of experiments, it was to be clarified what the colour changes of the Bismarck brown are based on. In the first experiment, 1 … 2 g spores were placed in test tubes filled with hydrochloric acid (pH = 2), distilled water (pH = 6) or sodium hydroxide (pH = 11). The aim was to test whether the colour change could be attributed to pH-related reactions of the dyes. Neither after 1 nor after 2 weeks were there any organoleptically recognisable colour changes on the spores. This finding led to a second series of experiments, varying the chemical matrix of the water, the temperature and the irradiation. For this purpose, about 0.2 g spores were mixed with 0.20 L water of different composition and temperature (Tab. 45) and observed in the laboratory between 18 March 1993 and 2 May 1993. The results of the experiment, the duration of which was based on the residence time of the spores in May and June 1992, are summarised in the table (Tab. 46).

Tab. 45 Experimental set-up to determine the stability of different spore colourations and reasons for the discolouration of the bismarck brown spores. The radiation source, 241.44 g uraninite (UO_2) with a specific activity of 9300 Bq kg^{-1}, was placed at a distance of 5 cm from the sample vessels BiBW, FuBW and LoBW (activity 311 Bq). Temperature: Average temperature during the experimental period.

Spore colour	Temperature	Water quantity	Bismarck brown	Foxin	Fluorescein
Tap water	19,1	0,20 L	BiLe – 0.22 g	FuLe – 0.24 g	LoLe – 0.2 g
Cold flooding water	19,0	0,20 L	BiKF – 0.22 g	FuKF – 0.24 g	LoKF – 0.2 g
Warm flooding water	26,2	0,20 L	BiWF – 0.22 g	FuWF – 0.24 g	LoWF – 0.2 g
Irradiated flood water	18,8	0,20 L	BiBW – 0.22 g	FuBW – 0.24 g	LoBW – 0.2 g

In addition to bismarck brown and fuchsine spores, spores stained with fluorescein were used, as this dye was said to be stable against external influences (Dr. M. STEINFATT, TU Clausthal, pers. comm.). Except in the samples with tap water, this could not be confirmed, as the samples LoBW, LoWF showed changes in the spores after one, the sample LoKF after five days. The spores LoBW irradiated with 311 Bq even turned black on the side facing the radiation source.

All other samples in the cold tap water (BiLe, FuLe) and irradiated flooding water (BiBW, FuBW) showed no to slight changes. In the “cold flooding water", the spores swelled slightly after two (BiKF) or three (FuKF) days.

The “warm flooding water” caused a clear swelling in the bismarck brown spores (BiWF) after one day, and a slight swelling in the fuchsia spores after five days. At the end of the 46-day experiment, no colour change was visible in either the bismarck brown or the chestnut spores.

None of the parameters pH, temperature, chemical matrix or radiation intensity is therefore responsible for the colour changes. It is possible that microbial activities are the cause of the colour change. However, this assumption could not be verified due to the lack of equipment.

7.2.5 Results and discussion

Since it was not possible to carry out continuous sampling during the test period, the flow velocity can only be estimated. From the feeding point, near the blind shaft 383 b on level -1620 (-1280 mNN), to the pumping point below level -1260 (-961.5 mNN), the bismarck brown spores had to cover -a vertical distance of d_v = 320 m and a horizontal -distance of d_h = 460 m, together d_g = 780 m. They needed at most the time between 11 May and 22 June 1992, i.e. 42 days. They needed at most the time between 11 May and 22 June 1992, i.e. 42 days. A minimum speed of v_s = 0.77 m h^{-1} is calculated (formula 44).

$$v_s = \frac{d_h + d_v}{t} = \frac{460\ \text{m} + 320\ \text{m}}{1008\ \text{h}} = 0{,}77\ \text{m h}^{-1} \qquad (44)$$

The tracer test and the tests with different probe types produced the following results:

- Stained lycopod spores are suitable as tracers in a flooded mine to determine flow conditions
- The chosen sampling method is suitable to recover spores
- Continuous sampling must begin immediately after the start of the experiment in order to be able to record the rate of spread of the spores.
- After 42 days, the water from levels -1620 and -1395 in the area of shaft 366 II b, level -1260 is homogeneously mixed
- The LydiA4 probe is suitable for abandoning spores in a mine

Tab. 46 Compilation of the results from the experiments with coloured spores. Temperature in °C. Explanation of abbreviations in Tab. 45. brownish: brownish.

Date		BiLe	FuLe	LoLe	BiKF	FuKF	LoKF
18.3.1993, 18:40	Water	clear	clear	clear	light brown	light brown	light brown
	Temperature	20.4	20.4	20.4	19.8	19.8	19.8
	Spores	-	-	-	-	-	-
19.3.1993, 8:32	Water	clear	clear	fluorescent	light brown	light brown	fluorescent
	Temperature	19.2	19.2	19.2	19.12	19.1	19.1
	Spores	-	-	-	-	-	-
20.3.1993, 10:44	Water	clear	clear	fluorescent	light brown	light brown	fluorescent
	Temperature	18.9	18.9	18.9	18.8	18.8	18.8
	Spores	-	-	-	slightly swollen	-	-
23.3.1993, 13:26	Water	clear	clear	fluorescent	light brown	light brown	fluorescent
	Temperature	18.9	18.9	18.9	18.9	18.9	18.9
	Spores	-	-	-	slightly swollen	slightly swollen	brownish. slightly swollen
29.4.1993, 19:33	Water	clear	clear	fluorescent	light brown	light brown	fluorescent
	Temperature	18.3	18.3	18.3	18.2	18.2	18.2
	Spores	-	-	-	slightly swollen	slightly swollen	brownish. slightly swollen
2.5.1993, 8:48	Water	clear	clear	fluorescent	light brown	light brown	fluorescent
	Temperature	18.9	18.9	18.9	19.0	19.0	19.0
	Spores	-	little puffed	little puffed	slightly swollen	slightly swollen	brownish. slightly swollen

Date		BiWF	FuWF	LoWF	BiBW	FuBW	LoBW
18.3.1993, 18:40	Water	light brown	light brown	light brown	light brown	light brown	light brown
	Temperature	19.8	19.8	19.8	19.8	19.8	19.8
	Spores	-	-	-	-	-	-
19.3.1993, 8:32	Water	light brown	light brown	fluorescent	light brown	light brown	fluorescent
	Temperature	28.5	28.5	28.5	19.0	19.0	19.0
	Spores	swollen	-	brownish	-	-	blackish
20.3.1993, 10:44	Water	light brown	light brown	fluorescent	light brown	light brown	fluorescent
	Temperature	24.4	24.4	24.4	18.7	18.7	18.7
	Spores	swollen	-	brownish	-	-	black. to the radiation source
23.3.1993, 13:26	Water	light brown	light brown	fluorescent	light brown	light brown	fluorescent
	Temperature	24.9	24.9	24.9	18.7	18.7	18.7
	Spores	swollen	slightly swollen	Swollen. brownish	-	-	black. to the radiation source
29.4.1993, 19:33	Water	light brown	light brown	fluorescent	light brown	light brown	fluorescent
	Temperature	30.5	30.5	30.5	17.9	17.9	17.9
	Spores	swollen	slightly swollen	Swollen. brownish	-	-	black. to the radiation source
2.5.1993, 8:48	Water	light brown	light brown	fluorescent	light brown	light brown	fluorescent
	Temperature	28.9	28.9	28.9	18.8	18.8	18.8
	Spores	swollen	slightly swollen	Swollen. brownish	-	-	black. to the radiation source

7.3 Temperature measurements

7.3.1 Energy sources

With a heat flux density of q = 70 … 95 mW m^{-2}, the Ore Mountains are among the areas with the largest heat fluxes in the new federal states (HURTIG & OELSNER 1979). From numerical modelling, a geothermal depth step of 40 m on average is calculated up to 12 km depth, which is higher below 14 km depth in the area of the Gera-Aue-Joachimsthal fault, and lower in the Flöhatal (OELSNER & HURTIG 1979).

At the Niederschlema/Alberoda uranium mine, the temperature of the flooding water is caused by various factors, three of which should be mentioned. Firstly, the geothermal depth level, secondly, the long-term cooling of the shafts and drifts to about 25 °C and thirdly, negligible radioactive decay processes in the flooding water and at the contact of the water with ore veins. In the deepest pit (-1800 level), the temperature is about 70 °C due to the geothermal gradient of 32 m. This is due in particular to the heat generation (Table 1). Heat generation (Tab. 47) from the decay of uranium, thorium and potassium diffusely distributed in the rock is particularly responsible for this (^{238}U, ^{235}U, ^{232}Th, ^{40}K, Tab. 48). Another non-negligible heat source influencing the geothermal depth stage is the post-kinematic Auer Granite (SEIM & TISCHENDORF 1990, JUST 1992, JUST 1980) and presumably the heat high of the Gera-Aue-Joachimsthal fault recognisable from the above-mentioned modelling. The heat production of the Auer granite presumably corresponds to that of the Eibenstock and Kirchberg granite and thus amounts to A = 3.0 … 6.7 µW m^{-3}. A substantially lower heat production with A = 1.7 µW m^{-3} is shown by the phyllites (JUST 1992).

As long as uranium was actively mined in the mine, cooling units ran at various levels to cool the mine ventilation to a temperature of 25 °C. This led to the cooling of the rock in the immediate vicinity around the mine workings. In the immediate vicinity around the mine workings, this led to the cooling of the rock, which must first be compensated for before the geothermal energy is available to heat the mine water.

Heat generation from the decay of the radioactive isotopes in uraninite (mainly ^{238}U, ^{235}U, ^{232}Th) dissolved in the mine water does not result in a decisive contribution to the temperature increase of the flooding water. Based on the specific heat capacity of the flooding water $c_p \approx 4.0$ J K^{-1}g^{-1} (seawater: c_p = 3.93 J K^{-1}g^{-1}, dest. water: c_p = 4.184 J K^{-1}g^{-1}) and a specific heat production of the uraninite ($^{238}U_{0,896}U^{235}{}_{0,006}Th_{0,0982}O$) of A = 7.98 10 ·$^{-2}$µW g^{-1} (78.94 % ^{238}U; 0.57 % ^{235}U; 8.61 % ^{232}Th), the following formula can be calculated 45 a heating rate of

$$w = \frac{A}{c_p} = \frac{7{,}98 \cdot 10^{-8}\ \mathrm{W\,g^{-1}}}{4{,}0\ \mathrm{J K^{-1} g^{-1}}} = 2{,}0 \cdot 10^{-8}\ \mathrm{K\,s^{-1}} \qquad (45)$$

per unit mass of uraninite and water. Although OBRIKAT & FUSBAN (1993) show by their analyses that the isotope distribution of uranium and thorium in water does not correspond to that of uraninite, a uniform isotope release should be assumed for a conservative estimation of the temperature increase in the flooding water. This means that with 36 · 10^6 m³ of flood water and 6 mg of uranium (expected value for the end of flooding) per litre of flood water, around 230,000 a would be necessary to cause a temperature increase of 1 K.

Tab. 47: Specific heat generation rates and relative frequencies of ^{238}U, ^{235}U, ^{232}Th, ^{40}K (BASALTIC VOLCANISM STUDY PROJECT 1981, quoted from SEIM & TISCHENDORF 1990).

	Unit	^{238}U	^{235}U	^{232}Th	^{40}K
Specific heat production *A*	µW kg^{-1}	94	579	26	30,2
relative frequency	%	99,276	0,720	100,0	0,01167

Tab. 48 Specific activity in Bq kg^{-1} of selected radionuclides in the fines of waste rock piles of different duration (ZETZSCHE 1994). All three waste rock piles are located in the area of the environmental register Niederschlema/Alberoda.

Stockpile no.	Service life	^{238}U	^{235}U	^{232}Th	^{40}K	^{226}Ra	^{210}Pb	^{136}Cs
208	1949	130 ± 50	6 ± 1	55 ± 12	880 ± 180	245 ± 50	200 ± 70	41 ± 9
296	1952	250 ± 70	11 ± 3	40 ± 10	910 ± 190	690 ± 140	350 ± 120	68 ± 15
371	1959	520 ± 100	24 ± 5	52 ± 12	1000 ± 210	670 ± 130	530 ± 150	27 ± 7

7.3.2 Measurements and evaluation methods

The detailed temperature measurements, which are still ongoing, are intended to provide insights into the hydrodynamics of the water in the mine workings. The results are presented together with those of the chapters “Further physicochemical measurements” (chapter 7.4), “Flow velocity” (chapter 7.5) and “The flooding of the Niederschlema/Alberoda mine” (chapter 7.6) have been incorporated into the discussion of the results (Chapter 7.7). There, a model conception of the flooding process in the Niederschlema-Alberoda mine is developed.

At the beginning of June 1992, the author submitted a concept to Wismut GmbH to ensure continuous monitoring of the flooding process in the flooding water by measuring pressure, temperature, redox potential, electrical conductivity and pH (Tab. 49). The aim of these physicochemical measurements is to clarify and record the hydrogeochemical, thermal and hydrodynamic processes during the flooding of the Niederschlema-Alberoda mine.

Overall objective

- Verification of the model through changes that have actually occurred

Temperature/electrical conductivity

- Structure of the flow behaviour during flooding of a level
- Increase/decrease in dissolved ions
- Convection/Diffusion/Turbulence
- Temperature stratification in the mine
- Mass and heat transport in the shafts and roadways

Print

- Breaking dams
- Observation of water rise/discontinuities
- Flood monitoring of larger cavities
- Effects of rainfall
- Ingress of additional water
- Pressure increases due to flow
- Mechanical stability of the mine workings

pH/Eh

- Determination of the possible solutions of certain elements
- Calculating phase equilibria

Tab. 49 Possible questions that can be clarified by measuring the physicochemical parameters in the Niederschlema/Alberoda mine.

For temperature measurement in the shafts 366 II b, 371 II b, 383 and 372 b, a portable temperature and water level probe was used, which has a resolution of 0.1 °C and is attached to a 500-metre-long stranded wire with centimetre divisions. Between 22 June 1992 and 14 September 1992, temperature, electrical conductivity and pressure probes from the company PIC/Munich were used, which had to be dismantled again due to damage to the plug connections and the electronics (complete failure on 25 August 1992). From 27 July 1994 to 5 August 1994 and from 6 September 1994 to 9 November 1994, an automatically recording temperature, electrical conductivity, pH and pressure probe (multi-parameter probe) from LogIn GmbH/Gommern was used in shaft 383, which was lost on 4 September 1994 due to corrosion of the steel cable. The measurements in the shafts 371 II b and 372 b were taken from the -990 level, in the 383 shaft from the -540 level and in the 366 II b shaft from working platforms which were mounted 5 … 7 m above the next level to be flooded. Additional measurements were carried out by DFA/Chemnitz on behalf of Wismut GmbH from 15.3.93 – 19.3.93, 30.3.93 – 6.4.93, 7.3.94 – 25.3.94 and 21.11.94 – 2.12.94 (DFA FERTIGUNGS- UND ANLAGENBAU-GESELLSCHAFT 1993, DFA FERTIGUNGS- UND ANLAGENBAU-GESELLSCHAFT 1994, C & E CONSULTING UND ENGINEERING GmbH 1994).

Tab. 50 Compilation of the framework data on the temperature measurements of the TU Clausthal and Wismut GmbH in the shafts 366 II b, 371 II b and 372 b.

Shaft	Beginning	Sump	Start of measurement	Measuring	Number	Temp. min.	Temp. max.
366 II b	Sole -990	Sole -1350	5.6.92	28.9.93	51	25.3 °C	41.0 °C
371 II b	Sole -990	Sole -1350	24.8.92	21.9.93	36	29.5 °C	40.9 °C
372 b	Sole -990	Sole -1620	21.12.92	14.9.93	20	36.3 °C	40.6 °C

On 5 June 1992, the first regular temperature measurements (vertical temperature profiles) began in the water column of several shafts. These reached depths of -1030 mNN in the 366 II b shaft -(between levels -1395 and -1350), -980 mNN in the -371 II b shaft (between levels -1350 and -1305) and -1140 mNN in the 372 b shaft (below level -1485). The measuring programme ended on September 28, 1993, after the probe in the 366 II b shaft -became entangled in 142.00 m water depth (-876.32 m a.s.l.) in inadequately disposed file waste and could -not be recovered. Details of the self-performed measurement programmes are listed in the table (Tab. 50).

In order to be able to represent the temporal development of the temperature distribution in the shafts, the temperatures at predetermined depths were calculated from the measured vertical temperature profiles of shafts 366 II b, 371 II b and 372 b by linear interpolation. From shafts 366 b, 296 II b, 371 and 383, where DFA/C&E measured, there were not enough measurement series available for such an evaluation. Between each level, the temperature was calculated at five depth points, the first at the level of the level, the other four evenly distributed between this level and the next level. For each of these points, which were about 5 m apart, a temperature t_i was calculated for the respective measurement date according to the formula 46 was calculated.

$$t_i = t_{i^+} + \left(\frac{t_{i^+} - t_{i^-}}{s_{i^+} - s_{i^-}} \right) \left(s_i - s_{i^+} \right) \qquad (46)$$

t_i : Temperature at the interpolated point
t_{i+} : Temperature at the measuring point above
t_{i-} : Temperature at the measuring point below
s_i : Depth of the interpolated point
s_{i+} : Depth of the measuring point above
s_{i-} : Depth of the underlying measuring point

The results of the above calculations are the temperature curves for shafts 366 II b, 371 II b and 372 b (Fig. 65, Fig. 68, Fig. 71).

Tab. 51: Compilation of framework data on temperature measurements by DFA/C&E on behalf of Wismut GmbH in shafts 366 II b, 371 II b, 372 b, 366 b, 296 II b, 371 and 383. *T*: temperature, Lf: electrical conductivity, pH: pH value, Eh: Eh value, *v:* flow velocity.

Shaft	Beginning	Swamp	Measurement data	Number	Parameter
296 II b	Sole -540	Sole -990	24.11.94, 25.11.94	2	*T*, Lf, pH, Eh
366 b	Sole -540	Sole -990	21.11.94, 22.11.94	3	*T*, Lf, pH, Eh
366 II b	Sole -990	Sole -1350	24.3.94, 25.3.94	2	*T*, Lf, pH, Eh
371	Sole -540	Sole -1080	28.11.94, 29.11.94	2	*T*, Lf, pH, Eh
371 II b	Sole -990	Sole -1350	30.3.93, 7.3.94, 8.3.94	3	*T*, Lf, pH, Eh
372 b	Sole -990	Sole -1620	15.3.93, 16.3.93, 17.3.93, 18.3.93, 19.3.93, 31.3.93, 1.4.93, 2.4.93, 5.4.93, 15.3.93, 16.3.93	11	*T*, Lf, pH, Eh, *v*
383	Sole -540	Sole -1260	1.12.94, 2.12.94	2	*T*, Lf, pH, Eh

Further measurements were carried out by DFA/C&E on behalf of Wismut GmbH (Tab. 51). The evaluation presented here only includes series of measurements taken when the probe was lowered and not when it was raised. The reason for this is the construction of the probe, which prevents a continuous flow around the sensors during recovery. Therefore, the measurements are not suitable for making correct statements about the physicochemical conditions in the respective water depth.

7.3.3 Explanations for the selection of the measurement series

Due to the large number of individual measurements (Tab. 50, Tab. 51), representative measurements had to be selected for each of the seven shafts. The selection criteria were completeness of the data set and characteristic temperature jumps, which are similar in most of the other measurement series. The descriptions of the respective temperature measurements also took into account findings from other temperature measurements carried out there. Own measurements were recorded by noting down the measured values, while the DFA/C&E used data loggers. Because of the different way of recording the data, the graphical representation methods differ slightly. Own measurements can be identified by points between the connecting lines of the measurement curve (e.g. Fig. 64), whereas the DFA/C&E measurements are represented by only one line (e.g. Fig. 62).

In the rest of the text, temperature increases or decreases are described. This always refers to a relative change from the bottom (lowest point of the shaft) to the top (water level). A first report on the findings from the measurements up to July 1993 was prepared within the framework of the cooperation agreement with Wismut GmbH (WOLKERSDORFER 1993), which is partly referred to here. The measurements up to December 1994 were recorded in a 2nd report on the cooperation agreement (WOLKERSDORFER 1995), which was already based on the content of this dissertation.

In the following chapters, the seven shafts are presented in ascending order of number. The first subsection of each chapter is a description of the vertical temperature profile. The second subsection is only present if there are enough temperature measurements from which a temporal temperature profile could be constructed. This results in a break in the numbering system, since, for example, chapter 7.3.4.1 is not followed by another chapter 7.3.4.2. This was accepted in order to maintain a clear structure.

7.3.4 Shaft 296 II b

7.3.4.1 Vertical temperature profile

At 33.1 … 33.2 °C, the water in shaft 296 II b is about 3 K colder than the water in other shafts at the same time (Fig. 62). At the level of level -990, the water has a temperature of 36.2 °C, as measured in shafts 366 b, 371 and 383.

At the transition from the filling point to the shaft (Fig. 69) the temperature decreases by 3 K over 4 m. These clear differences in the water temperature are equally reflected in the other physicochemical parameters as well as in the hydrochemical classification of the measuring points m-325 and m-332 in shaft 296 II b (chapter 6.3.1).

Another feature of the temperature profile in the shaft is the small temperature jump between -616 and -618 mNN, which divides -the water column into two water bodies, each with a different temperature. As the electrical conductivity measurements show, each of the two water bodies has a different electrical conductivity, thus a different chemical composition. Since the temperature difference of about 0.1 K is too small to cause a density stratification, both areas will mix with each other over time and form a uniform water body.

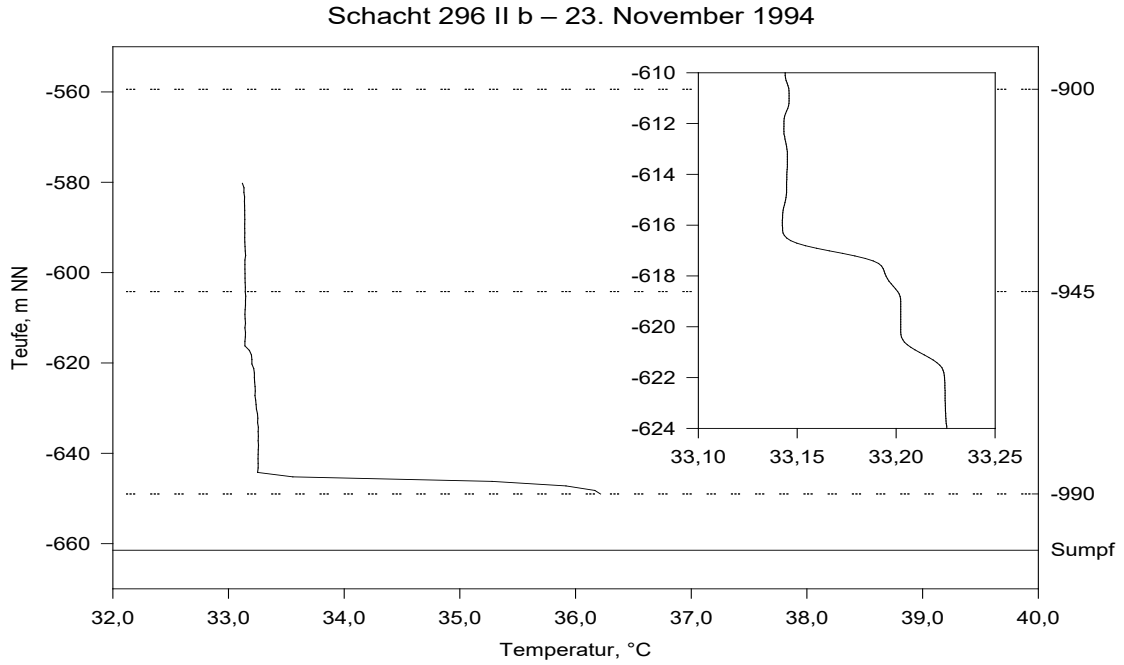

Fig. 62 Temperature profile of 23 November 1994 in shaft 296 II b with detailed representation of the temperature profile between -610 and -624 mNN (modified after DFA/C&E 1993/94).

7.3.5 Shaft 366 b

7.3.5.1 Vertical temperature profile

In shaft 366 b, all three measurements were stopped 11 … 17 m above the sump. Interestingly, the temperature above level -990 is -constant at about 35.3 °C (Fig. 63), without the drop in temperature above this main level observed in other shafts. There is a hint of a change at the level of the filling point in the measurement on 21 November 1994, whereas no influence seems to emanate from level -945.

The measurements in shaft 366 b suggest that influences emanating from the water surface have no discernible effect on the water temperature. On the contrary, water flowing into the shaft from the main levels seems to influence the temperature.

7.3.6 Shaft 366 II b

7.3.6.1 Vertical temperature profile

In the temperature profile of the IVth level (Fig. 69) of the 366 II b shaft, the temperature jump at level -1350 is striking (Fig. 64). Already during the first measurement on June 5, 1992, the aforementioned temperature and density layer was present, which – as could be shown on June 29, 1992 – is accompanied by a 4 … 5 m thick intermediate layer (temperature boundary layer). The upper and lower edges of the intermediate layer have a clear boundary; within the intermediate layer the temperature increases linearly with 1 … 2 K m^{-1}. As could be shown on 6 July 1992, the temperature jump takes place within a layer less than 10 cm thick. Thus, there is a distinct separation layer between the water in the shaft (shaft water) and the intermediate layer as well as between the intermediate layer and the water in the sump (sump water). In the course of 16 months, the lower edge sank by nine metres due to density currents, while the upper edge, apart from minor fluctuations in the metre range, maintained its depth position. This means that the intermediate layer continuously migrates into the shaft sump and becomes wider and wider.

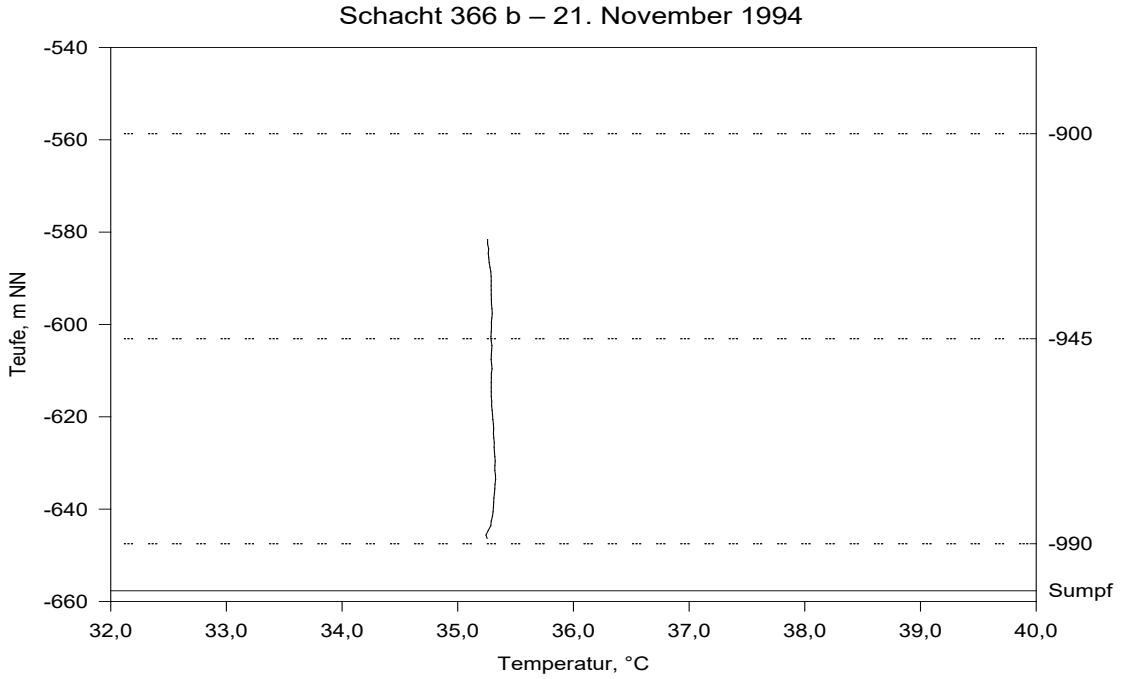

Fig. 63 Temperature profile of 21 November 1994 in shaft 366 b (modified after DFA/C&E 1993/94).

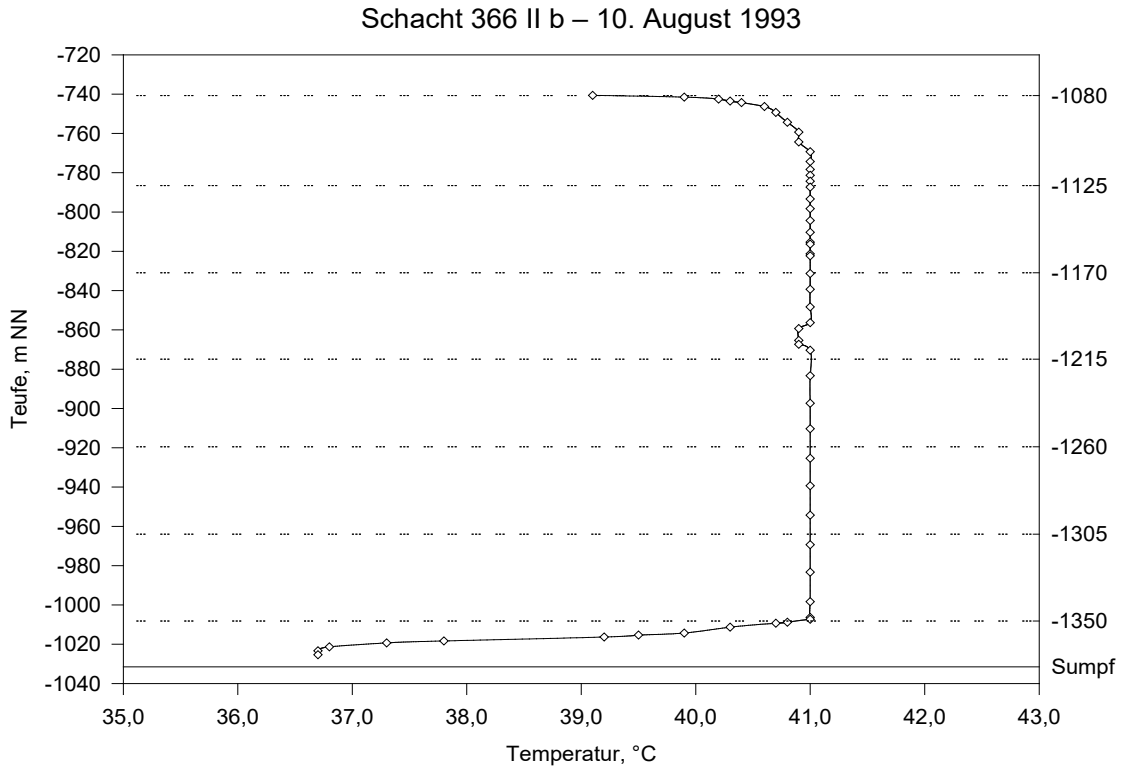

Fig. 64: Temperature profile of 10 August 1993 in shaft 366 II b.

At level -1170, a temperature increase of 0.1 K occurred shortly after flooding. On 15 February 1993 the difference was 0.8 K, on 1 March 1993 even 0.9 K. The cause of this increase is probably water from a cut pipeline 5 m north of the V. shaft compartment. From there, warmer, pressurised water flowed out of flooded areas of level -1170 already at the beginning of the flooding. A similar effect could be observed for three months (5 October 1992 … 4 January 1993) at level -1260, which, however, was not related to a single pipeline but to water from the roadway.

In order to check whether the temperature also changes horizontally, the horizontal temperature curve was investigated on 7 December 1992 in the II. shaft level 1 m above level -1305 (-962.71 mNN). In addition to the measured value in the middle of the IV. run, three values were determined in the II. run, about 20 cm from the III. run, the first being in the middle, the other two 50 cm each from the shaft wall (Fig. 69). All four readings consistently indicated a temperature of 40.1 °C.

Despite many smaller temperature variations in the profile measurements, three characteristic features of all measurements can be highlighted:

- Temperature drop after flooding of a battered invert
- Almost constant temperature between two struck soles
- Minor temperature changes in the filling point area

The temperature changes in the filling site area were -most consistent at level -1215. Since the flooding of this level in October 1992, there has been a temperature increase or decrease of up to 0.2 K in almost every measurement. At other levels, such a temperature increase was less pronounced.

7.3.6.2 Temperature curve over time

Two different areas are clearly visible in the temperature-time diagram of shaft 366 II b, each of which has a roughly constant temperature (Fig. 65). Both areas show a temperature increase, which amounts to about 9 … 10 K in the cooler area and 3 … 4 K in the warmer area. Due to the faster

warming of the cooler area, the temperature differences have decreased from 11 K to 4 K in the period under investigation.

In addition, five events stand out in the curve:

- 14.9.92 … 28.9.92 : Temperature rise by 2 K
- 30.11.92 : Incipient temperature drop in the shaft water body
- 25.1.93 : Temperature rise again in the shaft water body, temperature plateau in the sump water body.
- 1.3.93 : Maximum temperature in the shaft water body and temperature drop starting there
- 26.4.93 : Rise in temperature again in the sump water body

All events can also be documented in the two other shafts that were continuously measured at that time, which on the one hand indicates their large-scale significance and on the other hand the good hydraulic contact between the shafts. The reasons for the events cannot be reconstructed. Conceivable are the flooding of levels with simultaneous establishment of new hydraulic connections, stronger inflow of cold precipitation water as well as switching on or off mine water pumps or the changeover of the flooding process (for example on 6 January 1993).

However, it can be clearly seen that the two water bodies, separated from each other by a thermocline, did not mix for at least 15 months. At the same time, the temperature differences within the vertical water column of the sump water body or shaft water body were in the range of 1 K, which indicates their good convective mixing.

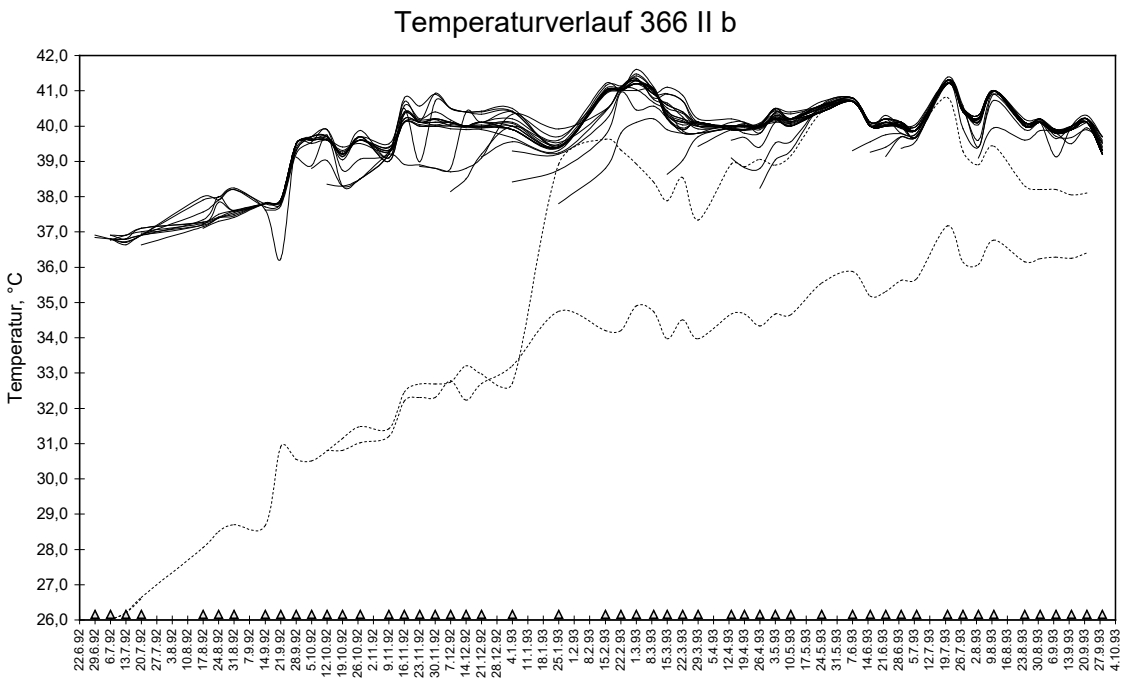

Fig. 65 Temperature curve in shaft 366 II b between 29 June 1992 and 28 September 1993. Each line corresponds to the temperature curve at a certain depth. The temperature curve in the sump water body is dashed. The triangles indicate the day of the measurement.

Whether the temperatures in the sump water body and the shaft water body have meanwhile equalised can no longer be determined, since the flooding of level -990 from May 1994 onwards meant that it was no longer possible to take measurements. The last temperature measurement by DFA/C&E on 25 May 1994 was interrupted at -760 mNN (between levels -1080 and -1125).

7.3.7 Shaft 371

7.3.7.1 Vertical temperature profile

In shaft 371, on 28/29.11.94, the temperature could only be -measured a few metres below level -990. It seems as if the temperature below this level is constant, but above it it drops by -0.2 K from 35.9 °C to 35.7 °C between the unstruck level -900 and -990 (Fig. 66). The small kink 8 … 9 m above the level of the floor is exactly at the level of the transition from the shaft to the filling point (Fig. 69) and proves that physico-chemical changes occur either there or, as can be observed in other shafts, at the level of the swing stage pit.

7.3.8 Shaft 371 II b (“Ellipse”)

7.3.8.1 Vertical temperature profile

In the 371 II b shaft, temperatures were measured from the -990 level. For this purpose, Wismut GmbH had mounted- a wooden working platform with a central opening above the V. shaft drift. The measurements could only be taken up to 325 m below the working platform because a dam had been- built in the shaft between levels -1350 and -1305. It was intended to prevent the exchange of radon during the operating phase.

Overall, the measurements show similarities with those of the 366 II b shaft in terms of the vertical and temporal temperature course (Fig. 67). Just as there, the temperature between two levels is mostly constant, shows a decrease after flooding a level and in some levels decreasing or increasing by up to 0.2 K.

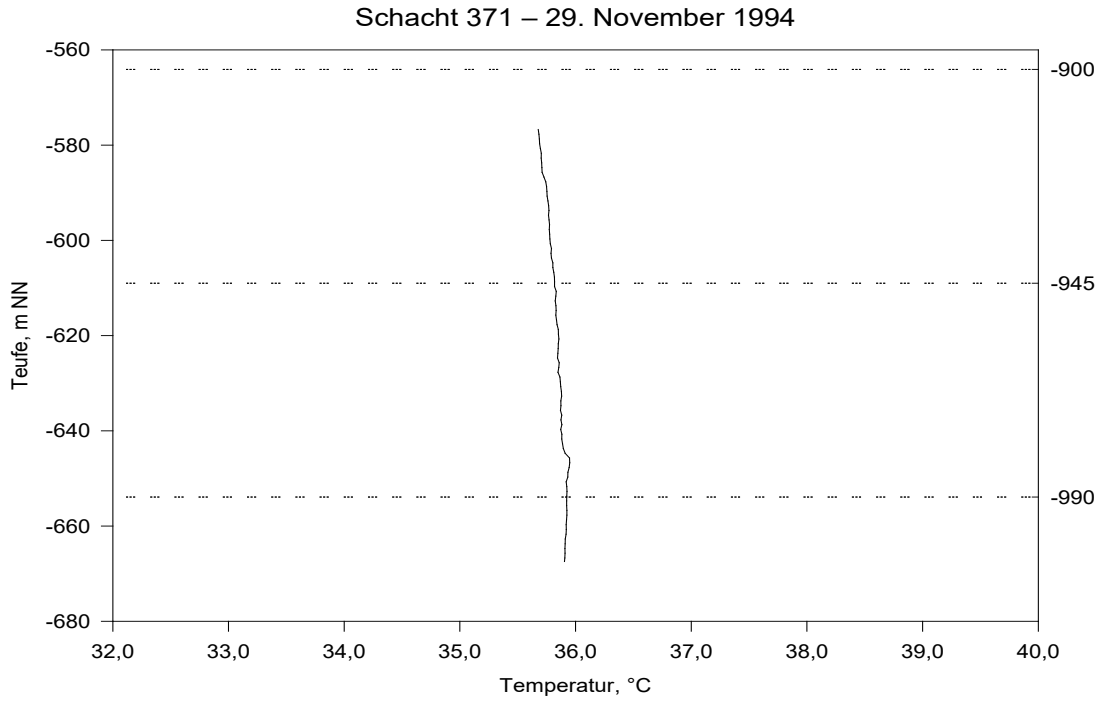

Fig. 66 Temperature profile of 29 November 1994 in shaft 371 (modified after DFA/C&E 1993/94).

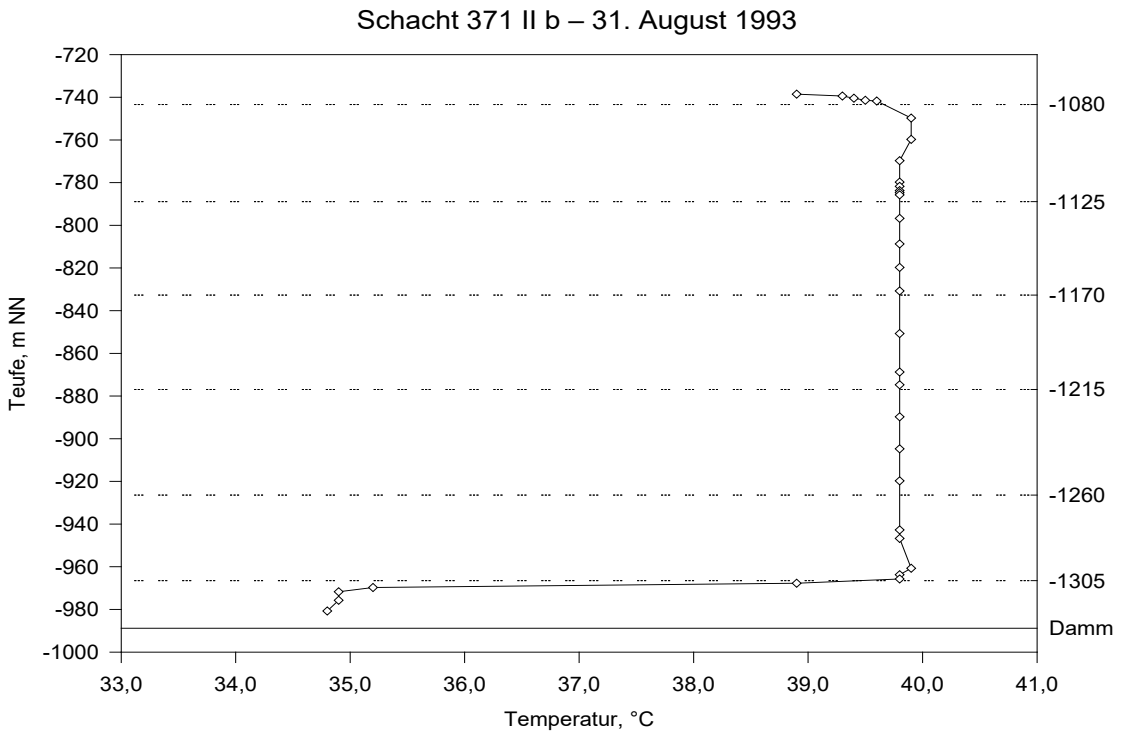

Fig. 67: Temperature profile of 31 August 1993 in shaft 371 II b.

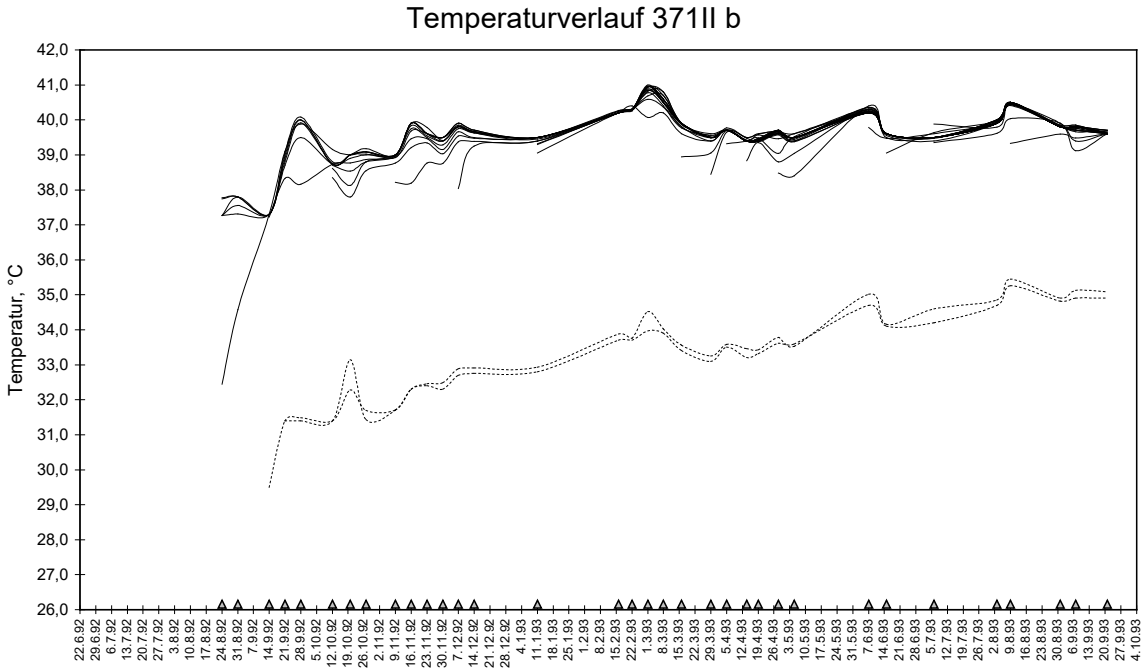

Fig. 68 Temperature curve in shaft 371 II b between 24 August 1992 and 21 September 1993. Each line corresponds to the temperature curve at a certain depth. The temperature curve in the sump water body is dashed. The triangles indicate the day of the measurement.

Below level -1305, a temperature jump of 6.5 K is noticeable, which is accompanied by an 8 m thick intermediate layer. Since the first more precise measurement (19 September 1992), its position and

thickness have hardly changed. The lower edge is at about -971 mNN, the upper edge at -966 mNN and thus exactly at the level of the bottom. The temperature difference between the shaft water body and the sump water body is also regularly 6 … 7 K.

From this, the temperature gradient in the intermediate layer is calculated as

$$\upsilon = \frac{\Delta t}{y} = \frac{6{,}5\ \mathrm{K}}{5\ \mathrm{m}} = 1{,}3\ \mathrm{K\,m^{-1}} \qquad (47)$$

However, the absolute temperature increased by about 4.5 K in the sump water body and 4.0 K in the shaft water body between 24 August 1992 and 8 March 1993.

7.3.8.2 Temperature curve over time

The temperature curve in the 371 II b shaft (Fig. 68) is similar to that in the 366 II b shaft. There are also two areas with clearly different temperatures, the difference between which ranges between 7 K and 5 K. A narrowing of the intermediate layer is not recognisable, but the sump water body warms up faster than the shaft water body. As the last temperature measurement before the invert -990 was flooded -shows, the density layer remained intact until 8 March 1994.

The temperature difference in the shaft water body is about 0.2 … 0.3 K lower than in shaft 366 II b. In general, the temperature of the shaft water body rises continuously from 37.5 °C to 41 °C until 1/2 March 1993, and then drops to 39.5 °C until the end of the measurement on 20 September 1993.

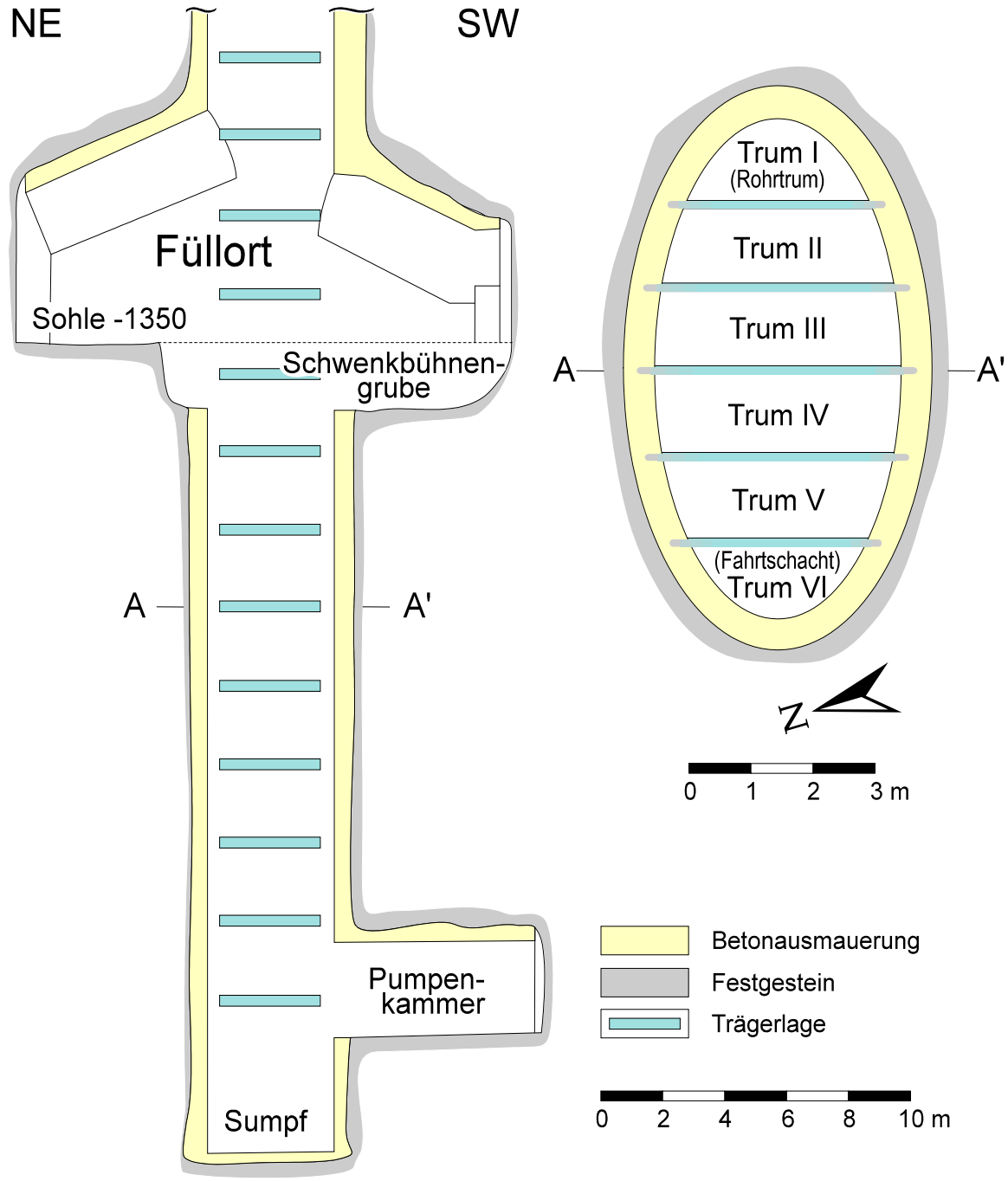

Fig. 69 Simplified vertical and horizontal section (“shaft slice”) of the 371 II b shaft. All the other shafts have basically the same cross-section, and the filling holes are also the same. Compared to the vertical section, the shaft slice is enlarged on a scale of 1:2 (according to original plans of SDAG Wismut).

7.3.9 Shaft 372 b (“Urban”)

7.3.9.1 Vertical temperature profile

Compared to shafts 366 II b and 371 II b, the temperature changes between the individual measurements in shaft 372 b were relatively small during the 38 weeks. The temperature was measured from level -990 to level -1485.

As the figure shows (Fig. 70), shaft 372 b can be divided into four areas based on the temperature measurements:

- Upper range with constant temperature: -1170 … surface
- medium range with falling temperature (Δt: 1 … 3 K): -1305 … -1170
- Transition zone: -1350 … -1305
- lower range with constant temperature: sump … -1350

In the lower range, the temperature remained approximately constant at 39 °C; the temperature drop in the middle range was initially 0.02 K m^{-1} (1 K/51 m) and decreased to 0.01 K m^{-1} (1 K/96 m) by the end of the measurement series, whereas in the upper range, it increased from 36 °C to 38 °C.

An interruption of the steady temperature increase in the middle area only occurs at the not completely damed levels. On 25 January 1993 and 16 February 1993 there was an inversion of 0.2 … 0.3 K at level -1350, which is possibly related to the change in flooding on 6 January 1993.

During the measuring campaign in March/April 1993, a probe from LogIn (Gommern) reached the greatest depth ever measured in the Niederschlema/Alberoda mine. There, temperature and electrical conductivity were measured down to just below level -1620 (-1283.6 mNN). Although the probe only travelled a few dm into the sump, there is no evidence of a drop in temperature similar to those in shafts 366 II b and 371 II b.

7.3.9.2 Temperature curve over time

A different, simpler temperature curve than in shafts 371 II b and 366 II b can be seen in shaft 372 b (Fig. 71). The different water depths have different water temperatures with a total difference of about 1 … 2 K. The water is not convectively mixed, but rather has a high temperature. The water is not convectively mixed, but has a wide transition area in which the temperature continuously decreases. Again, the tide change of 6 January 1993 is recognisable by a slight drop in temperature (0.5 K) in the upper part of the water column.

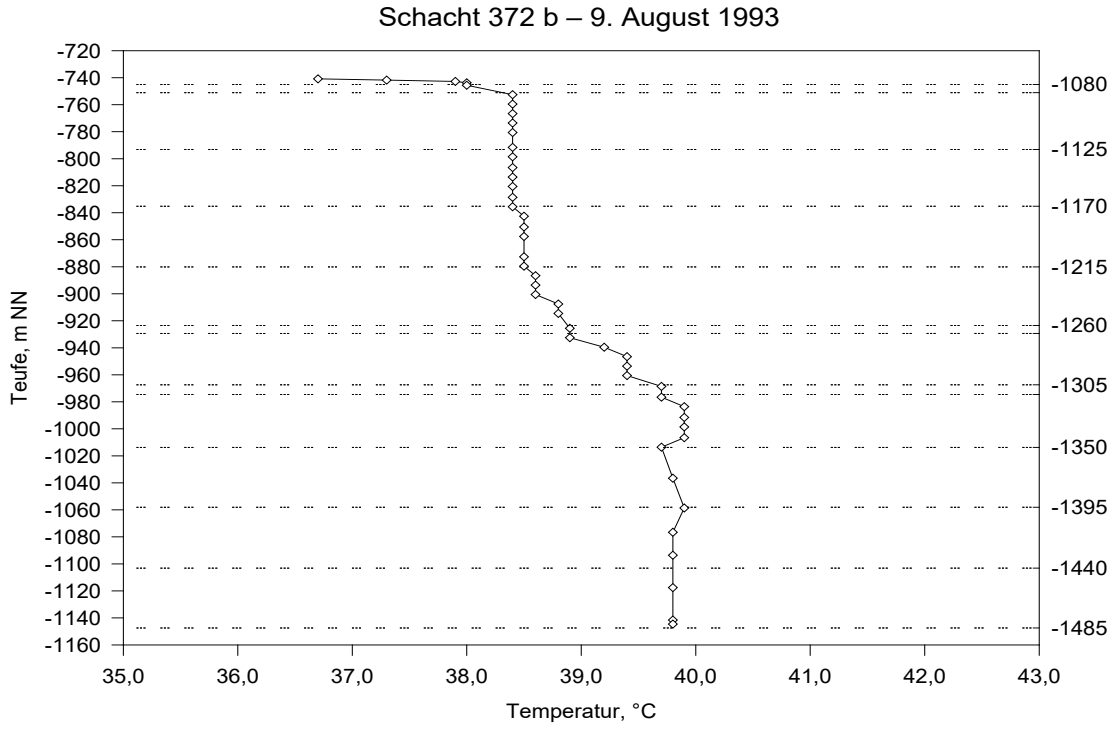

Fig. 70: Temperature profile of 9 August 1993 in shaft 372 b.

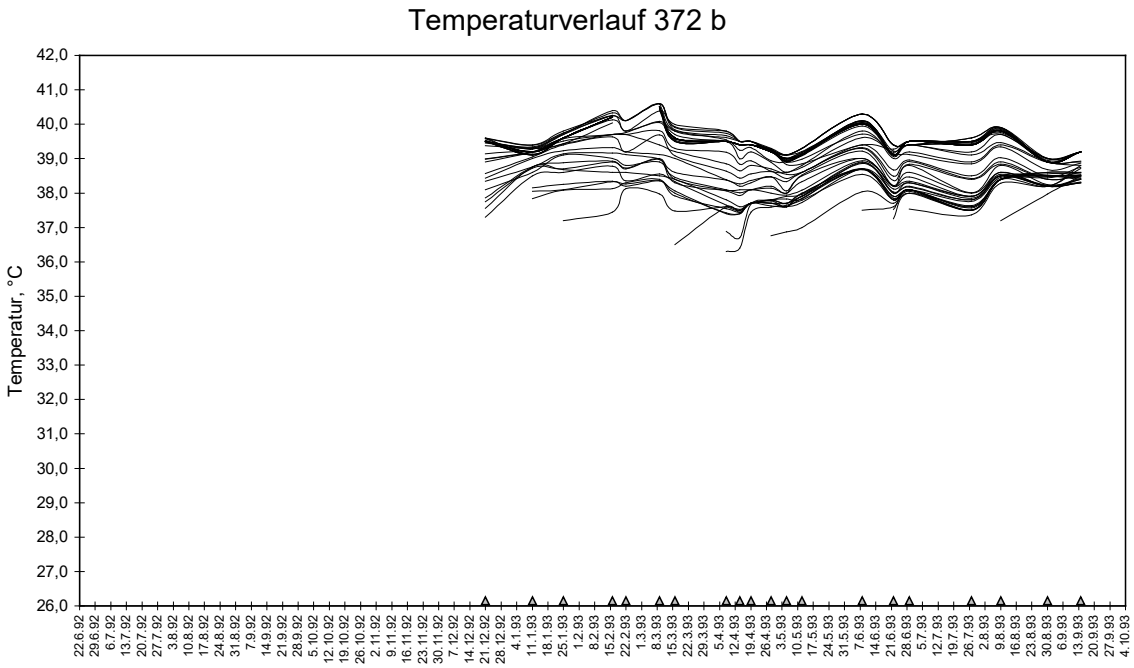

Fig. 71: Temperature curve in shaft 372 b between 21 December 1992 and 14 September 1993. The triangles indicate the day of the measurement.

7.3.10 Shaft 383

7.3.10.1 Vertical temperature profile

Below level -990, shaft 383 shows a constant temperature of about 36.3 °C up to the maximum measured depth of -740 mNN (Fig. 72). Bottom -1035 does not seem to have any influence on the shaft water temperature. The -conditions above level -990 are different. There, the temperature drops from 36.3 °C by 0.4 K to 35.9 °C, which can be attributed either to the inflow of cooler water from level -990 or cooling of the water from the surface. Taking into account the other physicochemical measurements, an inflow of water from the -990 bottom into the shaft is probable.

The own stationary measurement with the multiparameter probe of LogIn (Gommern) from 27.7.94 … 5.8.94 and 6.9.94 … 4.11.94 below level -990 shows that the temperature in the water body is subject to both long-term and short-term fluctuations (Fig. 73). The short-term fluctuations of 0.4 K are temperature variations that are to be expected with turbulent transport, since the turbulent convection cell always has slightly different temperatures at the same location during its movement.

In contrast to laminar flow, turbulent flow is flow that does not run in a straight line but breaks up into flow vortices with irregular velocity and pressure distribution. The transition from laminar to turbulent flow is described by the REYNOLDS number, which is a function of the velocity, density and viscosity of the fluid and the cross-section of the body through which it flows. In the cross-section of bodies with turbulent flow, the velocity profile is more uniform than that with laminar flow (GEBHART el al. 1988).

The causes of the long-term temperature changes cannot be stated with certainty due to the lack of long-term measurements, as in the three shafts described first. It could be the influence of cooler seepage water as well as the effects of large-scale convection in the mine workings.

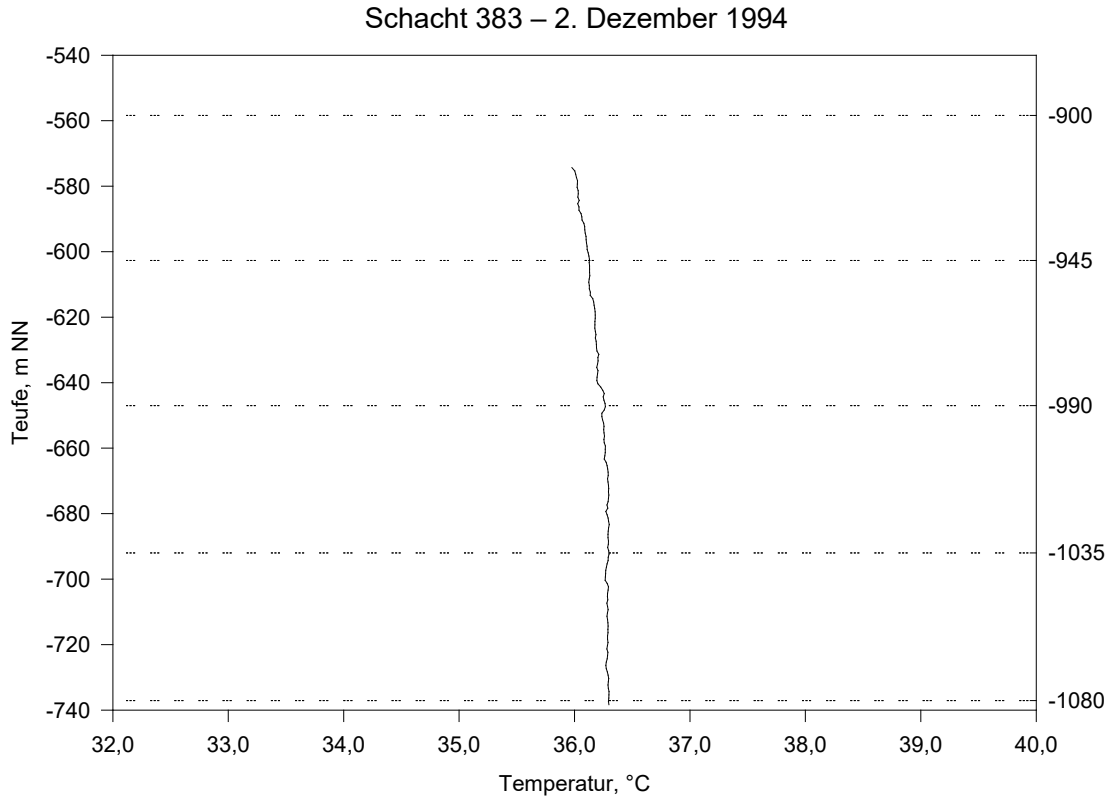

Fig. 72 Temperature profile of 2 December 1994 in shaft 383 (modified after DFA/C&E 1993/94).

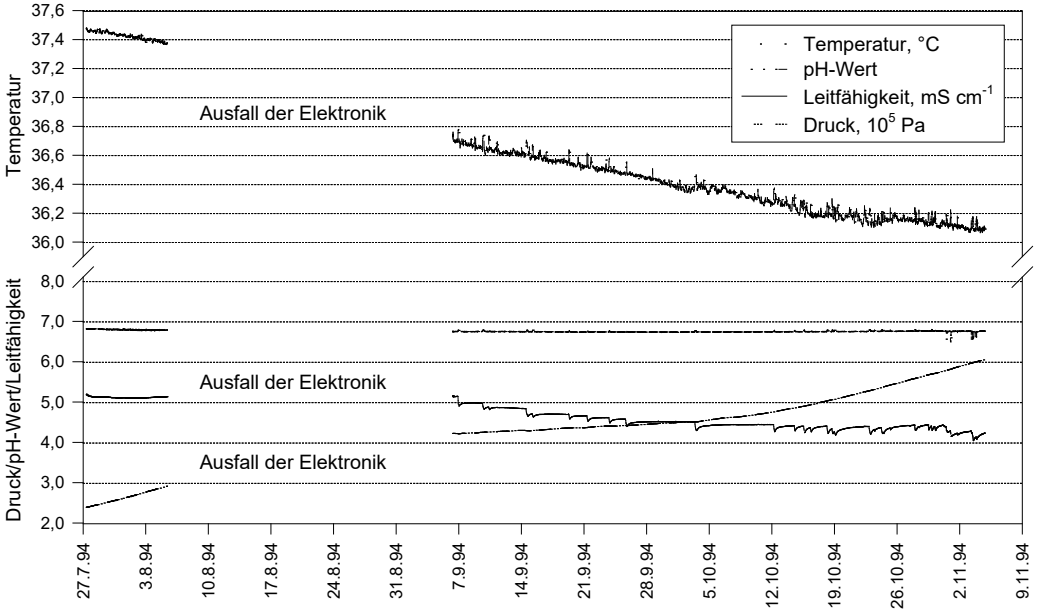

Fig. 73 Stationary temperature, electrical conductivity, pressure and pH-value measurements with the multi-parameter probe of LogIn (Gommern) in shaft 383 at -645.5 mNN (1.5 m above level -990) between 27 July and 4 November 1994.

7.4 Further physicochemical measurements

7.4.1 Electrical Conductivity

Electrical conductivity is used as a measure of the dissolved ions or dissociated substances in water.

It is a temperature-dependent quantity whose unit is S m^{-1} and is related to 25 °C temperature. Usually, measured electrical conductivity values are given in mS cm^{-1} or µS cm^{-1} (HÖLTING 1992).

By definition, the electrical electrical conductivity of a liquid is the reciprocal of a resistance measurement R between two electrodes of area F = 1 cm^2 and distance d = 1 cm:

$$K = \frac{1}{R} \cdot \frac{d}{F} \quad \left[\frac{1}{\Omega} \cdot \frac{m}{m^2} = Sm^{-1}\right] \tag{48}$$

Apart from one series of measurements (DFA: 8 March 1994), depth-dependent electrical conductivity measurements have a similar course, regardless of the shaft in which they were recorded. Three zones of varying thickness with rising or falling electrical conductivities are characteristic (Fig. 76), as can also be observed when a floor is flooded (Fig. 74).

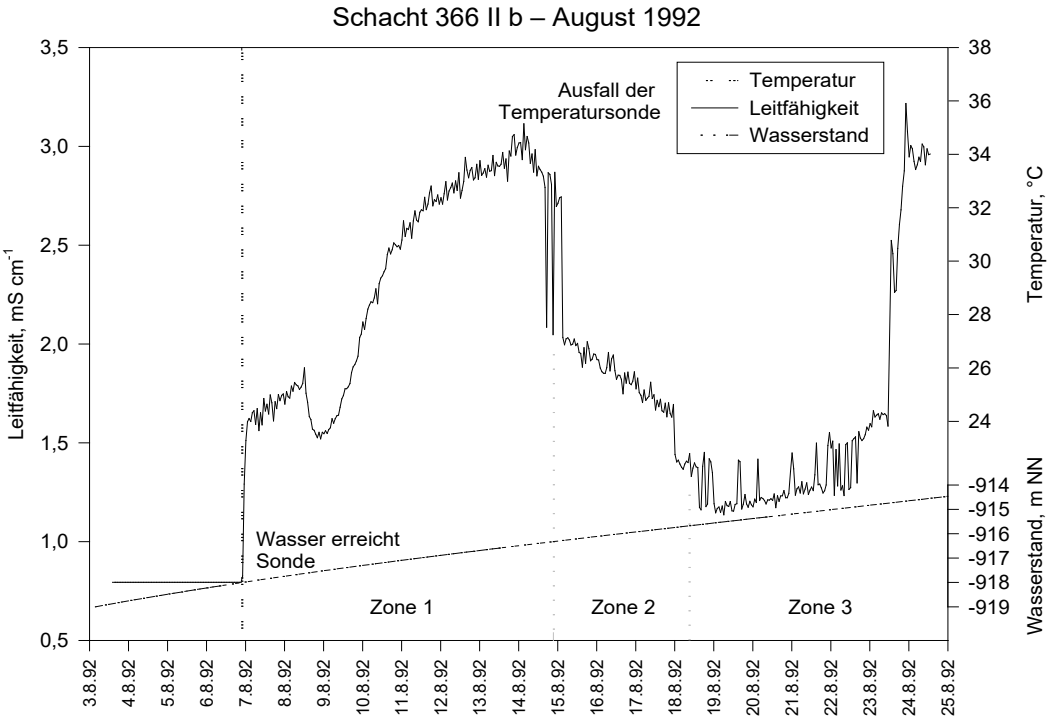

Fig. 74: Stationary temperature and electrical conductivity measurement at the level of level -1260 in shaft 366 II b between August 3 and 25, 1992. On July 24, 1992, at 1 p.m., at a water level of -923.35 mNN (5.35 m below ground -level-), the -probe -was -mounted at 918.-00 m -NN (1.50 m above ground level) to record the process during the rise of the mine water. The water level is derived from the interpolation of the water levels measured every 7… 14 days. Failure of the temperature probe due to corrosion of the plug connections on 15.7.92 at 7:00 am. Probes and data logger from PIC/Munich. Electrical conductivity increase between 7 August and 8 August possibly not due to water, but due to foam, as it was often present in shaft 366 II b (Fig. 91). The drop in electrical conductivity from August 14 to 15 coincides with the complete flooding up to the upper edge of the battered levels, that of August 18 with the complete flooding of the fill site. On 23 August, level -1260 was completely flooded. In zone 1 the electrical conductivity tends to increase, in zone 2 it decreases and in zone 3 it behaves inconsistently.

In the 1st zone, the electrical conductivity increases continuously up to a maximum value. It is between 1 and 18 m thick (n = 14, $\bar{x}$ = 7.3, med = 6 m), only in the 372 b shaft did it reach a clearly deviating value in March 1993 with a thickness of about 170 m. In March 1994, repeated measurements showed that it had also reached 6 … 14 m. Repeat measurements in March 1994 showed that the thickness had also decreased to 6 … 14 m.

Compared to the 1st zone, the 2nd zone is characterised by a steady decrease in electrical conductivity. Its thickness is 1 to 30 metres (n = 12, $\bar{x}$ = 7.5, med = 5 m), it is about as thick as the 1st zone. Again, the series of measurements in March 1993 in shaft 372 b deviate from the general picture, as zone 2 is about 45 m thick. The thickness had also decreased to 19 m during the repeat measurement in March 1994.

Below Zone 2, there is an area (Zone 3) in which the electrical conductivity shows a constant to decreasing trend. Locally, there are changes in electrical conductivity in this zone 3, which mostly occur at the level of the levels, as water flows into the shaft from there.

The absolute values of the electrical conductivity in the DFA/C&E measurements range between 3.70 mS cm^{-1} and 5.25 mS cm^{-1}, only in shaft 296 II b it was 1.79 … 2.93 mS cm^{-1}.

Fresh water flows into the 296 II b shaft, as evidenced by both the greater redox potential and the approx. 4 K lower water temperature compared to the other DFA measurements. The hydrogeochemical evaluation (chapter 6.3) of the analyses of shaft 296 II b confirms this different behaviour, as almost all analyses can be assigned to water type I. A characteristic of this type is the higher redox potential compared to the other DFA measurements. A characteristic of this type, compared to type G, is the less than half as large evaporation residue (Tab. 28), which explains the correspondingly lower electrical conductivity of the water in the 296 II b shaft.

As can be seen from the four figures (Fig. 75, Fig. 76, Fig. 77, Fig. 78), changes in electrical conductivity mostly take place at the levels of the floors. No changes are present at walled-off or unattached bases.

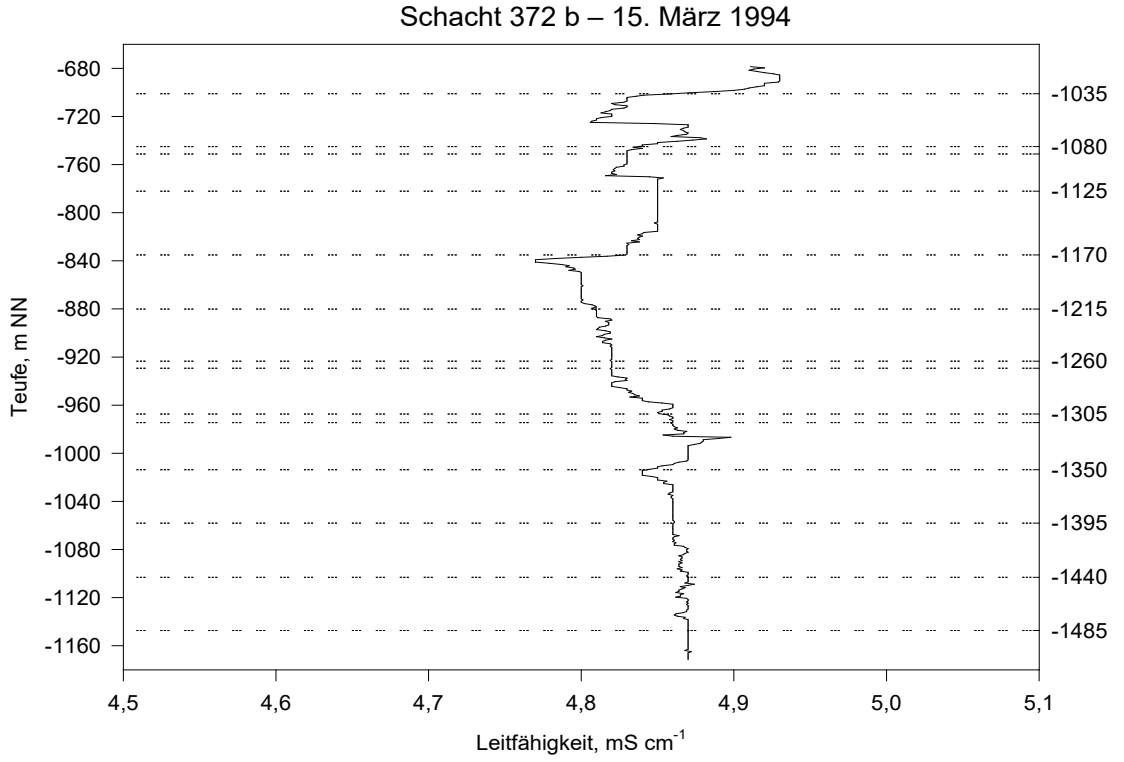

Fig. 75 Electrical conductivity measurements taken on 15 and 16 March 1994 in shaft 372 b between levels -990 and -1530. Graph compiled from moving averages of 10 individual measurements taken at intervals of 0.1 m (modified after DFA/C&E 1993/94).

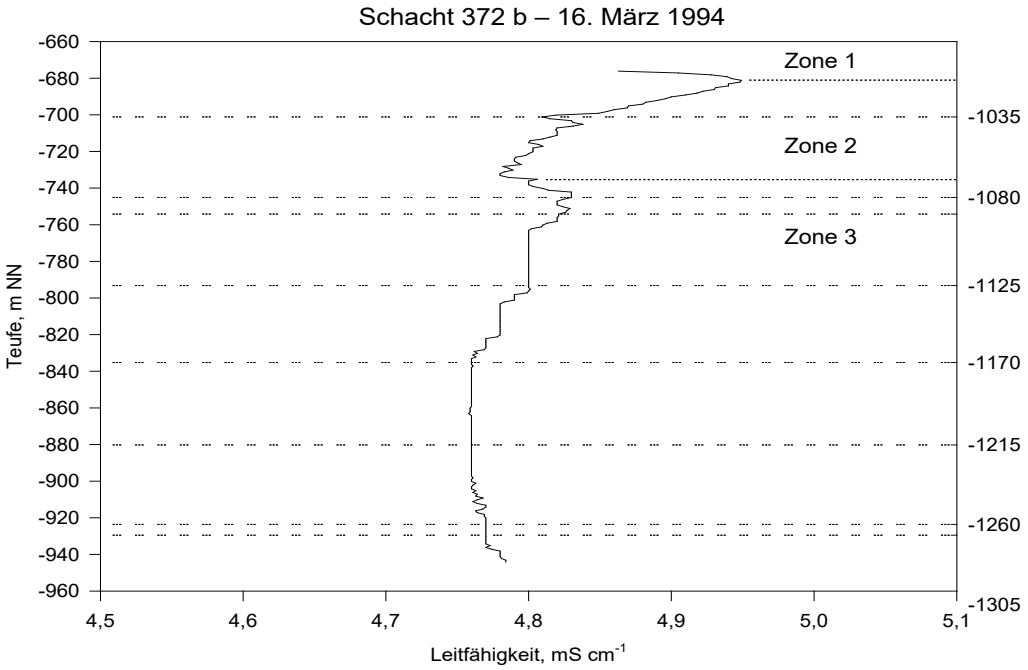

Fig. 76 Electrical conductivity measurement of 16 March 1994 in shaft 372 b between levels -990 and -1305. Graph compiled from moving averages of 10 individual measurements at intervals of 0.1 m (modified after DFA/C&E 1993/94).

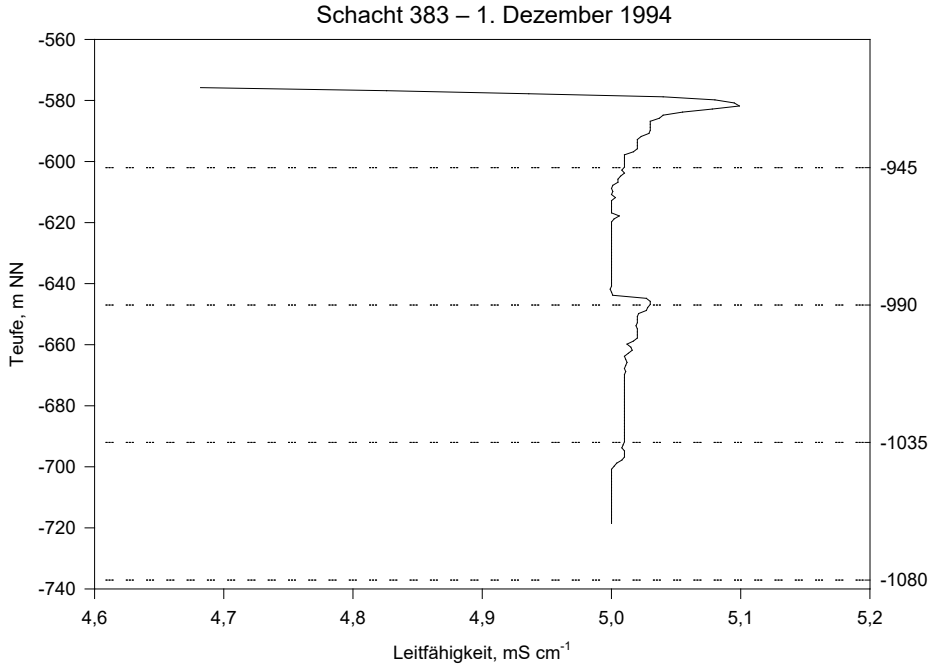

Fig. 77 Electrical conductivity measurement on 1 December 1994 in shaft 383 between levels -1080 and -990. The electrical conductivity increases rapidly in the top six metres. Graph compiled from moving averages of 10 individual measurements taken at intervals of 0.1 m (modified after DFA/C&E 1993/94).

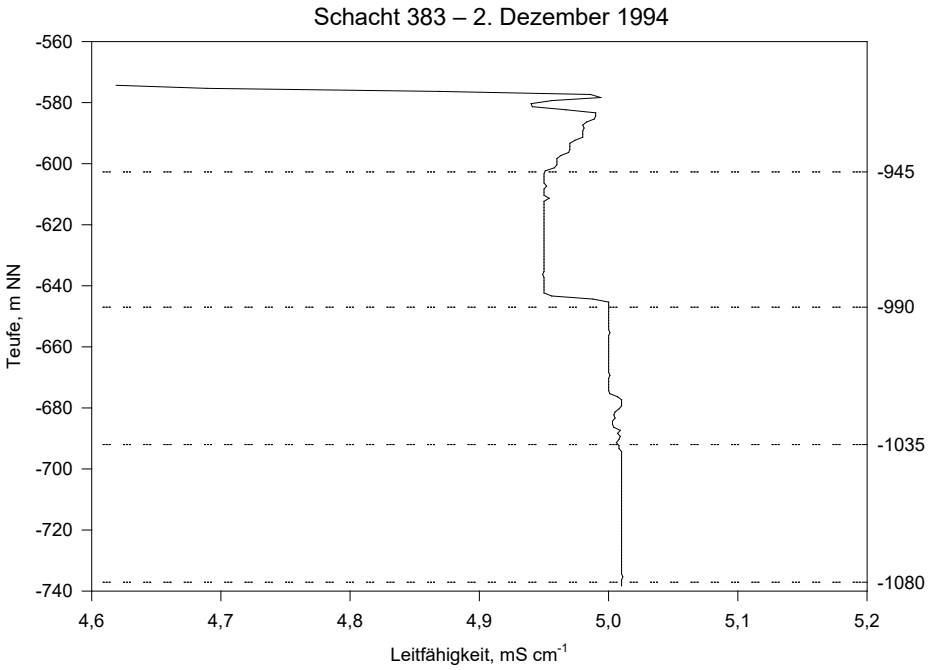

Fig. 78 Electrical conductivity measurement of 2 December 1994 in shaft 383 between levels -1080 and -990. Graph compiled from moving averages of 10 individual measurements at intervals of 0.1 m (modified after DFA/C&E 1993/94).

One of the largest changes in electrical conductivity, but also in pH, redox and temperature, was -measured on 8.3.94 in shaft 371 II b at the level of level -1305. There the electrical conductivity dropped abruptly from about 4.97 mS cm^{-1} by 0.15 mS cm^{-1} to 4.82 mS cm^{-1}. This condition was already observable on 30.3.93, when the electrical conductivity at the same level dropped by 0.18 mS cm^{-1} from 4.54 mS cm^{-1} to 4.36 mS cm^{-1}.

7.4.2 pH value

The pH value is the negative decadic logarithm of the hydrogen ion activity and has no unit:

$$pH = -\log \{H\}^{+} \quad (49)$$

STUMM & MORGAN (1981) refer to it as the “master variable” in hydrogeochemical systems, since the solubility of most mineral phases depends crucially on the pH value and, conversely, the solution of compounds influences the pH value.

At the Niederschlema/Alberoda mine, the absolute value of the level-dependent pH measurements ranges between 6.7 and 7.7 with an average of about pH 6.9.

Essentially, four pH-gradient courses can be distinguished in the shafts:

- pH value ±constant (Fig. 80; 366 b, 371 II b, 372 b)
- pH value increases with water depth (Fig. 81; 366 b, 372 b, 366 II b)
- pH value decreases with water depth (Fig. 79; 383, 366 b, 372 b)
- pH value shows inconsistent behaviour (Fig. 82; 371, 383, 296 II b).

None of the four curves is typical for a particular shaft; rather, the appearance of the curves changes without any recognisable system. For example, the pH value in shaft 372 b is almost constant on 16, 17, 18 and 19.3.93, on 15.3.93 it drops slightly and on 11.3.94 it rises slightly with increasing depth. The same applies to shaft 366 b, which showed a relatively constant pH value on 22.11.94 during the first measurement, a falling pH value during the second measurement on the same day and a rising pH value on 21.3.94.

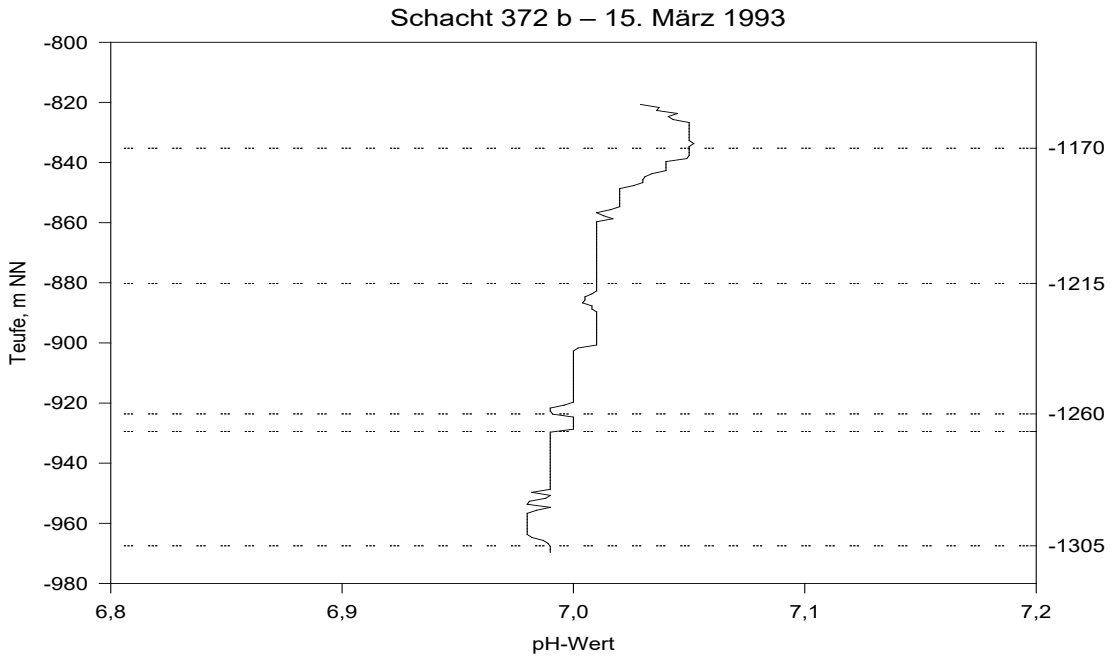

Fig. 79 pH measurement in shaft 372 b on 15 March 1993. Graph compiled from moving averages of 10 individual measurements taken at intervals of 0.1 m (modified after DFA/C&E 1993/94).

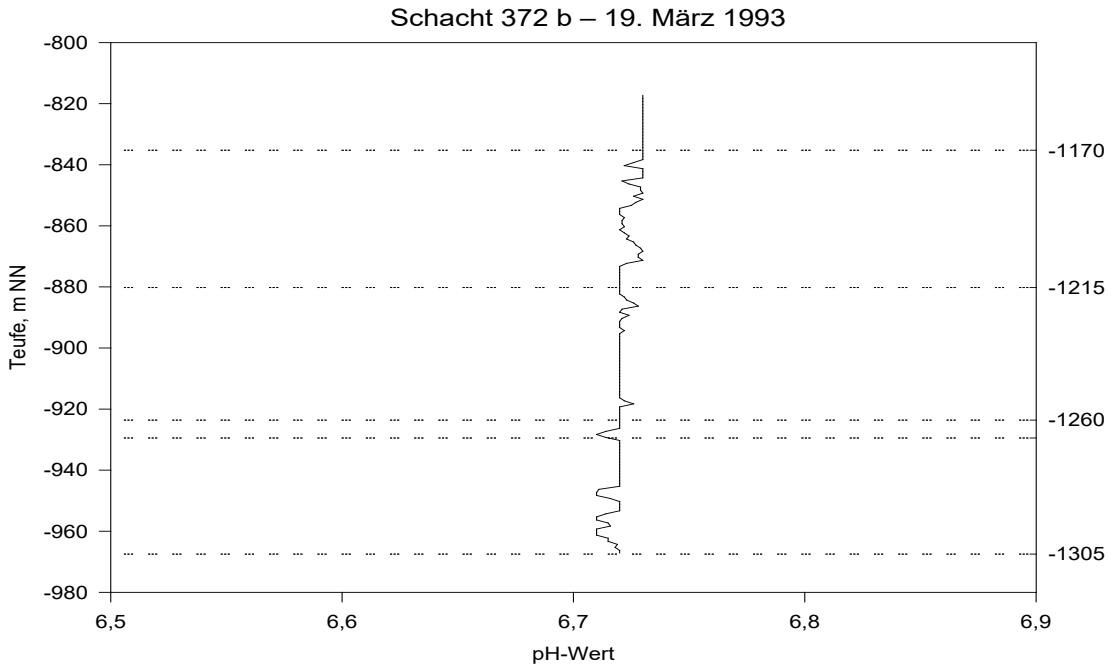

Fig. 80 pH measurement in shaft 372 b on 19 March 1993. Graph compiled from moving averages of 10 individual measurements at intervals of 0.1 m (modified after DFA/C&E 1993/94).

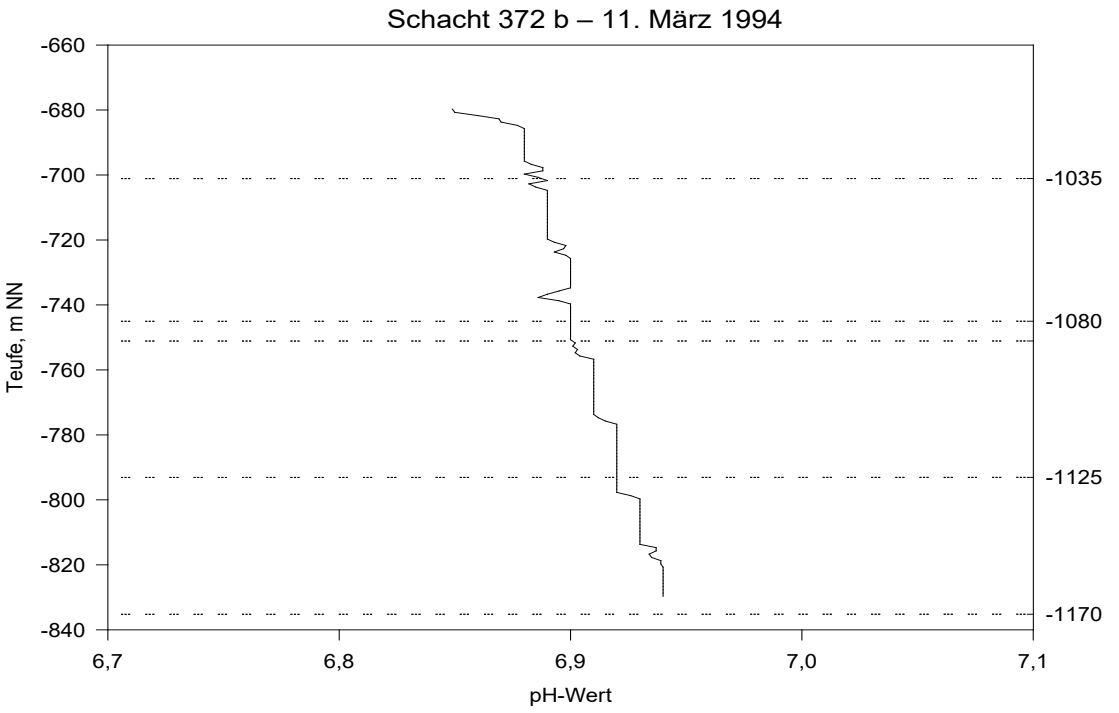

Fig. 81 pH measurement in shaft 372 b on 11 March 1994. Graph compiled from moving averages of 10 individual measurements taken at intervals of 0.1 m (modified after DFA/C&E 1993/94).

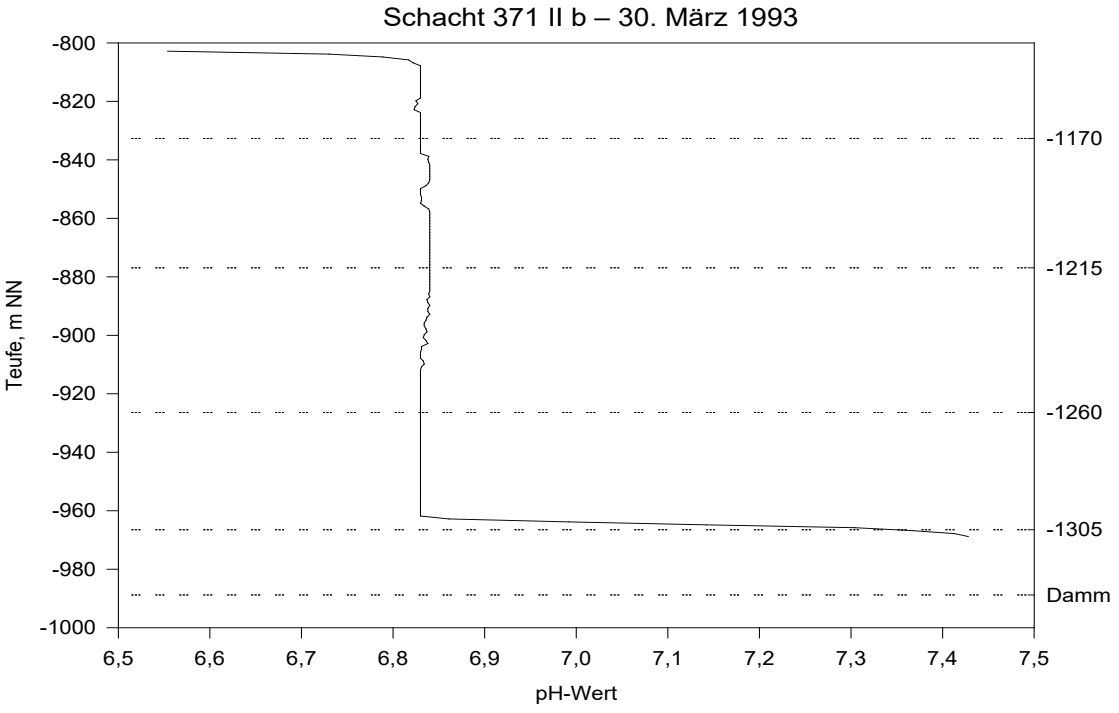

Fig. 82 pH measurement in shaft 371 II b on 30 March 1993. Graph compiled from moving averages of 10 individual measurements taken at intervals of 0.1 m (modified according to DFA/C&E 1993).

The level-dependent changes themselves are small with an average of 0.1 units, only in the shafts with non-uniform behaviour do they range between 0.2 … 0.9 units.

The small pH-value changes are possibly effects that can be explained by the pressure and temperature dependence of the equilibrium constant *K* of the calcite solution. Such pH changes have also been observed in lakes (ATKINS 1990). There, at constant temperature, constant ion activity product IAP = $\{Ca\}^{2+} - \{CO\}_3^{-2}$ and increasing pressure, the pH value decreases. These decreases, as observed in the Niederschlema/Alberoda mine, range from 0.1 … 0.2 pH units (STUMM & MORGAN 1981).

Other causes must be responsible for the larger pH value changes, which cannot be explained by the pressure and temperature dependence of the equilibrium constant alone. Since no depth-dependent water analyses are available, the true reasons cannot be found out. Presumably, however, the solution of carbonates in the concrete lining of the shafts increases the pH value.

From the measurement in shaft 371 II b (Fig. 82) it can be seen that the pH value below level -1305 suddenly increases by 0.6 units. This increase is accompanied by an equally sudden drop in temperature (Fig. 67). An explanation for this could not be found.

7.4.3 Redox potential

The redox potential of an aqueous system results from the relative activities of the oxidised and reduced water components. It is related to the potential of the standard hydrogen electrode, although the measurement is usually carried out by means of a platinum electrode. For conversion, a temperature-dependent constant must therefore be added to the measured value (VOIGT 1990). In terms of formula, this relationship is expressed by NERNST'S equation (STUMM & MORGAN 1981):

$$E_h = E_h^0 + \frac{RT}{nF} \ln\left(\frac{\prod_i \{Ox\}^{n_i}}{\prod_j \{Red\}^{n_j}}\right) = p_\varepsilon \cdot \frac{\ln(10) \cdot RT}{F} \qquad (50)$$

with

E_h^o	:	standard potential of the reaction, V
R	:	gas constant, 8.31441 J K^{-1} mol^{-1}
T	:	temperature, K
n	:	electrons involved in the reaction, 1
F	:	FARADAY constant, $9.64846 \cdot 10^4$ mol^{-1}
$\prod\{Ox\}, \{Red\}\prod$	:	Activities of the oxidised and reduced species, respectively, 1

At the present time, it has not been conclusively clarified whether the measurements of the redox potential in the Niederschlema-Alberoda mine correspond to the real redox potentials in the mine water. Probe manufacturers, measuring electrode manufacturers, DFA/C&E and Wismut GmbH are currently trying to find out to what extent the measured values are correct. It is certain that the calculation formulas, including the temperature correction and the correction to the hydrogen electrode, are correct and that the measuring probe delivers reproducible values in the laboratory. The extent to which the potential difference of about 100 mV in the rock between level -540 and the water surface affects the measurement of the redox potential could also not yet be determined. The destruction of the steel and data cable of a LogIn probe of the Engineering Geology Department may indicate that galvanic processes take place between the floor and the mine water. Their potential difference could mask the true redox potential of the mine water. A direct measurement of the redox potential at the surface of the mine water is currently not possible, because for safety reasons (too high radon, too low oxygen content of the mine air) it is not allowed to go down to the water surface. The only redox measurement directly in the mine water known to the author dates from 24 July 1992 and yielded a potential of 154 mV (Lf = 2.91 mS cm^{-1}, pH = 6.7, O_2 content = 0.6 mg L^{-1}). A H_2S outgassing in May 1992, which can be observed at redox potentials of -100 mV and above, was only local in character.

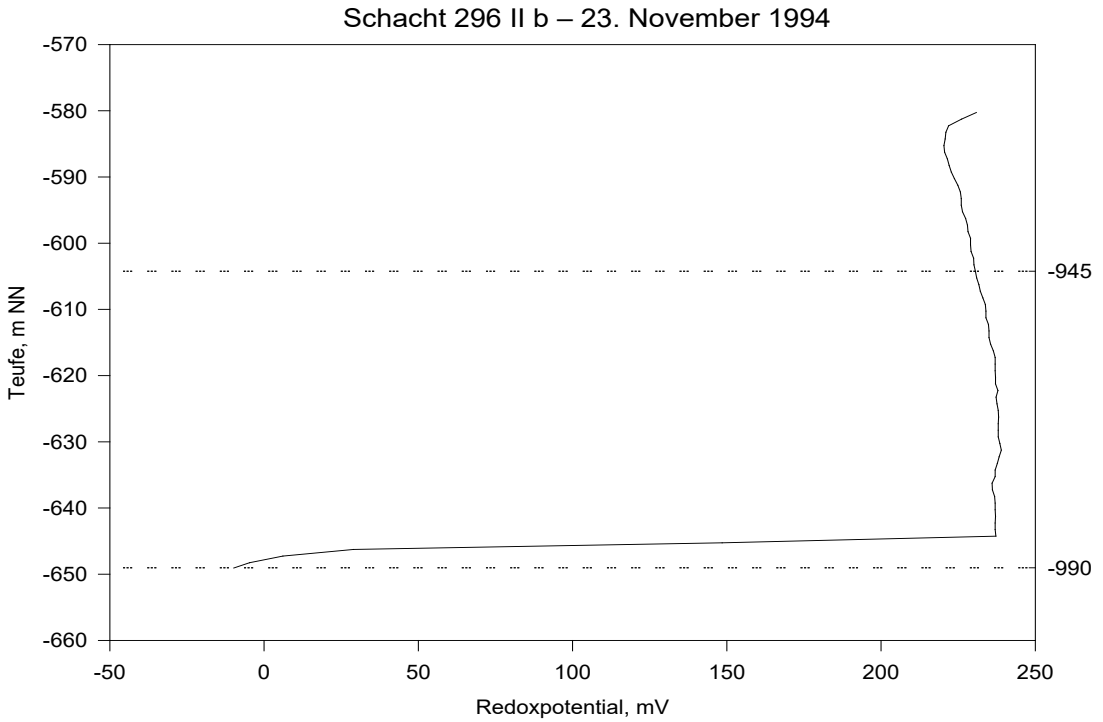

Fig. 83 Redox measurement in the 296 II b shaft on 23 November 1994. Graph compiled from moving average values of 10 individual measurements at intervals of 0.1 m (modified according to DFA/C&E 1993/94).

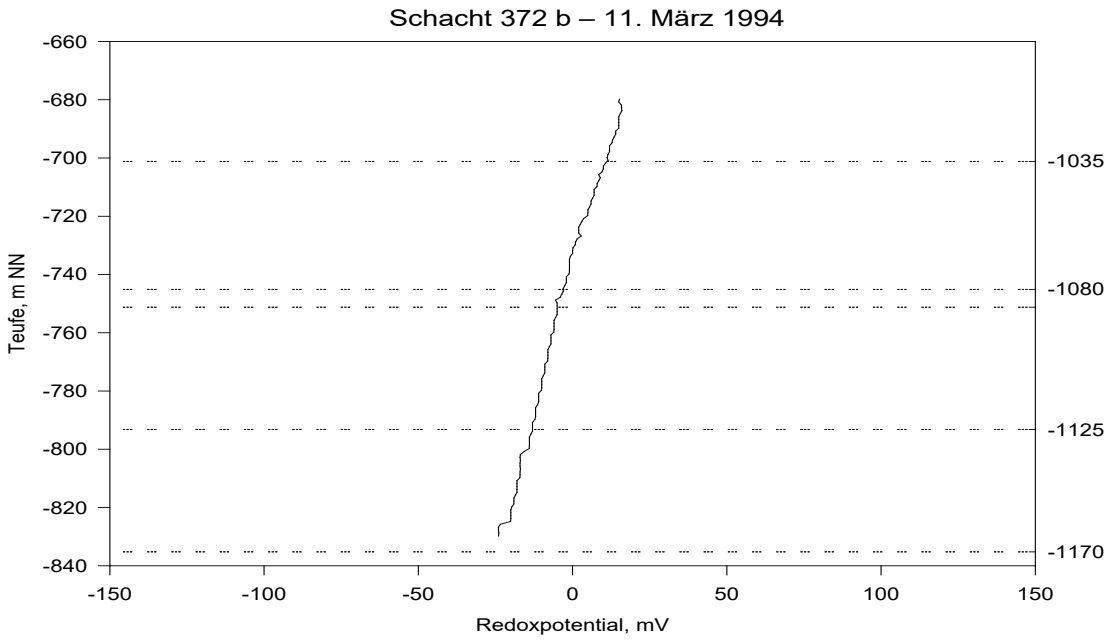

Fig. 84 Redox measurement in shaft 372 b on 11 March 1994. Graph compiled from moving average values of 10 individual measurements at intervals of 0.1 m (modified according to DFA/C&E 1993/94).

Only from the 296 II b shaft are redox potential measurements available that could correspond to the actual redox potentials in the mine water (Fig. 83). From the strong redox potential drop from approx.

250 mV to 0 mV at the level of level -990 it could be concluded that the measurements in the other shafts also correspond to the real conditions.

There is a substantial difference between shaft 296 II b and the other shafts in which the redox potential was measured, in that in the former the redox potential is clearly positive, whereas in the latter it becomes clearly negative starting from 0 … 50 mV. Only for the sake of completeness, a typical measurement from shaft 372 b is reproduced (Fig. 84).

7.5 Flow velocity

On 1 April 1993, the flow velocity was determined in shaft 372 b by LogIn (Gommern) using an FM 36(A) propeller probe of their own manufacture. The flow probe resolves in steps of 0.5 m min^{-1} and responds from about 0.6 m min^{-1} velocity. From the water surface at -795.5 m a.s.l. (between levels -1170 and -1125) to the highest measuring depth at -1280 m a.s.l. (level 1620), the measuring velocity was between 10.5 m min^{-1} and 12.2 m min^{-1}. A flow velocity ranging from 2.6 … 4.0 m min^{-1} and averaging 3.3 m min^{-1} was determined (Fig. 85). From level -1620 to level -1395 a relatively uniform velocity of 3.3 m min^{-1} prevails, which is only interrupted at level -1530. Above this point, there is an area with an irregular flow velocity, which is slightly higher on average.

Increases in flow velocities exist at the level or ventilation levels -1530, -1350, -1305, -1266 and -1215, decreases in level -1395, ventilation level -1356, top of fill location level -1305 and level -1260.

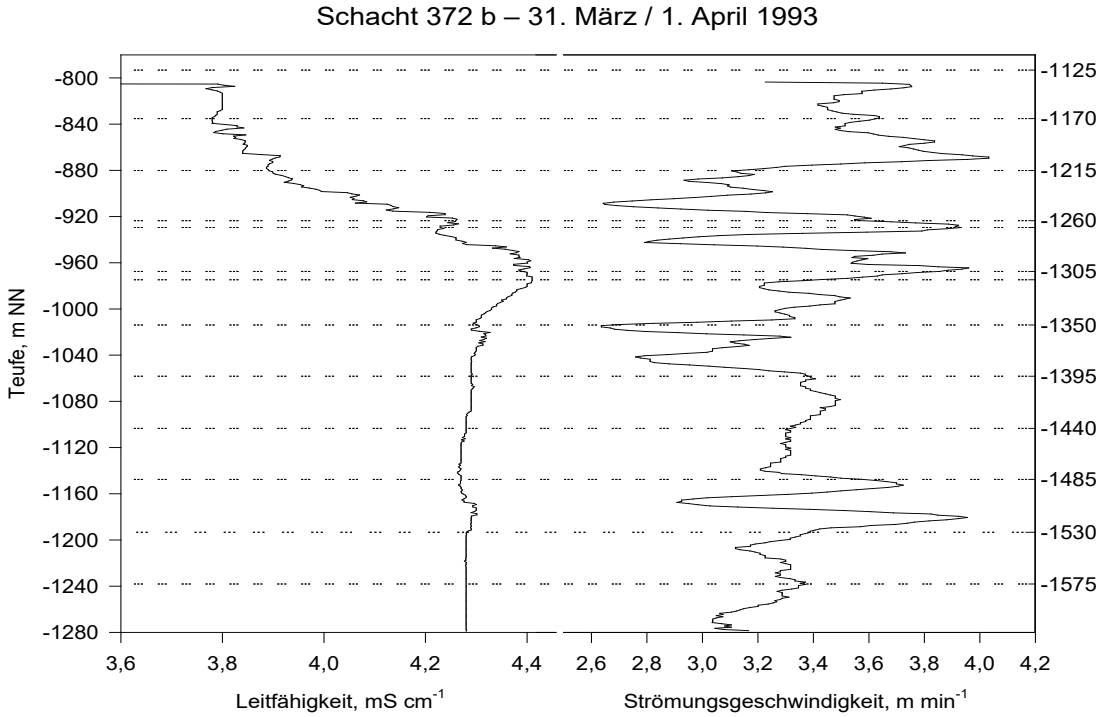

Fig. 85 Flow velocity and electrical conductivity in shaft 372 b on 1 April and 31 March 1993. Graph compiled from moving averages of 10 individual measurements taken at intervals of 0.1 m (modified according to DFA/C&E 1993/94). Changes in flow velocity are reflected in changes in electrical conductivity.

In an indirect way, the flow velocity could be determined on 3 May 1994 on level –990 in the access from crosscut –1406 to shaft 366 II b. There, a few days before, the flooding water had started to flow out of the shaft. A few days before, the flood water had begun to flow out of the shaft. By means of a drift body, the flow velocity at the water surface was determined to be 13.3 m min^{-1}, the inflowing water volume to be 3500 … 4000 $m^3 d^{-1}$ (daily inflow at that time about 4000 $m^3 d^{-1}$). Since the cross-

section of this access corresponds approximately to that of a shaft, the determined flow velocity can be regarded as a rough estimate of the velocity with which the water flows in the shaft.

The rate of rise of the water level due to the inflow of seepage water is negligible compared to the above rates. During the rise in the shafts it amounts to about 12 cm h^{-1}, during the flooding of a bottom 0.5 cm h^{-1}.

As the comparison of the above flow velocities (3 m min^{-1}, 13 m min^{-1}) with the velocity of the spores in the drift test shows (0.01 m min^{-1}), the flow velocity determined in chapter 7.2.5 represents a minimum value. Assuming a velocity of 3 … 13 m min^{-1}, the spores should have flowed between the feeding point and the extraction point after less than one day.

7.6 The flooding of the Niederschlema/Alberoda mine

7.6.1 Literature research

With a view to predicting the hydrogeochemical and hydrodynamic development of the Niederschlema/Alberoda mine, a literature search was carried out. At the same time, the research was intended to identify methods that can be used to keep the discharge of pollutants by the floodwater at the lowest possible level.

Unfortunately, of these papers (e.g. ACKMAN & RICHARD 1991, OLEM 1991, PFEUFER 1991, SINGH et al. 1985, ROGOZ & POSYLEK 1982, KESSERÜ et al. 1982) only a few contain a reference that would be applicable to Niederschlema/Alberoda, which can probably be attributed to the secrecy in the mining sector. Especially in the environmental field, mining companies try to withhold negative information, and a turn away from this company policy has only been noted recently (ROSIN 1994).

Numerous publications, partly edited by WIRTH ZUR OSTEN (1992), deal with the flooding of salt mines (e.g. BRENDEL et al. 1982, SITZ et al. 1982). Although the flooding of the Hope mine (HERBERT 1989) is a prime example of data collection during mine flooding, most of the information cannot be transferred to an ore mine. While the type of physical leaching of the salt is the most important issue in a salt mine, this process is insignificant in an ore mine.

In publications on flooded ore mines or mines to be flooded, the prediction of the resurgence process often plays a role (e.g. AURADA 1970, BROWN 1982, HANZLIK & VYDRA 1985, ROGOZ 1994, BANKS 1995). The result of the literature research, also carried out by WOLF (1995), is the realisation that rebound processes are usually incorrectly predicted. There are various reasons for this, including misjudgement of the groundwater level rise in unscored rock and long-term effects of average precipitation from past years (HANZLIK & VYDRA 1985). Only simple mine geometries can be predicted to a limited extent (BROWN 1982).

Publications that report on the dissolution and transport of pollutants from underground disposal sites occupy a large space. They can essentially be assigned to the disposal of radiotoxic and chemotoxic waste materials (e.g. NORDSTROM et al. 1989). In this type of work, transport processes in the surrounding rock are mostly of interest (e.g. NOWY 1993), rarely in the mine workings (e.g. JÄGER et al. 1990, UERPMANN 1980, BANKS 1995). Since, as explained in chapter 8.2 the main water transport in Niederschlema/Alberoda will take place via the workings and roadways, the aforementioned publications were only taken into account in the literature research if the geological-geometrical conditions were transferable.

A remarkable aspect, albeit for the abandonment of pyrite-bearing tailings, is described by GARGA et al. (1983). In order to minimise the oxidation of pyrite and the associated acid formation, they recommend flooding tailings after the end of mining. In Canadian tailings piles that were sealed off from atmospheric oxygen by flooding ponds (“abandonment lakes”), the seepage water in piles with a high pyrite content (15 … 17 %) had pH values of 6.9 after 32 years. In contrast, the seepage water of the top 15 cm of non-flooded areas of the same heap has a pH value of 2.5. The spatial proximity of

carbonate-rich rocks, where the water can enrich itself with carbonates, is advantageous for the successful creation of flood ponds (GARGA et al. 1983).

Despite the wide variety of issues addressed by the literature on mine flooding, they have in common some requirements for predicting recovery:

- Precise knowledge of the hydrogeological conditions
- Estimation of the amount of water flowing through the mine workings
- Investigation of the geological and geochemical situation

The most interesting work on mine flooding, some of whose results are transferable to Niederschlema/Alberoda, is by FERNANDEZ-RUBIO et al (1987). They present different possibilities to avoid acid mine drainage within the framework of hydrogeochemical conditions. The starting point of their proposals and considerations is the fact that pyrite oxidation is caused by the oxygen of mine ventilation and can be reduced by controlled flooding. Barrier structures, such as those proposed earlier for Niederschlema/Alberoda (WOLKERSDORFER 1992), also help to minimise the discharge of pollutants.

7.6.2 Main flooding methods and their results

The flooding of a mine serves different purposes. It is intended to prevent the underground cavity from collapsing and causing day fractures at the surface. Furthermore, the hydrogeological situation before mining began, in which atmospheric oxygen was not able to oxidise disulfide in the uncracked rock, should be restored as far as possible. But economic reasons also play a role, as it can cost several million DM annually to sump a mine.

Not all mines have the entire mine workings below the water level that naturally occurs after the end of flooding. To increase the stability of overlying workings, artificial measures would have to be taken to raise the water above the deepest water solution gallery (FERNANDEZ-RUBIO et al. 1987, SITZ et al. 1982). Although the Niederschlema/Alberoda mine belongs to this type of mine, such measures will not be discussed in more detail here, as raising the mine water above the level of the Markus-Semmler adit is not considered by either the authorities or Wismut GmbH.

In principle, four flooding methods can be distinguished:

- uncontrolled flooding (Fig. 86 a)
- Controlled flooding without water treatment and control mechanisms
- Controlled flooding without water treatment with control mechanisms (e.g. dams, Fig. 86 b, c, d).
- Controlled flooding with water treatment (with and without control mechanisms)

In all cases, it takes a considerable time for the contaminated mine water to improve its quality through natural mixing and exchange processes.

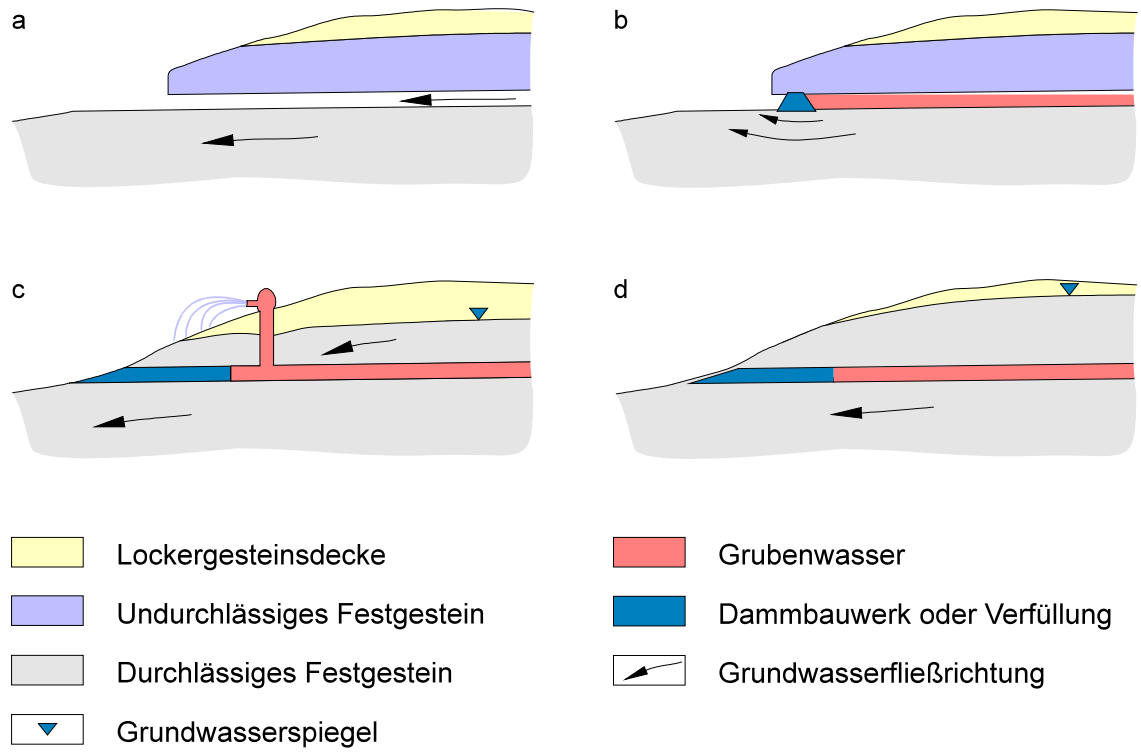

Fig. 86 Possibilities of discharging mine water into the surface water cycle. a: uncontrolled flooding; b, c: controlled flooding with dam structures; d: complete horizontal hermetisation of the mine workings (modified after FERNANDEZ-RUBIO et al. 1987).

The extent to which water quality improves over time can only be estimated on a case-by-case basis, if at all. The improvement in quality can take several decades, as demonstrated by the example of abandoned coal mines in Pennsylvania (LADWIG 1985, ERICKSON et al. 1982). Although the average sulfate content of the water there was approximately halved in 13 years, it still remained at a high level. The same studies show that in five out of nine investigated shafts a stratification developed in which qualitatively better water overlies qualitatively worse water. The stratification of the water body is reflected, among other things, in a sudden pH decrease, at which point its value drops by almost one unit. At the same time, the sulfate content increases regularly. Reasons for the stratification could be water inflows in the respective shafts or a density stratification similar to that in lakes or in the 296 II b shaft (ERICKSON et al. 1982, chapter 7.3.4.1). It depends on the individual case whether the controlled discharged water should be taken from the relatively uncontaminated or the contaminated water body. In any case, according to LADWIG (1985), IT must be avoided that too strong a lowering of the water level leads to further oxidation processes, i.e. acid formation, in the air-filled mine workings. Transferred to the Niederschlema/Alberoda mine, this would mean setting the flooding level as high as possible.

If necessary, *horizontal* hermetisation of the entire mine workings at the level of the water solution gallery can prevent the escape of pollutants (Fig. 86 d). A distinction is made between hermetisation against water and hermetisation against oxygen. In the first case, it must be ensured that no mine water reaches the surface via fault zones. Locatable fault zones must therefore be sealed from above ground as far as possible. BIAGLOW (1988) reports on the results of an incorrectly performed hermetisation, which led to an increase in the discharge of pollutants. In the second case, the mine workings are only sealed against the entry of oxygen so that pyrite oxidation is prevented, although this method is doubted by others as to its reliability (BARNES & CLARKE 1964).

Vertical hermetisation of the Niederschlema/Alberoda mine differs from that in Fig. 86 d in that it would not be the water solution gallery that would be hermetised, but the mine workings below the water solution gallery (Fig. 93). Hermeticisation has three advantages:

- fresh, oxygenated water cannot reach deeper parts of the mine via the mine workings, or can only do so with difficulty
- contaminated and non-contaminated water will not mix,
- water treatment may be avoidable.

7.6.3 Description of the flooding process

Although the flooding of the Niederschlema-Alberoda mine is very complex, as the seepage water flows into the mine workings via a large number of shafts, sumps and levels, an attempt will be made to outline the general process. The inflows into the most important shafts are described one after the other. Fig. 2 gives a basic representation of the processes.

Officially, the flooding of the Niederschlema/Alberoda mine started on 11 January 1991 with the shut-down of the main pump station at level -1710, but already on 24 April 1990 the auxiliary pump station at shaft 383 III b was shut down and the water flooded the deepest levels (Fig. 87, J. MEYER, G. FRÖHLICH, pers. comm.).

Every day, 9,000 … 15,000 m³ of seepage water (Wismut GmbH's term is "geological water") seeps into the Niederschlema-Alberoda mine workings (object 9). Part of the seepage water flows via the 296 b shaft into the 186 water reservoir, where water originating from the 240 level is also collected (approx. 4600 $m^3 d^{-1}$). From water reservoir 186, the seepage water reaches shaft 38 and sump I on level -546 via pipelines. About half of the seepage water accumulates at this shaft, sump I and sump II of sump section -546.

Until the flooding of level -990, the majority of all seepage water flowed into shaft 372 b, partly as a result of a test drilling on level -1176, which tapped large quantities of water. Furthermore, there were seepage inflows from the Oberschlema mining area via level -1035 (object 2). During a short period of time, water also flowed from level -540 into the 372 b shaft. Other notable inflows were observed at levels -1176, -1215 and -1086, and -water temporarily entered the -372b shaft via a pipeline at level -1620.

In the 296 II b shaft, seepage water flows in via a basin and a fall pipe at pump station -996. This water originates from level -726. At times, seepage water from pipelines was added at levels -1170, -1305, -945 and the shaft sump.

Much smaller quantities of seepage water flowed from level -1170 into shaft 366 II b. There was no active supply of seepage water there, any more than in shafts 371 II b and 371 b. The low temperatures in the shaft sumps of shafts 366 II b and 371 II b are therefore not, as stated in the Quarterly Report II/1993 (WISMUT GmbH 1993b), due to "colder […] feed waters". This is especially not because the temperature jump occurred consistently at the level of the swing stage pit!

Until the beginning of January 1993, further leachate infiltrated through pipes in the 371 II b shaft and the III die on the -1395 and -1620 levels. From 6 January 1993, the infiltrating water -was -discharged on the higher -1266, -1215 and -1170 levels.

A large part of the seepage inflow is controlled via flash tanks. Therefore, as long as the water level at an inflow point is below a flash tank, the water reaches below the mine water surface via pipelines from the tank. As soon as the basin is flooded, no more water flows from there into deeper mine areas.

Fig. 87: Partially flooded crosscut 1753 of level –1305 at the Niederschlema/Alberoda mine at the beginning of December 1992 (from FEDERAL MINISTER OF ECONOMICS 1993). The steel arch lining of a double-track line of the KSW 1097124/02 type with timber haulage made of round timber (SDAG WISMUT 1984) can be seen. The height of the track is about 3 m, the water level 0.5 m.

Pumps convey the water collected on level -540 via shaft 208 to the surface into the Bohrbach dust basin (formerly: industrial tailings pond, IAA) and the Zwickauer Mulde receiving watercourse. On average, the pumps lift 5,000 … 10,000 m³ of water per day, while 4000 … 7000 m³ flow into the mine workings and contribute to the rise in the mine water level. Until 20 May 1992, a turbine was also installed on the -720 level to generate electricity, which was actively operated with water from the -540 level. Since then, pumps have been pumping all the seepage water that can be collected on level 540 to the surface, thus enabling a controlled flooding process.

Another 5500 … 8200 $m^3\ d^{-1}$ of water originate from the Markus Semmler adit of the Schneeberg mine and enter the Schlemabach via the 15 II b shaft. The latter served as drinking water for SDAG Wismut and the town of Schlema until the early 1990s after arsenic reduction.

Compared to shafts 366 II b and 371 b, shaft 372 b, where the main water inflow occurred until the flooding of level -990, does not show substantially different temperatures. Only at level -1350 of shaft 372 b a clear temperature drop of 0.1 … 1.0 K can be observed -between April 28, 1993 and June 8, 1993, which is most probably due to the inflow of cold water. However, it can be seen from the profile that the cold water influence is no longer present after only a few metres in altitude. Similar effects are shown by the temperature profiles of the Hope and Adolfsglück shafts during their flooding (HERBERT 1989). There, the density stratification is primarily due to salinity. In UERPMANN (1980) there is an illustration of a shaft tube of the potash salt mining industry that has been flooded for 50 years, in which a more or less constant temperature decrease of 8 K can be observed over 100 metres in altitude, without there being any cold water inflows.

Apparently, the seepage water only causes a small, local temperature change. Due to the large energy content of the water already present in the mine (approx. $10 \cdot 10^6$ m³), the temperature is hardly affected by the additional 5 … 8‰ of water flowing in every week (approx. 0.01 K calculated temperature decrease). Convection in large areas of the mine (evidenced by the uniform temperature profiles of some shafts) also ensures rapid mixing of the water body.

7.6.4 General flooding process

After the mine water drainage was stopped, the mine water in the Niederschlema/Alberoda mine rose or rose in three phases (modified according to JÄGER et al. 1990):

1: Flooding of the levels, shafts and workings depending on the amount of inflowing water. Mainly vertical water movement due to the rising water.

2: Filling of the loosening zone. Vertical and hydrostatically induced horizontal water movement.

3: Restoration of the hydrogeological situation before the drainage of the mountain by mining.

In the following, the flooding process – as far as it is relevant for the question dealt with here – is briefly outlined.

During phase 1, the water rises continuously according to the principle of communicating pipes in the shafts (Fig. 88). Since the processes of flooding the floor and the roof are similar, these partial phases can be added to phase 1. However, it should not be ignored that the time for flooding the vertical mine workings is substantially shorter than that for the horizontal ones (ratio between 7:35 and 49:106 days, Fig. 88).

Due to temperature, mineralisation and gravity, the density of the water is not the same in every shaft. Therefore, the water levels in each of the investigated shafts will not be identical. For example, the difference in height in two connected 300 m high shafts (296 II b, 366 b, 371 b), in which water with the temperature 30 °C (ρ = 995.65 kg m^{-3}) and 40 °C (ρ = 992.2 kg m^{-3}) is located, is about 1 m. The water level in each shaft is therefore not identical.

To calculate the height difference, equation 52 can be used to calculate the height difference.

$$\frac{h_1}{h_2} = \frac{\rho_2}{\rho_1} \tag{51}$$

$$\Delta h = \frac{\rho_1 h_1 (1 - \frac{\rho_2}{\rho_1})}{\rho_2} \tag{52}$$

h_1 : Water level in shaft 1
h_2 : Water level in shaft 2
Δh : difference of the two water levels
ρ_1 : Density of the water in shaft 1
ρ_2 : Density of the water in shaft 2

In the uppermost 0 … 15 m, the front of the rising water (“Zone 1”) dissolves the already weathered, easily mobilisable minerals from the pit walls. This leads to an increase in substance concentrations in the water with a simultaneous increase in electrical conductivity (Fig. 77), which can be used as an indicator of water quality.

At the surface, the mine water is in solution equilibrium with the atmospheric oxygen, provided this has not been depleted by microbial processes above the rising water column. Therefore, apart from a few exceptions, the redox potentials in these uppermost metres are always greater than those below.

As the water rises, a zone of less oxidising conditions rises (“Zone 2”). The electrical conductivity is lower than that of zone 1, which is an indication of reduced overall mineralisation. Whether this zone causes less soluble phases to precipitate could not be determined with certainty. An example of this is given by the results of the physicochemical measurements in shaft 371 II b (Fig. 89, Fig. 90).

In the second phase – which is not completely separate from the first – the loosening zones around the mine cavities fill with water. Since the fissures are initially filled with air, material mobilisation takes place in this loosening zone, which is on average 1 m thick (chapter 8.2), as soon as the water flows through it. The water in the loosening zone will be transported both vertically and horizontally. Temperature will favour vertical transport (RUBIN 1981), solution gradients horizontal transport into and out of the matrix (GRISAK & PICKENS 1981, PFINGSTEN & MULL 1990). Which of the two processes will take place preferentially cannot be estimated at present.

Phase 3 represents the quasi-stationary state after the end of flooding, in which all drifts, excavation zones and the rock mass will be filled with water. Due to the low k_f-values *of* the rock, hardly any water flow on fault zones, but a weathering zone above the Markus-Semmler gallery, little seepage water will penetrate into greater depths of the mine workings. Rather, experience shows that – if no convection cycle is possible – the mine water body is overlayered by seepage water, as described by various authors (ERICKSON et al. 1982, LADWIG 1985, M. VESELIČ, pers. comm.).

In the mountains, flooding up to the Markus-Semmler adit will result in groundwater conditions similar to those existing before 1945. The groundwater levels will be directed towards the Schlemabach and the Zwickauer Mulde. Regardless of the choice of the future water outlet point, the amount of water flowing into the receiving water body will correspond to the water catchment area belonging to the mine. In the present case, this will be 5 … 9 · 10^6 m^3 a^{-1}.

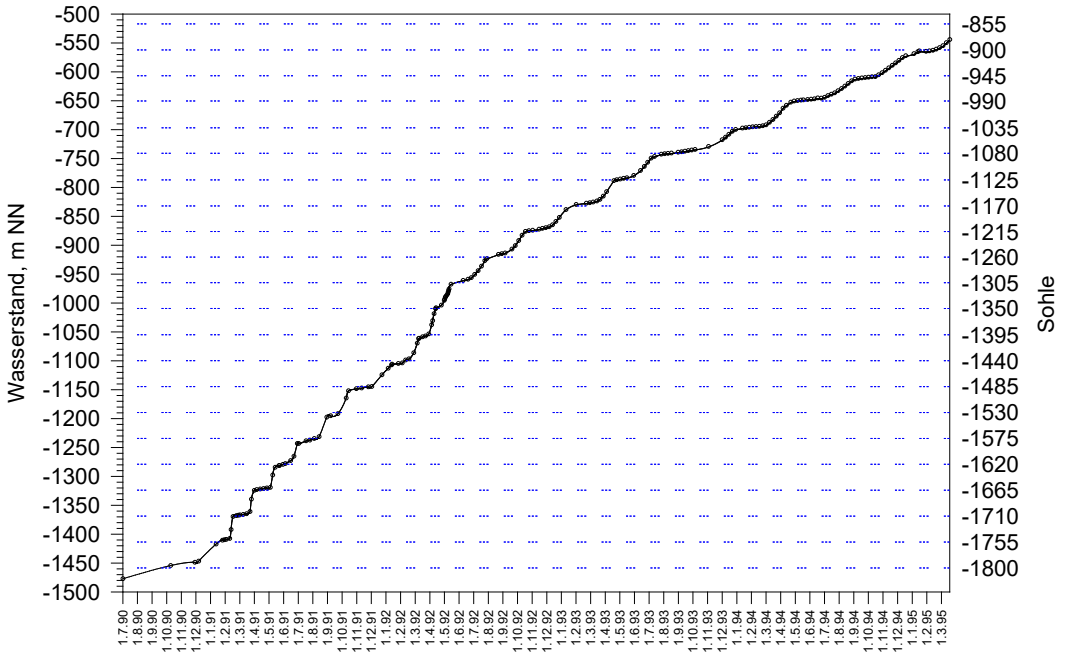

Fig. 88: Flooding curve of the water level in the Niederschlema/Alberoda mine between 1 July 1990 and 3 March 1995. Depicted on the basis of Wismut GmbH's own measurements and data.

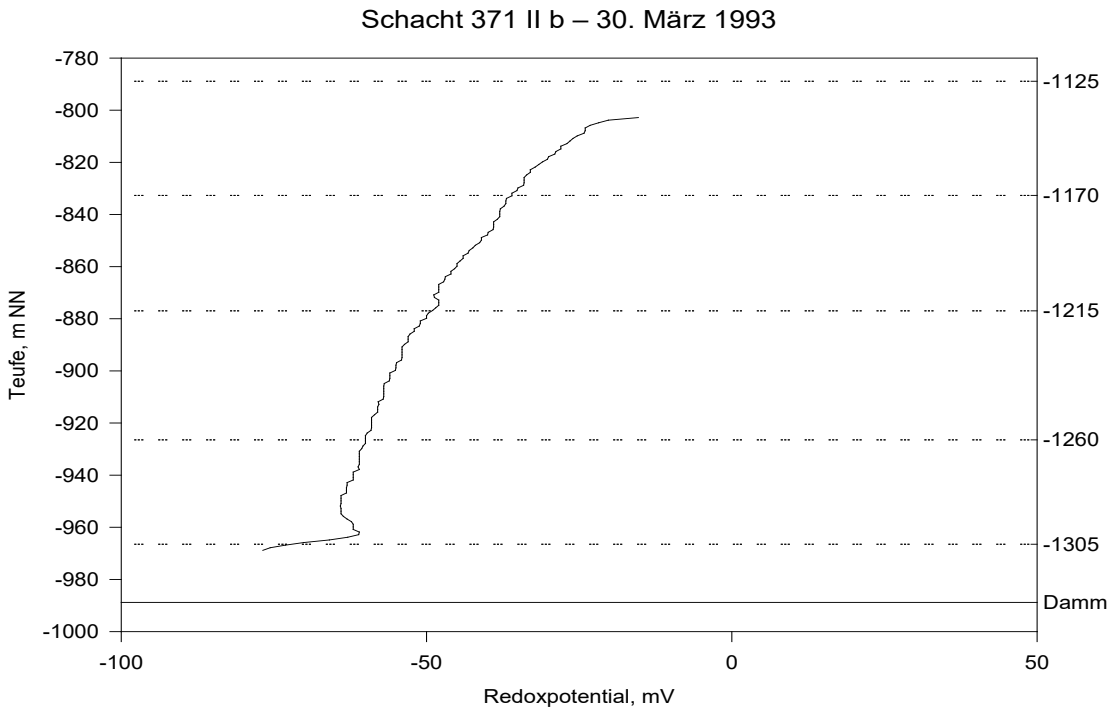

Fig. 89 Redox potential in the rising mine water of shaft 371 II b (modified after DFA/C&E 1993).

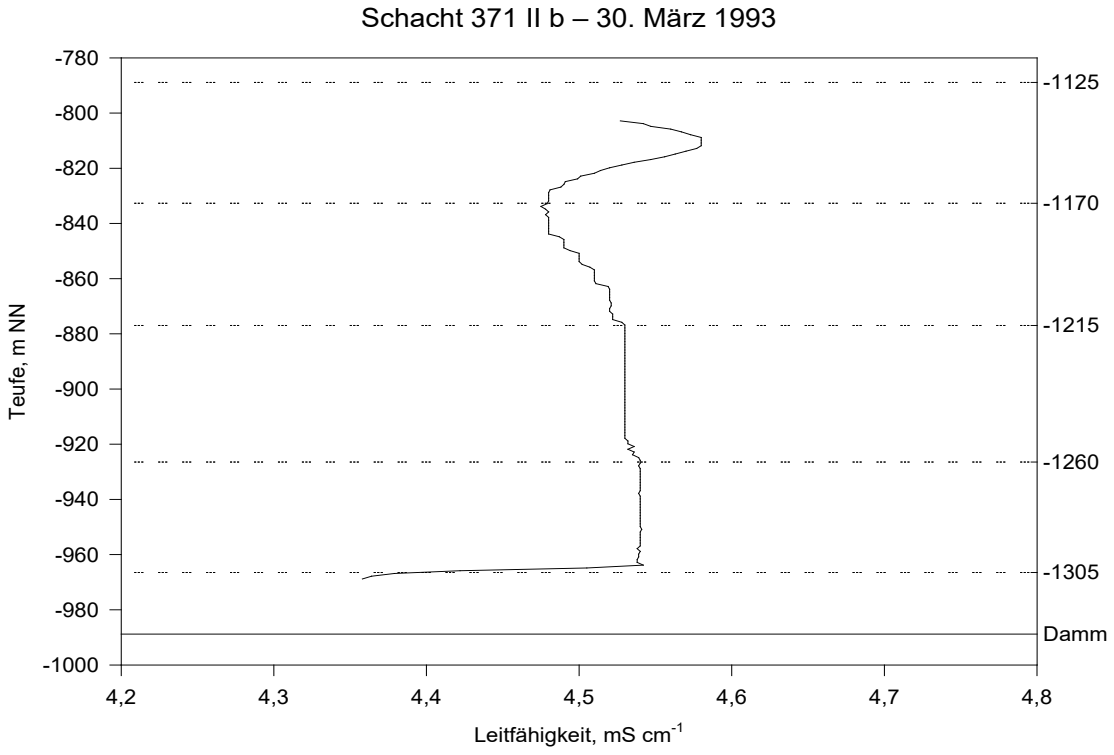

Fig. 90 Electrical conductivity in the rising mine water of shaft 371 II b (modified after DFA/C&E 1993).

7.7 Discussion and result

As the physicochemical measurements in seven shafts of the Niederschlema/Alberoda mine show, their hydrodynamic characteristics are similar in each case. Only shaft 372 b, above the level -1305, shows a deviating behaviour.

One of the most important similarities is that changes in a physicochemical parameter of the mine water occur in the same way in each shaft. This is clearly visible in the similar temperature curves of shafts 366 II b, 371 II b and 372 b (Fig. 65, Fig. 68, Fig. 71), but also in the electrical conductivity or pH measurements. In each shaft, two shaft water bodies and, if present, a sump water body can be distinguished.

The lower shaft water body is bounded at the top by the end of the fill site on the last struck bottom, the upper shaft water body is the part of the water above the fill site (Fig. 92, Fig. 69). Characteristics of the lower water body are relatively constant values in the physicochemical parameters, indicating good convective mixing, whereas the values in the upper water body change gradually towards the water surface. Convective flow is characterised by a regular or irregular change in flow direction and, for example, temperature ("oscillation", GEBHART et al. 1988). All stationary measurements in the shafts of the Niederschlema/Alberoda mine show a type of temperature or electrical conductivity oscillation in the lower water body (Fig. 73, Fig. 74, GEBHART et al. 1988, UERPMANN 1980).

These aforementioned features can be transferred to a detailed model of the flooding of the Niederschlema/Alberoda mine, assuming the presence of open thermosyphons or fluid circuits as described by GEBHART et al. (1988) and as investigated by BAU & TORRANCE (1981a, 1981b) (Fig. 92).

At the shaft walls and the bottom joints, the floodwater is heated if the rock temperature is higher than that of the water. The water surface and the shaft walls with temperatures below those of the floodwater, on the other hand, are cooled. Therefore, due to density differences, the heated mine water flows up the shaft walls, cools down in the near-surface area of the water body and sinks down in the centre of the shaft. Ideally, a laminar convection roll would form in most of the shafts of the Niederschlema-Alberoda mine, given the velocities and cross-sections. However, this is prevented because of the shaft installations (support layers, track laths, supply lines, Fig. 91) and the great wall roughness of the concrete lining. It can therefore be assumed that in the Niederschlema/Alberoda mine there are open water circuits (Fig. 92a, c) and open water circuits with an isothermal reservoir (Fig. 92b, d) in which the water flows turbulently and convectively.

Fig. 91: Mine water level in shaft 366 II b at the beginning of 1991. Shaft installations preventing laminar flow of the water are visible. The water surface (grey) is covered by foam. Image width about 2 m.

An isothermal reservoir is a sufficiently large fluid supply of constant temperature that is connected to the circuit and participates in the energy exchange.

Phase 1 of the resurgence process at the Niederschlema/Alberoda mine takes place in principle in four stages, alternating between open circuits, open circuits with isothermal reservoir and a closed circuit at the end. Due to the low permeabilities of the rock, flows through the rock are negligible.

Level I a

Seepage water collects in the shaft sumps and mixes with the quantities of non-sumped water already present there. These sump waters do not mix with the shaft water because the water flowing in from greater depths via the bottom has a lower density and overlaps the water in the sump. In the case of a developed convection cycle, the water flowing in via the invert can be understood in the sense of an inlet flow (KRANAWETTREISER 1989). A mixing of the two water bodies does not take place then.

Stage I b (Abb. 92a)

The water rises above the swamps, floods the first floor and begins to rise in the shafts. According to the principle of communicating tubes and the formula 46 the water levels adjust themselves. Shafts and invert, without sump, form an open circuit with two reservoirs. The bottom acts as a heater (Q), the shafts and the water surface as coolers relative to it.

As BAU & TORRANCE (1981b) and GEBHART et al. (1988) summarised, the water will flow convectively upwards and downwards alternately in the vertical sections due to density differences. Even a slightly different temperature of the shafts involved does not lead to any substantial change in the flow oscillation. Transferred to the mine model, this means mixing of the water in the roadway and the shafts. The sump water body is only involved in the flow if the density difference is smaller than about 2 g cm^3 (KRANAWETTREISER 1989). Oscillation is well documented from the long-term measurements and the resulting temperature curves.

Stage II (Fig. 92b)

With the onset of flooding of the next bottom, the two reservoirs merge into a uniform, approximately isothermal reservoir. BAU & TORRANCE (1981b) describe this case theoretically and experimentally. After a certain start-up phase, the temperature at the bottom reaches a maximum. The time span of the run-up phase is likely to be close to 0, since the energy input in Fig. 92b will not occur “suddenly” (energy input is expressed by the heating rate Q_1). Both the height of the maximum and the time span after which the system has cooled down to a fairly stable mean value are a function of the heating rate Q. Compared to the flow in stage I b, there is not a regular but an irregular up and down of the flow. Only in the steady state is there a homogeneous temperature distribution in the entire system. However, this is ruled out for a mine like the one at Niederschlema/Alberoda, as the rock temperature cannot be expected to equalise with the atmospheric temperature.

A behaviour exactly corresponding to that experimentally determined by BAU & TORRANCE (1981b) could be observed by the stationary measurement during the flooding of level -1260 in August 1992 (Fig. 74).

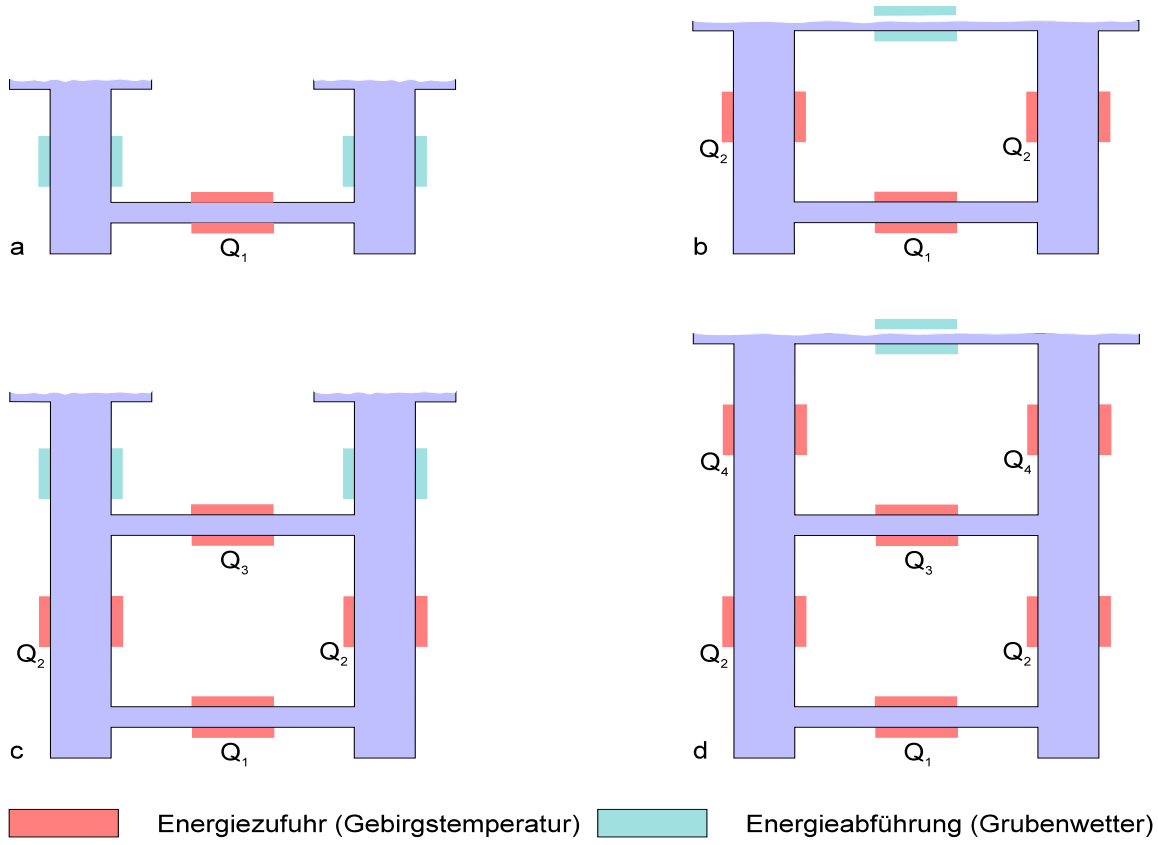

Fig. 92: Principle representation of the resurgence process in the Niederschlema/Alberoda mine as a combination of open and closed thermosyphons with free convection. a: Rise again in the shafts, energy supply from the levels, energy dissipation via the open shafts, shown as an open circuit with free convection and two reservoirs, b: Flooding of a level, energy supply from the completely flooded levels and the flooded shafts, energy dissipation at the water surface, shown as an open circuit with an equal temperature reservoir and free convection, c: Rise in the shafts above at least two flooded levels, shown as a combination of a closed circuit and an open circuit with two reservoirs, both with free convection, d: Flooding of a level above at least two fully flooded levels, shown as a closed circuit and an open circuit with an equal temperature reservoir, both with free convection. Heating rate $Q_4 > Q_3 > Q_2 > Q_1$.

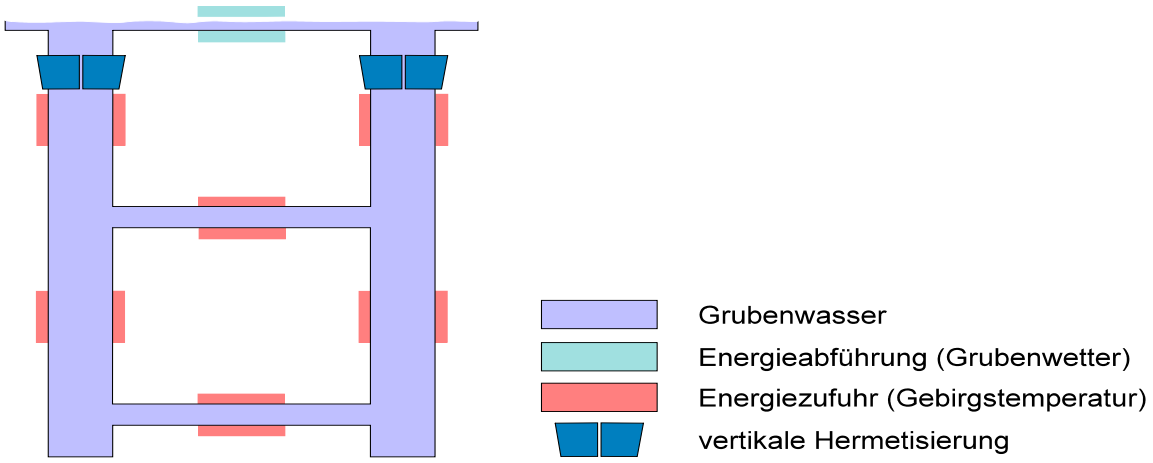

Fig. 93: Example of vertical hermetisation of a mine workings with pressure equalisation tubes for the time of flooding. The pressure equalisation pipes must be sealed after flooding of the vertical hermetisation to prevent water exchange between the water body below the hermetisation and the one above.

Stage III (Fig. 92c).

In stage III, the water in the shafts rises above the flooded bottom. Only the water below the fills is connected, but not that in the shafts. As shown by the numerous regular temperature measurements, the upper shaft water body cools down relatively quickly and only slowly takes on the temperature of the lower shaft water body. In addition, even if the seepage water temperature (approx. 20 °C) and the mine water temperature (approx. 40 °C) are assumed to be completely equal, there is a difference in density due to the difference in total mineralisation (1 g L^{-1} to 3 g L^{-1}), which prevents complete mixing. In addition, the flow field in the closed circuit of the lower shaft water body and the shaft geometry probably prevent mixing with the upper shaft water body. As soon as an intermediate layer of a certain thickness $Z(v, g, \rho_1, \rho_2)$ has formed between the lower and upper shaft water bodies, mutual influence is almost impossible (KRANAWETTREISER 1989).

In the closed circuit, temperature as well as flow velocity vary continuously, whereby certain, critical conditions can lead to the reversal of the flow direction, which can undergo a renewed reversal after a certain time (BAU & TORRANCE 1981b). In experiments, DAMERELL & SCHOENHALS (cited from BAU & TORRANCE 1981A, GEBHART et al. 1988) were able to demonstrate a continuous repetition of oscillating water movement for symmetrically heated, closed circuits.

Stage IV (Fig. 92d)

Stage IV differs from Stage II in that the connection of the two shafts is via more than one invert. Circulation can take place over one or both inverts, with flow preferentially over the invert with the lower flow resistance. Evidence of this behaviour is the result of the *Lycopodium* experiment in May 1992. Differently coloured spores were added to two shafts at two different depths, the numerical ratio of which indicated homogeneous mixing of the mine water over at least nine (!) levels after 5 weeks. From the experiments of BAU & TORRANCE (1981a) on asymmetrically heated open convection circuits, it can be concluded that shafts into which cold seepage water flows are also integrated into the convection circuit (specifically: shaft 372 b).

From the four-stage process of re-surge outlined above, the following summary emerges for the end of flooding with pumping out or overflowing of the water:

- End of flooding at stage III: upper shaft water body is not in convective contact with the rest of the mine water; nevertheless, contaminated water from other, also lower-lying mine workings constantly flows into the shaft due to pumping out of the water
- End of flooding at stage IV: the last flooded level is fully integrated into the water cycle, which is why contaminated water constantly reaches the surface

The only way to prevent the discharge and transport of pollutants would be to hermetise the mine workings as completely as possible vertically below the last level to be flooded (Fig. 93). It is essential to prevent or at least hinder the formation of large-scale convective cycles. Horizontal hermetisation by bricking off the filling points alone is not successful, as several walls have not been set (e.g. on level -990) and enable the circulation.

Finally, to illustrate the problem, let us quote from the work of BAU & TORRANCE (1981a), who write as the reason for their study in the first sentence:

“Free convection loops provide a means for circulating fluid without the use of pumps”.

8 Model presentation for mass transport

8.1 Introduction

Not only for environmental reasons, but also for business reasons, Wismut GmbH and the communities around Aue and Schlema must have an indication of the quantities of substances that the flooding water could dissolve and release if a conservative approach is taken. If a water treatment plant is built, its capacity, operating time and the necessary landfill space will depend on these quantities of material.

At an early stage, Wismut GmbH tried to estimate the quantities of metal that the flooding water could dissolve (SDAG WISMUT 1991). In its calculations, it assumed that most of the pollutants would be dissolved out of the small pieces of tailings remaining in the mine because of the large surface areas. The results of these rough calculations, which are only a rough estimate due to the lack of operational documents, are summarised separately for the individual elements in Tab. 55, whereby it cannot be assumed that all the substances in the tailings are mobilised, but only those in the weathered rims.

In the context of this work, it is shown that this is only a part of the rock mass available for dissolution. Along fractures and faults, further substances dissolve out of the solid rock and contribute to the increase of the mass concentration in the mine water. The aim of the following chapters is not to describe possible *sorption* or *desorption processes* between the mine water and the rock, but to give a conservative estimate of the quantities of elements that could pass from the rock matrix into the water through *mobilisation.*

8.2 Geotechnical assumptions

The following water pathways exist for the floodwater and seepage in a mine (Fig. 94), with the relative permeability decreasing from top to bottom within this listing:

- Stretches, shafts, hewing over
- Loosening zones
- Fissures, faults, ore veins
- Layer joints, bank joints, slate joints
- Microcracks
- Rock

The main water transport will take place in the drifts, shafts, overburden, loosening zones, fissures and faults with different velocities depending on the cross-section (chapter 7.5). In contrast, water movement in the crystalline rock matrix itself will play a subordinate role due to its low porosity, and thus also rock permeability (Tab. 52) (KARRENBERG 1981).

Tab. 52 Selected permeability coefficients and performance quotients (yields) of different rocks occurring in the Niederschlema/Alberoda deposit (k_f-values according to KRAPP 1983).

Rock	Rock permeability	Power quotients
	m s^{-1}	L s^{-1} m^{-1}
metamorphic limestone	10^{-3} ··· 10^{-2}	1 … 3
Keratophyr	10^{-3} ··· 10^{-2}	1 … 3
Quartzite	10^{-5} ··· 10^{-4}	0.6 … 0.8
Phyllites, Metamorphites	10^{-10} ··· 10^{-9}	0.001 … 0.01

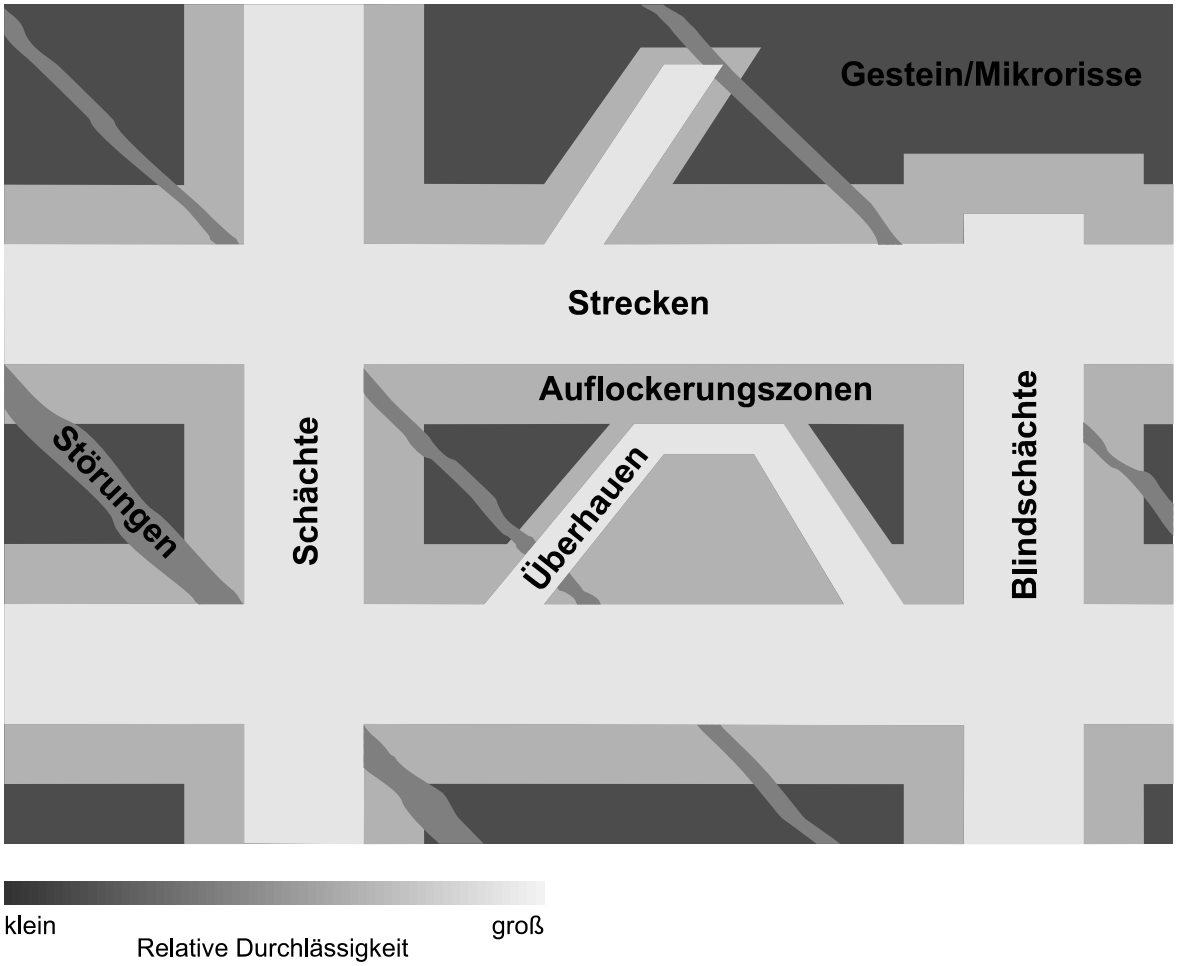

Fig. 94 Conceptual model of the water pathways in a mine (drawing of the roadway).

Tab. 53 Permeability as a function of fracture spacing (according to GEOLOGICAL SOCIETY ENGINEERING GROUP WORKING PARTY 1972, quoted from KARRENBERG 1981).

Fracture distance	Fracture distance d	Fracture number κ	Permeability k_f
	m	m^{-1}	$m\ s^{-1}$
Dense open partitions	< 0.06	> 16.7	10^{-6} … 10^{-4}
Narrow open partitions	0.06 … 0.60	16.7 … 1.7	10^{-9} … 10^{-6}
Wide open partitions	> 0.60	< 1.7	10^{-13} … 10^{-9}
No open partitions	Massive, dense	–	< 10^{-13}

Note: The values in Tab. 53 are not derived directly from the GEOLOGICAL SOCIETY ENGINEERING GROUP WORKING PARTY 1972. KARRENBERG (1981) may have combined the tables on pages 316 and 318. The way in which he arrived at the permeabilities given here is not comprehensible.

Some permeability coefficients as a function of fracture spacing, which can be taken as framework values, come from the British Geological Society (Tab. 53, quoted from KARRENBERG 1981).

Fissure numbers from the Niederschlema/Alberoda mine could not be found in the literature, so -fissure numbers were -determined at several points on level -540 on 2 February 1995 (Tab. 54). A relatively uniform picture emerged over the entire still accessible part. In most places the rock is only slightly disturbed, and even more strongly fractured areas were dry. The average fissure number is $\bar{\kappa} = 3$ ($s = 1.9$, $n = 44$), which suggests k_f-values of 10^{-9} … 10^{-7} m s^{-1} for the rock mass. If the measured values of the individual rock types of level -540, which represent 76 % of all rocks (Fig. 11), are weighted beyond this, the result is a fracture index of $\bar{\kappa} = 2$.

Another uncertainty when considering the possible waterway amalities is the depth of the loosening or relaxation zone around the drifts. It depends on various variables (G. REIK, R. STOLL, pers. comm.) and can therefore not be stated exactly:

- Technology of the driveway
- Route cross-section
- Lithology
- Thickness of the rock cover
- Expansion
- Tee-off length

MÜLLER-SALZBURG (1978) gives values of 0 … 3 m for the thickness, whereby maxima of 8 m can occur. MILITZER et al. (1986) give depths of 0.5 to 2.5 m for zones of loosening, and JACOBI & EVERLING (1981) consider values of 1.7 m to be realistic in solid rock. This information is confirmed by the geophysically determined depth of the excavation zone in the Niederschlema/Alberoda mine, which is slightly less than 1 m (STOLL & BAUER 1991). It is distributed over the entire mine area between a few centimetres and a maximum of 3 metres with a frequency maximum of 1 m (R. STOLL, pers. comm.). It is not possible at present to estimate the influence of the technology of flash blasting, which creates a flash zone extending 1 … 3 m around the roadway profile with new separation surfaces (ROSCHLAU 1994).

Since the size of the debris was not allowed to exceed a diameter of 0.15 m (G. FRÖHLICH, pers. comm.), a fragmentation of the rock in the loosening zone can be assumed, which corresponds to a fracture number of $\kappa = 6 \ldots 7$ m^{-1}. Thus, the coefficient of permeability of the loosening zone would be about $k_f = 10^{-7}$ m s^{-1}.

Between the excavation of an underground cavity and its flooding with water, oxygen-containing air circulates on the more or less wide-open fissures and oxidises a wide variety of minerals, as described in the example of uraninite (chapter 4.9). No information is available for Niederschlema/Alberoda on how far the reaction fringe extends into the rock, but it is probably a maximum of one to two millimetres (l_v in Fig. 95).

Tab. 54: Results of the fissure number measurements in the Niederschlema/Alberoda mine on level -540. ss: light-coloured phyllite, pd: coarse-grained metadiabas, td: banded metadiabas, fs: light-coloured fruity schist, G: granite.

No.	Measuring point lithology		fracture number κ, m^{-1}						n	$\overline{x}$	σ
1	Bottom -540, Qu. 900 a, B. K. 162, E-joint	ss	2	0	2				3	1	1.2
2	Bottom -540, Qu. 900 a, 17 m N' WQu. 900 a, W-Joint	ss	2	0	0	2	0	0	6	1	1.0
3	Sohle -540, F.-Str. 909, 115 m NW' Qu. 902, SW-Stoß	pd	4	4	3	1			4	3	1.4
4	Sohle -540, F.-Str. 909, 40 m NW' Qu. 905, NE-Stoß	td	4						1		
5	Sole -540, F.-Str. 909, Qu. 905, NE-Stoß	td	5	6	4	6			4	5	1.0
6	Sohle -540, F.-Str. 909, Qu. 906 a, SW-Stoß	fs	0	0	2				3	1	1.2
7	Sohle -540, F.-Str. 909, Qu. 906 a, NE-Stoß	fs	4	2					2	3	1.4
7'	Sole -540, F.-Str. 908, 10 m NW' Access 366 b, SW-Joint	fs	3	3	4	5			4	4	1.0
8	Sohle -540, F.-Str. 908, Access 383, Wetterstrecke, N-Stoß	fs	5	1	2	3	4		5	3	1.6
9	Sole -540, F.-Str. 907, Qu. 909, S-Joint	G	0	0	0	1			4	0	0.5
10	Sole -540, F. St. 907, 10 m SE' Qu. 908, SW thrust	fs	3	3	4	2			4	3	0.8
11	Sole -540, Qu. 908, surge tank 69, NE-strike	fs	5	5	3	4			4	4	1.0
	added up:								44	3	1.9

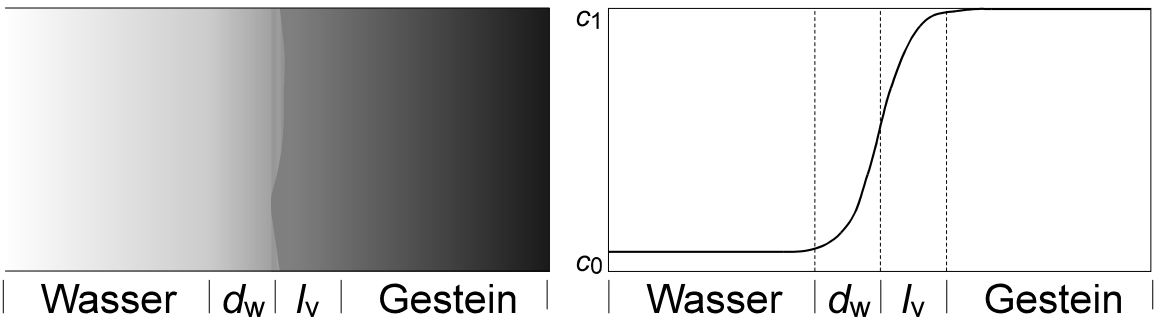

Fig. 95 Schematic representation of the reaction zones in solution processes on a rock matrix. c_1 and c_0 correspond to the relative concentrations $c_1 = 1.0$ and $c_0 = 0.0$ of a substance. d_w: Diffusion layer in the water, l_v: Reaction fringe in the rock.

8.3 "Back-of-the-envelope" calculations

The aforementioned geotechnical assumptions are the basis for calculating the available contact areas in the mine and the maximum quantities of contaminants that can be mobilised by the flooding water. It is assumed that the water completely mobilises the pollutants in the weathering crust and that its flow velocity is sufficiently high to always maintain a concentration gradient into the solution (Fig. 95).

The total porosity ϕ_T of the rock mass represents the sum of all porosities (NORTON & KNAPP 1977):

$$\phi_T = \phi_K + \phi_D + \phi_R \quad (53)$$

with

ϕ_T : Total porosity
ϕ_K : effective or kinematic porosity
ϕ_D : diffusive porosity
ϕ_R : residual porosity

The mine cavities can be classified accordingly:

$$\phi_{g,T} = \phi_{g,K} + \phi_{g,D} + \phi_{g,R} \quad (54)$$

where

$$\phi_{g,K} = \phi_{g,St} + \phi_{g,Sch} \quad (55)$$

$$\phi_{g,D} = \phi_{g,Ü} + \phi_{g,Su} + \phi_{g,B} \quad (56)$$

with

$\phi_{g,T}$: Total mine voids
$\phi_{g,K}$: effective mine voids
$\phi_{g,D}$: diffusive mine voids
$\phi_{g,R}$: residual mine voids = air-filled mine voids
$\phi_{g,St}$: mine voids of the roadways
$\phi_{g,Sch}$: mine voids of the shafts
$\phi_{g,Ü}$: mine voids of the Überhauen
$\phi_{g,Su}$: mine voids of the shaft sumps
$\phi_{g,B}$: mine voids of the blind sections

Since after the end $\phi_{g,T}$of flooding isϕ_T subset of , a quantity for the rock cavity must be introduced in addition to the mine cavity. This is understood in the following as $\phi_{h,T}$, with an equation 53 corresponding definition. Thus the total porosity is determined as

$$\phi_T = \phi_{g,T} + \phi_{h,T} \quad (57)$$

The corresponding areas of the porosities to

$$A(\phi_T) = A(\phi_{g,T}) + A(\phi_{h,T}) \quad (58)$$

However, only the effective total area A_w is of interest for the maximum amount of pollutant that can be mobilised:

$$A_w = A(\phi_K) + A(\phi_D) = [A(\phi_{g,K}) + A(\phi_{h,K})] + [A(\phi_{g,D}) + A(\phi_{h,D})] = A_g + A_k \quad (59)$$

Assuming that the area of the drift walls in $\phi_{g,R}$the Niederschlema/Alberoda mine is negligible (<1 %), the entire area of the drift walls is summarised as A_g. Due to the low fracturing of the rock, the consideration only includes the loosening zone around the drifts, whose area A_k is a subset of $A(\phi_{g,K})$ + $A(\phi_{g,D})$. The fracturing zone is homogeneously fissured in all three directions and all fractures are formed as plane± fissures.

The following data are used for the calculation (sources in brackets):

Total volume of the lines	V_{ges}	36.0 · 10^6 m³	(Tab. 3)
Total length of the driveways	l_s	4.16 · 10^6 m	(BÜDER & SCHUPPAN 1992)
Depth of the loosening zone	l_a	1.0 m	(STOLL & BAUER 1991)
Rock density	ρ	2.79 · 10^3 kg m^{-3}	(DALY et al. 1966, NORTON & KNAPP 1977)
Fissure number (loosening zone)	κ_a	7.0 m^{-1}	(Abb. 96)
Thick weathering rim	l_V	1 · 10^{-3} m	(–)

The following relationship applies to the calculation of the driveway inner surfaces, assuming that all driveways would have the same radius r_s:

$$A_g = 2 \cdot r_s \cdot \pi \cdot l_s \quad (60)$$

$$V_{ges} = r_s^2 \cdot \pi \cdot l_s \quad (61)$$

$$A = 2 \cdot \sqrt{\frac{V_{ges}}{\pi \cdot l_s}} \cdot \pi \cdot l_s = 2 \cdot \sqrt{V_{ges} \cdot \pi \cdot l_s} \quad (62)$$

The volume of the loosening zone, V_a, is determined by the following equation:

$$V_a = ((l_a + r_s)^2 - r_s^2) \cdot \pi \cdot l_s \quad (63)$$

A homogeneous degree of separation results in a fissure area A_k of

$$A_k = (l_a^2 + 2 \cdot l_a \cdot r_s) \cdot \pi \cdot l_s \cdot 3 \cdot \kappa_a \quad (64)$$

The effective total volume V_g is then calculated as follows

$$V_g = A_w \cdot l_v = (A_g + A_k) \cdot l_V \quad (65)$$

and its mass to

$$M_g = V_g \cdot \rho \quad (66)$$

The most relevant uncertainty factor is the assumption of a homogeneous aeration of the zone of loosening as well as its thickness. Various calculations depending on both variables show the percentage of A_{gw} and how it depends on the two variables (Fig. 96). It turned out that the proportion of A_g between the two minima (κ = 3 m^{-1}, l_a = 0.5 m) and maxima (κ = 8 m^{-1}, l_a = 3 m) amounts to 84 % to 99 % of the total inner surface A_w. Thus, within the given limits, the fissure number and the thickness of the zone of loosening have only a small influence on the effective total area A_w.

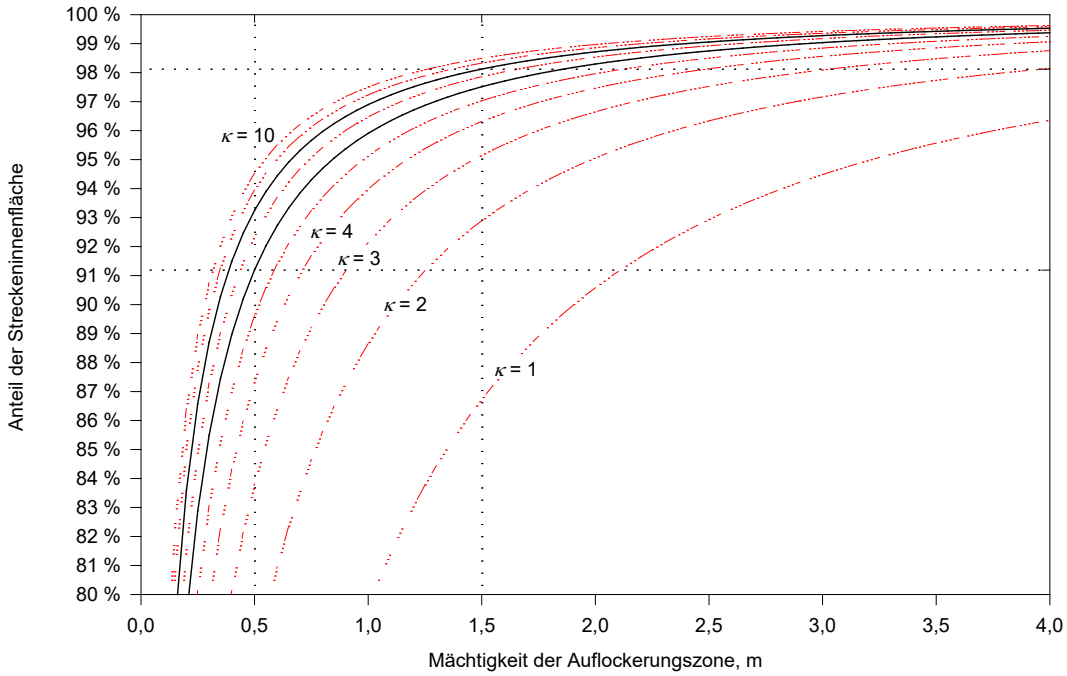

Fig. 96 Percentage of fissure areas A_k of the effective total area A_w as a function of the fissure number and the depth of the break-up zone l_a. Fissure areas from equation 64, inner surfaces of the break-up zone from equation 62.

Rounding the effective total mass to $0.1 \cdot 10^6$ t introduces an error of about ±8 %, so the average value used to calculate the maximum soluble pollutants is assumed to be $\kappa = 7.0$ m^{-1} and $l_a = 1.0$ m.

From the formulas 62, 64, 65 and 66 the total effective mass is calculated to be

- $M_g = 3.3 \cdot 10^6$ t

Tab. 55 Mobilisable pollutant reserves in the Niederschlema/Alberoda mine in t, last digit rounded (SDAG WISMUT 1991 and own calculations). A grain size of 5 cm and a thickness of the weathering rim of 0.1 cm were assumed for the heap material. The weathering rim then contains about 11 % of the mobilisable material quantities. “Debris material” refers to the total in the debris material, “of which mobilisable” refers to that in the weathering rim of the crushed material and “loosening zone” refers to the contaminant contents present in the loosening zone around the mine workings.

Element	Waste rock material	Thereof mobilisable	Loosening zone	Sum M_{max}, t
	t	t	t	t
Uranium	7000	810	20	830
Arsenic	11000	1270	100	1370
Nickel and cobalt	630	70	260	340
Bismuth	70	10	10	20
Zinc	1000	120	310	430
Copper	700	80	100	180
Lead	300	40	60	100
Antimony	300	40	10	50
Selenium	50	10	10	20
Radium 226	0.001	0.0001	$2.74 \cdot 10^{-7}$	0.0001

which together with the regional CLARKE values of the trace element distribution (Tab. 6) and the rock distributions (Fig. 11) lead to the calculation results in the table (Tab. 55). The mobilisable amounts of substances in the heap material were converted in such a way that from an idealised, round rock grain with a diameter of 5 cm, the substances in a 0.1 cm thick weathering rim are mobilised. This corresponds to about 11 % of the quantity remaining in the mine workings (SDAG WISMUT 1991 gives a grain size of 2 cm. However, this grain size seems too small from observations in the mine. If it is correct, the cleaning time would have to be multiplied by about 2).

8.4 Discussion and result

With regard to a possible complete treatment of the mine water, the question arises as to what time is necessary to treat the entire mine water, including the maximum soluble pollutants M_{max}. The following assumptions shall apply to estimate this time. To estimate this time, the following assumptions should apply, which have been partially substantiated by the physicochemical measurements:

- Withdrawal of type G water in the non-surface area
- Homogeneous mixing of the mine water
- Reduction of the mass concentrations through water withdrawal and the dissolution of new substances balance each other out (sufficiently large concentration gradient into the solution)
- Mass concentrations are constant until the last sampling day
- Diffusion into the rock matrix is less than diffusion into the mine water or solution.
- Pollutant content of the mine water only by dissolving the quantities M_{max}
- Pollutant supply through type S water is constant
- No technical barriers

The following values are the basis for calculation:

Water volume to be cleaned	V_{rei}	$36.0 \cdot 10^6$ m³
Annual water withdrawal	V_{ent}	$7 \cdot 10^6$ m³ a^{-1}
Mass concentration (type G, type S)	$\overline{x}_G$, $\overline{x}_S$	Tab. 28

Then the time t necessary for a complete cleaning of the water is calculated to:

$$t = \text{Feststoffterm} + \text{Grubenwasserterm} = \frac{M_{max} - V_{rei} \cdot \overline{x}_G}{V_{ent} \cdot (\overline{x}_G - \overline{x}_S)} + \frac{V_{rei} \cdot \overline{x}_G}{V_{ent} \cdot (\overline{x}_G - \overline{x}_S)} \qquad (67)$$

As the results (Tab. 56) show, a plant that consistently treats type G water from the mine workings would have to be operated for several decades or centuries, depending on which pollutant is to be removed. A complete mine water treatment down to pollutant levels corresponding to those of seepage water (type S) or even those of surface water is therefore questionable from an economic point of view.

Tab. 56: Treatment time of the mine water when type G water is extracted over the entire treatment period. All values rounded to two valid digits.

Element	Treatment time, a
Uranium	60
Arsenic	40
Nickel and cobalt	3.200
Bismuth	1.600
Zinc	820
Copper	4.400
Lead	2.200
Antimony	52.000
Selenium	28.000
Radium 226	280.000

9 Conclusions

Finally, the results of the investigations in the previous chapters will be used as a model to describe the hydrogeochemical-hydrodynamic development of the Niederschlema-Alberoda mine in the future and the quality of the water that will emerge from the mine at the end of the flooding.

Precipitation water enters the mine workings through the weathering zone of the rock and accumulates various cations and anions on its way. As soon as this seepage water hits a roadway or a shaft, it will continue to flow there and additionally absorb mining-related pollutants, the mass content of which will be greater the further the water has flowed in the mine workings. The comparison of the analyses from the level of the Markus Semmler adit with those of the seepage water shows this enrichment.

Since the permeability coefficients of the rocks are low and the water inflows into the mine workings decrease with increasing depth, only little seepage water will flow in at greater depths. As soon as the seepage water comes into contact with the mine water in a shaft, the mixing of the two types of water begins, the intensity of which depends on the current water level. Only a few weeks later, the former seepage water is homogeneously mixed with the mine water.

As has been shown, the pollutants accumulate depending on the solid phases present, with the carbonate solution being the most important controlling reaction. As soon as either the solution equilibrium of a phase is reached or a phase is no longer available, there is no further increase in the ions involved in the water. Relevant for the solution of solid phases are the redox potential and the pH value. As the calculation of the net neutralisation potential shows, no acidification of the mine water is to be expected at the Niederschlema-Alberoda mine, because the carbonates in the rock completely buffer the protons of the pyrite oxidation. A strong increase of the current mass contents in the mine water is therefore unlikely. On the other hand, the potential of the maximum available cations and anions shows that in the long term (at least four decades) there will be no improvement in the quality of the mine water, especially since the mine with its many shafts and drifts acts as an independently working circulating pump.

After the water has reached its maximum flood level, the seepage water will overlay the mine water until it is in density equilibrium with it.

Two opposing conditions can occur at the end of the flooding. Without vertical hermetisation, the Niederschlema/Alberoda mine will constantly have water with high pollutant contents, which will correspond to those of water type G, due to the mine geometry. Conversely, in the case of vertical hermetisation, water will be present on the last flooded level whose composition essentially corresponds to the geogenic background value. In terms of magnitude, this water has a chemism between that of the seepage water and that of the historical analyses.

In principle, the pollutant content of the floodwater to be discharged could be reduced by a treatment plant, the addition of chemicals or by controlling the flooding.

The most favourable way to prevent the discharge of contaminated mine water into the environment seems to be the construction of dams in all vertical mine workings that are in hydraulic connection with the last level to be flooded.

With regard to a possible water treatment plant, the following must be considered depending on the two final states of flooding shown above:

- In a water treatment plant that is operated for several decades, many tons of toxic treatment residues are continuously produced.
- From an economic point of view, it seems unjustifiable to treat water in which the mass concentrations of many constituents already correspond to the natural background level.

If the mine workings are hermetised as completely as possible, no water treatment plant is necessary for the Niederschlema/Alberoda uranium mine according to the results of the investigation presented here.

10 Literature

ACKMAN, T.E. & JONES, J.R. (1991): Methods to identify and reduce potential surface stream water losses into abandoned underground mines. – Environ Geol Water Sci, **17**: 227-232, 6 fig., 2 tab.; New York. https://doi.org/10.1007/BF01701703

AGRICOLA, G. (1994): Zwölf Bücher vom Berg- und Hüttenwesen (reprint). – 543 p.; Munich (Dt. Taschenbuch Verl.).

ALPERS, C.N. & NORDSTROM, D.K. (1990): Stoichiometry of mineral reactions from mass balance of acid mine waters at Iron Mountain, California. – Program with Abstracts – Geological Association of Canada, **15**: 1-2; Waterloo, ON, Canada.

ALTERMANN, M., LIEBEROTH, I. & SCHWANECKE, W. (1988): Gliederung der Lockergesteinsdecken der Mittelgebirge. – Z. f. angew. Geol., **34**: 302-306, 1 fig.; Berlin.

ALTERMANN, M. & WÜNSCHE, M. (1991): Source rocks and soil properties. – Z. geol. Wiss., **19**: 3-12, 5 fig., 3 tab.; Berlin.

AMERICAN BUREAU OF METAL STATISTICS (1994): Non-Ferrous Metal Data 1993 – 181 pp. (American Bureau of metal Statistics).

ANONYMOUS (1993): Uranium Supply of the World. – Atomwirtschaft Atomtechnik, **38**: 198-200.

ATKINS, P.W. (1990): Physikalische Chemie. – 2nd ed., 890 p.; Weinheim u.a. (VCH).

ATSCHEEV, B.N. (1967): Distributional regularities and localisation conditions of uranium mineralisation in the Schlema-Alberoda deposit (Russ.). – without pagination; SDAG Wismut (Unpublished report).

AURADA, K.D. (1970): Berechnung des Wiederanstiegsprozesses im Grubengebäude des Kupferschieferbergbaus in der Mansfelder Mulde mit Hilfe der Monte-Carlo-Methode. – Wasserwirtschaft Wassertechnik, **20**: 264-270, 6 fig., 3 tab.

BAAS BECKING, LGM., KAPLAN, IR. & MOORE, D. (1960) Limits of the Natural Environment in Terms of pH and Oxidation-Reduction Potentials. – J. Geol., **3**: 243-284, 34 fig.; Chicago. https://doi.org/10.1086/626659

BACHNER, D., BIESOLD, H. & UHLENBRUCK, H. (1993): Radiologische Erfassung, Untersuchung und Bewertung bergbaulicher Altlasten. – Atomwirtschaft Atomtechnik, **38**: 291-294.

BAIN, G.W. (1950): Geology of the fissionable materials. – Econ. Geol., **45**: 273-323, 4 fig., 4 tab.; Lancaster. https://doi.org/10.2113/gsecongeo.45.4.273

BALL, J.W., JENN, A.E. & CANTRELL, W.M. (1981): WATEQ3 – A Geochemical Model with Uranium added. – U.S. Geological Survey Open-File Report: 1-80, 2 Tab. https://doi.org/10.3133/ofr811183

BALL, J.W. & NORDSTROM, K.D. (1991): User's Manual for WATEQ4F, with revised Thermodynamic Data Base and Test Cases for Calculating Speciation of major, trace and redox Elements in natural Waters. – U.S. Geological Survey Open-File Report: 1-189, 2 Tab. https://doi.org/10.3133/ofr90129

BANKS, D. (1994): The Abandonment of the Killingdal Sulphide Mine, Norway: a Saga of Acid Mine Drainage and Radioactive Waste Disposal. – Mine Water and the Environment, **13** (3–4): 4 fig., 1 tab; Wollongong.

BARNES, I. & CLARKE, FE. (1964): Geochemistry of ground water in mine dranaige problems. – U.S. Geological Survey Professional Paper, **473, A**: 1-6; Washington. https://doi.org/10.3133/pp473A

BARTHEL, F.H. (1993): Uranium mining on the territory of the former GDR from 1945 to 1990 – Geol. Jb, **A 142**: 335-346, 2 fig., 5 tab.

BASAROVICH, H.S-S. (1992): Isotope-geochronological investigation of the Schlema-Alberoda deposit by means of the xenon-neutron induction method (in Russian). – 22 p., 8 fig., 1 tab.; Moscow (PhD thesis: Russian Academy of Sciences (Institute of Geochemistry and Analytical Chemie)).

BATES, R.L. & JACKSON, J.A. (1987): Glossary of geology. – 3rd ed., 788 p.; Alexandria (American Geological Institute).

BAU, H.H. & TORRANCE, K.E. (1981a): On the stability and flow reversal of an asymmetrically heated open convection loop. – J. Fluid. Mech., **109**: 417-433, 10 Fig. https://doi.org/10.1017/S0022112081001146

BAU, H.H. & TORRANCE, K.E. (1981b): Transient and Steady behaviour of an open, symmetrically-heated, free convection loop. – Int. J. Heat Mass Transfer, **24**: 597-609, 15 Fig. https://doi.org/10.1016/0017-9310(81)90004-1

BAUMANN, L. (1967): Zur Frage der varistischen und postvaristischen Mineralisation im sächsischen Erzgebirge. – Freiberger Forsch.-H., **C 209**: 15-38, 4 fig.; Freiberg.

BAUMANN, L. (1968): Die Mineralparagenesen des Erzgebirges – Charakteristik und Genese. – Freiberger Forsch.-H., **C 230**: 217-233; Freiberg.

BAUMANN, L. (1992): Zur Metallogenie des Erzgebirges sowie Darstellung einiger seiner bedeutenden Lagerstätten. – Schriftenreihe Gesellschaft Deutscher Metallhütten- und Bergleute, **64**: 1-30, 17 fig., 2 tab.; Clausthal-Zellerfeld.

BAUMANN, L. (1994): Ore parageneses of the Erzgebirge – history, results and problems. – Monograph Series on Mineral Deposits, **31**: 25-46, 11 fig.; Berlin.

BAUMANN, L., NIKOLSKIJ, I.L. & WOLF, M. (1979): Einführung in die Geologie und Erkundung von Lagerstätten. – 503 p., 151 fig., 44 tab.; Essen (Glückauf).

BECK, R. & WEBER, C.A. (1897): Ueber ein Torflager im älteren Diluvium des sächsischen Erzgebirges. – Z. dt. geol. Ges., **49**: 662-671, 1 fig.; Berlin.

BEEGER, D., MATHÉ, G., QUELLMALZ, W. & WEBER, W. (1988): Das sächsische Erzgebirge – Geologie, Bergbau und Kultur. – Veröffentlichungen aus dem Naturhistorischen Museum Wien, Neue Folge, **22**: 1-40, 49 fig., 1 pl.; Vienna.

BENEDIX, E.H., CASPER, S.J., DANERT, S., HÜBSCH, P., LINDNER, K.E., SCHMIEDEKNECHT, M. & SCHUBERT, R. (1991): Urania Pflanzenreich in vier Bänden – Viren Bakterien Algen Pilze. – 1st ed., 664 p., ill.; Leipzig Jena Berlin (Urania Verlag).

BIAGLOW, J.A. (1988): Study to determine the effectiveness of the hydraulic mine seal at Big Four Hollow Creek near Lake Hope State Park in southeastern Ohio – 169 p.; Dayton OH USA (Degree: Master's).

BLAIR, R.D., CHERRY, J.A., LIM, T.P. & VIVYURKA, A.J. (1980): Groundwater monitoring and contaminant occurrence at an abandoned tailings area, Elliot Lake, Ontario. – 411-430, Fig., 2 Tab.; Vancouver (First international conference on uranium mine waste disposal).

BLOWES, D.W., PTACEK, C.L., FRIND, E.O., JOHNSON, R.H., ROBERTSON, W.D. & MOLSON, J.W. (1994): Acid-Neutralization Reactions in inactive Mine Tailings Impoundments and their Effect on the Transport of dissolved Metals. – Proceedings, International Land Reclamation and Mine Drainage Conference, Pittsburgh, P.A.: 4 Fig., 1 Tab. https://doi.org/10.21000/JASMR94010429

BÖTTCHER, J., BÜDER, W., HAMANN, M., HAMANN, S., LINKERT, K-H., LIPP, U., MÜLLER, F., ROCHHAUSEN, D., ROSENHAHN, L., SCHRÖDER, B., SCHUPPAN, W. & SCHWARZE, K-H. (1991): Seilfahrt – Auf den Spuren des sächsischen Erzbergbaus. – In: WISMUT AG. – 2nd ed., 153 p.; Haltern (Doris Bode Verlag).

BOSECKER, K. (1980): Bakterielles Leaching – Metallgewinnung mit Hilfe von Bakterien. – Metall, **34**: 36-40; Berlin.

BREITHAUPT, A. (1849): Die Paragenesis der Mineralien: Mineralogisch, geognostisch und chemisch beleuchtet, mit besonderer Rücksicht auf Bergbau. – 276 p., 1 woodcut plate; Freiberg (Engelhardt).

BRENDEL, K., BRÜCKNER, G., KNITZSCHKE, G., SCHWANDT, A. & SPILKER, M. (1982): Montanhydrologische Aspekte zur Gewährleistung der Bergbausicherheit beim Abbau zechsteinzeitlicher Lagerstätten. – Z. geol. Wiss., **10**: 7-31, 13 fig.; Berlin.

BRINKMANN, R. & ZEIL, W. (1986): Abriß der Geologie – 2. Historische Geologie, Erd- und Lebensgeschichte. – 13th ed., 404 p.; Stuttgart (Enke).

BROWN, A. (1982): A validated theory of underground mine flooding. – Proceedings, 1st International Mine Water Congress, Budapest, Hungary: 411-428; Budapest.

BÜDER, W. & SCHUPPAN, W. (1992): Zum Uranerzbergbau im Lagerstättenfeld Schneeberg-Schlema-Alberoda im Westerzgebirge. – Schriftenreihe Gesellschaft Deutscher Metallhütten- und Bergleute, **64**: 203-221, 9 fig., 2 tab.; Clausthal-Zellerfeld.

BUNDESMINISTER FÜR WIRTSCHAFT (1992): Auswirkungen aus dem Uranbergbau und Umgang mit den Altlasten der Wismut in Ostdeutschland – Antwort der Bundesregierung auf die große Anfrage der Abgeordneten Dr. Klaus-Dieter Feige, Werner Schulz (Berlin) und der Gruppe BÜNDNIS 90/DIE GRÜNEN. – German Bundestag Printed Paper, **12**: 1-43; Bonn.

BUNDESMINISTER FÜR WIRTSCHAFT (1993): Wismut – Stand der Stillegung und Sanierung. – BMWI Documentation, **335**: 1-35; Bonn.

BUNDESMINISTER FÜR WIRTSCHAFT (1995): Wismut – Fortschritte der Stillegung und Sanierung. – BMWI Documentation, **370**: 1-34; Bonn.

BUNDESUMWELTMINISTERIUM (1994): Sanierung in den Uranbergberggebieten der Wismut – Zwischenbericht des Bundesumweltministers liegt. – Environment: 228-229; Bonn.

BUTTERMANN, G. (1988): Radioactivity and Radiation. – In: HANNS-SEIDEL-FOUNDATION: Chernobyl, Medicine, Technology. – 2nd ed., 98 p., 13 tab.; Percha (Schulz).

CARLÉ, W. (1975): Die Mineral- und Thermalwässer von Mitteleuropa. – 254-256 p.; Stuttgart (Wissenschaftliche Verlagsgesellschaft).

CARUCCIO, F.T., GEIDEL, G. & PELLETIER, A. (1980): The Assessment of a Stratum's capability to produce acidic drainage. – In: Symposium on Surface Mining Hydrology, Sedimentology and Reclamation. – 437-443, 5 fig.; Lexington (University of Kentucky).

C & E CONSULTING UND ENGINEERING GMBH (1994): Abschlussbericht (Teilleistung 6.2) über die Auswahl, Installation und Inbetriebnahme von Messsystemen zur Flutungkontrolle und Durchführung zusätzlicher Kontrollmessungen. – 14 p., 5 Tab., 54 Anl; Chemnitz (Unpublished report on order 1.3.1/8996/938/93).

CHARPENTIER, J.F. von (1778): Mineralogische Geographie der Chursächsischen Lande. – 432 p.; Leipzig (Crusius).

CHERVET, J. & COULOMB, R. (1958): Geochemical behaviour of uranium in the alteration cycle. – Proceedings II. Intern Conf Peaceful Uses Atomic Energy, **2**: 199-203.

CHILINGAR, G.V. (1956): Durov's Classification of Natural Waters and Chemical Composition of Atmospheric Precipitation in USSR: A Review. – Trans. Amer. Geophys. Union, **37**: 193-196, 3 fig., 1 tab; Washington DC. https://doi.org/10.1029/TR037i002p00193

DAENEKE & BÜSSER (1991): Konzeption zur Sanierung und Wiederurbarmachung im Uranerzbergbaugebiet Ronneburg. – In: STRAHLENMESSSTELLE GAMMA IM KATALYSE-INSTITUT KÖLN, BUNTSTIFT – FÖDERATION DER GRÜN-NAHEN LANDESSTIFTUNGEN UND BILDUNGSWERKE: Der Uranbergbau in der DDR und seine Folgen. – 2nd ed., 61-64 p.; Cologne (Strahlenmeßstelle GAMMA im KATALYSE-Institut).

DAHLKAMP, F.J. (1993): Uranium ore deposits. – 460 p.; Berlin (Springer). https://doi.org/10.1007/ 978-3-662-02892-6

DALÍ, S. & SCHIEBLER, R. (1990): Das geheime Leben des Salvador Dalí (The secret life of Salvador Dalí) – Autobiographie. – 3rd ed., 503 p.; Munich (Schirmer-Mosel).

DALY, R.A., EDWARD MANGER, G. & CLARK, S.P. jr (1966): Density of Rocks. – In: CLARK, S. P.: Handbook of physical constants. – 19-26, 5 Tab.; New York (Geological Society of America). https://doi.org/10.1130/MEM97-p19

DAVELER, S.A. & WOLERY, T.J. (1992): EQ6, A Computer Program for Reaction Path Modeling of Aqueous Geochemical Systems: Theoretical Manual, User's Guide, and Related Documentation (Version 7.0). – 338 p., 17 fig., tab.; Livermore (Lawrence Livermore National Laboratory).

DAVIS, J.C. (1986): Statistics and Data Analysis in Geology. – 2nd ed., 646 p.; New York u.a. (John Wiley & Sons).

DEUTSCHER VERBAND FÜR WASSERWIRTSCHAFT UND KULTURBAU (1992): Anwendung hydrogeochemischer Modelle. – Schriftenreihe des Deutschen Verbandes für Wasserwirtschaft und Kulturbau, **100**: 344, fig.; Hamburg, Berlin.

DFA FERTIGUNGS- UND ANLAGENBAU-GESELLSCHAFT (1993): Report on the performance of physicochemical measurements in the flooded part of the Schlema-Alberoda uranium mine. – 19 p., 3 Tab., 25 Anl; Chemnitz (Unpublished report).

DFA FERTIGUNGS- UND ANLAGENBAU-GESELLSCHAFT (1994): Zwischenbericht (Teilleistung 6.2) über die Auswahl, Installation und Inbetriebnahme von Meßsystemen zur Flutungkontrolle und Durchführung zusätzlicher Kontrollmessungen. – 10 p., 3 Tab., 28 Anl; Chemnitz (Unpublished report on order 1.3.1/8996/938/93).

DIN GERMAN INSTITUTE FOR STANDARDISATION E.V. (1991): DIN 17 224. springs: Standards. – 7th ed., 400 p.; Berlin u.a. (Beuth).

DIN GERMAN INSTITUTE FOR STANDARDISATION E.V. (1993a): DIN 18 130. subsoil, tests and test equipment: determination of the water permeability coefficient: laboratory tests. Erkundung und Untersuchung des Baugrunds: Normen, Bd 113. – 6th ed., 393 p.; Berlin u.a. (Beuth).

DIN DEUTSCHES INSTITUT FÜR NORMUNG E.V. (1993b): DIN 4188. wire sieve trays for test sieves. – : Exploration and investigation of the subsoil: standards. – 6th ed., 393 p.; Berlin u.a. (Beuth).

DIN DEUTSCHES INSTITUT FÜR NORMUNG E.V. (1994): DIN 4049. Hydrology: Part 1 (December 1992), Part 2 (April 1990), Part 3 (October 1994). – Berlin u.a. (Beuth).

DOERFFEL, K. (1965): Beurteilung von Analyseverfahren und -ergebnissen. – 2nd ed., 98 p., 25 fig.; Berlin (Springer). https://doi.org/10.1007/978-3-642-85753-9

DOUGLAS, H. & KLEINE-BROCKHOFF, T. (1991): Hot Earth from the Cold War. – Die Zeit, **7.6.1991**: 15-17, 8 fig.

DYBEK, J. (1962): Zur Geochemie und Lagerstättenkunde des Urans. – Clausthaler Hefte zur Lagerstättenkunde und Geochemie, **1**: 1-163, 24 fig., 33 tab.; Berlin.

EHRLICH, H.L. (1963): Bacterial Action on Orpiment. – Econ. Geol., **58**: 991-994, 1 fig.; Lancaster. https://doi.org/10.2113/gsecongeo.58.6.991

EHRLICH, H.L. (1964): Bacterial Oxidation of Arsenopyrite and Enargite. – Econ. Geol., **59**: 1306-1312, 3 fig., 2 tab.; Lancaster. https://doi.org/10.2113/gsecongeo.59.7.1306

ERBACHER, O. (1928): Gmelins Handbuch der anorganischen Chemie: Radium und Isotope. – 8th ed., 80 p., 4 fig.; Berlin (Verlag Chemie).

ERICKSON, P.M., KLEINMANN, R.L.P., POSLUSZNY, E.T. & LEONARD-MAYER, P.J. (1982): Hydrogeochemistry of a large mine pool. – Proceedings, 1 stInternational Mine Water Congress, Budapest, Hungary: 27-42, 7 Fig., 2 Tab.

FEIGE, K-D. (1992): Auswirkungen aus dem Uranbergbau und Umgang mit den Altlasten der Wismut in Ostdeutschland – Rede des Bundestagsabgeordneten Dr. Klaus-Dieter Feige. – Verhandlungen des Deutschen Bundestages – Stenographische Berichte, **12**: 10217-10218; Bonn.

FERNANDEZ-RUBIO, R., FERNANDEZ-LORCA, S. & ESTEBAN ARLEGUI, J. (1987): Preventive techniques for controlling acid water in underground mines by flooding. – Intern. J. Mine Water, **6**: 39-52, 11 fig.; Budapest. https://doi.org/10.1007/BF02498104

FIX, P.F. (1955): Hydrocheochemical Exploration for Uranium. – U.S. Geological Survey Professional Paper, **300**: 667-671, 4 tab.; Washington.

FÖRSTER, W. (1990): Altlasten des Erzgebirges. 3rd International KfK/TNO Congress on the Remediation of Contaminated Sites. Karlsruhe 1990 – Kluver Academic Publishers: 137-144, 1 Fig., 2 Tab.

FRANZKE, H.J., BANKWITZ, P. & BANKWITZ, E. (1992): The fracture tectonics of the Harz Mountains and its foreland according to satellite photos. – Z. geol. Wiss., **20**: 209-218; Berlin.

FRIEDRICH-EBERT-STIFTUNG (1992): Wismut und die Folgen des Uranbergbaus. – Series Wirtschaftspolitische Diskurse, **31**: 1-44; Bonn.

GAERTNER, H.-R. von (1944): Die Schichtgliederung der Phyllitgebiete in Thüringen und Nordbayern und ihre Einordnung in das stratigraphische Schema. – Jahrbuch des Reichsamts für Bodenforschung für 1941, **62**: 54-80, Taf. 3-4; Berlin.

GANS, I. (1978): Monitoring requirements for waste water from uranium mines. – Schriftenreihe Gesellschaft Deutscher Metallhütten- und Bergleute, **34**: 111-122; Clausthal-Zellerfeld.

GARGA, V.K., SMITH, H.R. & SCHARER, J.M. (1983): Abandonment of acid generating mine tailings. – Proceedings of the Panamerican Conference on Soil Mechanics and Foundation, **7**: 613-626, 5 fig., 13 refs; Sao Paulo, Brasil.

GARRELS, R.M. (1955): Some thermodynamic relations among the uranium oxides and their relation to the oxidation states of the uranium ores of the Colorado Plateaus. – Am. Min., **40**: 1004-1021, 7 Fig., 1 Tab.

GATZWEILER, R. & MAGER, D. (1993): Altlasten des Uranbergbaus. – Die Geowissenschaften, **11**: 164-172, 10 Fig., 1 Tab.; Weinheim.

GEBHART, B., JALURIA, Y., MAHAJAN, R.L. & SAMMAKIA, B. (1988): Buoyancy-Induced Flows and Transport. – 1001 p.; Berlin (Springer).

GENSER, C. (1932): Über die Entstehung und die Natur radioaktiver Quellen. – Geologische Rundschau, **23**: 188-237, 4 fig., 4 tab., 1 pl.; Berlin. https://doi.org/10.1007/BF01803460

GENSER, C. (1933): Radioaktive Heilquellen in Deutschland. – Z. dt. geol. Ges., **85**: 482-495, 3 fig., 1 pl.; Berlin.

GEOLOGICAL SOCIETY ENGINEERING GROUP WORKING PARTY (1972): The preparation of maps and plans in terms of engineering geology. – Quarterly Journal of Engineering Geology, **5**: 293-382, ill., tab.; Edinburgh. https://doi.org/10.1144/GSL.QJEG.1972.005.04.01

GEOLOGICAL SURVEY OF SWEDEN, SWEDISH UNIVERSITY OF AGRICULTURAL SCIENCES (1991): Abstracts of the 2nd International Symposium on Environmental Geochemistry. – In: SELINUS, O. – no pagination; Uppsala (Geological Survey of Sweden).

GERMANOV, A.J., BATULIN, S.G., VOLKOV, G.A., LISITSIN, A.K. & SEREBRENNIKOV, V.S. (1958): Some regularities of uranium distribution in underground water. – Proceedings II. Intern Conf Peaceful Uses Atomic Energy, **2**: 161-177.

GESELLSCHAFT DEUTSCHER CHEMIKER, FACHGRUPPE WASSERCHEMIE (1982): Deutsche Einheitsverfahren zur Wasser-, Abwasser- und Schlammuntersuchung – physikalische, chemische, biologische und bakteriologische Verfahren. – 3rd ed., loose-leaf collection; Weinheim (Verlag Chemie).

GOTTSCHALK, G. & KAISER, R.E. (1976): Einführung in die Varianzanalyse und Ringversuche: Soforthilfe für die richtige statistische Auswertung von Datengruppen. – 165 p.; Mannheim (B.I. Hochschultaschenbücher).

GOTTSCHALK, V.H. & BUEHLER, H.A. (1912): Oxidation of Sulphides. – Econ. Geol., **7**: 15-34, 3 Tab.; Lancaster. https://doi.org/10.1144/GSL.QJEG.1972.005.04.01

GRAUPNER, A. (1928/29): Das phyllitische Kerngebiet des Ostthüringer Hauptsattels. – Beiträge zur Geologie von Thüringen, **2**: 82-105, 113-144, 8 fig., 2 tab., 1 map; Erfurt.

GRISAK, G.E. & PICKENS, J.F. (1981): An analytical solution for solute transport through fractured media with matrix diffusion. – J. Hydrol., **52**: 47-57, 7 Fig., 1 Tab.; Amsterdam. https://doi.org/10.1144/GSL.QJEG.1972.005.04.01

COCKS, R. (1992): Contamination of ground and surface waters in the Ronneburg uranium mining area. – Water Air Soil: 24-26, 4 Fig., 1 Tab.

HAMANN, M. & HAMANN, S. (1990): Der Uranerzbergbau der SDAG-Wismut im Raum Schneeberg-Aue-Schlema und seine Mineralien (I) – Zur Geschichte des Bergbaus im Westerzgebirge. – Mineralien Welt, **2**: 35-42; Haltern.

HANZLIK, J. & VYDRA, J. (1985): Liquidation of abandoned mine excavations by flooding. – Proceedings, 2nd International Mine Water Congress, Granada, Spain: 953-965, 6 Fig., 2 Tab.

HARLASS, E. & SCHÜTZEL, H. (1965): Zur paragenetischen Stellung der Uranpechblende in den hydrothermalen Lagerstätten des westlichen Erzgebirges. – Z. f. angew. Geol.: 569-582, 20 fig.; Berlin.

HECHT, G. (1974): Wässer. – In: HOPPE, W. & G. SEIDEL: Geologie von Thüringen. – 1000 S. (VEB Hermann Haack).

HENNINGSEN, D. & KATZUNG, G. (1992): Einführung in die Geologie Deutschlands. – 4th ed., 228 p.; Stuttgart (Enke).

HENTSCHEL, B. & SCHEFFLER, A. (1991): Regionalführer Sachsen. – 198 p.; Berlin (Tourist Verlag).

HERBERT, H-J. (1989): Geochemical processes during the flooding of the Hope potash salt mine. Final report of the geochemistry sub-project of the Hope FE project – 62 p., 4 tab., 72 fig. in the appendix; Neuherberg (gsf report).

HÖLTING, B. (1992): Hydrogeologie: Einführung in die allgemeine und angewandte Hydrogeologie. – 4th ed., 415 p.; Stuttgart (Enke).

HOHL, R. (1985): Die Entwicklungsgeschichte der Erde. – 6th ed., 703 p.; Hanau/Main (Dausien).

HOPPE, W. & SEIDEL, G. (1974): Geologie von Thüringen. – 1000 S. (VEB Hermann Haack).

HOTH, K., LORENZ, W., HIRSCHMANN, G. & BERGER, H-J. (1979): Lithostratigraphische Gliederungsmöglichkeiten regionalmetamorphen Jungproterozoikum am Beispiel des Erzgebirges. – Z. geol. Wiss., **7**: 397-404, 2 fig.; Berlin.

HURTIG, E. & OELSNER, C. (1979): The Heat Flow Field on the Territory of the German Democratic Republic. – In: CERMÁK, V. & RYBACH, L.: Terrestrial heat flow in Europe. – 186-190, 3 fig.; Berlin u.a. (Springer). https://doi.org/10.1007/978-3-642-95357-6_18

INTERNATIONAL MINE WATER ASSOCIATION (1991): Proceedings of the 4th International Mine Water Congress. – In: UNIVERSITY OF LJUBLJANA. – 326 + 366 p.; Ljubljana (University of Ljubljana).

INTERNATIONAL MINE WATER ASSOCIATION (1994): Mine Water and the Environment. Proceedings of the 5th International Mine Water Congress. – In: UNIVERSITY OF NOTTINGHAM. – 871 p.; Nottingham (University of Nottingham).

JACKS, G. (1984): Effect of acid rain on soil and groundwater in Sweden. – In: YARON, B.: Ecological Studies: Pollutants in porous media – the unsaturated zone between soil surface and groundwater. – 296 p.; Berlin u.a. (Springer). https://doi.org/10.1007/978-3-642-69585-8_9

JACOBI, O. & EVERLING, G. (1981): Praxis der Gebirgsbeherrschung. – 2nd ed., 576 p.; Essen (Glückauf).

JÄGER, B., OBERMANN, P. & WILKE, F.L. (1990): Studie zur Eignung von Steinkohlebergwerken im rechtsrheinischen Ruhrkohlebezirk zur Untertagverbringung von Abfall- und Reststoffen. – In: STATE OFFICE FOR WATER AND WASTE NORTH RHINE-WESTPHALIA. – 628 p.; Düsseldorf (LWA Study).

JAEGER, H. (1959): Graptolithen und Stratigraphie des jüngsten Thüringer Silurs. – Abh. d. Dt. Akad. Wiss. Bln. Kl. f. Chemie etc, **2**; Berlin.

JANDEL SCIENTIFIC (1992): TableCurve for Windows 1.2 User's Manual. – D-40699 Erkrath (Jandel Scientific GmbH).

JANDEL SCIENTIFIC (1994a): SigmaPlot for Windows 2.0 User's Manual. – D-40699 Erkrath (Jandel Scientific GmbH).

JANDEL SCIENTIFIC (1994b): SigmaStat for Windows 1.0 User's Manual. – D-40699 Erkrath (Jandel Scientific GmbH).

JANISCHEWSKIJ, E.M. & KONSTANTINOW, W.M. (1962): Der Einfluß tektonischer und lithologischer Faktoren auf die Uranvererzung im Erzgebirge. – Z. f. angew. Geol., **8**: 124-128, 5 fig.; Berlin.

JENS, U. (1991): Gesetz zu dem Abkommen vom 16. Mai 1991 zwischen der Regierung der Bundesrepublik Deutschland und der Regierung der Union der Sozialistischen Sowjetrepubliken über die Beendigung der Tätigkeit der Sowjetisch-Deutschen Aktiengesellschaft Wismut – Rede des Bundestagsabgeordneten Dr. Uwe Jens. – Verhandlungen des Deutschen Bundestages – Stenographische Berichte, **12**: 4288; Bonn.

JURJOVEC, J., BLOWES, D.W. & PTACEK, C.J. (1995): Acid Neutralization in Mill Tailings and the Effect of Natrojarosite Addition. – Proceedings of Sudbury '95 – Mining and the Environment, **I**: 29-38, 5 fig., 1 tab; Sudbury, Ontarion, Canada.

JUST, G. (1980): Die Bestimmung von Thorium, Uran und Kalium in Magmatiten als Beitrag zur petrophysikalisch-petrochemischen Interpretation regionaler geophysikalischer Arbeiten. – Z. geol. Wiss., **5**: 525-536, fig., tab.; Berlin.

JUST, G. (1992): Distribution of radioactive elements and heat production in the Erzgebirge. – Geophys. Publ. Univ. Leipzig, **4**: 93-101, 6 fig., 5 tab.; Berlin.

KÄSS, W. (1991): Moderne Methoden der hydrologischen Markierungstechnik. – Water Calendar: 24-49.

KAISER, R.E. & GOTTSCHALK, G. (1976): Elementare Tests zur Beurteilung von Messdaten – Soforthilfe für statistische Tests mit wenigen Messdaten. – 1st ed., 96 p.; Mannheim (B.I. Hochschultaschenbücher).

KAISER, R.E. & MÜHLBAUER, J.A. (1983): Elementare Tests zur Beurteilung von Messdaten – Soforthilfe für statistische Tests mit wenigen Messdaten. – 2nd ed., 96 p.; Mannheim (B.I. Hochschultaschenbücher).

KARLSCH, R. (1993): "Ein Staat im Staate" – Der Uranbergbau der Wismut AG in Sachsen und Thüringen. – Aus Politik und Zeitgeschichte – Beilage zur Wochenzeitung Das Parlament, **43**: 14-23, 4 Tab.; Bonn.

KARRENBERG, H. (1981): Hydrogeologie der nichtverkarstungsfähigen Festgesteine – 284 p., 83 fig. https://doi.org/10.1007/978-3-7091-7037-3

KAUL, A. (1991): Bergbauliche Altlasten in den neuen Ländern. – Umwelt, **1991**: 529-533, 3 fig.; Bonn.

KESSERÜ, Z., KEMPF, J., DUCKSTEIN, L. & CASTI, J. (1982): A bifurcation theory model of minewater inrushes. – Proceedings, 1st International Mine Water Congress, Budapest, Hungary: 346-375, 8 Fig., 1 Tab.

KIRCHHEIMER, F. (1978): Das Uran und seine Geschichte. – 371 p.; Stuttgart (Schweizerbart).

KOCZY, F., TOMIC, E. & HECHT, F. (1957): Zur Geochemie des Urans im Ostseebecken. – Geochim. Cosmochim. Acta, **11**: 86-102; Oxford, New York, Paris, Frankfurt. https://doi.org/10.1016/0016-7037(57)90007-8

KÖLLING, M. (1988): Vom berechneten Sättigungsindex zur Reaktion im Wasser [From calculated saturation index to reaction in water]. – Z. dt. geol. Ges., **139**: 393-405, 6 fig., 2 tab.; Hannover. https://doi.org/10.1016/0016-7037(57)90007-8

KOSSMAT, F. (1927): Gliederung des varistischen Gebirgsbaues. – Abh. des Sächsischen Geologischen Landesamtes: 1-39, 2 fig., 2 pl.

KRANAWETTREISER, J. (1989): Technische Hydromechanik. Vol. 2. – In: PREISSLER, G. & BOLLRICH G. – 1st ed., 680 p.; Berlin (VEB Verlag für Bauwesen).

KRAPP, L. (1983): Determination of regional rock-mass permeabilities. – Bulletin of the international Association of Engineering Geology, **26-27**: 443-447, 3 fig. https://doi.org/10.1007/BF02594256

KRUMBIEGEL, G. & KRUMBIEGEL, B. (1981): Fossilien der Erdgeschichte. – 406 p.; Stuttgart (Enke).

KUBACH, I. & WEIGEL, F. (1977): Gmelin-Handbuch der anorganischen Chemie: Radium und Isotope. – 8th ed., 1-131 p., 1 fig.; Berlin u.a. (Springer).

KUYUMCU, H., STOLL, R. & VIEHWEG, M. (1994): Die Berücksichtigung des geologischen Umfeldes für die Bewertung der Altlasten des Erzbergbaus in Sachsen und Thüringen. – VDF Journal, **1994**: 28-31, 2 Fig., 2 Tab.; Essen.

LADWIG, K.J. (1985): Hydrologic aspects of acid mine drainage control. – Bureau of mines Information Circular, **V**: 12-18, 4 Fig., 1 Tab.

LANGE, G., MÜHLSTEDT, P., FREYHOFF, G. & SCHRÖDER, B. (1991): Uranerzbergbau in Thüringen und Sachsen – ein geologisch-bergmännischer Überblick. – Erzmetall, **44**; Weinheim.

LANGMUIR, D. (1978): Uranium Solution – mineral equilibria at low temperatures with applications to sedimentary ore deposits. – Geochim. Cosmochim. Acta, **6**: 547-569, 23 Fig., 3 Tab.; Oxford, New York, Paris, Frankfurt. https://doi.org/10.1016/0016-7037(78)90001-7

LAPAKKO, K. (1990): Solid Phase Characterisation in conjunction with Dissolution Experiments for prediction of Drainage Quality. – In: DOYLE, F. M.: Mining and Mineral Processing Wastes. – 81-86, 2 fig. (Proceedings of the Western Regional Symposium on Mining & Mineral Processing Wastes).

LAPAKKO, K.A. & N WESSELS, J. (1995): Release of Acid from Hydrothermal Quartz-Carbonate hosted Gold-Mine Tailings. – Proceedings of Sudbury '95 – Mining and the Environment, **I**: 139-148, 3 fig., 1 Tab; Sudbury, Ontarion, Canada.

LEUTWEIN, F. (1957): Alter und paragenetische Stellung der Pechblende erzgebirgischer Lagerstätten. – Geologie, **6**: 797-805, 1 fig., 2 tab.; Berlin.

LEUTWEIN, F. & WEISE, L. (1962): Hydrogeochemische Untersuchungen an erzgebirgischen Gruben- und Oberflächenwässern. – Geochim. Cosmochim. Acta, **26**: 1333-1348, 2 fig., 13 tab.; Oxford, New York, Paris, Frankfurt. https://doi.org/10.1016/0016-7037(62)90058-3

LOPATKINA, A.P. (1964): Characteristics of migration of uranium in the natural waters of humid regions and their use in the determination of the geochemical background for uranium. – Geochem. Intern., **4-6**: 465-471.

LORENZ, W. (1979): Lithostratigraphy, lithology and lithofacies of metamorphic complexes. – Z. geol. Wiss., **7**: 405-418, 3 fig., 2 tab.; Berlin.

LORENZ, W. & HOTH, K. (1990): Lithostratigraphy in the Erzgebirge – concentration, development, problems and perspectives. – Abh. d. Staatl. Mus. f. Min. a. Geol. z. Dresden, **37**: 7-35; Leipzig.

LUNDGREN, D.G. & SILVER, M. (1980): Ore leaching by bacteria. – Ann. Rev. Microbiol., **34**: 263-283. https://doi.org/10.1146/annurev.mi.34.100180.001403

MAGER, D. & VELS, B. (1993): Wismut; an example for the uranium industry in eastern Europe? – Research, Planning and Operation – Preussag AG, **18**: 126-132.

MAURIN, V. & ZÖTL, J. (1960): Untersuchung der Zusammenhänge unterirdischer Wässer mit besonderer Berücksichtigung der Karstverhältnisse. – Beiträge zur alpinen Karstforschung: 1-179; Vienna.

MAYR, A. (1953): Blütenpollen und pflanzliche Sporen als Mittel zur Untersuchung von Quellen und Karstwässern. – Anz. Österr. Akad. d. Wissensch. Math. nat. Kl.: 94-98; Vienna.

MEINEL, G. (1993): Possible relationships between uranium deposits and cratonisation using the example of Thuringia. – Geowiss. Mitt. Thüringen, **1**: 59-63, 1 Fig., 1 Tab.; Weimar.

MEYER, A-G. (1976): Statistical methods. – 138 p.; Essen (Verlag Glückauf).

MICROSOFT CORPORATION (1993a): Microsoft Excel 5.0a User's Guide. – 891 p.; D-85716 Unterschleissheim (Microsoft Corporation).

MICROSOFT CORPORATION (1993b): Microsoft Visual Basic 3.0 Programmer's Guide. – 711 p.; D-85716 Unterschleissheim (Microsoft Corporation).

MICROSOFT CORPORATION (1994): Microsoft Access 2.0 User Manual. – 900 p.; D-85716 Unterschleissheim (Microsoft Corporation).

MILITZER, H., SCHÖN, J. & STÖTZNER, U. (1986): Angewandte Geophysik im Ingenieur- und Bergbau. – 2nd ed., 419 p., 341 fig., 53 tab.; Stuttgart (Enke).

MOENKE, H. (1956): Untersuchungen zur Geochemie des Arsens am Quellwasser und Eisenoxydhydratabsätzen der Saalfelder "Feengrotten". – Chemie der Erde, **18** : 89-91, 1 Tab.; Jena.

MORIN, K.A. (1990): A case study of data quality in routine chemical analyses of acid mine drainage. – Program with Abstracts – Geological Association of Canada: 91; Waterloo, ON, Canada.

MRNA, F. & SATTRAN, V. (1980): Short review of geology and metallogeny of the Krusné hory (Erzgebirge) Mts. – Ore metal, **33**: 145-149, fig., tab.; Stuttgart.

MÜHLSTEDT, P. (1992): Der Uranbergbau in Sachsen und seine Besonderheiten in exogenen Lagerstätten. – Schriftenreihe Gesellschaft Deutscher Metallhütten- und Bergleute, **64**: 183-201, 10 fig., 5 tab.; Clausthal-Zellerfeld.

MÜLLER-SALZBURG, L. (1978): Der Felsbau. Vol. 3 – 945 p., 612 fig., 50 plates; Stuttgart (Enke). https://doi.org/10.1007/978-3-662-58198-8

MURAKAMI, Y., FUJIWARA, S., SATO, M. & OHASHI, S. (1958): Chemical prospecting of uranium deposits in Japan. – Proceedings II. Intern Conf Peaceful Uses Atomic Energy, **2**: 131-139.

NEAVILLE, C.C. (1989): Simulation of ground- and surface-water flow in the Globe area, Arizona. – Water-Resources Investigations Report, **WRI 88-4220**: 577-579, fig.; Reston, VA, United States.

NORDSTROM, D.K. (1977): Hydrogeochemical and microbiological factors affecting the heavy metal chemistry of an acid mine drainage system. – 230 p.; United States (Degree: Doctoral).

NORDSTROM, D.K. & ALPERS, C.N. (1995): Remedial Investigation, Decisions and Geochemical Consequences at Iron Mountain Mine, California. – Proceedings of Sudbury '95 – Mining and the Environment, **II**: 633-642, 2 fig., 1 tab; Sudbury, Ontarion, Canada.

NORDSTROM, D.K., BALL, J.W., DONAHOE, R.J. & WHITTEMORE, D. (1989): Groundwater chemistry and water-rock interactions at Stripa – Geochim. Cosmochim. Acta, **53**: 1727-1740, 16 fig., 2 tab.; Menlo Park, CA, United States. https://doi.org/10.1016/0016-7037(89)90294-9

NORDSTROM, D.K., OLSSON, T., CARLSSON, L. & FRITZ, P. (1989): Introduction to the hydrogeochemical investigations within the International Stripa Project. – Geochim. Cosmochim. Acta, **53**: 1717-1726, Fig., 8 Tab.; Menlo Park, CA, United States.

NORDSTROM, D.K., PLUMMER, N.L., LANGMUIR, D., BUSENBERG, E., MAY, H.M., JONES, B.F. & PARKHURST, D.L. (1990): Revised Chemical Equilibrium Data for Major Water-Mineral Reactions and their Limitations. – American Chemical Society Symposium Series – Chemical Modeling of Aqueous Systems II, **416**: 398-413, 2 Tab. https://doi.org/10.1021/bk-1990-0416.ch031

NORDSTROM, D.K., PLUMMER, L.N., WIGLEY, T.M.L., WOLERY, T.J., BALL, J.W., JENNE, E.A., BASSETT, R.L., CRERAR, D.A., FLORENCE, T.M., FRITZ, B., HOFFMAN, M., HOLDREN JR. , G.R., LAFON, G.M., MATTIGOD, S.V., MCDUFF, R.E., MOREL, F., REDDY, M.M., SPOSITO, G. & THRAILKILL, J. (1979): A Comparison of Computerized Chemical Models for Equilibrium Calculations in Aqueous Systems. – American Chemical Society Symposium Series – Chemical Modeling of Aqueous Systems: 857-892, 12 tab. https://doi.org/10.1021/bk-1979-0093.ch038

NORTON, D. & KNAPP, R. (1977): Transport phenomena in hydrothermal systems: the nature of porosity. – American Journal of Science, **277**: 913-936, 10 fig., 3 tab.

NOWY, W. (1993): Repository for low- and intermediate-level waste. – Felsbau, **11**: 67-71, 7 fig.; Essen.

OBRIKAT, D. & FUSBAN, H.U. (1993): Bestimmung von Uranisotopen in Wasser. – Bundesamt für Strahlenschutz Jahresbericht 1993, **1993**: 146-149, 2 fig., 3 tab.; Braunschweig.

OELSNER, O.W. (1951): Die Abhängigkeit der Paragenese erzgebirgischer Lagerstättenbezirke vom Intrusionsalter der zugehörigen Granite. – Freiberger Forsch.-H., **C 3**: 24-34; Freiberg.

Oelsner, O.W. (1958): Die erzgebirgischen Granite, ihre Vererzung und die Stellung der Bi-Co-Ni-Formation innerhalb der Vererzung. – Geologie, **7**: 682-697, 5 fig., 6 pictures; Berlin.

OELSNER, C. & HURTIG, E. (1979): Zur geothermischen Situation im Erzgebirge. – Freiberger Forsch.-H., **C 350**: 7-17, 5 fig.; Freiberg.

OFFICE OF WATER RESOURCES RESEARCH (1975): Acid mine water – a bibliography. – In: U.S. DEPARTMENT OF COMMERCE. – 563 S. (National Technical Information Service).

OLEM, H. (1991): Minerals and mine drainage. – Research Journal WPCF, **63**: 472-475.

PAČES, T. (1969): Chemical equilibria and zoning of subsurface water from Jáchymov ore deposit, Czechoslovakia. – Geochim. Cosmochim. Acta, **33**: 591-609, 6 Fig., 6 Tab.; Oxford, New York, Paris, Frankfurt. https://doi.org/10.1016/0016-7037(69)90017-9

PÄLCHEN, W., RANK, G., LANGE, H. & TISCHENDORF, G. (1987): Regionale Clarkewerte – Möglichkeiten und Grenzen ihrer Anwendung am Beispiel des Erzgebirges (DDR). – Chemie der Erde, **47**: 1-17, 3 fig.; Jena.

PAUL, R. (1991): Das Wismut-Erbe – Geschichte und Folgen des Uranbergbaus in Thüringen und Sachsen. – 191 p.; Göttingen (Die Werkstatt).

PFEUFER, J. (1991): Maßnahmen zum Schutz des Trinkwassers im Nebengestein bei der Stillegung des Eisenberges Leonie in Auerbach (Opf.). – Erzmetall, **44**: 30-38, 9 fig.; Weinheim.

PFINGSTEN, W. & MULL, R. (1990): Transport processes in fractured aquifers. – DGM, **34**: 116-123, 9 fig., 1 tab.

PHILIPSBORN, H. von (1967): Tafeln zum Bestimmen der Minerale nach äußeren Kennzeichen. – 2nd ed., 319 p., 289 fig.; Stuttgart (Schweizerbart).

PIETZSCH, K. (1951): Abriß der Geologie von Sachsen. – 1st ed., 160 p., 30 fig., 24 plates; Berlin (Volk und Wissen Volkseigener Verlag).

PIETZSCH, K. (1962): Geologie von Sachsen (Bezirke Dresden, Karl-Marx-Stadt und Leipzig). – 870 p., 300 fig., 1 tab.; Berlin (VEB Deutscher Verlag der Wissenschaften).

RACKLEY, R.I. (1976): Origin of Western-States Type Uranium Mineralization. – In: WOLF, K. H.: Handbook of strata-bound and stratiform ore deposits. – 89-156, 22 fig.; Amsterdam (Elsevier). https://doi.org/10.1016/B978-0-444-41407-6.50006-4

RÖHNSCH, W. & ETTENHUBER, E. (1993): Radiologische Erstbewertung bergbaulicher Altlasten in den neuen Bundesländern. – Bundesamt für Strahlenschutz Jahresbericht 1993, **1993**: 141-141, 1 Fig.; Braunschweig.

ROGOŻ, M. & POSYLEK, E. (1982): Prediction of water inflow to mines using modified trend methods. – Proceedings, 1 stInternational Mine Water Congress, Budapest, Hungary: 258-276, 4 fig.; Budapest.

ROGOŻ, M. (1994): Computer Simulation of the Process of Flooding up a Group of Mines. – Proceedings, 5th International Mine Water Congress, Nottingham, U.K., **1**: 369-377, 3 fig., 1 tab.; Nottingham.

ROSCHLAU, H. (1994): Bohr- und Sprengarbeiten im Uranerzbergbau der AG/SDAG Wismut. – Erzmetall, **47**: 411-416, 480-488, 627-631, 28 fig., 4 tab.; Weinheim.

ROSIN, N. (1994): Minerva – Editorial Note. – Mining Environmental Management, **2**: 3.

RUBIN, H. (1981): Thermal convection in a nonhomogeneous aquifer. – Journal of Hydrology, **50**: 317-331, 7 fig.; Amsterdam.

RUNGE, W. & BÖTTCHER, J. (1994): Stillegung und Sanierung des ostdeutschen Uranerzbergbaus. – Atomwirtschaft Atomtechnik, **39**: 194-190, 4 Fig., 4 Tab.

RUNNELLS, D.D. & LINDBERG, R.D. (1981): Hydrochemical Exploration for Uranium Ore Deposits: Use of the Computer Model WATEQFC. – Journal of Geochemical Exploration, **15**: 37-50, 11 fig., 3 tab.; Amsterdam. https://doi.org/10.1016/0375-6742(81)90054-6

SÄNGER, H. (1993): Die Flora und Vegetation im Uranbergbergviervier Ronneburg – Pflanzensoziologische Untersuchungen an Extremstandorten. – Ökologie und Umweltsicherung, **A76**: 227, fig., tab.; Kassel.

SAKER, I. & JORDAN, H. (1977): Zu hydrogeologischen Eigenschaften der Verwitterungszonen erzgebirgischer Gneise. – Z. f. angew. Geol., **23**: 606-611, 5 fig.; Berlin.

SAKER, I. & JORDAN, H. (1979): On hydrogeological properties of the weathering zones of porphyries and sandstones. – Z. f. angew. Geol., **25**: 588-597, 8 fig., 3 tab.; Berlin.

SCHADE, M. (1982): On the thermodynamic analysis of the geochemical behaviour of uranium in the hypergenesis zone. – Z. f. angew. Geol., **28**: 524-530, 5 fig., 1 tab.; Berlin.

SCHIFFNER, C. (1908): Radioaktive Wässer in Sachsen. – 1-57, 16 fig., 15 tab.; Freiberg (Craz & Gerlach).

SCHIFFNER, C. & WEIDIG, M. (1909): Radioaktive Wässer in Sachsen. – 59-144, 35 Fig., 36 Tab.; Freiberg (Craz & Gerlach).

SCHIFFNER, C., WEIDIG, M. & FRIEDRICH, R. (1911): Radioaktive Wässer in Sachsen. – 145-216, 51 Fig., 52 Tab.; Freiberg (Craz & Gerlach).

SCHRÖDER, B. & LIPP, U. (1990a): Der Uranerzbergbau der SDAG-Wismut im Raum Schneeberg-Aue-Schlema und seine Mineralien (I) – Zur Geologie und Mineralogie der Lagerstätte Schlema-Alberoda. – Mineralien Welt, **2**: 42-47; Haltern.

SCHRÖDER, B. & LIPP, U. (1990b): The uranium ore mining of SDAG-Wismut in the Schneeberg-Aue-Schlema area and its minerals (II). – Mineralien Welt, **3**: 21-44; Haltern.

SHCHUROV, V.P. & TIMOFEYEV, E.V. (1966): The structural ore control in hydrothermal ore deposits. – Z. f. angew. Geol., **12**: 185-188, 3 fig.; Berlin.

SCHÜTTMANN, W. (1992): German uranium for Russian bombs. – Frankfurter Allgemeine Zeitung, **22.4.92**.

SCHULZ, H.D. & KÖLLING, M. (1992): Grundlagen und Anwendungsmöglichkeiten hydrochemischer Modellprogramme. – Schriftenreihe des Deutschen Verbandes für Wasserwirtschaft und Kulturbau, **100**: 1-96, 7 fig., tab.; Hamburg.

SCHUPPAN, W., BÜDER, W. & LANGE, G. (1994): On Uranium mineralization in the vein deposits of the Western Erzgebirge, Germany. – Monograph Series on Mineral Deposits, **31**: 191-207, 8 fig., 2 tab.

SDAG WISMUT: see also WISMUT GMBH.

SDAG WISMUT (1984): Roadways with steel arch support – ABB No. 7112/01. – In: Bergbaubetrieb AUE: Technologie Streckenvortrieb Werkstandard. – 55-60, 3 fig., 5 tab.; Chemnitz (self-published by SDAG Wismut).

SDAG WISMUT (1991): Untersuchungen zur Bewertung und Begutachtung der Flutung des Lagerstättenteiles bis zur Sohle -990. – no pagination; Chemnitz (internal project outline).

SDAG WISMUT, CLAUSTHAL TECHNICAL UNIVERSITY (1991): Cooperation agreement between SDAG Wismut and Clausthal Technical University. – 6 p.; Chemnitz.

SEIM, R. (1990): Geochemistry of Sediments. – In: SEIM, R. & G. TISCHENDORF: Grundlagen der Geochemie. – 632 p.; Leipzig (Dt. Verl. für Grundstoffindustrie).

SEIM, R. & TISCHENDORF, G. (1990): Grundlagen der Geochemie. – 632 p., 1 supplement; Leipzig (Dt. Verl. für Grundstoffindustrie).

SHUKOLYUKOV, Y.A., MESHIK, A.P. & BASAROVICH, C.S-S. (1990): Xe-Xe_{SN} age of uranium veins in Erzgebirge deposit, Germany. – Abstracts Geological Society of Australia, **27**: 92; Sydney.

SHUKOLYUKOV, Y.A., MESHIK, A.P., KRYLOV, D.P. & PRAVDIVTSEVA, O.V. (1994): Current Status of Xe-Xe_{SN} Dating. – Noble Gas Geochemistry and Cosmochemistry: 125-146, 18 Fig., 1 Tab.

SHUKOLYUKOV, Y.A., SOKOLOVA, N.T., MESHIK, A.P., BASAROVICH, C.S-S. & BARSUKOV, V.L. (1992): The age of pitchblende in the quartz-calcite-uraninite veins of the Schlema-Alberoda deposit (Erzgebirge, Germany). – News of the Russian Academy of Sciences – Geological Series, **1**: 78-91 (in Russian), 8 fig., 3 tab.; Moscow.

SIGG, L. & STUMM, W. (1994): Aquatische Chemie – eine Einführung in die Chemie wässriger Lösungen und natürlicher Gewässer. – 3rd ed., 498 p.; Zurich (Verl. der Fachvereine).

SINGH, R.N., DENBY, B. & REED, S.M. (1985): The Effect of Groundwater re-establishment on the Settlement of Opencast Mine Backfills in the United Kingdom. – Proceedings, 2nd International Mine Water Congress, Granada, Spain: 803-816, 8 fig.; Grananda/Spain.

SITZ, P., HÄFNER, F. & LANGE, W. (1982): Possibilities of inflow control in potash mining and notes on the preservation of underground mine workings. – Z. geol. Wiss., **10**: 141-151, 4 fig.; Berlin.

SOKOLOVA, N.T. & ACHEYEV, B.N. (1972): Causes of localization of uranium mineralization in contact-metamorphism aureoles of granitoids. – Geochemistry International, **9**: 1067-1077, 3 fig., 3 tab.

SPERLING, B. & MERKEL, B. (1992): Modellierung geogener Grundwasserbeschaffenheit am Beispiel des fränkischen Keupers. – Schriftenreihe des Deutschen Verbandes für Wasserwirtschaft und Kulturbau, **100**: 201-320, fig.; Hamburg, Berlin.

STAMM, P. von (1993): Hot Earth from the Cold War. – Kosmos, **89**: 52-59, 9 ill.; Stuttgart.

STANGE, K. (1970): Angewandte Statistik – Eindimensionale Probleme. – 592 p., 227 fig.; Berlin (Springer). https://doi.org/10.1007/978-3-642-85602-0

STEMPROK, M. (1992): Geochemical development of the Krusné hory/Erzgebirge granite pluton exemplified on its Czechoslovak part. – Geophys. Publ. Univ. Leipzig, **IV**: 51-63, 10 fig.; Berlin.

STOBER, I. (1995): Die Wasserführung des kristallinen Grundgebirges. – 191 p., 81 fig., 16 tab.; Stuttgart (Enke).

STOLL, R. & BAUER, D. (1991): Anwendung geophysikalischer Verfahren zur Kontrolle und Überwachung technologischer Teilprozesse im untertägigen Erzbergbau. – Neue Bergbautechnik, **21**: 427-431, 11 Fig., 1 Tab.

STRASBURGER, E., NOLL, F., SCHENK, H., SCHIMPER, A.F.W., SITTE, P., ZIEGLER, H., EHRENDORFER, F. & BRESINSKY, A. (1991): Lehrbuch der Botanik für Hochschulen. – 33rd ed., 1030 p., 1023 fig., 50 tab.; Stuttgart Jena New York (Gustav Fischer Verlag).

STRÜBEL, G. & ZIMMER, S.H. (1982): Lexikon der Mineralogie. – 363 p., 159 fig.; Stuttgart (Dt. Taschenbuch Verl.).

STRUNZ, H. (1982): Mineralogische Tabellen. – 8th ed., 621 p.; Leipzig (Akademische Verlagsanstalt).

STUMM, W. & MORGAN, J.I. (1981): Aquatic chemistry – An introduction emphasizing chemical equilibria in natural waters. – 2nd ed., 780 p.; New York (Wiley & Sons).

THALHEIM, K. & FIEDLER, H.J. (1990a): Granulometric and mineralogical composition of base sediments of the Pleistocene overburden on metamorphic and igneous bedrock in the Osterzgebirge. – Abh. d. Staatl. Mus. f. Min. a. Geol. z. Dresden, **37**: 143-154, 4 fig., 4 tab.; Leipzig.

THALHEIM, K. & FIEDLER, H.J. (1990b): Granulometric and mineralogical composition of middle sediments of the Pleistocene overburden on metamorphic and magmatic bedrock in the Osterzgebirge. – Abh. d. Staatl. Mus. f. Min. a. Geol. z. Dresden, **37**: 155-168, 3 fig., 3 tab.; Leipzig.

TISCHENDORF, G. (1986): Variscan Ensialic Magmatism and Metallogenesis in the Ore Mountains – Modeling of the Process. – Chemie der Erde, **45**: 75-104, 7 fig., 6 tab.; Jena.

TISCHENDORF, G. & UNGETHÜM, H. (1965): Zur Anwendung von Eh-pH-Beziehungen in der geologischen Praxis. – Z. f. angew. Geol., **11**: 57-67, 9 fig.; Berlin.

TISCHENDORF, G. & UNGETHÜM, H. (1968): Einige Überlegungen zur Frage der Bildungsbedingungen erzgebirgischer Mineralparagenesen. – Freiberger Forsch.-H., **C 230**: 127-137, 4 Fig., 1 Tab.

TOLER, L.G. (1982): Some Chemical Characteristics of Mine Drainage in Illinois – U.S. Geological Survey Water-Supply Paper, **2078**: 1-47, 10 fig., 5 tab.; Washington.

UERPMANN, E-P. (1980): Hydrogeologische Fragen bei der Endlagerung radioaktiver Abfälle. – 128 p., 21 fig., 5 tab.; Clausthal (dissertation TU Clausthal).

UNIVERSITY OF MINING AND METALLURGY IN KRAKÓW (1994): Abstracts of the 3rd International Symposium on Environmental Geochemistry. – In: RYBICKA, H. & W. S. SIKORA. – 473 p.; Kraków (University of Mining and Metallurgy).

VESELIČ, M. & TREBUŠAK, I. (in press): Bibliography of the International Mine Water Association. – (International Mine Water Association). – This bibliography never appeared in print, but can alternatively be found at https://www.IMWA.info/content/list-of-journals.html

VOGEL, G. & ANGERMANN, H. (1984): dtv-Atlas zur Biologie. – 223 p., 111 fig., tab.; Stuttgart (Dt. Taschenbuch Verl.).

VOIGT, H-J. (1990): Hydrogeochemie – Eine Einführung in die Beschaffenheitsentwicklung des Grundwassers. – 310 p.; Berlin u.a. (Springer).

WAGENBRETH, O. (1990): Bergbau im Erzgebirge. – 504 p.; Leipzig (Dt. Verl. für Grundstoffindustrie).

WALTER, R., GIESE, P., WALTHER, H.W. & DILL, H.G. (1992): Geologie von Mitteleuropa. – 5th ed., 561 p.; Stuttgart (Schweizerbart).

WEIDIG, M. (1912): Radioaktive Wässer in Sachsen. – 217-359 p., 73 fig., 81 tab.; Freiberg (Craz & Gerlach).

WEIGEL, F. (1977): Gmelin-Handbuch der anorganischen Chemie: Radium und Isotope. – 8th ed., 132-435 p.; Berlin u.a. (Springer).

WENRICH-VERBEEK, K.J. (1977): Uranium and coexisting element behaviour in surface Waters and associated Sediments with varied sampling Techniques used for Uranium Exploration. – J of Geochemical Exploration, **8**: 337-355, 6 Fig., 6 Tab.; Amsterdam. https://doi.org/10.1016/ 0375-6742(77)90060-7

WERNER, A.G. (1791): Neue Theorie von der Entstehung der Gänge mit Anwendung auf den Bergbau besonders den freybergischen – *Nouva theoria de origine venarum officiis et operibus metallifossorum in primis Freibergensium accomodata*. – Freiberg.

WIRTH ZUR OSTEN, U. (1992): Einfluß der Lagerstättenverhältnisse und der Petrographie auf die Anlage der horizontalen und vertikalen Auffahrungen von Kalisalzbergwerken in Sachsen-Anhalt. – 69 p., 25 fig.; TU Clausthal (diploma thesis).

WISMUT GMBH: see also SDAG WISMUT.

WISMUT GMBH (1993a): Der Sanierungsbetrieb Aue gestern und heute. – Dialog – Werkzeitschrift der Wismut GmbH: 16-21, 9 fig.

WISMUT GMBH (1993b): Assessment of the changes in chemical-physical parameters in the rebounding mine water in the II. quarter 1993. – 21 p., 5 fig., 4 tab.; Chemnitz (internal report).

WISMUT GMBH (1994a): Ergebnisse der Umweltüberwachung und Sanierungstätigkeit 1993 – Sanierungsbetrieb Aue. – 68 p.; Chemnitz (Wismut GmbH).

WISMUT GMBH (without, 1994b): Ronneburg, Seelingstädt – Schwerpunkte der Sanierung in der Ostthüringer Wismut-Region. – Wismut GmbH Chemnitz, Public Relations Department: 1-16; Chemnitz.

WOLERY, T.J. (1992): EQ3NR, A Computer Program for Geochemical Aqueous Speciation-Solubility Calculations: Theoretical Manual, User's Guide, and Related Documentation (Version 7.0). – 246 p., 7 fig.; Livermore (Lawrence Livermore National Laboratory). https://doi.org/10.2172/138643

WOLERY, T.J., JACKSON, K.J., BOURCIER, W.L., BRUTON, C.J., VIANI, B.E., KNAUSS, K.G. & DELANY, J.M. (1990): Current Status of the EQ3/6 Software Package for Geochemical Modeling. – American Chemical Society Symposium Series – Chemical Modeling of Aqueous Systems II, **416**: 104-116, 2 fig.; Washington. https://doi.org/10.1021/bk-1990-0416.ch008

WOLF, L. (1991): Die Niederterassen der Zwickauer Mulde, der Chemnitz und der Zschopau. – Z. geol. Wiss., **19**: 347-363, 5 fig.; Berlin.

WOLF, R. (1995): Der Wiederanstiegsprozess des Grubenwassers bei der Flutungen von Bergwerken. – 37 p., 22 fig.; TU Clausthal (student research project).

WOLKERSDORFER, Ch. (1992): Remediation of the Wismut uranium mines. – Water, Air and Soil, **6**: 28-29, 1 fig.

WOLKERSDORFER, Ch. (1993): 1st report on the cooperation agreement between WISMUT GmbH and the Department of Engineering Geology. – 59 p., 29 fig., 16 tab.; Clausthal (Unpublished report).

WOLKERSDORFER, Ch. (1994): Changes in mine water hydrology during the flooding of an abandoned uranium mine in the Erzgebirge/Saxonia/Germany. – Abstracts of the 3rd International Symposium on Environmental Geochemistry, Kraków: 447-448, 1 fig., 1 tab.

WOLKERSDORFER, Ch. (1995): 2nd Report on the Cooperation Agreement between WISMUT GmbH and the Department of Engineering Geology. – 107 p., 45 fig., 16 tab.; Clausthal (Unpublished report).

YAMANE, T. (1976): Statistik – Ein einführendes Lehrbuch. – 858 p., 15 tables; Frankfurt/M. (Fischer).

ZENTRALES GEOLOGISCHES INSTITUT (1968): Grundriß der Geologie der Deutschen Demokratischen Republik. – 623 p.; Berlin (Akademie Verlag).

ZENTRALINSTITUT FÜR PHYSIK DER ERDE (1989): Silicic Magmatism and Metallogenesis of the Erzgebirge. – Veröffentlichungen des Zentralinstituts für Physik der Erde, **107**: 1-316; Berlin.

ZETZSCHE, C. (1994): Determination of regional Clarke values for the lithosphere and the hydrosphere in the Schlema-Alberoda area. – without pagination; Freiberg (Unpublished final report on contract 1/39-2/00151/93).

11 Directories

11.1 List of abbreviations

≪ much smaller than
≫ much bigger than
{X}Chemical activity of the substance X
a, *b axes*
(aq) solute (in reaction equations)
Aspecific heat production
AAplite
AASAtomic Absorption Spectroscopy
ADPAdenosine diphosphate
AGStock corporation
$_g$ Total area of the track walls
$_k$ AFace of the loosening zone
ANOVAVariance Analysis (Analyses of Variance)
APP acid production potential
ARAbdamp residue
AStreet $_s$ cross-section
ATPAdenosine triphosphate
Affective$_w$ area of the line walls
AWÜAbwetterüberhauen
B.K. Drilling chamber
BqBecquerel
bräunli. Brownish
cconcentration
C&EConsulting & Engineering
CFDComputational Fluid Dynamics
COVcovariance
cspecific$_p$ heat capacity
COD chemical oxygen demand
dAir gap , plate spacing
DDR German Democratic Republic
DEVDeutsche Einheitsverfahren
DFADeutsche Fertigungs- und Anlagenbau GmbH
dtotal$_g$ flow length
d $_h$ horizontal flow path
DINGerman Institute for Standardisation e.V.
dsdark slates
ds/kdark limestone-bearing slates
dseDolomite Selenide Formation
dvertical$_v$ flow path
dThickness$_w$ of the diffusion area
ebedle brown spar formation
ebaIron baryte formation
EhEh value
ENEuronorm
ENEOst-North-East
ESEEast-South-East
et al. and co-workers
pale fruit slates
FFace
F-StrField section
fbafluorbarytic lead ore formation
flgFluorite quartz formation
FlWÜFlughwayoverhauled
FRFilter residue
fshell fruit slate
fs/kslFruit slate with pebble slate layers
gGravitational constant
light mica slates
GGranite
(g) gaseous substance (in reaction equations)
g(1-, *n-1*) probability
Gfree^o enthalpy
GBqGigabecquerel
Ges. Die
GHGtotal hardness
Limited liability company
gshelle Glimmerfelse
hHeight
H_o, *HNull*$_1$ *hypothesis* , counter hypothesis
h_1, *hWater level*$_2$
hmbaHematite baryte formation
iGeneral counter
IAAIndustrial settling plant
ISOInternational Standardizing Organization
kLime
KbBiotitkersanit
kbGravelly Blendy Formation
Kb/KhLamprophyre
kPermeability$_f$ *coefficient*
KhChlorite kersanite
KHcarbonate hardness
kkuComb quartz-calcite-uranite formation
Solubility $_L$ product
CPSU Communist Party of the “Soviet Union
krsbCarbonates-Antimonides-Formation
krsfcarbonate sulphide formation
ksAlaunschiefer
ks/kCarboniferous limes (ochre lime)
ks/lAlum and siliceous slate
l_a Depth of the loosening zone
l_s Total length of the driveways
lThickness$_v$ *of* the weathering bark
Lf, electrical conductivity
Lit. literature
LogInCompany LogIn GmbH, Gommern
LPGLand Agricultural Production Cooperative
LUTLaboratory for Environmental Technology, Jena
LydiALycopodium task probe
mMeasuring station of the Wismut
Mmolar mass
max. max.
medmedian
M_g Effective total mass
mguMagnesium carbonate pitchblende formation
minMinimum
MioMillions
MSD relative standard deviation (mean standard deviation)
MSSMarkus-Semmler-Stollen
mNNmeter Normal Zero
nSample number
NNorth
N’ north
n.b. not determined
n.n. not detectable
NENorth-East
Net NPNetto Neutralisation potential
NKHNoncarbonate hardness
NNENorth-North-East
NNWN North North West
NPNeutralisation potential
NWNorth-West
NW’ northwest
nQuantity$_x$ *of substance*
OFMOberflussmeisterei
OICOlder Intrusive Complex
pDifference distance (DUNN test)
pPrint
PW probability
pd coarse-grained metadiabase
pers. comm. personal communication
pHpH value
Polymetallic. Polymetallic formation
PVAPolyvinyl alcohol
PVC polyvinyl chloride
qheat flux density
QTest size (DUNN Test)
QWater volume per time
Q() deposit-specific limit index
$Q_{1,2}$, $_3$, heating $_4$ rate
q_1, *qIdentifier*$_2$ log-As-Ca-U

qasQuartz arsenide formation
qhmquartz-hematite formation
qks/wquartz-cassiterite/tungsten formation
qsMain quartzite
qsfQuartz Fluorite Formation
Crosscut
R electrical resistance
r-test NALIMOV TEST (outlier test)
rCorrelation² coefficient
RadAkRadioactivity
Rstatistical$_k$ rank
rPearson$_P$ correlation coefficient
rRadius$_s$ of the ramps
sStandard deviation (sample)
shelle phyllite (muscovite-biotite schist)
(s) solid (in reaction equations)
Sstatistical security
SSouth
SAGSoviet Joint Stock Company
SaSiWaCollecting point for seepage water
SDAGSoviet German Joint Stock Company
SESouth-East
SE ‘ southeast
SEDSocialist Unity Party of Germany
SISaturation index
SISystème International d’Unités, International System of Units
skHornfels , Skarnoide
SKW stationScrew-type cold water station
sshell phyllite
ss/fsPhyllite , light fruit schists
ss/kscarbonaceous dark phyllite
SSESouth-South-East
SSWSouth-South-West
StSaturation level
SWSouth-West
t time
TTemperature
tdbanded metadiabase
TOCTotal Organic Carbon
TU, TUCTechnical University of Clausthal
Type GMine water
Type IIntermediate waters
Type SSickerwaters
uilateral$_{(n),\ 1-\alpha}$ probability for $\sqrt{n,1-\alpha}$
u.N. below the detection limit
udfine-grained , homogeneous metadiabase
ud/tdfine-grained and banded metabiabase
USSRUnion of Soviet Socialist Republics
uqkUran quartz calcite formation
V_{ent} annual water withdrawal
VTotal$_{ges}$ *volume of* routes
VTotal$_{rei}$ volume to be cleaned
vMinimum$_s$ flow velocity
vSpeed$_x$
wHeating speed
WismutSDAG Wismut, Wismut AG, Wismut GmbH
WNWWest-North-West
WQuWeather crosscut
WSWWest-South-West
$\overline{x}$ Mean value
xThreshold$_{(n),\ 1-\alpha}$ *value*
x_i, *xvalue*$_n$
yThickness of the intermediate layer
YICYounger Intrusive Complex
Zstatistical test variable

critical value (statistics)
ϑ Temperature in °C
Cliff number
Variance (population)
Degree of freedom
Density
Standard deviation (population)
ϕ_D diffusive porosity
$\phi_{g,B}$ Pit cavity of the blind sections
$\phi_{g,D}$ Diffusive pit cavity
$\phi_{g,K}$ Effective pit cavity
$\phi_{g,R}$ residual cavity
$\phi_{g,Sch}$ Pit cavity of the shafts
$\phi_{g,St}$ Pit cavity of the roadways
$\phi_{g,Su}$ Pit cavity of the shaft sumps
$\phi_{g,T}$ total cavity
$\phi_{g,Ü}$ Pit cavity of the overhauen
ϕ_{hD} Diffusive rock cavity
ϕ_{hK} Effective rock cavity
ϕ_{hT} total rock cavity
ϕ_K Effective or kinematic porosity
ϕ_R residual porosity
ϕ_T Total porosity

11.2 List of figures

11.3 List of tables

12 Curriculum vitae

Curriculum Vitae

Birthday	: 17 February 1964
Place of birth	: Schwabach/Mfr., Germany
Nationality	: German
Parents	: Horst Wolkersdorfer, master radio and television mechanic Roswitha Wolkersdorfer née Steiner, Managing Director
Marital status	: Married to Ulrike née Biller since 30.6.1990

Training

1970 – 1974	: Wendelstein Primary School
1974 – 1975	: Wendelstein Secondary School
1975 – 1984	: Gymnasium Roth (mathematics and science branch)
^{10}1984 – ^{9}1986	: Friedrich-Alexander University Erlangen-Nuremberg, geology studies
^{10}1986 – ^{4}1989	: Clausthal University of Technology, geology studies
1989	: Diploma thesis on lead-zinc deposits of the Northern Limestone Alps

German Armed Forces

^{1}1990 – ^{3}1990	: Basic training air force, Roth/Mfr.
^{3}1990 – ^{4}1990	: Cologne Air Force Command
^{4}1990 – ^{12}1990	: Geological Service, Air Force Support Command Karlsruhe

Employment relationships

1989	: Computer operator, Quelle, Fürth
1991 – 1995	: Research assistant to Univ.-Prof. G. Reik, Ph.D., Clausthal University of Technology (Department of Engineering Geology)

Scholarship

1988	: Tyrolean Provincial Government Innsbruck
1991 – 1993	: Hanns Seidel Foundation Munich

13 Table and figure appendix

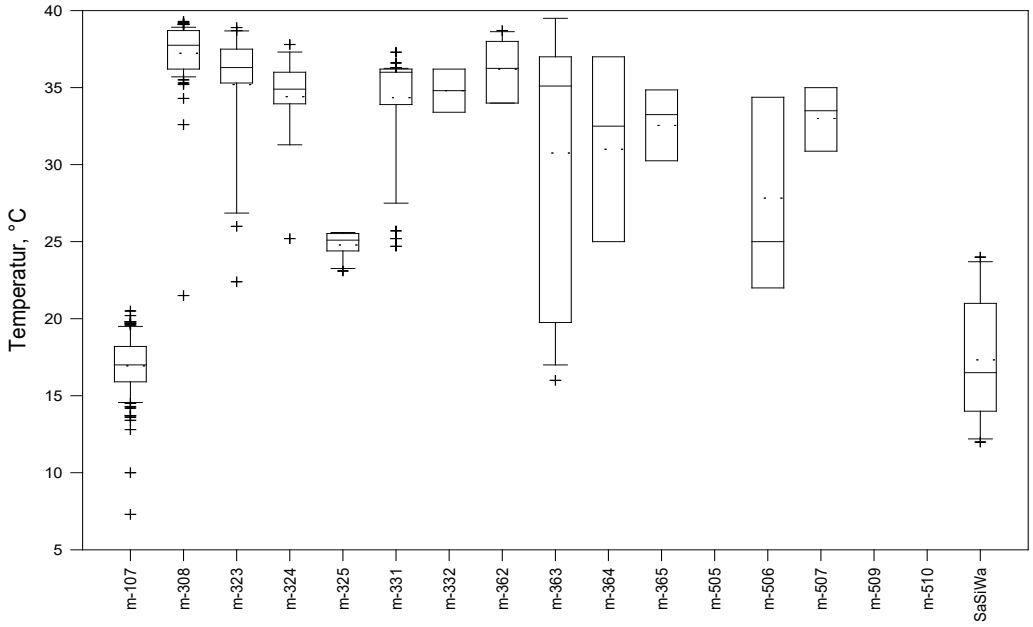

Fig. 97: Boxplot of the measured temperature values. SaSiWa: Collection point for seepage water (m-315, m-316, m-318, m-320, m-501, m-503, m-504, w-68 and w-92).

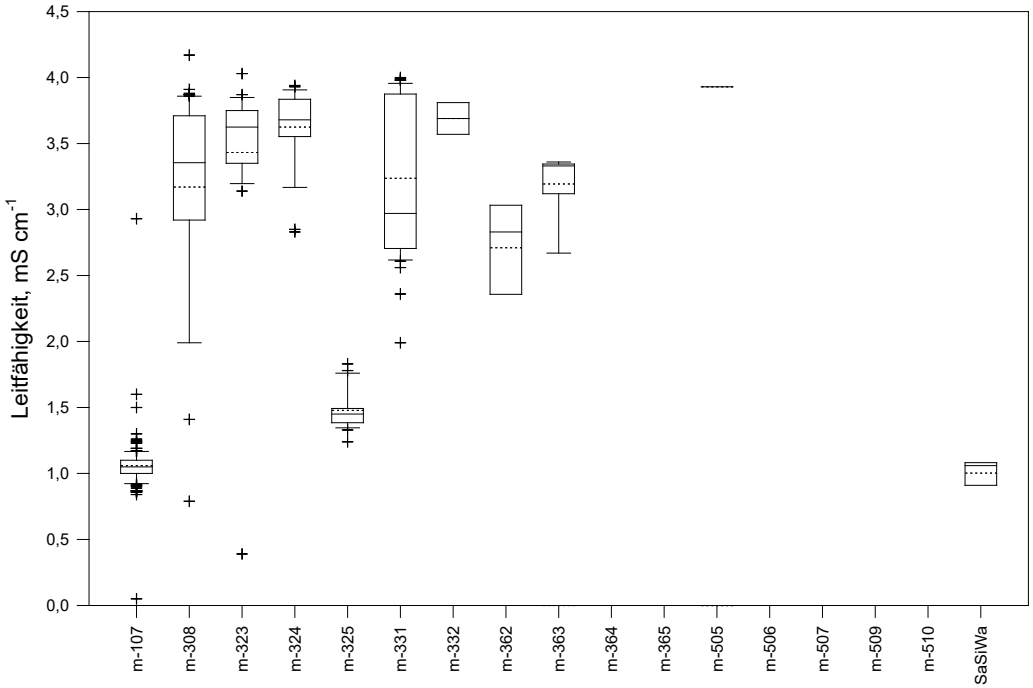

Fig. 98: Boxplot of electrical conductivity measurements. SaSiWa: Collection point for seepage water (m-315, m-316, m-318, m-320, m-501, m-503, m-504, w-68 and w-92).

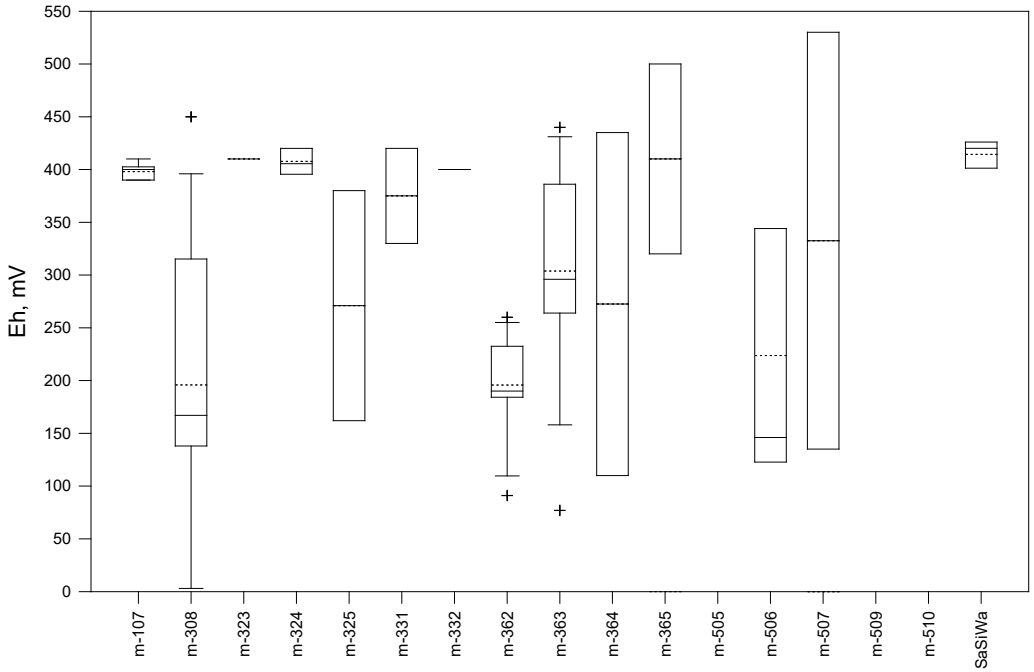

Fig. 99: Boxplot of the measured values of the redox potential. SaSiWa: Collection point for seepage water (m-315, m-316, m-318, m-320, m-501, m-503, m-504, w-68 and w-92).

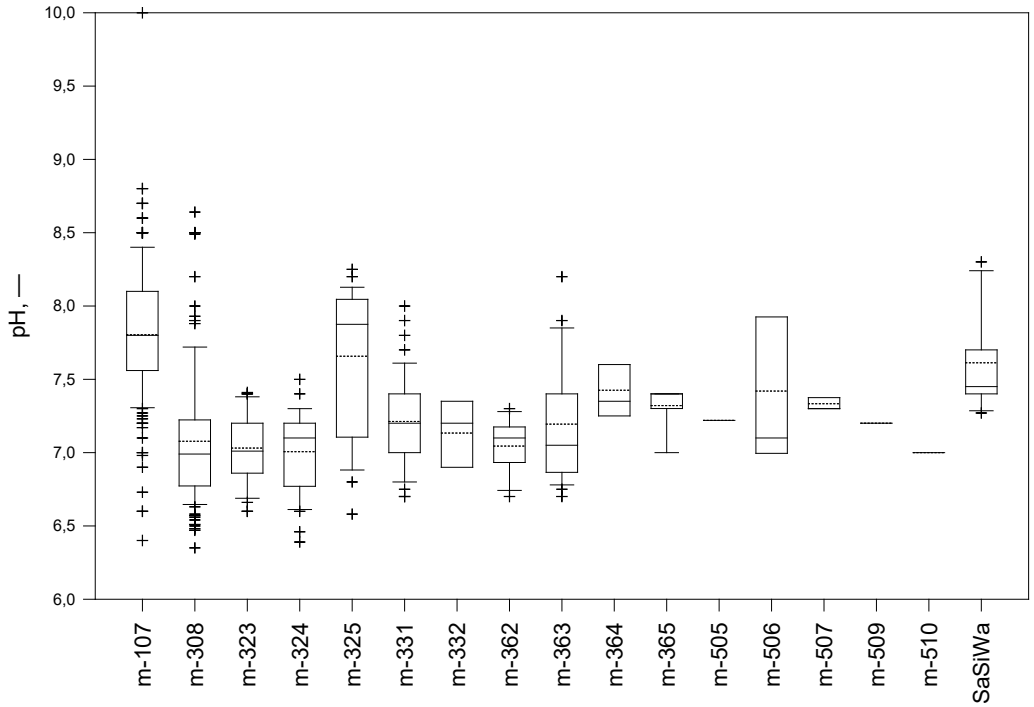

Fig. 100: Boxplot of the measured pH values. SaSiWa: Collection point for leachates (m-315, m-316, m-318, m-320, m-501, m-503, m-504, w-68 and w-92).

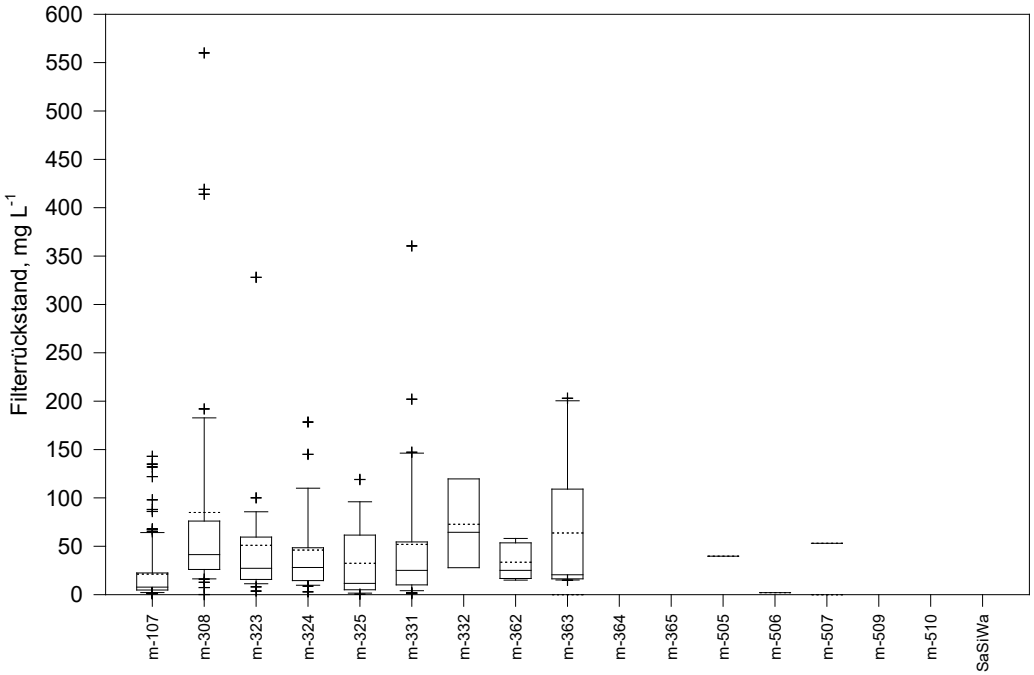

Fig. 101: Boxplot of the mass of the filter residue. SaSiWa: Collection point leachates (m-315, m-316, m-318, m-320, m-501, m-503, m-504, w-68 and w-92).

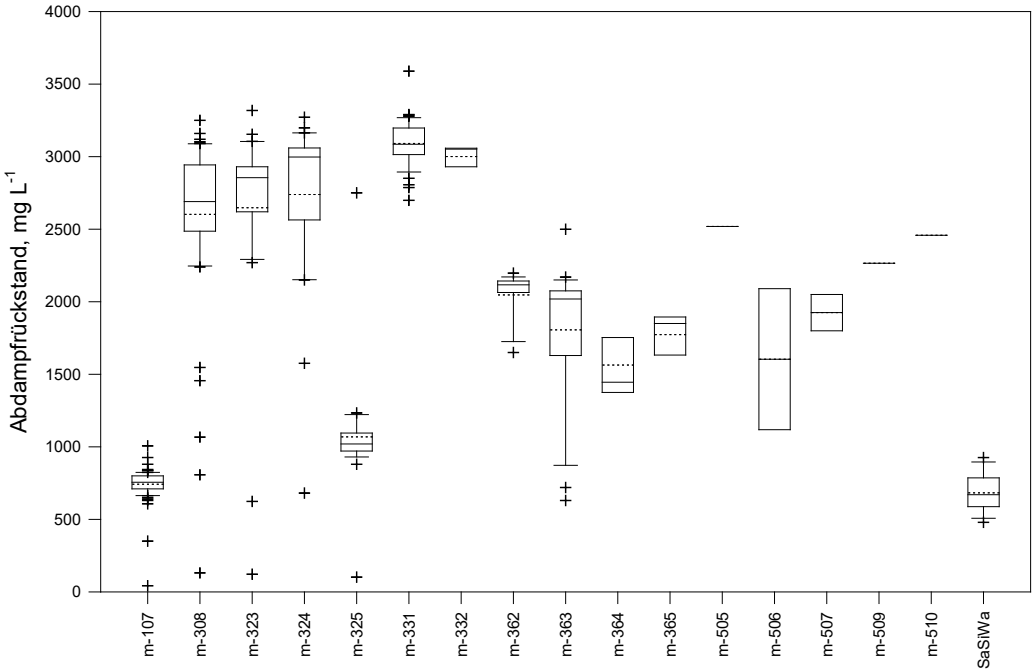

Fig. 102: Boxplot of the mass of the evaporation residue. SaSiWa: Collective measuring point leachates (m-315, m-316, m-318, m-320, m-501, m-503, m-504, w-68 and w-92).

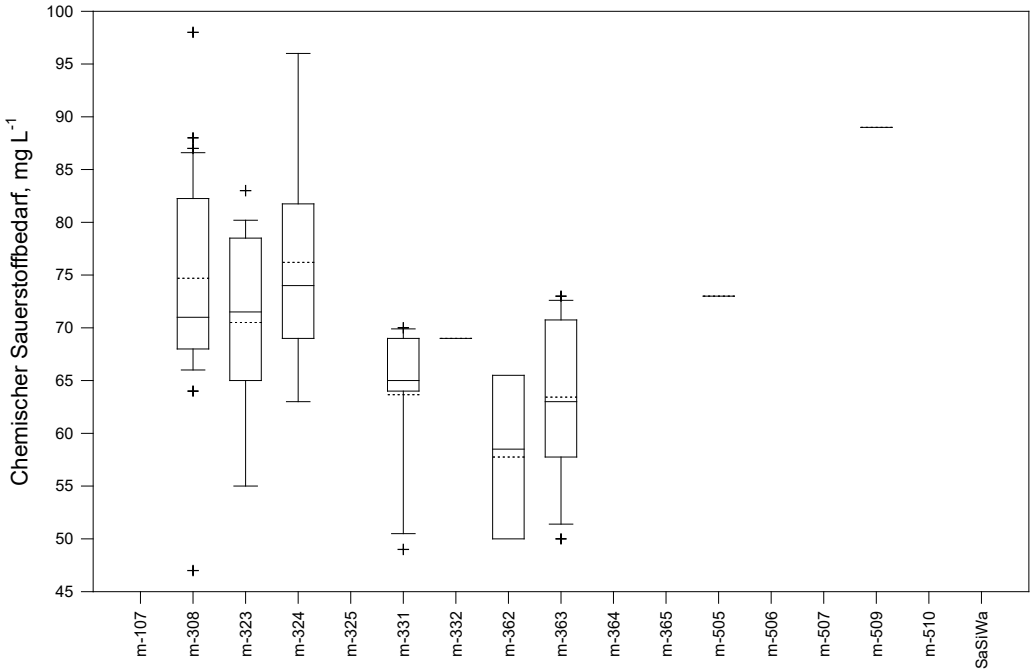

Fig. 103: Boxplot of the chemical oxygen demand. SaSiWa: Collective measuring point leachates (m-315, m-316, m-318, m-320, m-501, m-503, m-504, w-68 and w-92).

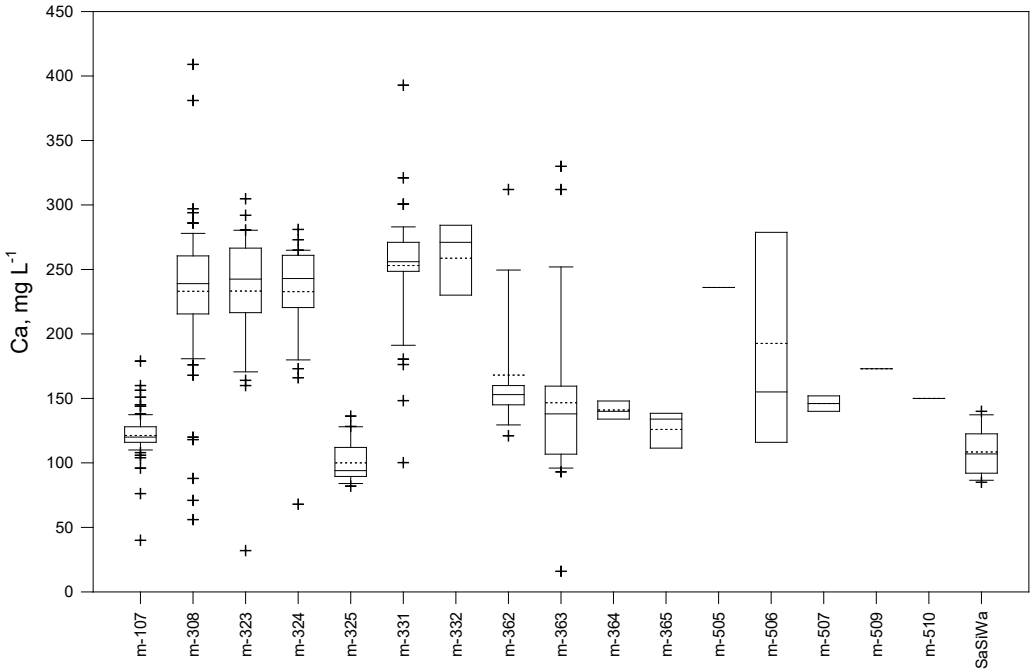

Fig. 104: Boxplot of the mass concentration of calcium. SaSiWa: Collective measuring point leachates (m-315, m-316, m-318, m-320, m-501, m-503, m-504, w-68 and w-92).

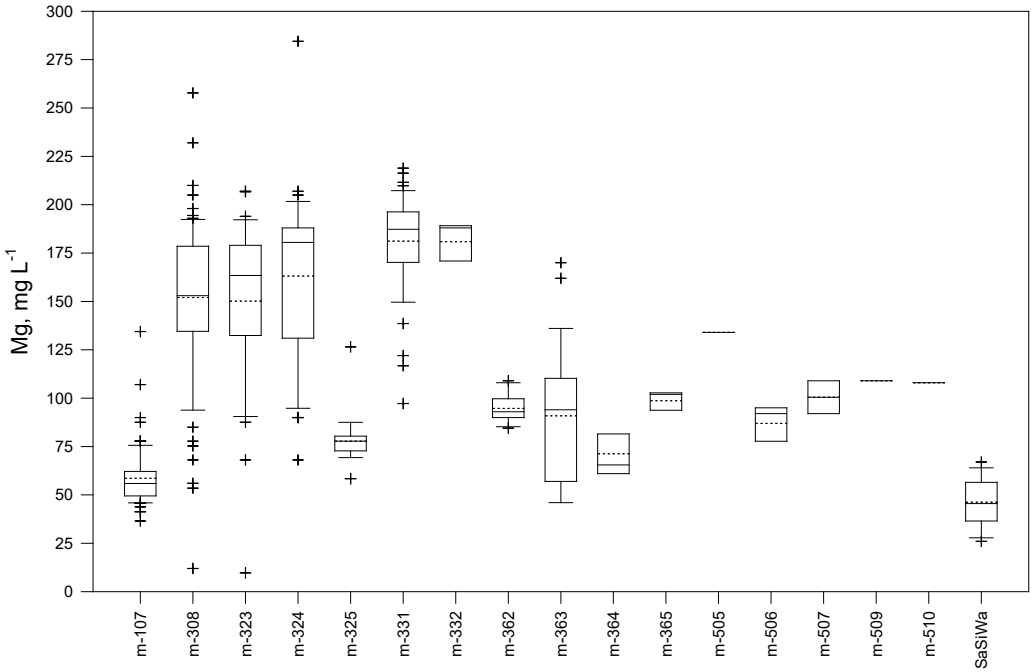

Fig. 105: Boxplot of the mass concentration of magnesium. SaSiWa: Collective measuring point leachates (m-315, m-316, m-318, m-320, m-501, m-503, m-504, w-68 and w-92).

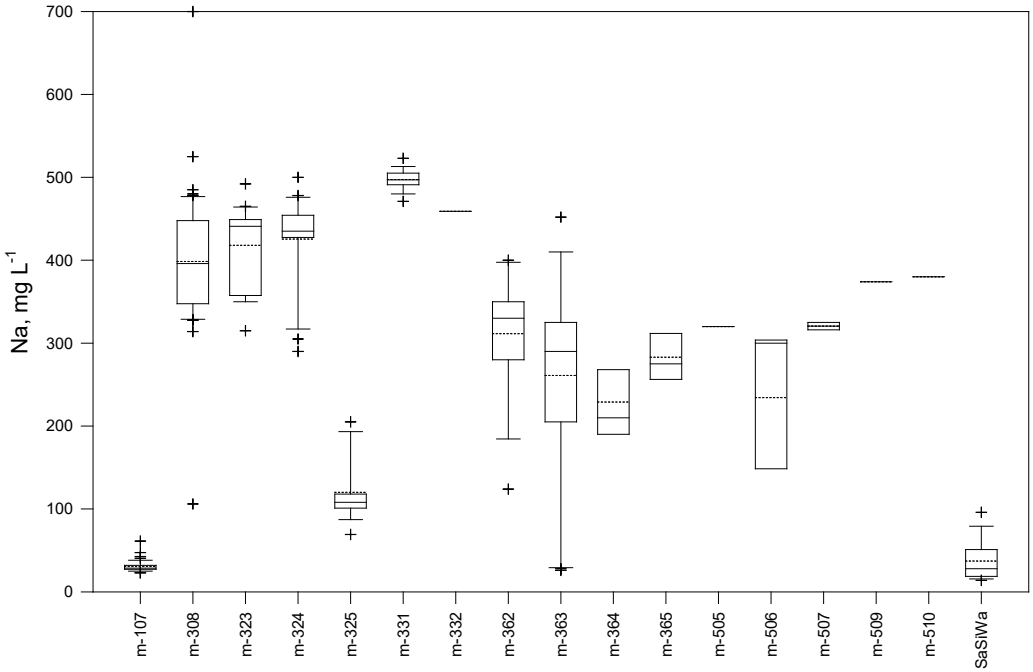

Fig. 106: Boxplot of the mass concentration of sodium. SaSiWa: Collective measuring point leachates (m-315, m-316, m-318, m-320, m-501, m-503, m-504, w-68 and w-92).

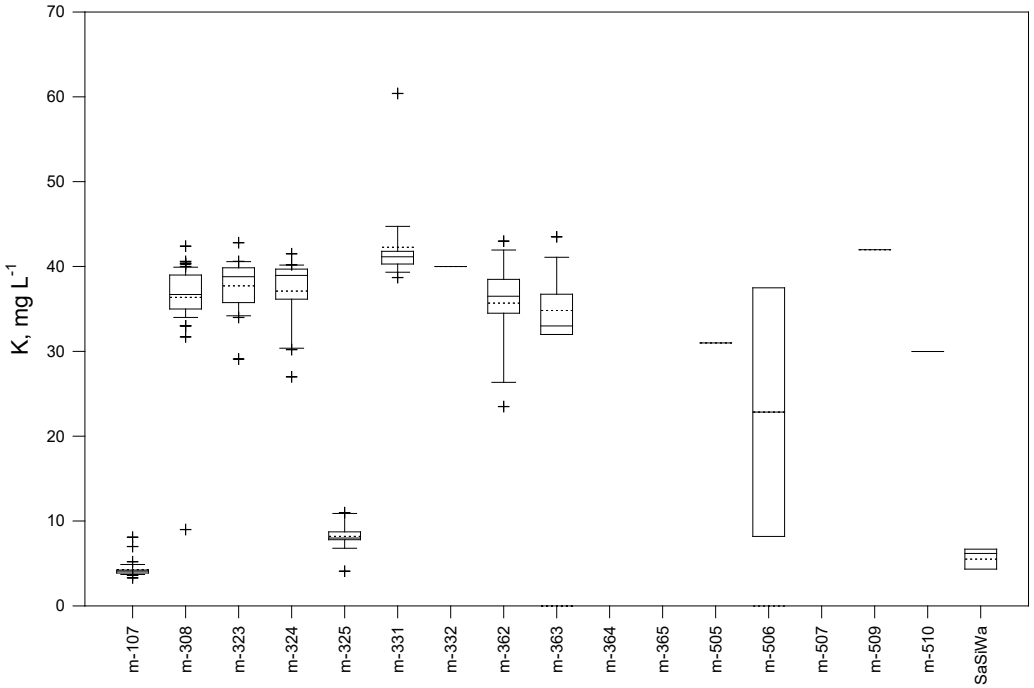

Fig. 107: Boxplot of the mass concentration of potassium. SaSiWa: Collective measuring point leachates (m-315, m-316, m-318, m-320, m-501, m-503, m-504, w-68 and w-92).

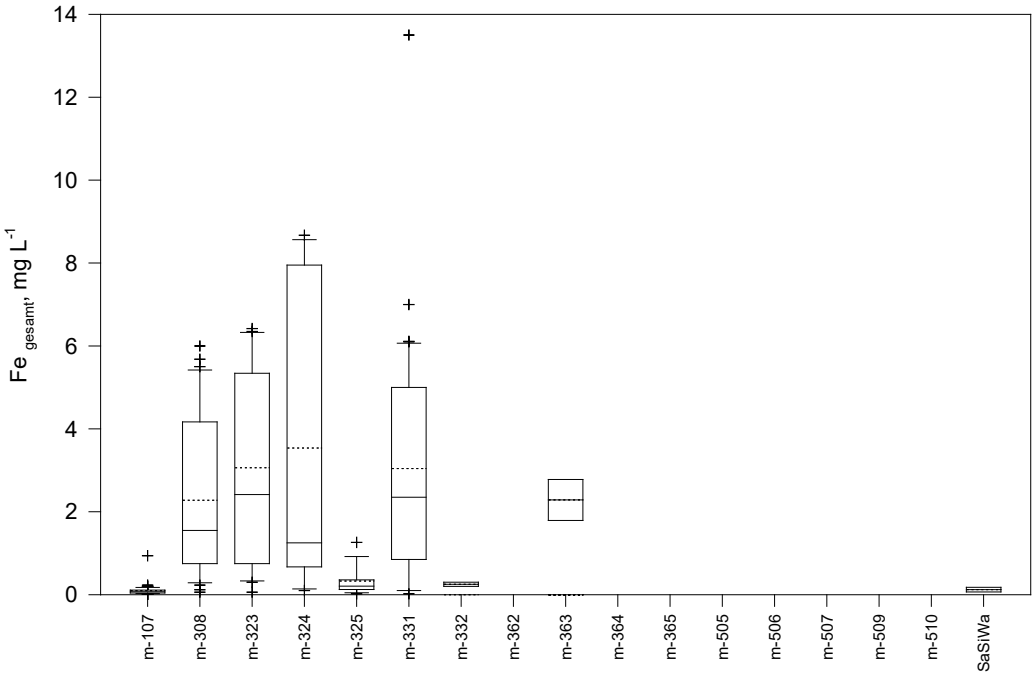

Fig. 108: Boxplot of the mass concentration of total iron. SaSiWa: Collective measuring point leachates (m-315, m-316, m-318, m-320, m-501, m-503, m-504, w-68 and w-92).

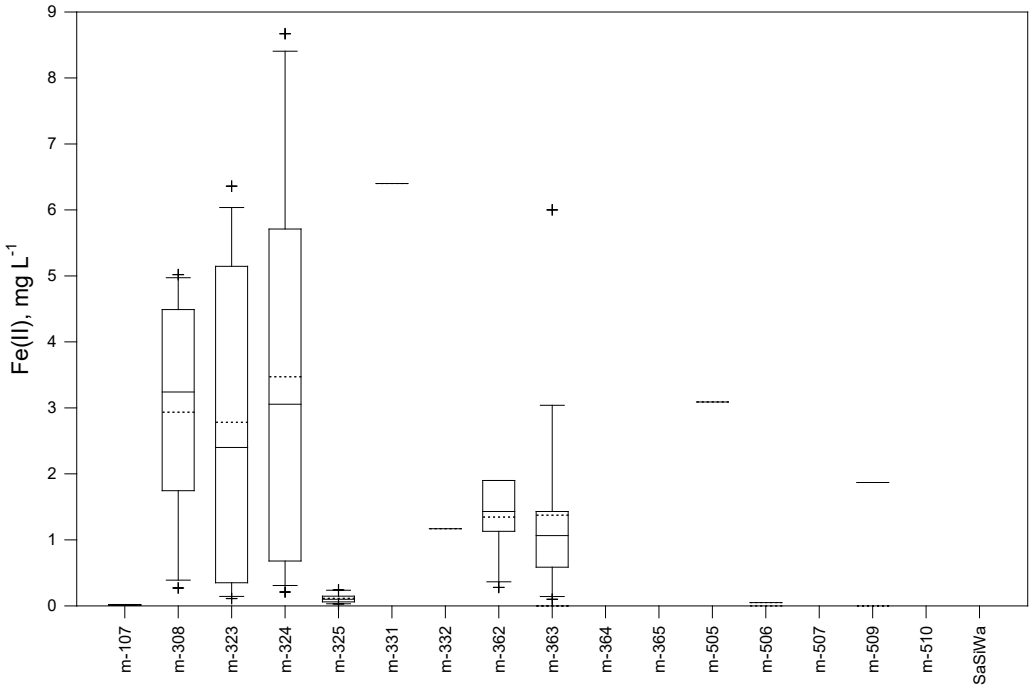

Fig. 109: Boxplot of the mass concentration of iron (II). SaSiWa: Collective measuring point leachates (m-315, m-316, m-318, m-320, m-501, m-503, m-504, w-68 and w-92).

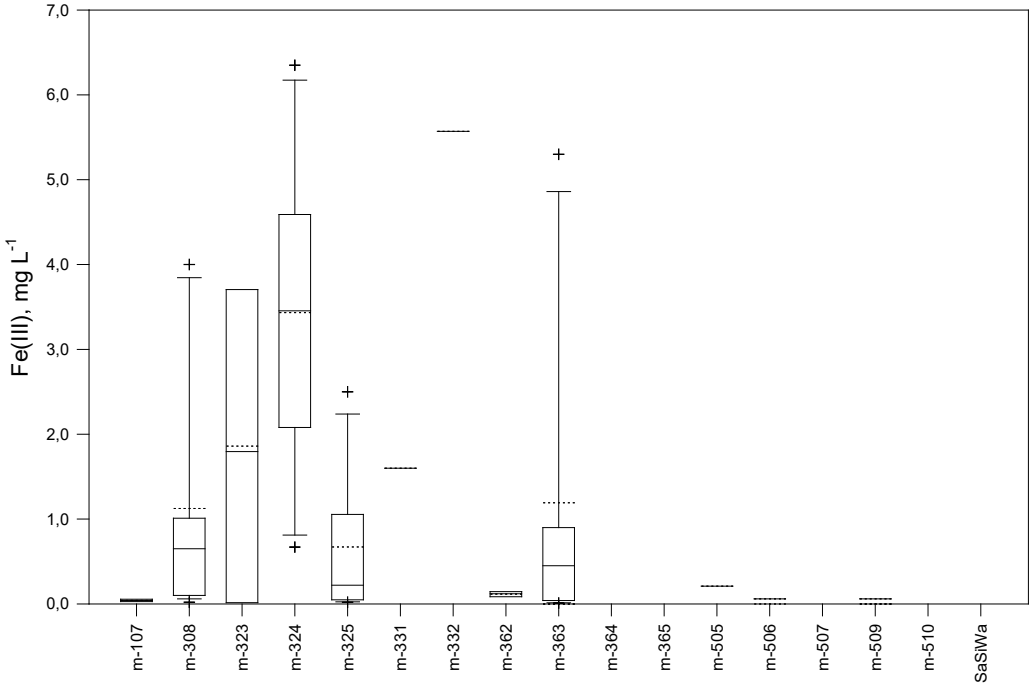

Fig. 110: Boxplot of the mass concentration of iron (III). SaSiWa: Collective measuring point leachates (m-315, m-316, m-318, m-320, m-501, m-503, m-504, w-68 and w-92).

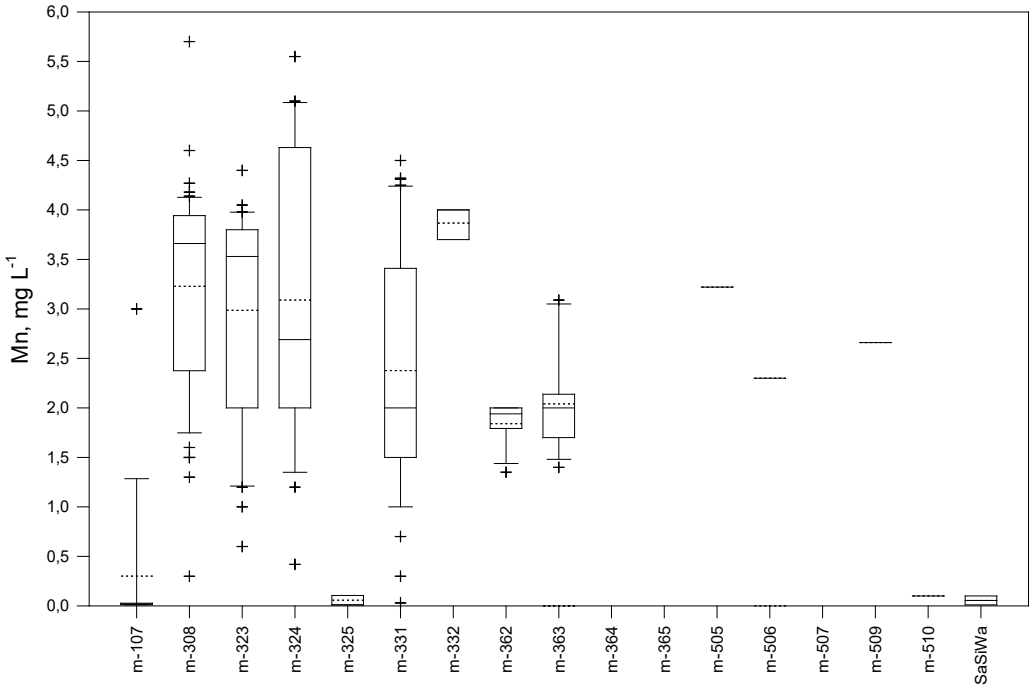

Fig. 111: Boxplot of the mass concentration of manganese. SaSiWa: Collective measuring point leachates (m-315, m-316, m-318, m-320, m-501, m-503, m-504, w-68 and w-92).

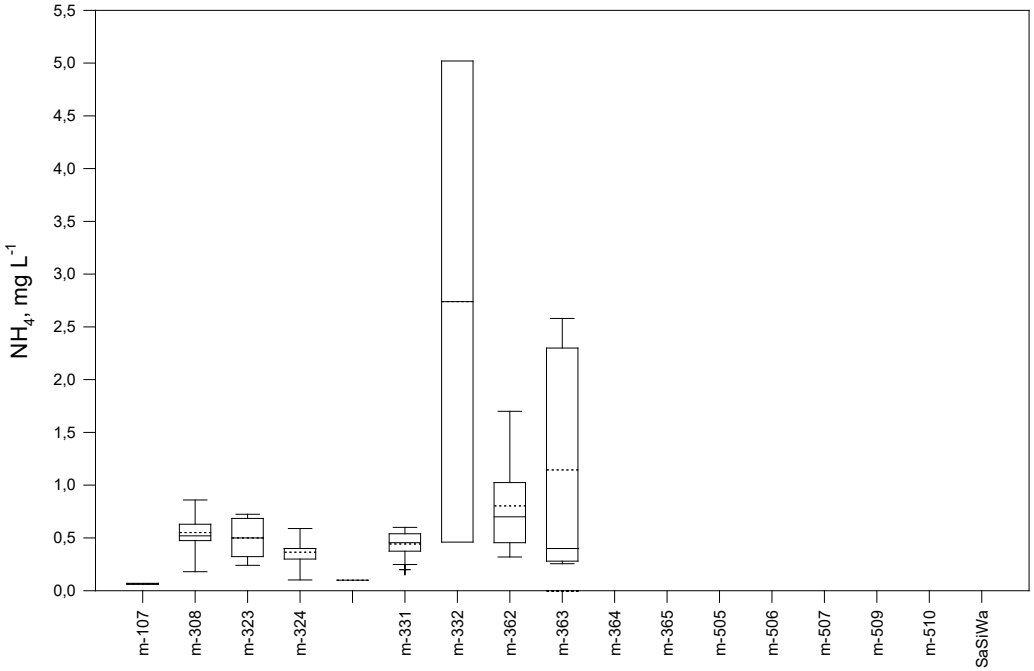

Fig. 112: Boxplot of the mass concentration of NH_4^+. SaSiWa: Collection point leachates (m-315, m-316, m-318, m-320, m-501, m-503, m-504, w-68 and w-92).

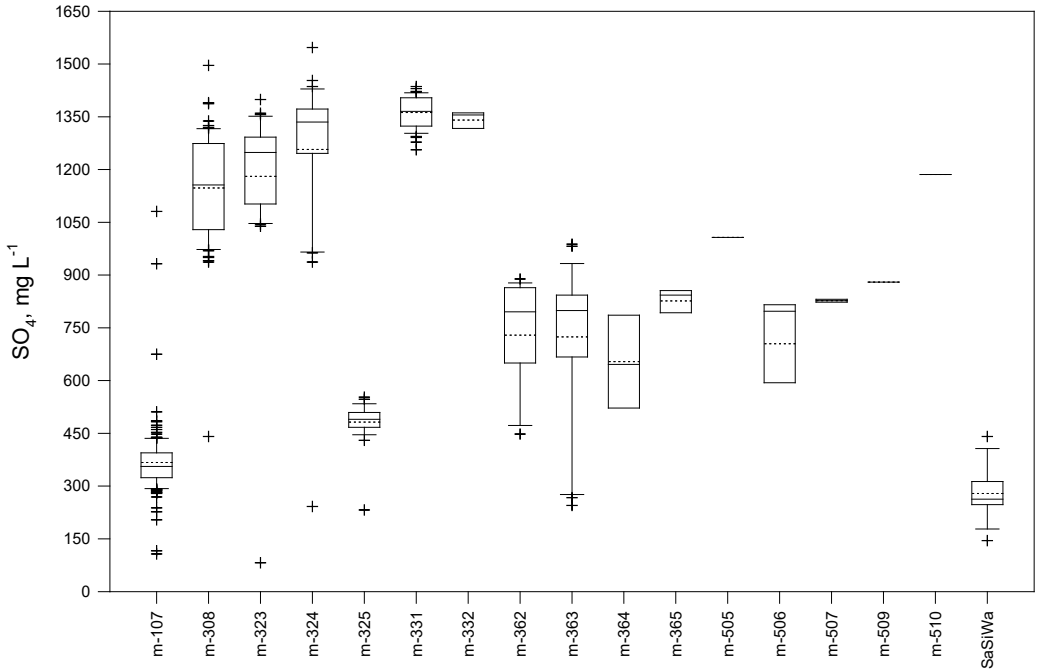

Fig. 113: Boxplot of the mass concentration of sulphate. SaSiWa: Collective measuring point leachates (m-315, m-316, m-318, m-320, m-501, m-503, m-504, w-68 and w-92).

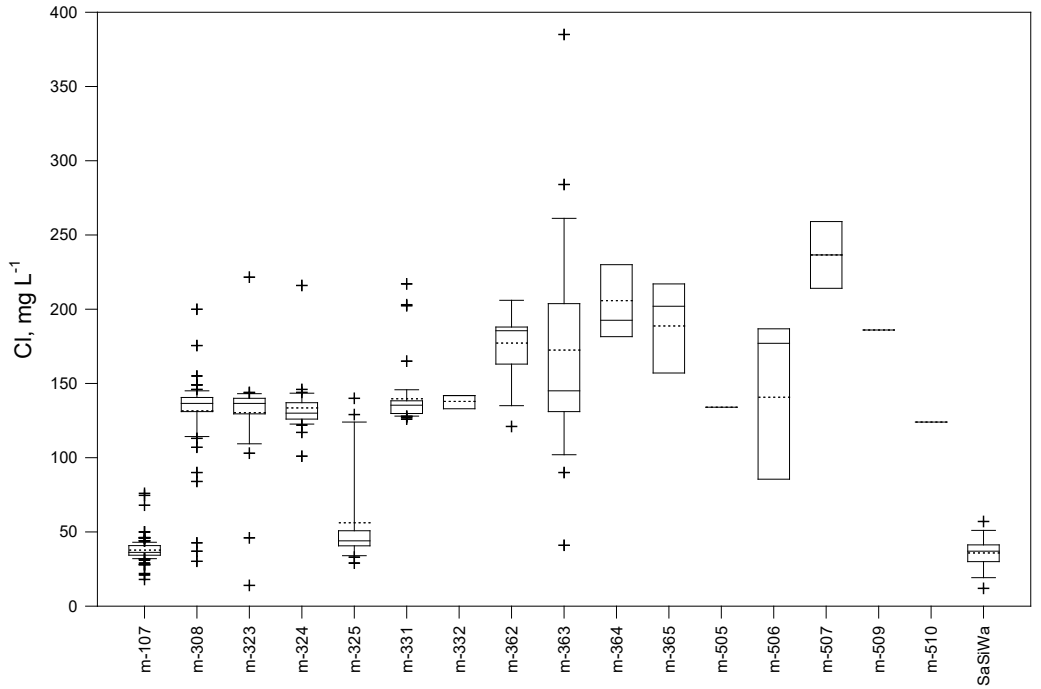

Fig. 114: Boxplot of the mass concentration of cloride. SaSiWa: Collection point leachates (m-315, m-316, m-318, m-320, m-501, m-503, m-504, w-68 and w-92).

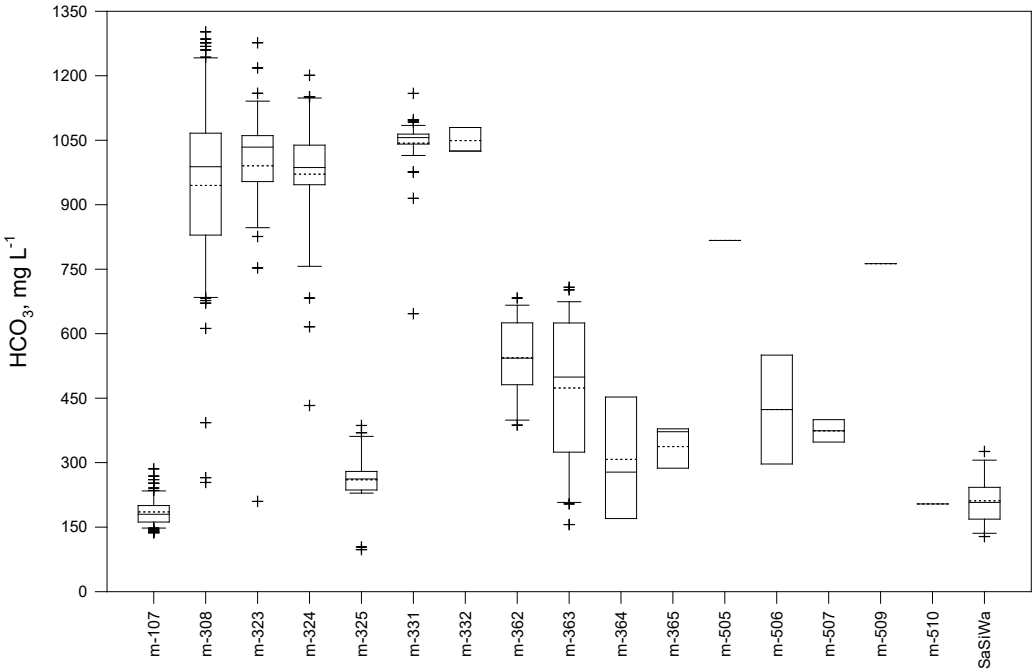

Fig. 115: Boxplot of the mass concentration of hydrogen carbonate. SaSiWa: Collective measuring point leachates (m-315, m-316, m-318, m-320, m-501, m-503, m-504, w-68 and w-92).

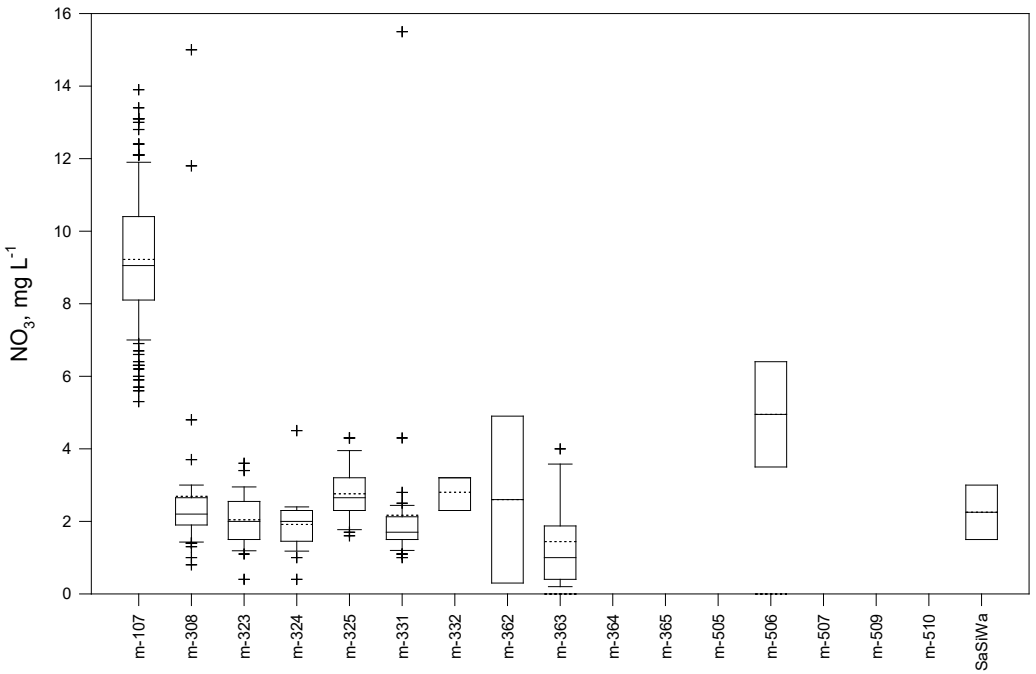

Fig. 116: Boxplot of the mass concentration of nitrate. SaSiWa: Collective measuring point leachates (m-315, m-316, m-318, m-320, m-501, m-503, m-504, w-68 and w-92).

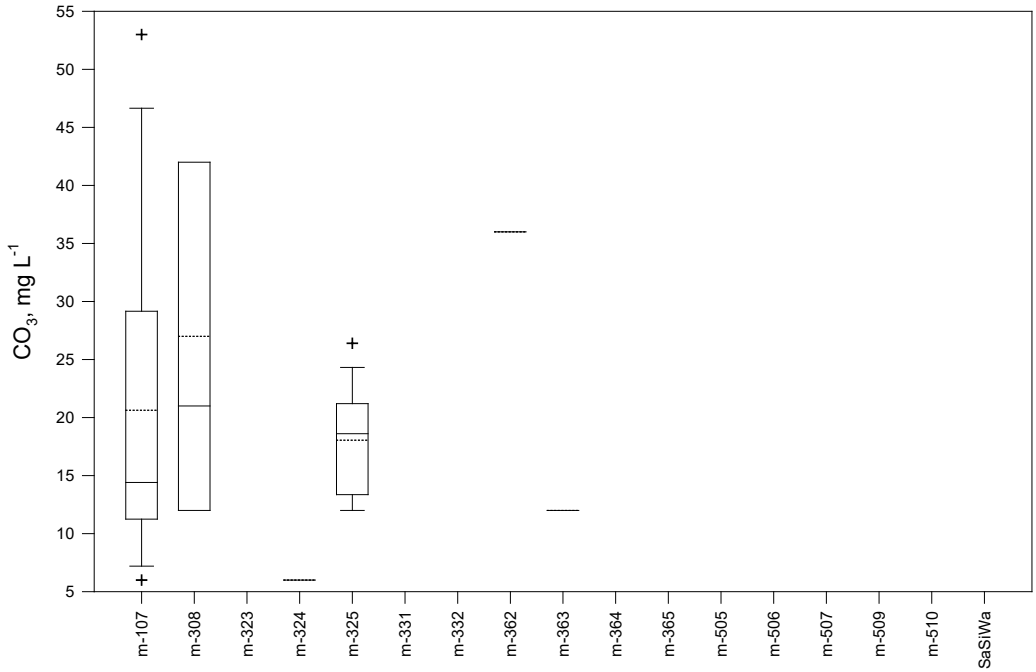

Fig. 117: Boxplot of the mass concentration of carbonate. SaSiWa: Collective measuring point leachates (m-315, m-316, m-318, m-320, m-501, m-503, m-504, w-68 and w-92).

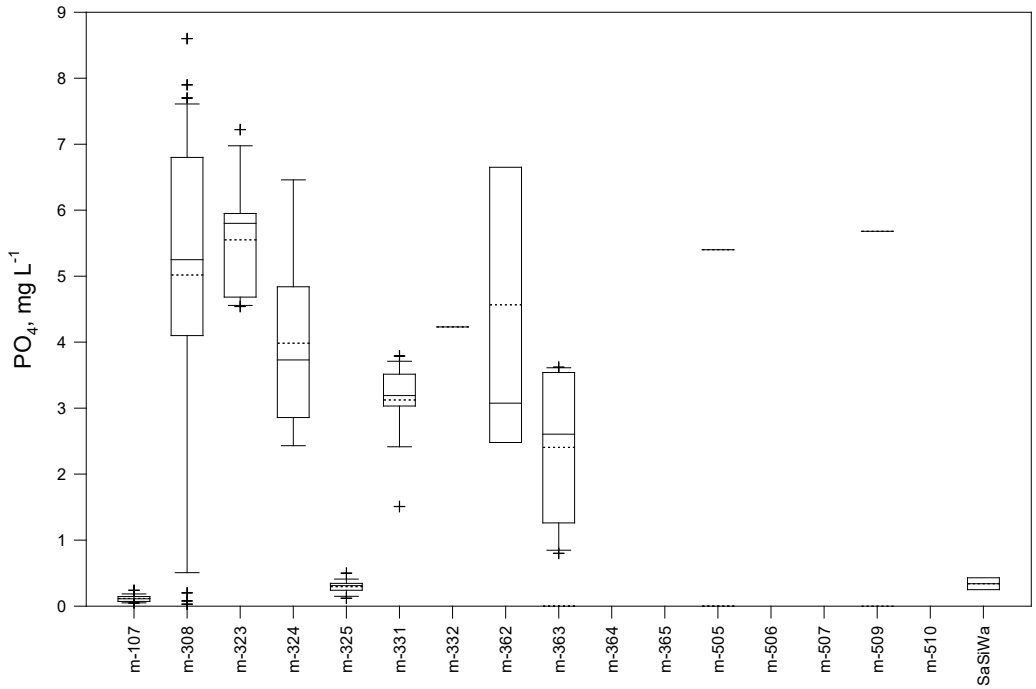

Fig. 118: Boxplot of the mass concentration of phosphate. SaSiWa: Collective measuring point leachates (m-315, m-316, m-318, m-320, m-501, m-503, m-504, w-68 and w-92).

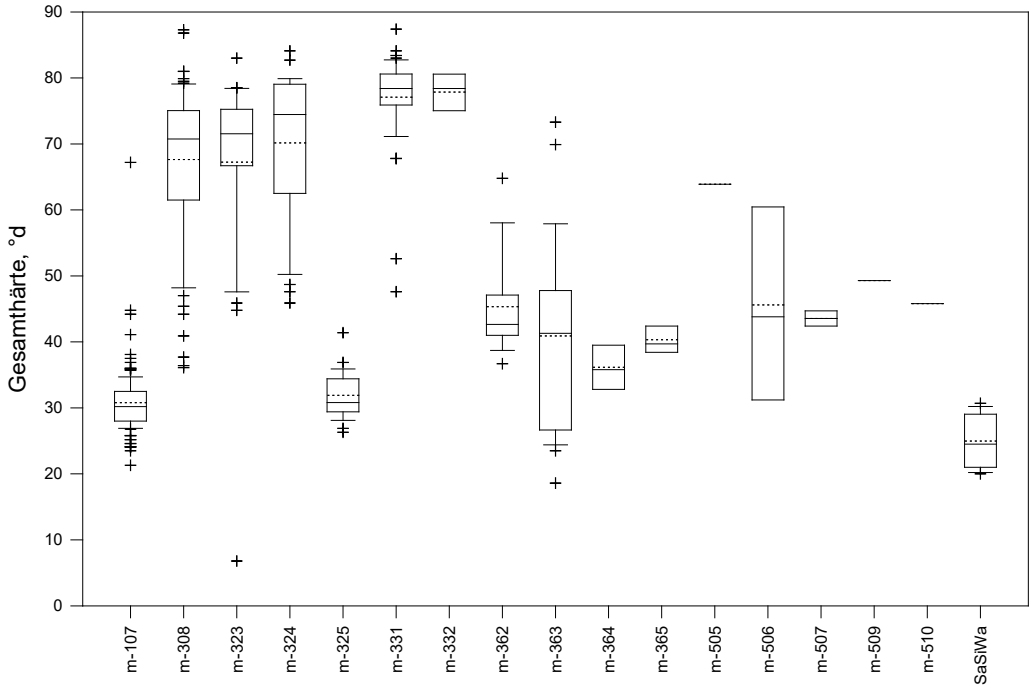

Fig. 119: Boxplot of the value of total hardness. SaSiWa: Collective measuring point leachates (m-315, m-316, m-318, m-320, m-501, m-503, m-504, w-68 and w-92).

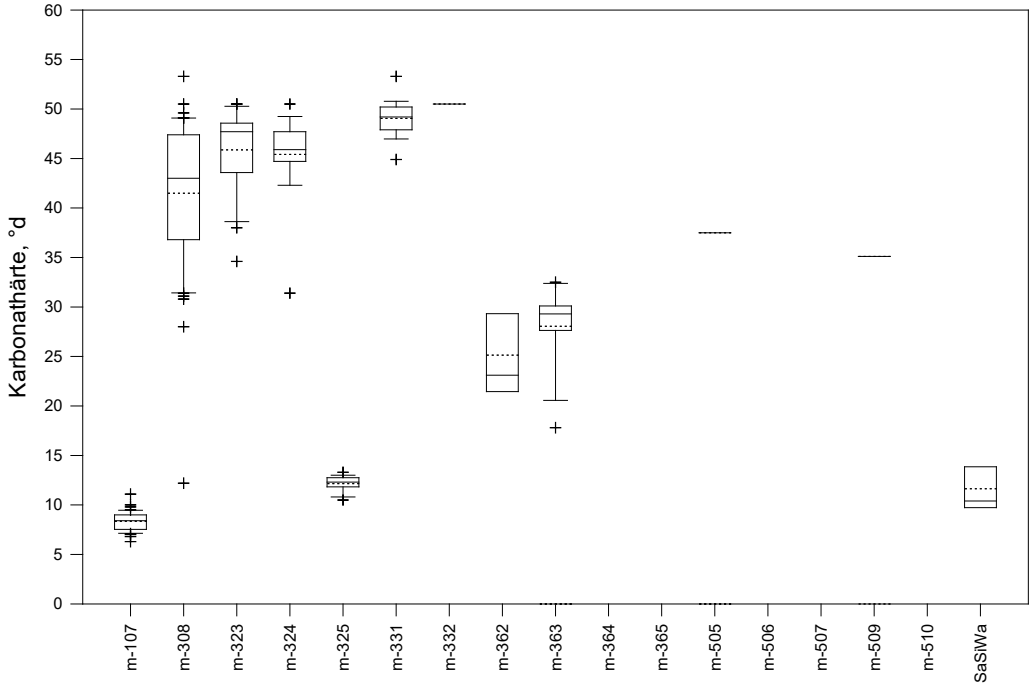

Fig. 120: Boxplot of the carbonate hardness value. SaSiWa: Collective measuring point leachates (m-315, m-316, m-318, m-320, m-501, m-503, m-504, w-68 and w-92).

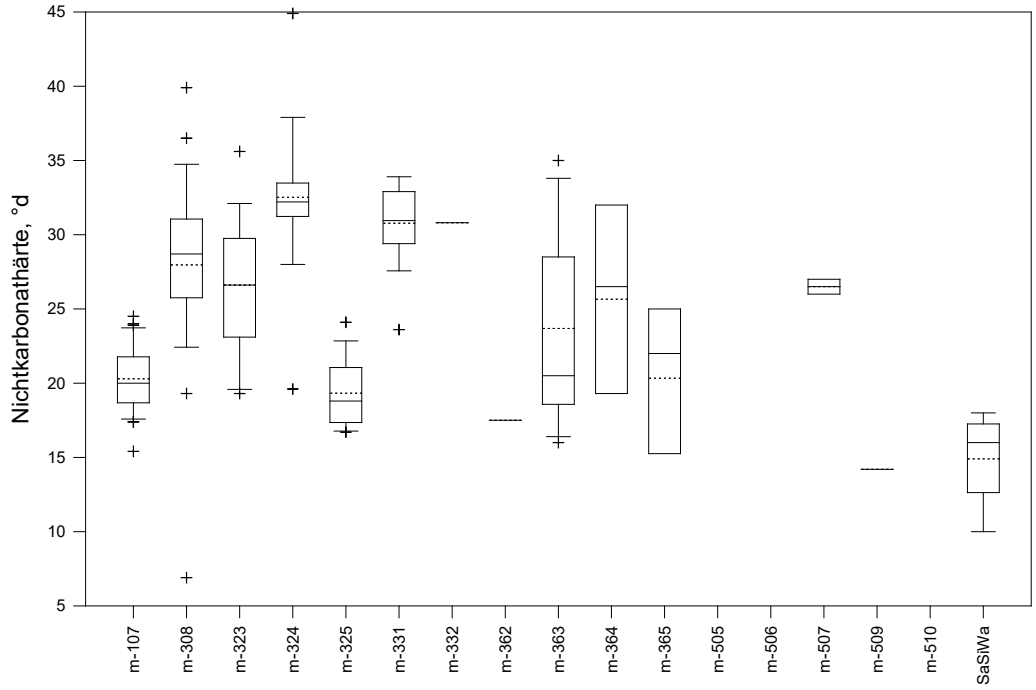

Fig. 121: Boxplot of the value of non-carbonate hardness. SaSiWa: Collective measuring point leachates (m-315, m-316, m-318, m-320, m-501, m-503, m-504, w-68 and w-92).

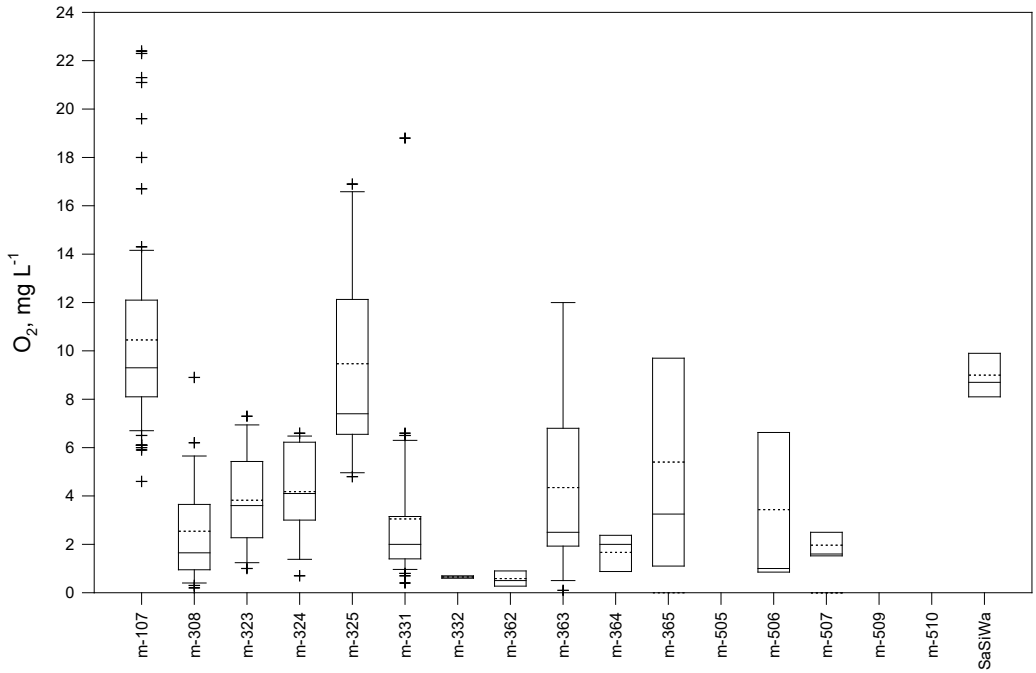

Fig. 122: Boxplot of the mass concentration of free oxygen. SaSiWa: Collective measuring point leachates (m-315, m-316, m-318, m-320, m-501, m-503, m-504, w-68 and w-92).

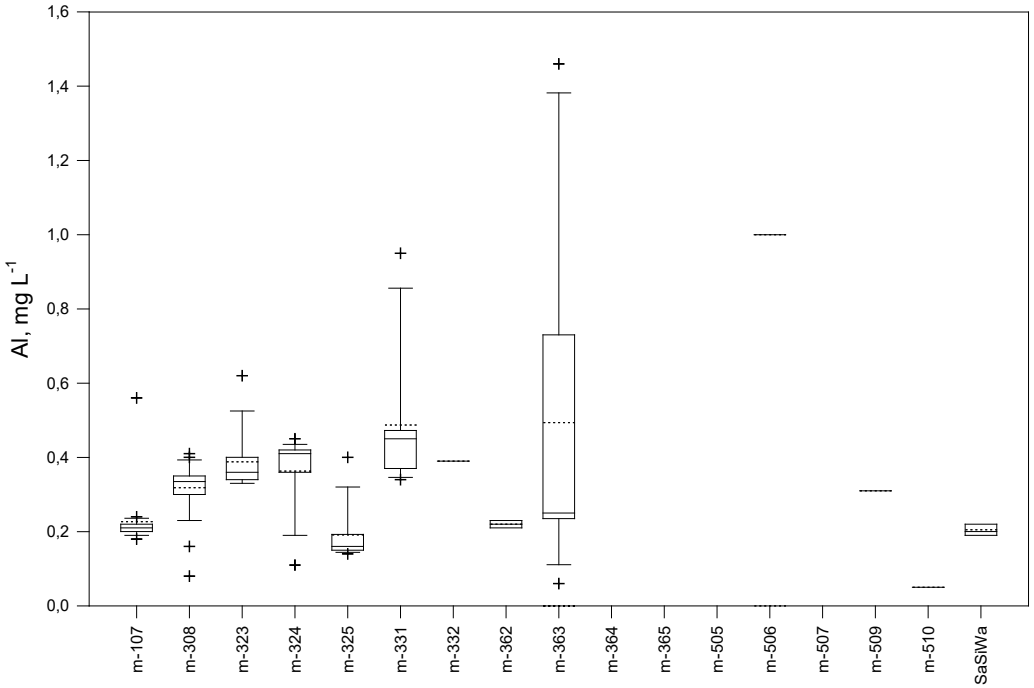

Fig. 123: Boxplot of the mass concentration of aluminium. SaSiWa: Collective measuring point leachates (m-315, m-316, m-318, m-320, m-501, m-503, m-504, w-68 and w-92).

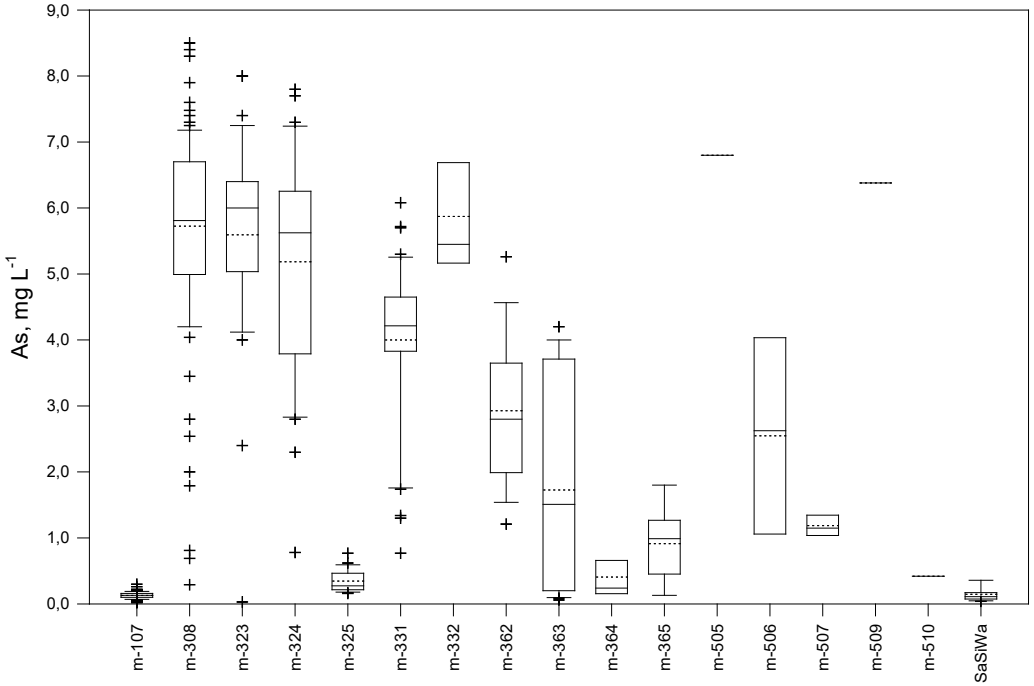

Fig. 124: Boxplot of the mass concentration of arsenic. SaSiWa: Collective measuring point leachates (m-315, m-316, m-318, m-320, m-501, m-503, m-504, w-68 and w-92).

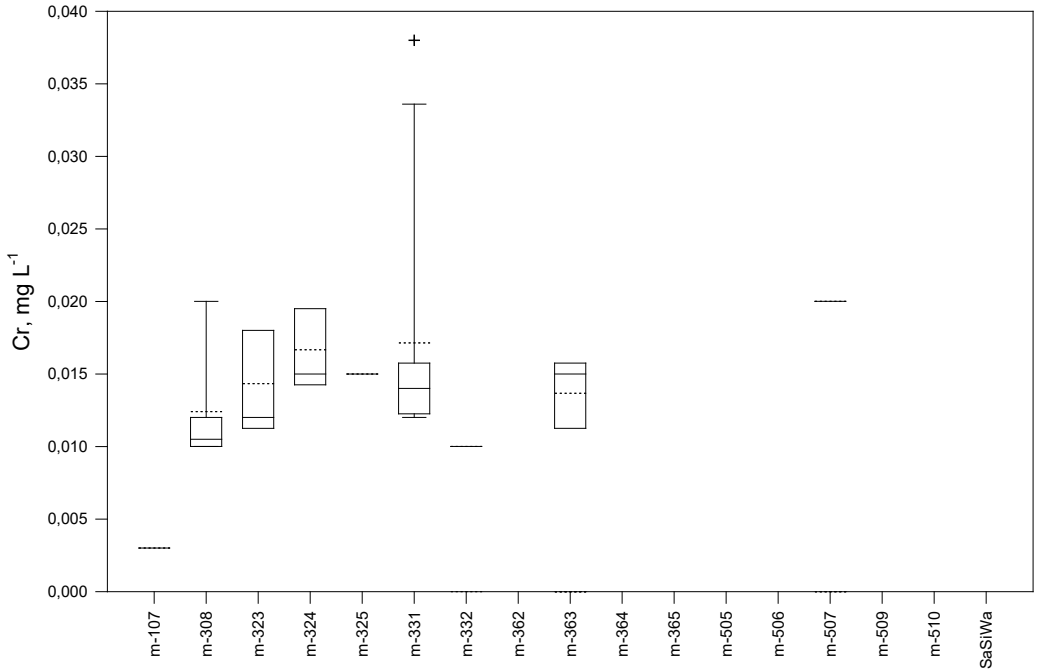

Fig. 125: Boxplot of the mass concentration of chromium. SaSiWa: Collective measuring point leachates (m-315, m-316, m-318, m-320, m-501, m-503, m-504, w-68 and w-92).

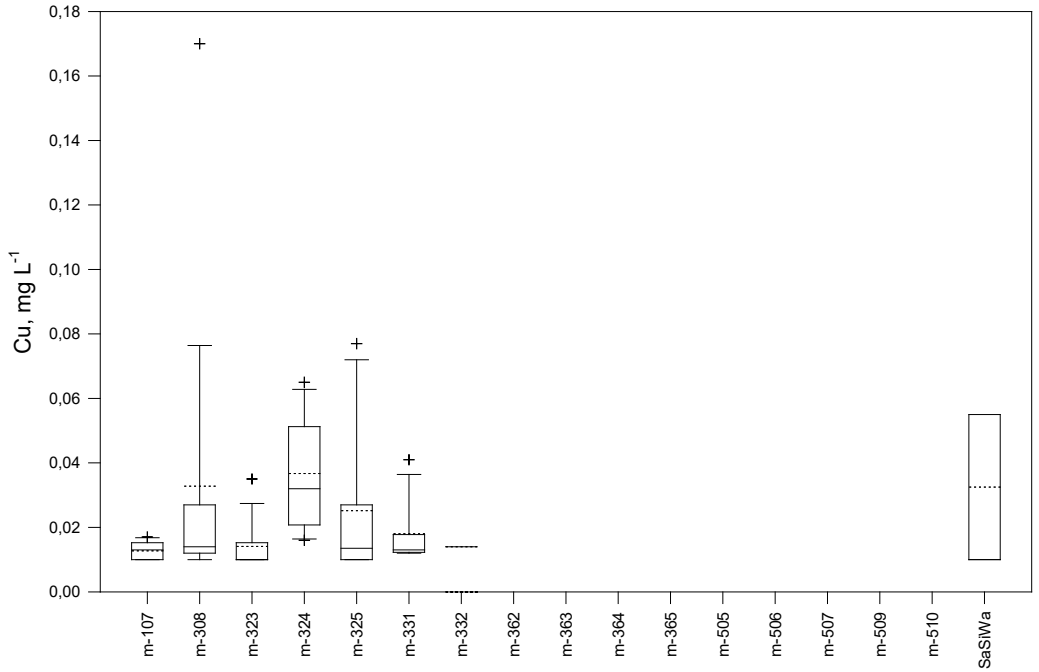

Fig. 126: Boxplot of the mass concentration of copper. SaSiWa: Collective measuring point leachates (m-315, m-316, m-318, m-320, m-501, m-503, m-504, w-68 and w-92).

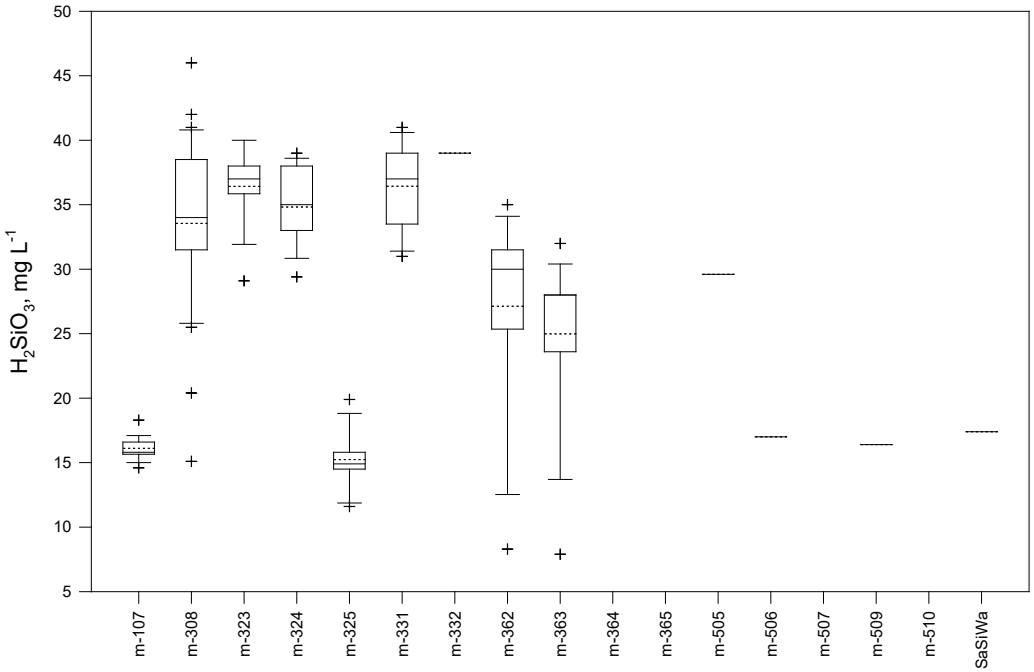

Fig. 127: Boxplot of the mass concentration of silicate. SaSiWa: Collective measuring point leachates (m-315, m-316, m-318, m-320, m-501, m-503, m-504, w-68 and w-92).

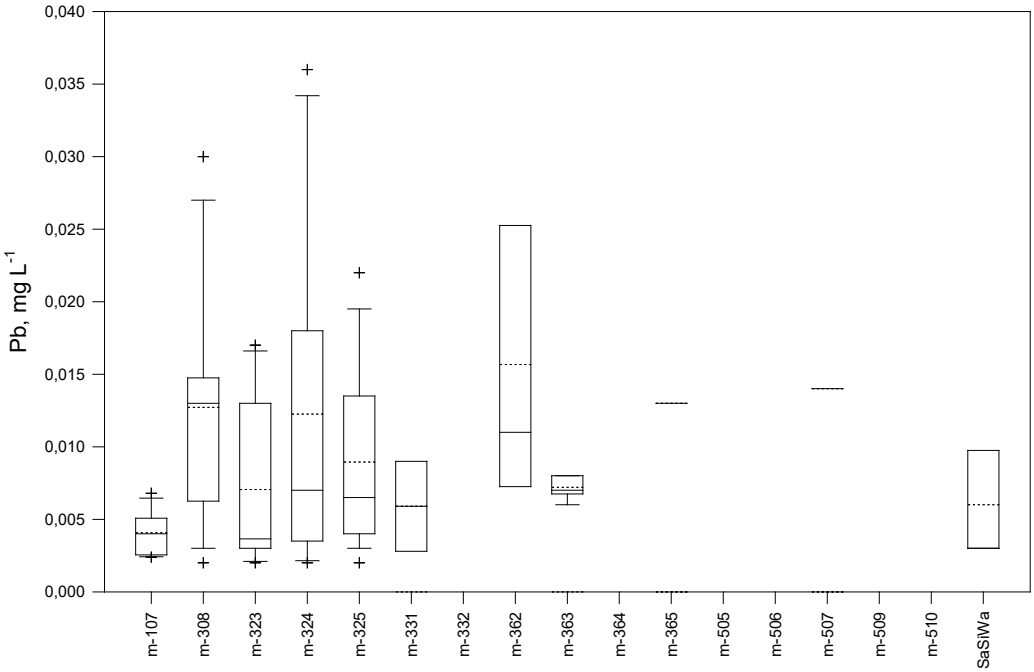

Fig. 128: Boxplot of the lead mass concentration. SaSiWa: Collective measuring point leachates (m-315, m-316, m-318, m-320, m-501, m-503, m-504, w-68 and w-92).

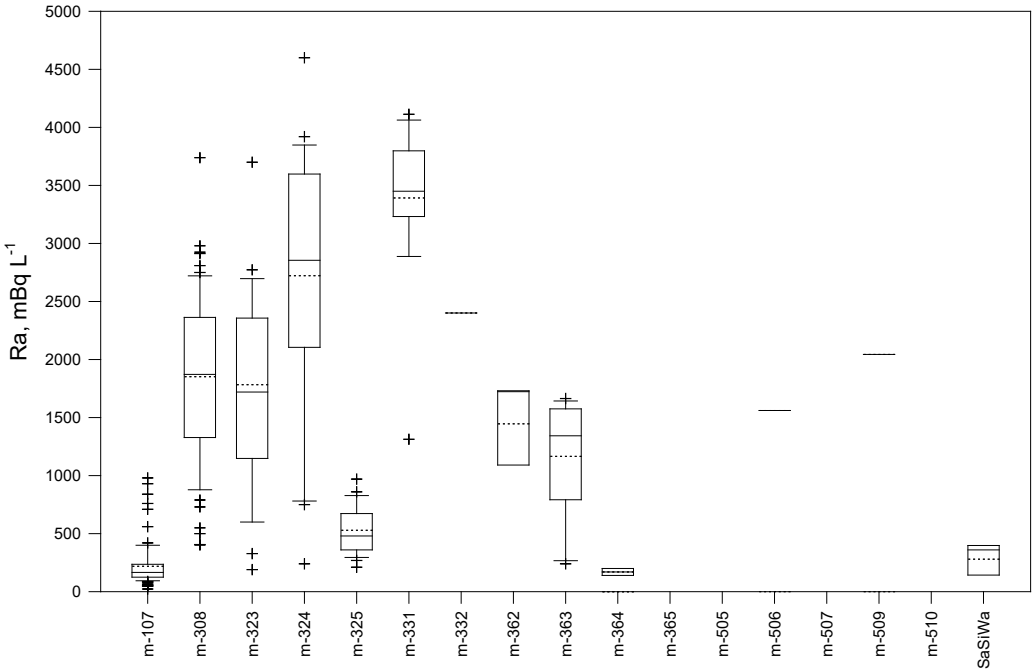

Fig. 129: Boxplot of radium activity. SaSiWa: Collective measuring point leachates (m-315, m-316, m-318, m-320, m-501, m-503, m-504, w-68 and w-92).

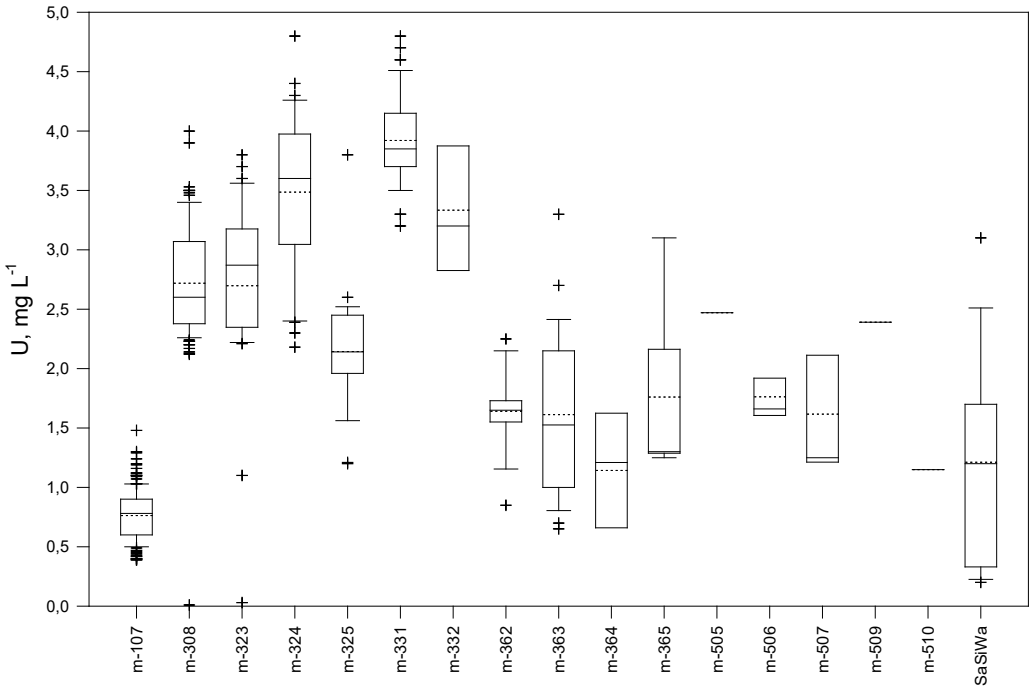

Fig. 130: Boxplot of the uranium mass concentration. SaSiWa: Collective measuring point leachates (m-315, m-316, m-318, m-320, m-501, m-503, m-504, w-68 and w-92).

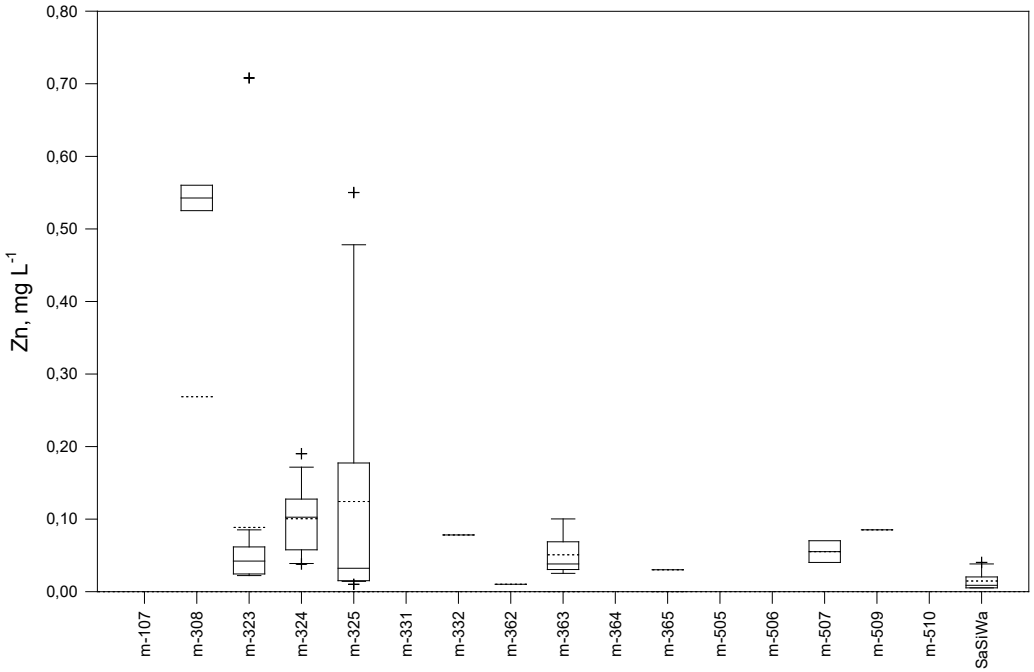

Fig. 131: Boxplot of the mass concentration of zinc. SaSiWa: Collective measuring point leachates (m-315, m-316, m-318, m-320, m-501, m-503, m-504, w-68 and w-92).

Tab. 57: Results of the multiple comparison (DUNN test) between the individual measuring points with the parameters As, U, Ca, Mg, Na, SO_4^{2-}, Cl and HCO_3^-. The numbers indicate in the lower section for how many parameters the test value $Q < 1$, in the upper section for how many parameters $Q > 10$. The larger the numerical value in the table, the more similar the measuring points are.

Meßstelle	m-107	m-308	m-315	m-316	m-318	m-320	m-323	m-324	m-325	m-331	m-332	m-362	m-363	m-364	m-365	m-501	m-503	m-504	m-505	m-506	m-507	m-509	m-510	w-68	w-92
m-107		7					1		4											3					1
m-308																	1								
m-315	8																								
m-316	8		8																						
m-318	6		8	8																					
m-320	8		8	7	6																				
m-323		7	1			1																			
m-324		1	3	3	1	2	3																		
m-325		2	2		1		5																		
m-331	1		3	3	3	3	2	6																	
m-332	3	1	4	4	2	4	3	8		6															
m-362	1	1	4	2	3	3	2	6	1	8	7														
m-363		4	4	3	3	2	7	7	7	6	6	6													
m-364	1	1	4	3	2	2	2	7	5	7	7	7	8												
m-365	2	1	4	2	3	2	6	7	7	7	7	8	8	8											
m-501	7		8	7	8	7		4	2	5	5	5	5	6	6										
m-503	2		7	5	4	4	1	4		3	4	6	5	6	4	6									
m-504	1	3	1	1	1	1	6		8	1		1	7	2	7	2	1								
m-505	3	3	3	3	2	3	4	6	5	1	6	5	6	5	5	4	4	4							
m-506		2	1		1		6		6	1		2	7	1	7			6	5						
m-507			1		1				1	1		1	1	1	1	1		1		1					
m-509		1					1	1		1	1								1						
m-510	1		1		1				1	1		1	1	1	1	1	1	1		1	1				
w-68	7		8	7	7	7	1	5	1	6	6	6	5	7	6	8	7	2	5				1		
w-92	1	2	3	3	2	2	1	6	4	6	6	7	7	8	7	5	5	3	6	2	1		1	5	

Tab. 58: Mine water: Results of the correlations of individual parameters of the outlier-free water analyses from the Niederschlema/Alberoda mine. For legend see p. 79.

	As	U	SO4	Cl	Ca	Mg	pH	AR	HCO3	Na	GH °dH	K	Temp °C	Mn	NO3	KH °dH	Ra	CSB	PO4	Al	EH(mV)	H2SiO3	Zn	O2	Pb	Leitf	FR	Ni	Fe(II)	Fe g	NKH °dH	NO2	Fe(III)	Cu	Cr
As		+	+	-	+	+	-	+	++<	+	+	+	+	+	-	+	+	+	++<	+	-	+	+	-	-	+	+	+	+	+	+	-	+	-	-
U	<		++<	-	+	++<	-	++<	++<	++<	++<	+	+	+	-	++<	++<	-	-	+	+	+	-	-	-	+	-	+	+	+	+	-	+	-	+
SO4	<	<		-	++<	+	-	++<	++<	++<	++<	+	+	+	-	++<	+	+	-	+	+	++<	-	-	-	+	-	+	+	+	+	-	+	-	+
Cl	<	<	<		-	-	+	-	-	-	-	+	-	-	-	+	-	+	+	-	-	-	+	-	+	+	-	-	+	-	-	+	-	++<	+
Ca	<	<	<	<		+	-	++<	+	+	++<	+	+	+	-	+	+	+	+	+	+	+	+	-	-	+	+	+	+	-	+	+	+	-	+
Mg	<	<	<	<	<		+	+	++<	++<	++<	+	+	+	-	++<	+	+	+	+	+	++<	-	-	-	+	-	+	+	+	++<	-	+	-	-
pH	<	>	>	<	<	>		-	-	-	-	-	-	+	-	+	-	-	-	-	+	-	+	+	-	+	+	-	+	+	+	-	+	+	+
AR	<	<	<	<	<	<	>		++<	++<	++<	++<	+	+	-	++<	++<	+	+	+	+	++<	+	-	-	+	-	+	+	+	+	-	+	-	+
HCO3	<	<	<	<	<	<	<	<		++<	++<	+	+	+	-	++<	+	+	+	+	+	++<	-	-	-	+	-	-	+	+	+	-	+	-	-
Na	<	<	<	>	<	<	>	<	<		++<	+	+	+	+	++<	++<	+	-	+	+	++<	-	-	-	++<	-	+	+	++<	+	-	+	-	+
GH °dH	<	<	<	<	<	<	>	<	<	<		+	+	+	-	++<	+	+	+	+	+	++<	-	-	-	+	-	+	+	+	++<	+	+	-	-
K	<	<	<	<	<	<	>	<	<	<	<		-	+	-	+	+	+	+	+	+	+	+	+	-	++<	-	+	-	+	+	-	+	-	++<
Temp °C	<	<	<	>	<	<	<	<	<	<	<	>		-	-	-	+	-	+	+	--<	-	-	--<	+	+	-	+	--<	-	-	-	-	-	---
Mn	<	<	>	>	<	<	>	<	>	<	<	<	>		+	++<	+	+	+	+	+	+	+	-	-	+	+	++<	+	+	+	-	+	-	-
NO3	>	<	>	<	>	<	>	>	>	>	>	>	>	<		-	-	-	-	-	+	-	-	-	-	-	+	-	+	+	-	+	-	-	+
KH °dH	<	<	<	>	<	<	>	<	<	<	<	<	<	<	>		+	+	+	-	++<	++<	-	-	-	++<	-	-	+	++<	+	-	+	-	-
Ra	<	<	<	<	<	<	>	<	<	<	<	<	>	<	>	<		-	-	-	+	+	-	+	-	+	-	+	+	+	+	-	+	-	-
CSB	<	>	>	>	>	>	>	>	>	>	>	>	>	>	<	>	>		+	-	-	-	+	+	+	+	+	+	+	-	-	-	+	+	+
PO4	<	>	>	>	<	>	<	>	>	>	>	>	<	>	<	>	>	<		+	-	+	+	-	+	+	+	+	+	-	+	-	+	+	+
Al	>	<	>	>	<	>	>	>	>	>	<	<	>	>	>	>	>	<	>		+	+	-	+	-	+	+	+	-	-	+	++<	-	-	+
EH(mV)	>	<	>	>	<	>	>	<	>	>	<	<	<	<	>	<	>	>	>	>		+	-	+	-	+	-	+	+	++<	++<	+	-	+	-
H2SiO3	<	<	<	<	<	<	>	<	<	<	<	<	>	<	>	<	<	>	<	<	<		-	--	-	++<	+	-	+	++<	+	-	+	-	-
Zn	>	>	>	>	>	>	>	>	>	>	>	>	>	>	>	>	>	<	<	>	>	>		--	+	-	-	+	+	-	+	-	-	+	+
O2	<	>	<	>	<	<	<	<	<	<	<	>	<	>	>	>	>	>	>	>	>	<<	<<		+	-	+	./.	++<	-	-	-	+	./.	+
Pb	>	<	<	>	<	<	<	<	<	<	<	>	>	>	>	<	>	<	>	>	>	<	<	>		--<	+	+	+	--<	-	-	-	-	-
Leitf	<	<	<	<	<	<	>	<	<	<	<	<	>	<	<	<	<	>	>	>	<	<	<	>	<		-	-	+	+	+	-	-	-	-
FR	>	<	<	<	>	>	>	>	>	>	>	>	<	>	<	>	>	>	>	>	>	>	>	>	>	>		-	+	+	-	-	-	-	+
Ni	>	>	>	>	>	>	>	>	>	>	>	>	>	<	>	>	>	>	>	>	>	>	>	./.	>	>	>		-	+	+	-	+	-	-
Fe(II)	<	<	<	>	<	<	<	<	<	<	<	>	<	<	>	<	>	>	>	>	>	<	>	<	>	<	>	>		++<	+	-	-	+	+
Fe g	<	<	>	>	>	<	>	>	<	<	<	<	>	<	>	<	<	<	<	>	<	<	<	>	<	<	>	>	<<		+	-	+++	--<	-
NKH °dH	<	<	<	>	<	<	>	<	<	<	<	>	>	<	>	<	<	>	>	>	<	<	>	<	>	<	>	<	<	./.		-	+	+	-
NO2	>	>	>	>	<	>	>	>	>	>	>	>	>	>	<	>	>	>	>	<	>	>	>	>	>	>	>	>	>	>	>		-	-	+
Fe(III)	>	<	<	>	>	<	>	<	>	>	<	>	>	<	>	<	<	>	>	>	>	>	>	>	>	>	>	>	>	>	>	>		-	+
Cu	<	<	<	<	>	<	>	>	<	<	<	>	>	<	>	<	>	<	>	>	>	<	<	./.	>	>	>	>	<	<	<	>	>		+
Cr	<	>	>	<	>	<	>	>	>	>	>	<	>	>	>	>	>	>	>	<	>	>	>	>	>	>	>	>	>	<	>	>	>	>	
Co	>	>	>	>	>	>	>	>	>	>	>	>	./.	<	>	>	>	>	>	>	<<	>	>	./.	>	<<	>	<	>	>	>	>	<<	<<	>
Mo	>	<	<<	>	<<	>	<<	<<	<<	>	<<	>	<<	<<	<<	<<	>	>	>	>	<<	<<	>	>	>	>	<<	>	>	./.	>	>	>	>	>
Sr	<	<	<	>	>	<	>	<	<	<	<	>	>	<	>	<	<	>	>	>	>	<<	>	>	>	<	>	>	<	>	>	>	>	>	>
TOC	<	>	>	<	<	<	>	>	>	>	>	<	>	<	>	>	>	>	>	<	./.	>	>	./.	>	>	>	>	>	<	>	./.	>	<<	<<
F	>	>	>	>	>	>	>	>	>	>	>	>	>	>	>	>	>	>	>	>	>	>	>	./.	>	>	>	>	>	>	<	>	./.	>	>

Tab. 59: Seepage water: Results of the correlations of individual parameters of the outlier-free water analyses from the Niederschlema/Alberoda mine. Legend see p. 79.

	As	U	SO4	Cl	Ca	Mg	pH	HCO3	Na	GH °dH	K	Mn	NO3	KH °dH	Ra	PO4	Al	H2SiO3	O2	Pb	Leitf	FR	Ni	Fe(II)	Fe g	NKH °dH	Cu	CO3	Sr	F
As		+	-	+	-	-	+	+	-	-	-	+	+	+	-	++<	-	-	+	++<	-	-	+	-	+	--<	++	+	++	-
U	<		-	+	+	-	+	++<	+	-	-	+	-	++<	-	+	-	--<	+	+	+	-	-	+	-	-	+	-	++<	-
SO4	<	<		-	+	+	-	-	+	+	+	-	-	-	-	--<	+	+	-	-	+	+	+	+	+	++<	-	++<	--	+
Cl	>	<	>		+	+	+	+	-	+	-	+	+	+	+	-	+	-	-	++<	+	-	+	+	-	-	++<	++<	++<	+
Ca	>	>	>	>		+	-	+	-	+	-	++<	-	-	+	--<	-	-	-	+	+	+	-	-	-	+	+	-	--	+
Mg	<	<	<	>	>		-	+	+	++<	+	-	-	-	++<	-	+	+	-	-	-	-	+	+	+	++<	-	++<	--	+
pH	>	>	>	<	<	>		+	+	+	-	++<	-	+	+	-	-	-	+	-	+	+	-	+	-	-	-	+	+++	-
HCO3	>	<	>	<	>	>	<		+	+	+	-	-	+	+	+	-	-	-	+	+	+	+	+	-	-	+	+	++	-
Na	>	>	>	<	<	>	>	<		-	+	+	-	++<	+	-	-	-	+	--	+	+	-	++	+	+	-	./.	+	+
GH °dH	<	>	<	<	<	<	>	>	>		+	-	-	-	+	--<	+	+	-	-	+	+	-	+	+	++<	+	++	---	+
K	<	>	>	<	>	<	>	>	<	>		++	-	+	+	--<	-	+	./.	-	+	-	-	++	+	+	-	./.	-	+
Mn	>	>	>	>	<	>	<	>	>	<	>		++<	-	-	./.	+++	./.	./.	./.	-	./.	---	./.	-	./.	./.	./.	./.	./.
NO3	>	<	>	>	>	<	>	<	<	<	>	<		-	-	-	++<	-	-	+	-	-	-	-	+	+	+	-	+	+
KH °dH	<	<	<	>	>	>	>	<	<	<	>	>	<		++<	+	-	-	./.	-	+	+	-	+	-	--<	-	./.	+	-
Ra	<	>	>	<	>	<	<	<	<	<	>	>	<	<		-	-	-	-	-	-	-	-	-	-	-	--	+	./.	+
PO4	<	>	<	>	<	<	>	>	>	<	<	./.	>	>	>		-	-	./.	-	-	+	+	-	--<	--<	-	./.	./.	-
Al	>	>	<	>	>	>	>	<	>	>	>	>	<	<	>	<		-	./.	++	+	--	+	-	+	++	-	./.	+	++<
H2SiO3	<	<	>	>	>	>	>	>	>	>	>	./.	>	>	>	>	>		./.	+	+	+	+	-	-	+	+	./.	./.	-
O2	<	>	>	>	<	<	<	<	>	>	./.	./.	<	./.	>	./.	./.	./.		./.	+	+	./.	./.	-	-	./.	--	./.	./.
Pb	<	>	>	<<	>	>	>	>	<<	>	>	./.	>	>	>	>	>	>	./.		-	---	+	./.	++	-	+++	./.	+	+
Leitf	>	>	>	>	<	>	>	>	>	>	>	>	>	>	>	>	>	>	<	>		+	+	+	+	+	-	-	./.	+
FR	<	>	<	<	>	>	>	>	>	>	>	./.	<	>	>	>	>	>	>	>	>		+	./.	+	-	./.	+	./.	---
Ni	>	>	>	>	>	>	>	>	>	>	>	>	>	>	<	>	<	>	./.	>	>	>		./.	++<	+	-	./.	++<	-
Fe(II)	>	>	>	>	>	>	>	>	>	>	>	./.	>	>	>	>	<	>	./.	./.	>	./.	./.		./.	-	./.	./.	./.	-
Fe g	>	>	>	>	>	>	>	>	>	>	>	>	>	>	>	<	<	>	>	>	>	>	<	./.		+	+	./.	-	+
NKH °dH	<	<	<	<	>	<	<	<	>	<	<	./.	<	<	<	<	<	>	>	>	<	>	>	>	>		-	./.	./.	+
Cu	<	>	>	<	>	>	>	>	>	>	>	./.	>	>	>	>	<<	>	./.	>	>	./.	>	./.	>	>		./.	./.	-
CO3	>	>	<	<	>	<	>	>	./.	<	./.	./.	>	./.	>	./.	>	./.	>	./.	>	>	./.	./.	./.	./.	./.		./.	./.
Sr	>	<	>	<	>	>	<<	>	>	>	>	./.	>	>	./.	./.	>	./.	./.	>	./.	./.	<<	./.	>	./.	./.	./.		./.
F	>	>	>	>	>	>	>	>	>	>	>	./.	>	>	>	>	<	>	./.	>	>	<<	>	>	>	>	>	./.	./.	

Tab. 6o: Compilation of the open mine space (in m³) of the Niederschlema/Alberoda deposit (Wismut GmbH, Dienstsache 4.0.28/254, ca. 1991). Classification of the cascades ("mining sections") according to BÜDER & SCHUPPAN (1992). The table does not contain information on the Oberschlema mine (object 2). MS: Markus Semmler adit. Total sum is calculated, starting from level -1800, by adding the open cavity of the respective levels. Total cascade is the sum of the cavity of all levels of the cascade.

Bottom	open mine space	Total	Cascade	Total
MS	55.664	28.785.937		
-30	75.152	28.730.273		
-60	273.752	28.655.121		
-90	485.559	28.381.369		
-120	571.192	27.895.810		
-150	467.064	27.324.618		
-180	708.254	26.857.554		
-210	568.563	26.149.300		
-240	488.031	25.580.737	Cascade I:	3.693.231
-270	427.781	25.092.706		
-300	636.622	24.664.925		
-330	593.866	24.028.303		
-360	629.421	23.434.437		
-390	700.440	22.805.016		
-420	751.928	22.104.576		
-450	699.610	21.352.648		
-480	785.601	20.653.038		
-486	26.072	19.867.437		
-510	716.791	19.841.365		
-540	1.197.040	19.124.574	Cascade II:	7.165.172
-546	98.794	17.927.534		
-585	875.574	17.828.740		
-630	1.069.639	16.953.166		
-636	55.190	15.883.527		
-675	913.030	15.828.337		
-720	1.044.529	14.915.307		
-726	50.484	13.870.778		
-765	863.252	13.820.294		
-810	1.053.705	12.957.042		
-816	58.016	11.903.337		
-855	901.342	11.845.321		
-900	914.672	10.943.979		
-906	31.113	10.029.307		
-945	772.996	9.998.194		
-990	1.272.873	9.225.198	Cascade III:	9.975.209
-996	64.078	7.952.325		
-1035	743.307	7.888.247		
-1080	763.755	7.144.940		
-1086	34.437	6.381.185		
-1125	655.306	6.346.748		
-1170	598.322	5.691.442		
-1176	21.298	5.093.120		
-1215	570.068	5.071.822		
-1260	484.996	4.501.754		
-1266	35.615	4.016.758		
-1305	778.311	3.981.143		
-1350	622.545	3.202.832	Cascade IV:	5.372.038
-1356	23.918	2.580.287		
-1395	530.688	2.556.369		
-1440	450.256	2.025.681		
-1485	397.207	1.575.425		
-1530	308.522	1.178.218		
-1575	201.777	869.696		
-1620	317.195	667.919		
-1626	41.750	350.724		
-1665	142.395	308.974		
-1710	143.127	166.579	Cascade V:	2.556.835
-1755	13.273	23.452		
-1800	10.179	10.179	Cascade VI:	33.631

Tab. 61: List of minerals described from the Niederschlema/Alberoda deposit (SCHRÖDER & LIPP 1990a, 1990b). More frequent minerals are in italics (J. MEYER, pers. comm.). The formulae are given according to STRUNZ (1982), STRÜBEL & ZIMMER (1982) or by PHILIPSBORN (1967), English mineral names according to BATES & JACKSON (1987).

No.	No. WATEQ4F	Name	English Name	Formula
1		Aguilaritaguilarite	$AgSeS_4$	
2		Aikinitaikinite	2PbS-CuS-BiS_{223}	
3	445	Acanthitacanthite	AgS_2	
4		Actinolite actinolite	$Ca_2(Mg,Fe)_5[(OH,F)\|SiO_{411}]_2$	
5		Allargentumallargentum	ε-(Ag,Sb)	
6		Allemontitallemontite	Sb-As	
7		Almandinalmandines	$FeAl_{32}[SiO]_{43}$	
8		Anatasanatase	TiO_2	
9		Andraditandradite	$CaFe_{32}[SiO]_{43}$	
10	17	Anhydrite anhydrite	$Ca[SO]_4$	
11		Ankerite anchorite	$CaFe[CO]_{32}$	
12	494	***annabergite***	annabergite	$Ni_3[AsO_{42}]$-8HO_2
13		***Antimony***	antimony	Sb
14		Apatitapatite	, phosphorite	$Ca_5[F\|(PO_4)_3]$
15		Apophylliteapophyllite	$KCa_4[F\|(SiO_{410})_2]$-8HO_2	
16	21	Aragonitaragonite	$CaCO_3$	
17		Argentitargentite	AgS_2	
18		Argentopyritargentopyrite		$AgFeS_{23}$
19		***Arsenic***	arsenic	As
20		Arsenolampritarsenolamprite		α-As
21	497	Arsenolite arsenolite	AsO_{23}	
22		***Arsenopyrite***	arsenopyrite	FeAsS
23		Atelestitatelestite	$Bi_2[O\|OH\|AsO_4]$	
24		Auripigmentauripigment	AsS_{23}	
25	620-622/625/626	***Autunite***	autunite, calcouranite	$Ca[_2UO\|PO_{42}]$·10(12–10)H_2O
26	144	***barite***	barite	$Ba[SO]_4$
27		Becquerelitebecquerelite		6$[UO\|_2(OH)_2]$-$Ca(OH_2)$-4HO_2
28		Berzelianiteberzelianite	$CuSe_2$	
29		Beyerite beyerite	$CaBi_2[O\|CO_3]_2$	
30		Bieberitbieberite	$Co[SO_4]$-7HO_2	
31		Bismuthinitebismuthine	, bismuthinite	BiS_{23}
32		Bornitebornite	, erubescite	$CuFeS_{54}$
33		Bournonitebournonite	2PbS-CuS-SbS_{223}	
34		Bravoitbravoite	$(Ni,Fe,Co)S_2$	
35	12	***Calcite***	calcite	$CaCO_3$
36		Cannizzaritecannizzarite		$PbBiS_{3511}$
37		***Carnotite***	carnotite	$K_2[UO\|_2(VO_4)_2]$-3HO_2
38		Cassiteritecassiterite	, tinstone	SnO_2
39	365	Cerussitcerussite	$PbCO_3$	
40	250	***Chalcopyrite***	chalcopyrite	$CuFeS_2$
41		Chalcosine chalcocite	, chalcosine	CuS_2
42		***Chloantite***	chloanthite	$NiAs_3$
43	125/49	***chlorite***	chlorite	$(Mg,Fe)_3[(O,OH)_2\|AlSiO_{310}]$
44		Cinnabaritecinnabarite	HgS	
45		***Clausthalite***	clausthalite	PbSe
46		***Cobaltine***	cobaltite	CoAsS
47	577	***Coffinite***	coffinite	$U[SiO]_4$
48	246	Covellincovelline	, covellite	CuS
49		Crookesitecrookesite	$(Cu,Tl,Ag)_2Se$	
50		Cubanitecubanite	$CuFeS_{23}$	
51		Curitcurite	3PbO-8UO-4HO_{32}	
52	11/401	Dolomite dolomite	$CaMg[CO]_{32}$	
53		Dyscrasitdyscrasite	$AgSb_3$	
54		Emplektitemplectite	CuS-BiS_{223}	
55		Epidotepidote	, pistacite$Ca_2(Fe,Al)Al_2[O\|OH\|SiO\|SiO_{427}]$	
56		***erythrite***	erythrite	$Co_3[AsO_{42}]$-8HO_2
57		Eukairiteucairite	α-CuSe-$AgSe_{22}$	
58	62	***Fluorite***	flourite	CaF_2
59		Fourmarieritefourmarierite		8$[UO\|_2(OH)_2]$-2$Pb(OH_2)$-4HO_2
60		***Galenite***	galena, galenite	PbS
61	18	Gypsum	$Ca[SO_4]$-2H_2O	
62	110	Goethitgoethite	-FeOOH	
63		Garnet (Grossular)	garnet	$CaAl_{32}(SiO_4)_3$
64		Guanajuatiteguanajuatite		$Bi_2(Se,S)_3$
65	600	Gummitgummite	, gummy matter	Formulas see Tab. 9
66	108	***hematite***	hematite	FeO_{23}
67		Hessonite	$Ca_3(Al,Fe)_2[SiO_4]_3$	
68		Klockmanniteklockmannite		CuSe

No.	No. WATEQ4F	Name	English Name	Formula
69		Cobalt pentlandite	cobalt pentlandite	$(Co,Ni,Fe)_9S_8$
70		***Copper***	copper	Cu
71		Lautitlautite	CuAsS	
72		Limonite limonite	, brown hematite	-FeOOH
73		***Iollingite***	lollingite	$FeAs_2$
74		Luzonitluzonite	$CuAsS_{34}$	
75	107	Magnetite magnetites	$(FeFe^{3+2+})FeO^{3+}{}_4$	
76	235	Malachite malachite	$Cu_2[(OH)_2\|CO_3]$	
77	189	Manganite manganite	-MnOOH	
78		Marcasite marcasite	FeS_2	
79		Maucheritemaucherite	$NiAs_{<32}$	
80		Mgriitmgriite	$(Cu,Fe)_3AsSe_3$	
81		Miargyritmiagyrite	$AgSbS_2$	
82	415	Millerite millerite	, nickel pyrites	β-NiS
83		Molybdenite molybdenites		MoS_2
84		Muscovite Muscovite	$KAl_2[(OH,F)_2\|AlSiO_{310}]$	
85		Naumannitnaumannite	$AgSe_2$	
86		***nickeline***	nickeline	NiAs
87		Orthoclase field spar	$K[AlSiO]_{38}$	
88		Para-Rammelsbergite	pararammelsbergite	$NiAs_2$
89		***Pharmacolite***	pharmacolite	$CaH[AsO_4]$-$2H_2O$
90		Polybasitepolybasite	$8(Ag,Cu)_2S$-SbS_{23}	
91		Proustiteproustite	$AgAsS_{33}$	
92	197	Psilomelanpsilomelane	$(Ba,Mn^{2+}\ldots)_3(O,OH)_6MnO_{816}$	
93		Pyrargyritepyrargyrite	$AgSbS_{33}$	
94	114	***Pyrite***	iron pyrite	FeS_2
95	183	Pyrolusite pyrolusite	β-MnO_2	
96		Pyromorphite pyromorphite		$Pb_5[Cl\|(PO_4)_3]$
97	53	Pyrophyllite	$Al_2[(OH)_2\|SiO_{410}]$	
98		Pyrostilpnite pyrostilpnite		$AgSbS_{33}$
99		Pyrrhotinepyrrhotite	FeS	
100	101	Quartz quartz	SiO_2	
101		***Rammelsbergite***	rammelsbergite	$NiAs_2$
102	501	Realgarrealgar	AsS_{44}	
103	190/564	Rhodochrosite Rhodochrosite	$MnCO_3$	
104		Rößleritrosslerite	$MgH[AsO_4]$-$7HO_2$	
105		***Safflorite***	safflorite	$CoAs_2$
106		***scheelite***	scheelite	$Ca[WO]_4$
107		Schorltourmaline	, achroite	$NaFeAl_{36}[(OH)_{1+3}\|(BO_3)_3\|SiO_{618}]$
108		***Selenium***	selenium	-Se
109	94	***Siderite***	siderite	$FeCO_3$
110		***Silver***	silver	Ag
111		Scorodite scorodite	, pitticite	$Fe^{3+}[AsO_4]$-$8HO_2$
112		Skutteruditscutterndite	$CoAs_3$	
113		Smythitsmythite	FeS_{34}	
114	286	***Sphalerite***	shalerite, zinc blende	α-ZnS
115		Stephanite stephanite	5 AgS-SbS_{223}	
116		Sternbergite Sternbergite		$AgFeS_{23}$
117		Stetefeldtitstetefeldite	$AgSb_{1-22-1}(O,OH,H_2O)_7$	
118		***Symplesite***	symplesite	$Fe_3{}^{2+}[AsO_{42}]$-$8HO_2$
119	37	Talktalc	$Mg_3[(OH)_2\|SiO_{410}]$	
120		Tennantittennantite	$CuAsS_{33.25}$	
121		Tetrahedral tetrahedrite	$CuSbS_{33.25}$	
122	629	***Torbernite***	torbernite	$Cu[UO\|PO_{242}]$-10(12-8)H_2O
123		***Tujamunit***	tyuyamonite	$Ca[UO\|VO_{242}]$-$5HO_2$
124		Ullmannitullmannite	NiSbS	
125		Umangitumangite	$CuSe_{32}$	
126	573	***Uraninite***	uraninite	UO_2
127	632	Uranophanuranophane	$CaH_2[UO\|SiO_{242}]$-$5HO_2$	
128		Uranopilituranopilite	$[_26UO\|5(OH)_2\|SO_4]_2\cdot 12H_2O$–$1H_2O$	
129		Uranospinituranospinite	$Ca[UO\|AsO_{242}]$-$10HO_2$	
130		Vaesitvaesite	NiS_2	
131		***Weilit***	weilite	$CaH[AsO]_4$
132		Whewellitwhewellite	$Ca[_2CO_4]$-HO_2	
133		***Bismuth***	bismuth	Bi
134	145	Witheritwitherite	$BaCO_3$	
135		***Wolframite***	wolframite	$(Mn,Fe)WO_4$
136		Wollastonite Wollastonite		$Ca_3[SiO]_{39}$
137		Wurzitwurtzite	β-ZnS	
138		Xanthoconxanthoconite	$AgAsS_{33}$	
139		Zeunerite	$Cu[_2UO\|AsO_{42}]\cdot 10(16–10)H_2O$	
140		Zippeitzippeite	$[_26UO\|3(OH)_2]3SO_4]_{22}\cdot 12H_2O\cdot 3HO$	